HOKKAIDO UNIVERSITY

Title	Electron Microscopic Studies on Plant Viruses
Author(s)	SHIKATA, Eishiro
Citation	Journal of the Faculty of Agriculture, Hokkaido University, 55(1), 1-110
Issue Date	1966-04
Doc URL	https://hdl.handle.net/2115/12816
Type	departmental bulletin paper
File Information	55(1)_p1-110.pdf

Hokkaido University Collection of Scholarly and Academic Papers : HUSCAP

ELECTRON MICROSCOPIC STUDIES ON PLANT VIRUSES

By

Eishiro SHIKATA

Department of Botany, Faculty of Agriculture
Hokkaido University
Sappro, Japan

Contents

I. Introduction 2
II. Materials 4
III. Determination of magnification of an electron microscope and measurement of size of virus particles 5
A. Measurement of magnification with grating replica films 6
1. Schrinkage of replica films 6
2. Distortion of replica films 9
3. Fluctuation of magnification of an electron microscoope determined by grating replica films 9
B. Measurements of magnification with Dow latex particles 12
1. Increase in particle diameter by contamination in the electron microscope 12
2. Fluctuation of magnification of an electron microscope determined by Dow latex particles 13
3. Discrepancy of diameter between shadowed and unshadowed latex particles 20
C. Discussion and conclusions 20
IV. Tobacco mosaic virus 24
A. Shape and size of tobacco mosaic virus 24
B. Tobacco mosaic virus stained by phosphotungustic acid 26
C. Effect of heat on tobacco mosaic virus 26
D. Effect of hydrogen ion concentration on tobacco mosaic virus . . . 35
E. Effect of hydrogen peroxide on tobacco mosaic virus 38
F. Effect of formalin on tobacco mosaic virus 47
G. Effect of sodium nitrite on tobacco mosaic virus 49
H. Effect of ultraviolet light on tobacco mosaic virus 52
I. Effect of X-ray on tobacco mosaic virus 55
J. Effect of detergent on tobacco mosaic virus 60

[Journ. Facul. Agr., Hokkaido Univ., Sapporo, Vol. 55, Pt. 1, 1966]

K. Ultrathin sectioning 60
L. Discussion and conclusions 61
V. Potato virus X 67
A. Size and shape of potato virus X 67
B. Effect of hydrogen ion concentration on potato virus X 75
C. Effect of ultraviolet light on potato virus X 76
D. Ultrathin sectioning 77
E. Discussion and conclusions 78
VI. Barley stripe mosaic virus 79
A. Isolation and purification of barley stripe mosaic virus 79
B. Size and shape of barley stripe mosaic virus 80
C. Barley stripe mosaic virus stained by phosphotungustic acid and potassium chloride 82
D. Effect of detergent on barley stripe mosaic virus 82
E. Discussion and conclusions 83
VII. Rice dwarf virus 84
A. Isolation of rice dwarf virus from diseased rice plant 84
B. Isolation of rice dwarf virus from diseased Echinochloa crus-galli Beauv. 86
C. Isolation of rice dwarf virus from viruliferous leafhoppers 86
D. Size and shape of rice dwarf virus 87
E. Ultrathin sections of diseased rice leaves 91
F. Ultrathin sections of infective leafhoppers 92
G. Discussion and conclusions 94
VIII. Summary 100
IX. Literature 102
X. Figures

I. Introduction

One of the most outstanding achievements in virology during the past 30 years was the determination of the size and shape of virus particles under the electron microscope.

Furthermore, it became possible to study the fine structures of virus particles and the sites of virus multiplication in different host cells by means of recently improved techniques for specimen preparation. The development of numerous improved techniques followed closely the remarkable progress of high resolution electron microscopes.

Difficulties for application of electron microscopes to biological studies have been, at the beginning, derived from the fundamental character of the electron beam. It is necessary to keep the passage of the electron beam in a high vacuum. Thus no material lenses can be used for the electron microscope, and the specimen to be observed should be placed in a high vacuum.

Despite improved techniques of specimen preparation, such discrepancy between light and electron microscope may sometimes cause difficulties for specimen preparation or misunderstanding in the interpretation of results obtained. After the first successful electron microscopic studies of isolated tobacco mosaic virus and potato virus X particles by KAUSCHE *et al.* (1939), improvements in the preparation techniques had a great impact on virus research. Among them, most important improvements are: metallic shadow casting introduced by WILLIAMS and BACKUS (1949-a), staining method perfected by HALL (1955), ultrathin sectioning accomplished by Pease, and Baker (1948), and negative staining invented by BRENNER and HORNE (1959). Each of these techniques made a greatly significant contribution to electron microscopic studies of viruses.

There had been no information available in regard to electron microscopy of plant viruses in Japan until 1949, notwithstanding the fact that YOSHII (1943) had already pointed out in 1943 the necessity of electron microscopic studies of plant viruses.

The author began working on the electron microscopic study of plant viruses in 1949; his studies were concerned with tobacco mosaic virus, potato virus X, barley stripe mosaic virus, and rice dwarf virus. After the introduction of ultrathin sectioning, this technique was applied by the author to tobacco mosaic virus disease, potato virus X disease, and, most extensively, to rice dwarf virus disease.

The experiments described now have been carried out over a period of 14 years, from 1949 to 1962, at the Botanical Institute, Faculty of Agriculture, Hokkaido University, Sapporo, Japan, using various models of electron microscopes available in Japan.

The author wishes to sincerely thank Prof. EMER. of Hokkaido University, Teikichi FUKUSHI, and Prof. Daiki MURAMA for their kind suggestions and encouragement throughout the experiments.

The author also thanks Dr. Karl MARAMOROSCH of the Boyce Thompson Institute, Yonkers, New York, for his suggestions during the preparation of this manuscript.

The author is indebted to Dr. Taro TAKEYAMA, Mr. Giichi SATO, Mr. Goro TOMITA, Prof. Katsuhichi HIRATO, and Dr. Teruo KUNISHIGE, for their kind help in using the electron microscopes, and to Prof. Yoshio TAKAHASHI and Mr. Shōichiro TAKAHASHI for their kindness in permitting the use of a high resolution electron microscope and in helping to keep our electron microscope in best condition throughout the experiments. The author expresses sincere thanks to Prof. Tokio NEI and Dr. Ikuo KIMURA for their kind help

during some of the experiments.

II. Materials

Tobacco mosaic virus: Five or six-leaved yonug plants of *Nicotiana tabacum* L. var. White Burley or *N. sylvestris* SPEG. et COMES. were incoculated with tobacco mosaic virus. After 20 to 30 days, young infected leaves were harvested and frozen at −20°C to 30°C for experiments. Infectivity of virus material was tested on leaves of *Nicotiana glutinosa* L. plants by half-leaf methods.

Potato virus X: The virus was inoculated into leaves of tomato plants (*Lycopersion esculentum* MILL. var. *Marglobe*) or tobacco plants. After 20 to 30 days, young affected leaves were harvested and frozen at −20°C to −30°C. Four strains of potato virus X were used in the experiments; strain X-5 isolated from potato plant *Solanum tuberosum* L. var. Norin-1 shows severe necrotic symptoms on leaves of *Datura stramonium* L. and tomatoes. Strain X-68 was isolated from a potato plant var. Oojiro. This strain shows mosaic symptoms on leaves of tomato and tobacco plants. Strain X-C_1 obtained from a crinkle mosaic diseased potato plant var. Benimaru shows slight mosaic on leaves of tomato and tobacco plants. X-I_{43} was isoloted from a symptomless potato plant var. Danshaku. Faint mottling appears on the infected leaves but disappears in the summertime. Strains X-5, X-68, and X-I_{43} were isolated by Dr. Nobuyuki OSHIMA at Hokkaido Agricultural Experiment Station (OSHIMA 1959).

Barley stripe mosaic virus: Young barley plants (*Hordeun Sativum* L. var. Moravia) and sweet corn (*Zea mays* L. var. Golden Bantam) were inoculated with barley stripe mosaic virus. About 30 days later, affected leaves were harvested and frozen at −20°C to −30°C.

Rice dwarf virus: Rice plants (*Oryza sativa* L. var. Nōrin 20) and *Panicum crus-galli* L. var. Shirosanpaku were inoculated with infective leafhoppers (*Nephotettix cincticeps* UHLER). After 30 to 40 days following inoculation, the leaves showed typical symptoms of yellowish white specks spreading along the veins. These leaves were harvested and used in the experiments.

The insect vectors were placed in insect proof cages on healthy or diseased rice plants. Viruliferous leafhoppers were tested individually on seedlings of rice plants in glass tubes, about 30 to 40 cm long, and 3 to 4 cm in diameter, closed at the upper end with a thin nylon cloth.

Electron microscope and ultramicrotome: The electron microscopes used in the experiments were as given in Table 1.

TABLE 1. Electron Microscopes used for Experiments

	Model of Electron microscopes	Lens system	Direct magnification	Resolution	Accelerating voltage
HU-4	Hitachi Co.	Magnetic, 2 stage	5,000-12,000	50 Å	50 KV.
HU-7	"	" "	2.000-15,000	25 Å	50
JEM-4B	Japan electron optics Co.	" 3 stage	500-20,000	30 Å	50
JEM-4C	"	" "	500-30,000	20 Å	50
JEM-T1	"	" 2 stage	2,500- 5,000	50 Å	50
JEM-5L	"	" 3 stage	600-50,000	10 Å	50, 80, 100
JEM-5Y	" (double condenser)	" "	500-200,000	8 Å	"

Specimens for ultrathin sections were fixed in 1% osmic acid solution buffered with 1/100 M phosphate at pH 7.2 to 7.4 containing 0.2 M sucrose and then dehydrated with graded alcohol. These specimens were embedded in methacrylate and cut into thin sections by means of the ultramicrotomes (JUM-4 or 5, Japan Electron Optics Laboratory Co.) equipped with glass knives.

Dow latex particles used in the experiments were 580 G (260 mμ), 15 N-2 (340 mμ), 15 N-8 (511 mμ), 15 N-23 (138 mμ), and LS-057 (264 mμ).

III. Determination of magnification of an electron microscope and measurement of size of virus particles

In general, the size of virus particles, as determined by an electron microscope using magnification graphs made by grating replicas, includes approximately a 10 to 20% error.

The diffraction grating is one of the reliable scales and it has therefore been used to determine magnification of the electron microscope for a long time. The diffraction grating has to be implemented by replica films of the gratings and by the determination of magnification with the help of grating replica films.

Dow latex particles have been reported useful for the determination of the size of virus particles, as reported by BACKUS and WILLIAMS (1948, 1949). The determination of electron microscope magnifications with the latex particles was further improved in 1950 (Gerould, 1950—a, b ;, KERN and KERN, 1950).

In our own experiments, diffraction glass gratings with 960 grooves per mm or 1200 grooves per mm, crosswise ruled at right angles, were employed (Figs. 1, 2).

A. Measurements of magnification with grating replica films

1. Shrinkage of replica films

To make the grating replicas, the "filmy replica technique" (FUKAMI, 1955) was employed throughout the experiments. This is a two-step replica method using acetyl cellulose films for the first replica and then carbon films for the second replica.

MORITO *et al.* (1956) and Akashi *et al.* (1956) reported that the replica film of methylmethacrylate showed 1 to 2% shrinkage after stripping from glass grating, but no results have been reported regarding shrinkage of acetylcellulose film replicas.

An area of the graduation mark on a vanier caliper was replicated with an acetylcellulose film. After stripping, the length of the same area on both

TABLE 2. Shrinkage of Acetylcellulose Films

Expt. number	Immediately after stripping	Per cent of shrinkage						
		Hours after stripping						
		3	6	20	24	48	72	96
1	2.0	2.66	2.94	3.60	3.46	3.73	3.00	3.73
2	2.0	2.66	2.80	3.33	3.33	3.73	3.73	3.73
3	2.0	2.4	2.66	2.94	2.94	3.20	3.47	3.53
4	2.0	2.0	2.80	2.94	2.80	3.33	3.47	3.47
5	1.47	2.0	2.66	3.33	3.33	3.73	3.67	3.60
Average	1.9	2.3	2.8	3.2	3.2	3.5	3.6	3.6

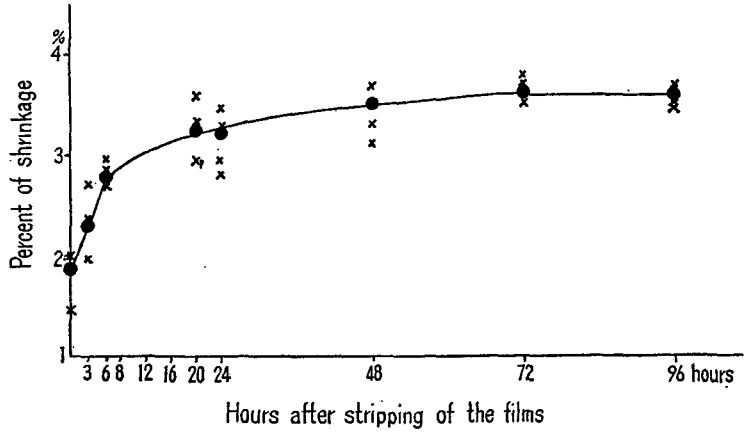

Diagram 1. Schrinkage of Acetylcellulose Films

the vanier caliper and the replica film were accurately measured with a light microscope.

The calculated shrinkage of 5 acetyl films is shown in Table 2 and Diagram 1.

Immediately after removing the films, approximately 2% shrinkage of acetylcellulose films occurred. The films continued to shrink for 48 to 72 hours. at room temperature. After 3 days there was little shrinkage. About 3.6% shrinkage of acetylcellulose films occurred within 3 days after removing from the glass grating.

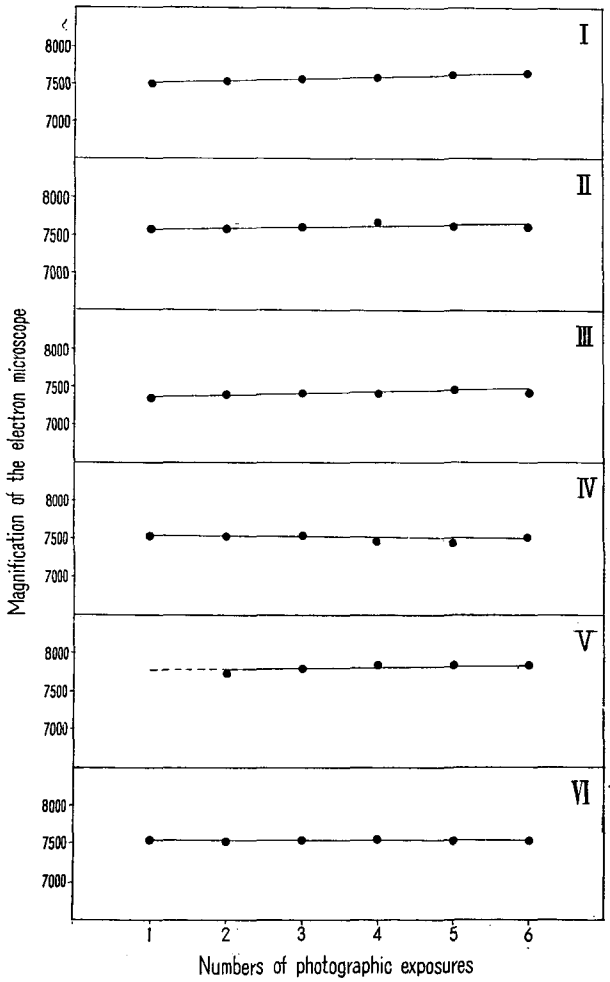

Diagram 2. Changes of Grating Replica Films in the electron mieroscope

TABLE 3. Changes of Grafting Replica Films

Expt. number	Values calculated, (mm)	No. of grooves	Average distance of grooves, (mm)	Magnification
I-1	30.1	4	7.53	7500
2	30.3	4	7.58	7540
3	30.3	4	7.58	7540
4	30.55	4	7.64	7620
5	30.65	4	7.66	7640
6	30.55	4	7.64	7620
II-1	30.4	4	7.60	7570
2	30.4	4	7.60	7570
3	30.6	4	7.65	7630
4	30.8	4	7.70	7680
5	30.5	4	7.63	7600
6	30.5	4	7.64	7620
III-1	29.45	4	7.36	7340
2	29.75	4	7.44	7410
3	29.7	4	7.43	7400
4	29.75	4	7.44	7410
5	29.85	4	7.46	7440
6	29.8	4	7.45	7420
IV-1	30.3	4	7.58	7550
2	30.3	4	7.58	7550
3	30.3	4	7.58	7550
4	30.3	4	7.50	7480
5	30.0	4	7.50	7480
6	30.1	4	7.53	7500
V-1	—	—	—	—
2	29.0	4	7.25	7230
3	29.35	4	7.34	7310
4	29.3	4	7.38	7350
5	29.5	4	7.38	7350
6	29.45	4	7.36	7340
VI-1	30.3	4	7.58	7550
2	30.25	4	7.56	7540
3	30.25	4	7.56	7540
4	30.25	4	7.56	7540
5	30.25	4	7.56	7540
6	30.25	4	7.56	7540

2. Distortion of replica films

A drop of diluted latex (Dow latex 580 G) was dried on replica films supported by brass grids. Photographic exposures were then made from the specimens in an electron microscope. In these experiments the following distortions of the replica films were observed.

a) When 6 photographs were made from 6 different areas in a replica film, average spacing of grooves of each 6 photographs differed considerably.

b) The grooves on the replica films were made crosswise at right angles, but average spacings between crossed grooves varied considerably.

c) Although crosswise grooves did not form a right angle, the latex particles on the same replica films showed regular circles.

It is apparent that the distorted films described above cannot be used for calculating the accurate magnification of an electron microscope. Therefore, silica was evaporated on the carbon films, as reported by BRADFORD and VANDERHOFF (1955), in order to prevent such distortions. As a result, it was easy to make wide replica films without being distorted during preparation and by electron beams.

In order to investigate distortion of silica coated replica films after irradiation by an electron beam, fresh replica films were placed in the JEM-4B electron microscope and 6 successive photographic exposures of the same area were made at intervals of 3 minutes under conditions of high intensity of irradiation with beam current of 10 μA. As shown in Table 3, Diagram 2, no noticeable distortions and shrinkages of silica carbon films occurred under the electron bombardment.

3. Fluctuation of magnification of an electron microscope determined by grating replica films

In these experiments, investigations of possible errors in each photograph were made for 6 months under usual working conditions for virus observation. (JEM-4B, intermediate lens current was

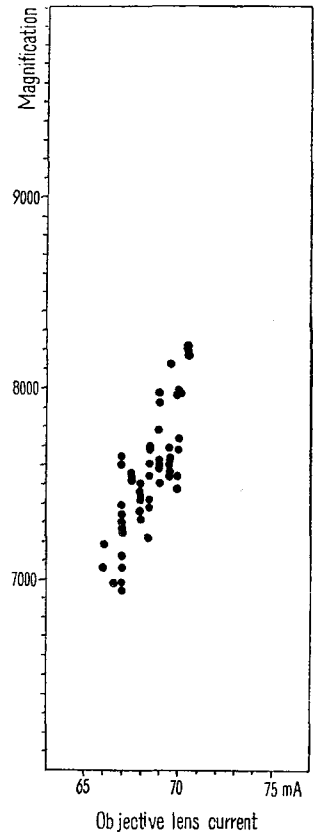

Diagram 3.
Fluctuation of Magnification of JEM-4 Electron Microscope Calculated by Grating Replica Films

14 mA, projective lens, switch No. 5). Specimen holders used in the experiments were taken at random out of lots of more than 10 holders for each grating replica.

As shown in Table 4 and Diagram 3, magnifications calculated with grating replicas under the conditions mentioned above fluctuated between about 7,000 and 8,000, and objective lens current also fluctuated between 66 mA and 70.5 mA. This proved that the position of the specimen in the electron microscope was very variable.

TABLE 4. Fluctuation of Magnification of JEM-5 Electron Microscope Calculated by the Grating Replica Films

Exposure numbers	Values measured (numbers of grooves) (mm)	Average distance of grooves, (mm)	Conditions of JEM-4B			Magnification
			Inter. lens (mA)	Project. lens	Object. lens (mA)	
S- 967	37.0 (5)	7.40	14	5 *	68.5	7380
S- 968	29.8 (4)	7.45	"	"	"	7420
S- 969	29.4 (4)	7.35	"	"	"	7320
S- 970	21.6 (3)	7.20	"	"	66.0	7180
S- 971	21.0 (3)	7.00	"	"	66.5	6980
S- 972	35.4 (5)	7.08	"	"	66.0	7060
S- 979	35.0 (5)	7.00	"	"	67.0	6980
S- 980	35.5 (5)	7.10	"	"	"	7070
S- 981	42.0 (6)	7.00	"	"	"	6980
S-1003	40.0 (5)	8.00	"	"	70.0	7980
S-1004	31.1 (4)	7.78	"	"	"	7740
S-1006	37.4 (5)	7.48	"	"	"	7460
S-1007	38.0 (5)	7.60	"	"	"	7580
S-1008	37.3 (5)	7.46	"	"	"	7440
S-1014	32.6 (4)	8.15	"	"	69.5	8120
S-1015	31.8 (4)	7.95	"	"	69.0	7920
S-1030	33.0 (4)	8.25	"	"	70.5	8220
S-1031	33.0 (4)	8.25	"	"	"	8220
S-1032	32.9 (4)	8.22	"	"	"	8200
S-1045	24.0 (3)	8.00	"	"	69.0	7980
S-1047	31.2 (4)	7.80	"	"	"	7770
S-1069	30.1 (4)	7.53	"	"	68.5	7500
S-1070	30.3 (4)	7.58	"	"	"	7540
S-1071	30.3 (4)	7.58	"	"	"	7540

Exposure numbers	Values measured (numbers of grooves) (mm)	Average distance of grooves, (mm)	Conditions of JEM-4B			Magnification
			Inter. lens (mA)	Project. lens	Object. lens (mA)	
S-1072	30.6 (4)	7.65	14	5 *	68.5	7620
S-1073	30.7 (4)	7.68	"	"	"	7640
S-1074	30.6 (4)	7.65	"	"	"	7620
S-1100	23.0 (3)	7.67	"	"	67.0	7640
S-1101	30.5 (4)	7.63	"	"	"	7600
S-1105	30.4 (4)	7.60	"	"	69.5	7570
S-1106	30.4 (4)	7.60	"	"	"	7570
S-1107	30.6 (4)	7.65	"	"	"	7620
S-1108	30.8 (4)	7.70	"	"	"	7670
S-1109	30.5 (4)	7.63	"	"	"	7600
S-1110	30.6 (4)	7.64	"	"	"	7620
S-1111	30.2 (4)	7.55	"	"	"	7530
S-1112	30.3 (4)	7.57	"	"	"	7540
S-1113	30.3 (4)	7.57	"	"	"	7540
S-1123	40.0 (5)	8.00	"	"	70.0	7980
S-1124	31.9 (4)	7.98	"	"	"	7950
S-1125	31.7 (4)	7.93	"	"	"	7900
S-1176	30.5 (4)	7.63	"	"	69.0	7600
S-1177	30.6 (4)	7.64	"	"	"	7620
S-1178	38.0 (5)	7.60	"	"	"	7580
S-1179	30.3 (4)	7.58	"	"	"	7540
S-1245	30.3 (4)	7.58	"	"	67.5	7540
S-1246	30.2 (4)	7.55	"	"	"	7530
S-1247	30.4 (4)	7.60	"	"	"	7570
S-1248	34.8 (5)	69.6	"	"	67.0	6940
S-1250	32.8 (4)	8.20	"	"	70.5	8180
S-1257	28.6 (4)	7.15	"	"	67.0	7120
S-1258	36.4 (5)	7.28	"	"	"	7250
S-1259	36.5 (5)	7.30	"	"	"	7280
S-1260	29.3 (4)	7.33	"	"	"	7300
S-1261	29.4 (4)	7.35	"	"	"	7340
S-1262	30.0 (4)	7.50	"	"	"	7480

* Switch number of projector lens control.

B. Measurements of magnification with Dow latex particles

1. Increase in particle diameter by contamination in the electron microscope

BRADFORD and VANDERHOFF (1955) reported that the diameter of Dow latex particles varied considerably, depending on the different kinds of metals used for the supporting grids.

In order to investigate the variation in particle diameter under an electron beam, Dow latex particles (580 G, 15 N–7) were diluted and dried on grating replica films supported by brass grids. The specimen was then placed in the JEM–4B electron microscope and 6 successive photographic exposures were made of the same area, at intervals of 3 minutes, under high intensity of irradiation and beam current of 10 μA. The results are shown in Table 5 and Diagram 4. The diameters of Dow latex particles of 15 N–7 and 580 G on the collodion films supported by brass grid increased by about 5.3 and 9.5% respectively, after about 20 minutes, during which time 6 successive photographic exposures of the same area were made under conditions of continuous

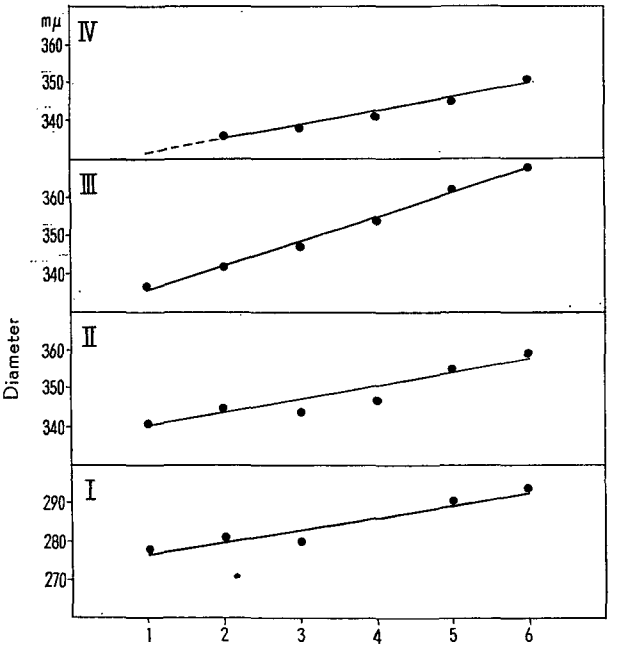

Diagram 4. Increase in the Diameter of Dow Latex Particles under an Electron Beam

TABLE 5. Increase in the Diameter of Dow Latex Particles Exposed to an Electron Beam

Expt. No.	Exposures No.	Dow latex	Diameter of latexes measured, (mm)	Magnification by gratings	Diameter of latexes, (mμ)
I	1	580G	31.3	7500	278
	2		31.8	7540	281
	3		31.6	7540	280
	4		—	(7620)	— over focus
	5		33.3	7640	291
	6		33.6	7620	294
II	1	15N-7	39.0	7570	341
	2		39.2	7570	345
	3		39.4	7630	344
	4		39.9	7680	347
	5		40.5	7600	355
	6		41.0	7620	359
III	1	15N-7	37.0	7340	336
	2		38.0	7410	342
	3		38.0	7400	347
	4		39.4	7410	354
	5		40.2	7440	362
	6		41.0	7420	368
IV	1	15N-7	—	—	—
	2		36.4	7230	336
	3		37.1	7310	338
	4		37.6	7350	341
	5		38.1	7350	345
	6		38.6	7340	351

irradiation by the intense electron beam (Figs. 3, 4).

2. Fluctuation of magnification of an electron microscope determined by Dow latex particles.

During a series of experiments over a 7-month period, Dow latex particles (15 N-7, 15 N-8, 580 G) were used to measure magnifications under the same conditions mentioned in chapter III, A. 3.

As shown in Tables 6 or 9 and Diagram. 5 to 8, magnifications calculated

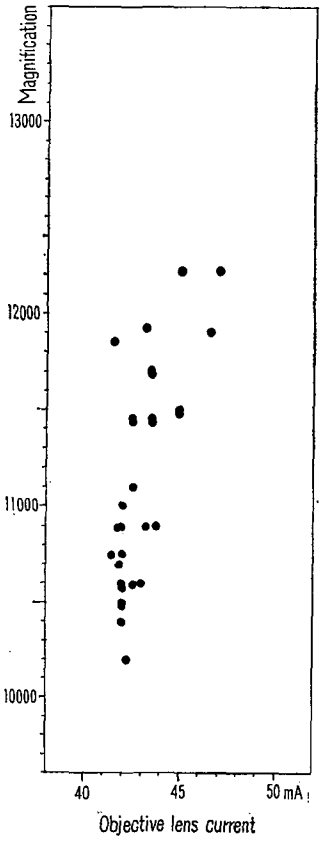

Diagram 5.

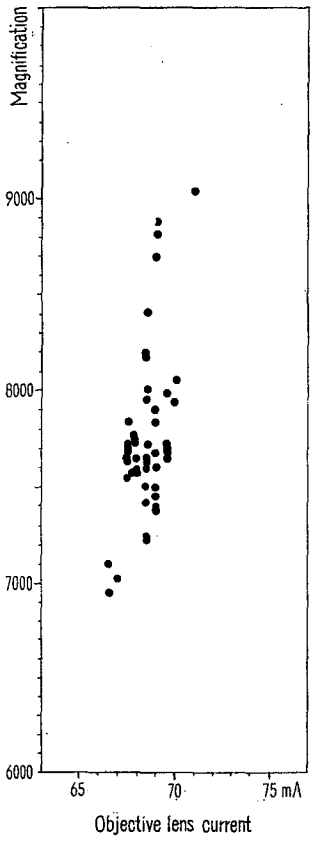

Diagram 6.

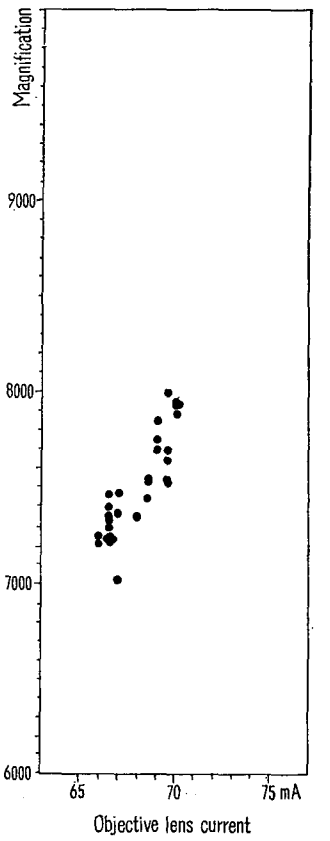

Diagram 7.

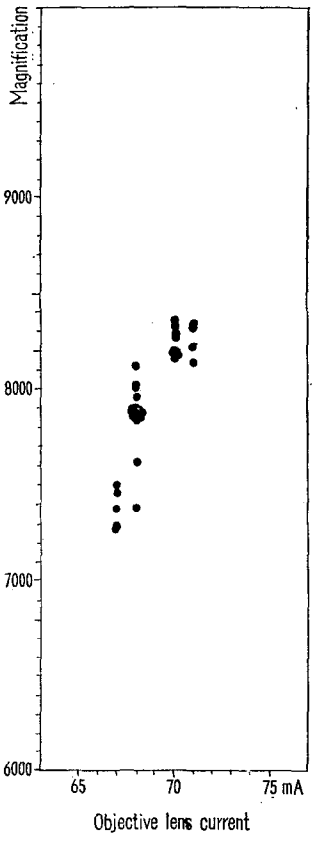

Diagram 8.

Diagram 5. Fluctuation of Magnification of a HU-7 Electron Microscope Calculated by Using Dow Latex 580-G
Diagram 6. Fluctuation of Magnification of a JEM-4 Electron Microscope Calculated by Using Dow Latex 580-G
Diagram 7. Fluctuation of Magnification of a JEM-4 Electron Microscope Calculated by Dow Latex 15 N-7
Diagram 8. Fluctuation of Magnification of a JEM-4 Electron Microscope Calculated by Using Dow Latex 15 N-7

TABLE 6. Fluctuation of Magnification of a HU-7 Electron Microscope Calculated by using Dow Latex 580 G

Exposure numbers	No. of particles	Average diameter of latex (× 1/15 mm)	Projective lens current (mA)	Objective lens current (mA)	Magnification
2726A	20	44.0	50	42	10400
2726B	8	45.5	〃	〃	10750
2773	1	47.6	〃	42.5	11460
2767	1	51.2	〃	45.0	12200
2770	3	48.6	〃	〃	11500
2772	3	〃	〃	〃	11500
2786	3	46.1	〃	42.0	10900
2787	6	46.5	〃	〃	11000
2788	1	44.8	〃	〃	10600
2790	1	〃	〃	42.5	10600
2792	1	47.0	〃	〃	11100
2806	20	44.8	〃	42.0	10600
2807	4	44.4	〃	〃	10500
2819	7	45.5	〃	41.5	10750
2820	6	44.4	〃	42.0	10500
2821	9	45.2	〃	41.95	10700
2855	1	43.1	〃	42.2	10200
2850	17	46.1	〃	41.8	10900
2857	8	44.8	〃	43.0	10600
2981	1	48.4	〃	42.5	11460
2982	1	50.4	〃	43.2	11920
2985	1	48.4	〃	43.5	11460
2989	1	48.4	〃	〃	11460
2987	1	49.5	〃	〃	11700
2988	1	〃	〃	〃	11700
2989	2	50.1	〃	41.5	11850
3029	1	50.4	〃	46.75	11900
3030	4	51.6	〃	47.0	12200
3031	1	46.1	〃	43.75	10900
3033	1	〃	〃	43.2	10900

TABLE 7. Fluctuation of Magnification of a JEM-4 Electron Microscope Calculated by using Dow Latex 580 G

Exposure numbers	No. of particles	Average diameter of latexes (× 1/15 mm)	Inter. lens current (mA)	Project. lens switch	Object. lens current (mA)	Magnification
S-751	4	30.0	14	5	66.5	7100
S-752	7	29.7	〃	〃	67.0	7020
S-756	2	31.4	〃	〃	68.5	7420
S-762	5	32.4	〃	〃	69.0	7680
S-763	10	32.3	〃	〃	69.5	7650
S-764	5	32.4	〃	〃	〃	7680
S-765	1	32.6	〃	〃	〃	7720
S-766	3	31.7	〃	〃	68.5	7500
S-767	1	30.6	〃	〃	〃	7250
S-768	3	30.6	〃	〃	〃	7250
S-770	1	33.2	〃	〃	69.0	7840
S-771	2	34.1	〃	〃	70.0	8060
S-774	7	33.9	〃	〃	69.5	8000
S-775	11	33.4	〃	〃	69.0	7900
S-778	12	29.4	〃	〃	66.5	6950
S-781	10	32.3	〃	〃	68.0	7650
S-787	14	37.2	〃	〃	69.0	8810
S-788	20	37.5	〃	〃	〃	8860
S-789	2	36.8	〃	〃	〃	8700
S-791	13	32.1	〃	〃	68.0	7600
S-792	10	33.9	〃	〃	68.5	8000
S-793	12	38.2	〃	〃	71.0	9030
S-798	2	33.7	〃	〃	68.5	7960
S-799	3	34.7	〃	〃	68.0	8200
S-810	2	33.6	〃	〃	70.0	7950
S-823	9	34.7	〃	〃	68.5	8200
S-824	6	35.6	〃	〃	〃	8410
S-859	5	33.2	〃	〃	67.5	7840
S-860	2	32.6	〃	〃	〃	7720
S-861	2	32.6	〃	〃	〃	7720
S-862	2	32.3	〃	〃	〃	7650
S-863	2	32.3	〃	〃	〃	7650
S-864	6	32.4	〃	〃	〃	7680
S-865	4	31.9	〃	〃	〃	7550
S-866	2	32.2	〃	〃	68.0	7600
S-867	5	32.1	〃	〃	67.5	7580
S-868	7	32.6	〃	〃	〃	7720
S-869	5	32.8	〃	〃	〃	7760
S-870	12	32.7	〃	〃	〃	7740
S-871	3	31.3	〃	〃	69.0	7400
S-872	7	31.7	〃	〃	〃	7500
S-873	1	32.2	〃	〃	〃	7600
S-875	5	31.3	〃	〃	〃	7400
S-876	5	31.5	〃	〃	〃	7450
S-877	9	32.6	〃	〃	69.5	7700
S-878	4	32.2	〃	〃	68.5	7600
S-879	8	32.3	〃	〃	〃	7650
S-881	2	32.6	〃	〃	〃	7720
S-882	2	32.3	〃	〃	〃	7650

TABLE 8. Fluctuation of Magnification of a JEM-4 Electron Microscope Calculated by using Dow Latex 15 N-7

Exposure numbers	No. of particles	Average diameter of latexes (× 1/15 mm)	Inter. lens current (mA)	Project. lens switch	Object. lens current (mA)	Magnification
S-1114	2	39.3	14	5	69.5	7700
S-1116	2	39.5	〃	〃	〃	7750
S-1117	3	40.0	〃	〃	70.0	7850
S-1118	6	39.0	〃	〃	69.5	7650
S-1120	2	38.5	〃	〃	〃	7550
S-1121	3	38.5	〃	〃	〃	7550
S-1122	2	39.5	〃	〃	〃	7750
S-1127	4	40.3	〃	〃	70.0	7900
S-1130	2	40.5	〃	〃	〃	7940
S-1131	3	40.5	〃	〃	〃	7940
S-1132	5	40.3	〃	〃	〃	7900
S-1133	2	40.5	〃	〃	〃	7940
S-1136	2	40.8	〃	〃	69.5	8000
S-1139	2	39.8	〃	〃	69.5	7780
S-1144	3	40.0	〃	〃	69.0	7850
S-1145	2	39.5	〃	〃	〃	7750
S-1146	2	39.3	〃	〃	〃	7700
S-1180	2	37.5	〃	〃	68.0	7350
S-1181	1	38.0	〃	〃	68.5	7450
S-1183	1	39.0	〃	〃	〃	7650
S-1184	2	39.0	〃	〃	〃	7650
S-1186	2	37.0	〃	〃	66.0	7250
S-1187	2	36.8	〃	〃	〃	7210
S-1188	3	37.0	〃	〃	66.5	7250
S-1190	2	37.0	〃	〃	〃	7250
S-1191	2	37.3	〃	〃	〃	7300
S-1192	1	38.0	〃	〃	〃	7450
S-1197	3	37.0	〃	〃	〃	7250
S-1198	1	37.0	〃	〃	〃	7250
S-1200	2	37.8	〃	〃	〃	7400
S-1201	2	37.5	〃	〃	〃	7350
S-1202	1	37.5	〃	〃	〃	7350
S-1227	1	35.9	〃	〃	67.0	7030
S-1228	2	37.6	〃	〃	〃	7380
S-1229	2	38.0	〃	〃	〃	7450

TABLE 9. Fluctuation of Magnification of a JEM-4 Electron Microscope Calculated by using Dow Latex 15 N-8

Exposure numbers	No. of particles	Average diameter of latexes (× 1/15 mm)	Inter. lens current (mA)	Project. lens switch	Object. lens current (mA)	Magnification
S-1233	2	56.0	14	5	67.0	7300
S-1234	1	56.0	〃	〃	〃	7300
S-1235	1	56.5	〃	〃	〃	7380
S-1236	2	57.3	〃	〃	〃	7450
S-1237	2	57.5	〃	〃	〃	7500
S-1241	2	64.0	〃	〃	70.0	8350
S-1242	2	64.0	〃	〃	71.0	8350
S-1243	2	63.5	〃	〃	70.0	8300
S-1254	1	56.5	〃	〃	68.0	7380
S-1256	3	58.5	〃	〃	〃	7620
S-1263	1	63.0	〃	〃	70.0	8220
S-1264	1	63.5	〃	〃	〃	8300
S-1265	2	64.0	〃	〃	〃	8350
S-1267	2	63.0	〃	〃	〃	8220
S-1268	2	62.8	〃	〃	〃	8200
S-1269	1	63.0	〃	〃	〃	8220
S-1271	2	63.0	〃	〃	71.0	8220
S-1273	2	62.5	〃	〃	〃	8150
S-1274	2	64.0	〃	〃	〃	8350
S-1281	2	60.5	〃	〃	68.0	7900
S-1282	2	61.25	〃	〃	〃	8000
S-1283	2	60.5	〃	〃	〃	7900
S-1284	2	60.5	〃	〃	〃	7900
S-1285	2	61.0	〃	〃	〃	7960
S-1286	2	60.5	〃	〃	〃	7900
S-1287	2	60.5	〃	〃	〃	7900
S-1288	2	60.25	〃	〃	〃	7880
S-1289	2	62.25	〃	〃	〃	8130
S-1292	1	61.5	〃	〃	〃	8020

with Dow latexes under the same conditions fluctuated from about × 7,000 to × 8,500 in JEM-4 and from about × 10,200 to × 12,000 in HU-7.

The position of the specimen grid in the electron microscope is very

critical with regard to magnification. Fluctuation of objective lens current values ranged from 66.5 mA to 71.0 mA in JEM-4 and from 41 mA to 47 mA in HU-7. These objective lens current values are dependent on the variation of accelerating voltages and on the differences in length of each specimen holder. Therefore, it is better to use only one holder in one experiment either for measuring the magnification or for the study of virus particles.

TABLE 10. Increase of the Diameter of Pd-shadowed Dow Latex 15 N-8 (511 mμ)

Exposure numbers	Unshadowed		Shadowed		
	Diameter of latexes (× 1/15 mm)	No. of particles	Diameter of latexes (× 1/15 mm)	No. of particles	Diameter of 15 N-8 calculated
S-1305	64.85	4	65.5	2	516
S-1306	62.5	1	65.0	1	531
S-1308	64.5	1	65.0	1	515
S-1309	63.0	1	64.0	1	520
S-1310	64.2	1	66.0	1	525
Average					521.4
% of Increase					2.03%

TABLE 11. Increase in the Diameter of Pd-shadowed Dow Latex 15 N-7 (340 mμ)

Exposure numbers	Unshadowed		Shadowed		
	Diameter of latexes (× 1/15 mm)	No. of particles	Diameter of latexes (× 1/15 mm)	No. of particles	Diameter of 15 N-7 calculated
S-1317	37.0	2	37.46	5	344
S-1318	38.25	4	38.81	8	345
S-1325	41.0	2	42.25	2	350.5
S-1328	40.5	3	41.85	7	351.5
S-1329	41.0	3	41.5	2	344
S-1330	40.75	2	41.83	3	349
	41.5	2	43.5	2	356
S-1331	39.5	2	41.4	3	356
S-1332	40.0	3	41.83	3	356
S-1336	40.93	3	41.75	2	355
S-1337	42.0	2	42.62	4	345
S-1338	41.0	2	42.0	2	348
S-1339	42.5	1	43.25	2	346
Average					349.1
% of Increase					2.68%

3. Discrepancy of diameter between shadowed and unshadowed latex particles

KERN ahd KERN (1950) reported that the average diameters of the shadowed latex particles were positively larger than those of unshadowed latex particles. In order to investigate these particle diameters, latex particles (15 N–7, 15 N–8) were dried on a collodion membrane supported by a brass grid, and then shadowed. Afterward a drop of latex particles was dried again on these shadowed membranes. Photographic exposures were made in the area showing both shadowed and unshadowed latexes. Measurements were made of the diameters of latexes at right angles to the shadowing direction.

The experimental results shown in Table 10 and 11 are as follows: Diameters of palladium shadowed latex particles of 15 N–8 were found to be larger than unshadowed ones by about 2%, while 15 N–7 latexes increased in diameter by about 2.7%.

C. Discussion and conclusions

In order to calculate the magnifícation of photographs of virus specimens, most applied electron microscopists previously employed the "magnification graph", which had been made by using grating replicas. However, it is very difficult to find the fluctuation of magnification in each electron micrograph from the "magnification graph". If the Dow latexes were not photographed together with virus particles, the distortion of the electron microscope could not be recognized and, consequently, the length of virus particles on those photographic plates could be calculated with a wide range of distortion.

As a result of measurements by grating replicas or by Dow latex particles, it has been found that the possible error in measurements of magnification of the electron microscope was about 10 to 20%. Therefore, it is desirable to measure the magnification of electron micrographs separately.

There are two methods for measuring the magnification of electron micrographs. One is the method that uses the grating replica films for support. But this is not convenient for the determination of magnifications higher than 20,000, and it is very hard to shadow sufficiently the virus specimen, because surfaces of the replicas are not smooth. The other method is the use of latex particles. It has been reported that wide ranges of magnification can be measured by the method using latex particles of various diameters as an indicator of determination of magnification of the electron microscope (BRADFORD and VANDERHOFF, 1955).

Latex particle solutions mixed with virus, or sprayed on the supporting films after virus specimens had been dried, are of great advantage in deter-

mination of size of virus particles in each electron micrograph.

To determine the magnification of the electron microscope by means of latex particles, it is necessary to consider some of the factors which may cause errors in the calculation of magnifications (BRADFORD and VANDERHOFF, 1955; GEROULD, 1950-b; KERN and KERN, 1950). These are: a) changes in the size of latex particles during preservation; b) contamination by the electron beam; c) discrepancy between diameters of shadowed and unshadowed particles.

TABLE 12. Increase of an Average Diameter of Latex 580 G Preserved for 3 Years

Diameters of latex particles	No. of particles
272	21
274	10
275	9
276	11
277	26
278	10
280	23
281	12
282	40
283	11
285	24
286	20
287	18
288	12
289	10
291	12
293	8
Total number of latex	271
Average diameter	282 mμ
Standard deviation	5 mμ

As shown in Table 12 and 13, it was observed that average particle diameters of Dow latex 580 G spheres increased by 8 to 8.4% when dispersed in distilled water and preserved at 3° to 5°C for 3 years, but there was practically no change in the standard deviations of measurements. This obviates the necessity to reexamine the diameter of latex particles just before use.

BRADFORD and VANDERHOFF (1955) reported that the particle diameter

TABLE 13. Homogeneity in Diameter of Latex 580 G Preserved for 3 Years

Electron microscope	Exposure numbers	Inter. lens current (mA)	Project. lens current (mA)	Object. lens current (mA)	Diameter of latexes (× 1/15 mm)	No. of particles	Average diameter of latexes	Standard deviation
HU-7	1		50.0	42.0	44.0*	2		
					44.5	7	44.73	0.34
					45.0	11		
	2		50.0	42.0	45.5	1		
					46.0	5	46.06	0.32
					46.5	2		
	3		50.0	45.0	50.0	7	50.13	0.35
					51.0	1		
	4		50.0	42.5	44.0	2		
					44.5	2		
					45.0	7	45.20	0.64
					45.5	4		
					46.0	5		
	5		50.0	41.5	45.5	1		
					46.0	4	46.07	0.34
					46.5	2		
	6		50.0	42.0	45.0	6	45.0	0
	7		50.0	41.95	45.5	3		
					46.0	5	45.89	0.38
					46.5	1		
	8		50.0	41.8	46.5	12	46.65	0.61
					47.0	5		
JEM-4B	1	14.0	5**	67.0	29.5*	2		
					30.0	3	30.0	0.38
					30.5	2		
	2	"	"	69.5	32.0	2		
					32.5	4	32.65	0.48
					33.0	3		
					33.5	1		
	3	"	"	69.5	34.0	4	34.21	0.27
					34.5	3		
	4	"	"	69.0	33.5	4	33.82	0.25
					34.0	7		
	5	"	"	66.5	29.0	1		
					29.5	7	29.67	0.83
					30.0	3		
					30.5	1		
	6	"	"	68.0	32.5	6		
					33.0	3	32.75	0.35
					33.5	1		

Electron micro-scope	Exposure number	Inter. lens current (mA)	Project. lens current (mA)	Object. lens current (mA)	Diameter of latexes (× 1/15 mm)	No. of Particles	Average diameter of latexes	Standard deviation
	7	〃	〃	69.0	37.0 37.5 38.0	2 5 7	37.67	0.37
	8	〃	〃	69.0	37.0 37.5 38.0 38.5	3 3 10 1	37.76	0.43
T-1	1			5	22.5 ×22.5	5	22.5	
	2			2	22.0 ×22.0	5	22.0	
	3			3	80.0** ×80.0	3	80.0	
	4			2	22.0 ×22.0	2	22.0	
	5			4	23.5×23.5 24.0×23.5 24.0×24.0	2 1 1	23.75 ×23.63	
	6			2	23.0 ×23.0	2	23.0	

increased 4 to 13% when copper grid supports were used. It was within the limit of error of the measurements when stainless steel grid supports were used.

Dow latex particles of 15 N-7 and 580 G on the collodion films supported by a brass grid increased their diameter by about 5.3% and 5.7%, respectively, after about 20 minutes, when 6 successive photographic exposures of the same area were made under conditions of continuous irradiation by the intense electron beam.

In order to reduce the influence of contamination, observation of specimens should be made as rapidly as possible under high vacuum conditions in low electron beam intensity. Photographing less than three areas in different grid openings of the same specimen grid should be made to minimize the effect of bombardment by electron beams.

The reasons for the discrepancy in diameters of shadowed and unshadowed particles have not been reported. The discrepancy depends upon conditions of the electron microscope used, kinds of shadowed metals, and thickness of shadowing on the latexes. It is desirable to employ the unshadowed latex particles for electron microscopic calibration. However, for shadowed virus

particles it is necessary to calculate their size and to compare it with the diameter of shadowed latex particles.

It is concluded that the fluctuation in magnification of the electron micrographs for separate specimens can be minimized by using Dow latex particles if adequate attention is paid to the possible causes of error in measurements.

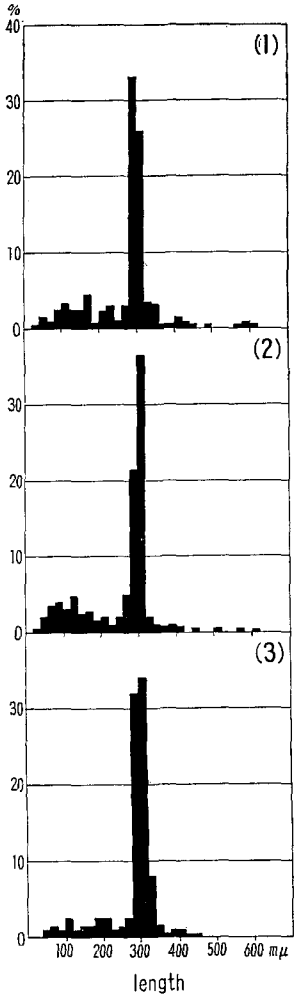

(1),(2),(3) are the same as mentioned in Table 14

Diagram 9. Length Distribution of Tobacco Mosaic Virus Particles as Compared with Dow Latex Particles

IV. Tobacco mosaic virus

A. Shape and size of tobacco mosaic virus

The virus was purified by means of repeated salting out with ammonium sulfate and precipitation with acid at the isoelectric point. The resulting material was dissolved in a phosphate buffer solution at pH 7.0 and then diluted 1 : 100 to 2,000 with distilled water for electron microscopic preparations. The virus in unpurified crude sap was also photographed, using an electron microscope. 10 to 20 gm of young leaves of diseased or *N. sylvestris* plants were ground in a mortar and the expressed sap was centrifuged at 3,500 rpm for 30 minutes and then the supernatant fluid frozen at −20°C overnight. After thawing, the sap was centrifuged at 16,000 rpm for 30 minutes. The supernatant fluid was diluted 1 : 5,000 with distilled water and than dried on the supporting membranes.

Since KAUSCHE *et al.* (1939) published the first electron micrographs of tobacco mosaic virus particles, and showed that they were rod-shaped, 150 to 300 mμ long and 15 mμ wide, a great number of papers have appeared concerning the morphological aspects of this virus. As shown in Figs. 5 and 6, rod-shaped virus particles have been demonstrated both in chemically purified solutions and in crude sap. Table 14, 15 and Diagram 9 show the results

TABLE 14. Length Distribution of Tobacco Mosaic Virus Particles as Compared with Dow Latex Particles

Length of Virus Particles	Number of Particles Measured			Total Number	Length of Virus Particles	Number of Particles Measured			Total Number
	(1)	(2)	(3)			(1)	(2)	(3)	
mμ					mμ				
10	0	0	0	0	340	3	1	3	7
20	0	0	0	0	350	3	1	0	4
30	1	1	0	2	360	6	3	3	12
40	0	1	0	1	370	1	1	1	3
50	3	5	0	8	380	0	2	0	2
60	1	3	2	6	390	0	3	1	4
70	2	5	1	8	400	1	2	1	4
80	1	10	2	13	410	4	3	2	9
90	3	9	1	13	420	0	0	0	0
100	4	8	0	12	430	1	0	1	2
110	4	3	3	10	440	2	0	0	2
120	4	10	4	18	450	0	0	1	1
130	4	10	0	14	460	1	2	0	3
140	3	9	2	14	470	0	0	0	0
150	4	4	4	12	480	0	0	0	0
160	3	6	1	10	490	0	0	0	0
170	6	5	1	12	500	1	0	0	1
180	6	6	2	14	510	0	0	0	0
190	2	2	2	6	520	0	1	1	2
200	0	4	3	7	530	0	0	0	0
210	3	5	2	10	540	0	0	0	0
220	3	4	3	10	550	0	0	0	0
230	3	1	1	5	560	1	0	0	1
240	5	3	1	9	570	0	1	0	1
250	0	5	2	7	580	0	0	0	0
260	3	3	1	7	590	1	0	0	1
270	1	7	1	9	600	1	0	0	1
280	8	13	4	25	610	0	1	0	1
290	47	13	13	73	620	2	0	0	2
300	45	74	53	172	630	0	0	0	0
310	44	99	48	191	640	0	0	0	0
320	28	50	24	102					
330	7	8	14	29	Total	276	407	209	892

(1) Purified virus (Latex 580 G)
(2) Crude sap virus (Latex 15 N-7)
(3) Crude sap virus (Latex 15 N-8)

TABLE 15. Length of Tobacco Mosaic Virus Particles

Virus Preparations	(1)	(2)	(3)	Average
No. of Particles Measured	180	264	157	601
Average Length (mμ)	298	301	302	300.5
Standard Deviations	13	8	13	12.5
Standard Error	0.79	0.49	1.04	0.50

(1) (2) (3) are the same as mentioned in Table 14

of measurements of the length of virus particles as determined by latex 580 G, 15 N-7, and 15 N-8. According to these measurements, tobacco mosaic virus has an average length of 300 mμ. There are little differences between length distributions of purified and crude sap virus, as measured by three kinds of latexes. The diameter of shadowed virus particles, which were parallel to the shadowing direction, was about 15 to 20 mμ.

B. Tobacco mosaic virus stained by phosphotungstic acid.

An equal volume of 20% phosphotungstic acid (PTA) was added to a purified virus solution and then preserved for 2 to 12 hours at 0° to 5°C. The supernatant solution was diluted 1 : 10 to 100 with distilled water and then dried on collodion membranes.

As shown in Figs. 6 to 9, PTA-stained tobacco mosaic virus particles more clearly showed their structure than unstained or KCl-stained particles. A fine thread-like structure running along the long axis appeared in the center of these particles. This thread-like line was more clearly defined near the end of a particle than in the center.

C. Effect of heat on tobacco mosaic virus

Series 1. The virus suspension, purified by chemical methods, was diluted 1 : 10 or 1 : 100 with distilled water and dialyzed overnight through cellophane against running tap water, to remove salts. The suspensions were poured into test tubes and heated at 70°, 80°, and 90°C for 10 minutes, respectively. When observed by an electron microscope, the virus particles were aggregated into dense masses, so that the shape of individual virus particles could not be recognized. Therefore, further purification of the virus was carried out by tryptic digestion and electrophoretic fractionation (TODD 1927). However, similar results were obtained irrespective of further purification. The results showed that virus particles in dialyzed solution were coagulated into amorphous

large masses and deposited, when heated in a test tube. Accordingly, further experiments were carried out by heating the diluted, dialyzed virus suspensions on the collodion membranes which were placed in saturated steam at desired temperatures.

A drop of a dialyzed virus suspension was placed on the collodion film and heated at 60°, 70°, 80°, 90°, and 95°C for ten minutes; at 70°C for 5, 10, 20, 30, and 40 minutes; at 80°C for 5, 10, 20 and 30 minutes, respectively.

About 3.5 ml of the same preparation was heated in a small glass tube under the same conditions as mentioned above. After cooling, the treated virus suspensions were inoculated into the leaves of *N. glutionsa* plants.

The virus particles in the dialyzed solution had a tendency toward end-to-end aggregation. When such preparations were heated at 60°C for ten minutes, and 70°C for 5 to 40 minutes, the virus particles showed a tendency to aggregate into networks, while those heated at 80°C for 5 to 30 minutes represented a lot

TABLE 16. Infectivity and Particle Length of Heated and Dialyzed Tobacco Mosaic Virus Suspensions

Treatment	Length of Particles					No. of Particles	Infectivity*
	Globular Particles	Shorter than 233 mμ	233–367 mμ	367–500 mμ	Longer than 500 mμ		
Untreated		16.6%	48.0%	20.2%	15.3%	535	185
60°C–10 min		10.7	39.1	13.8	36.3	289	219
70°C "		29.9	50.8	11.8	7.5	254	133
80°C "		67.6	22.4	7.9	2.1	290	54
90°C "	100%						0
95°C "	100						0
Untreated		16.6	48.0	20.2	15.3	535	249
70°C–5 min		22.4	41.5	22.8	13.4	299	228
" 10 "		16.1	62.1	10.2	12.4	354	209
" 20 "		44.6	49.4	6.1		316	216
" 30 "		72.8	25.8	1.4		286	168
" 40 "		72.4	26.4	1.2		322	174
Untreated		16.6	48.0	20.2	15.3	535	210
80°C–5 min		38.0	53.2	5.4	3.5	316	189
" 10 "		55.9	39.3	4.5		265	69
" 20 "	(24.0%)	80.9	15.5	3.6		219	6
" 30 "	100%						0

* Total lesions inoculated with treated virus suspensions on 30 leaves of *N. glutinosa*

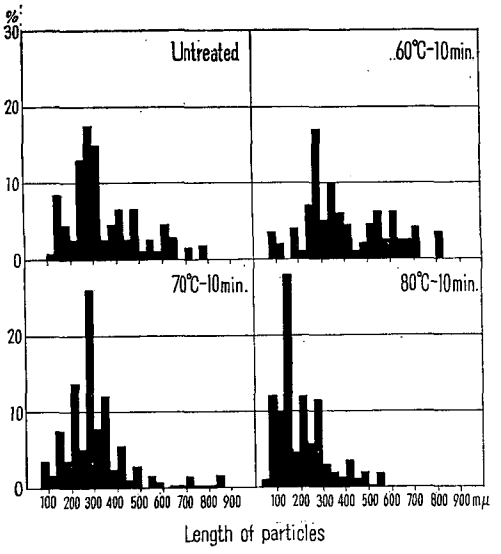

Diagram 10. Length Distribution of Virus Particles in the Dialyzed Suspension of Chemically Purified Tobacco Mosaic Virus, Treated by Heat

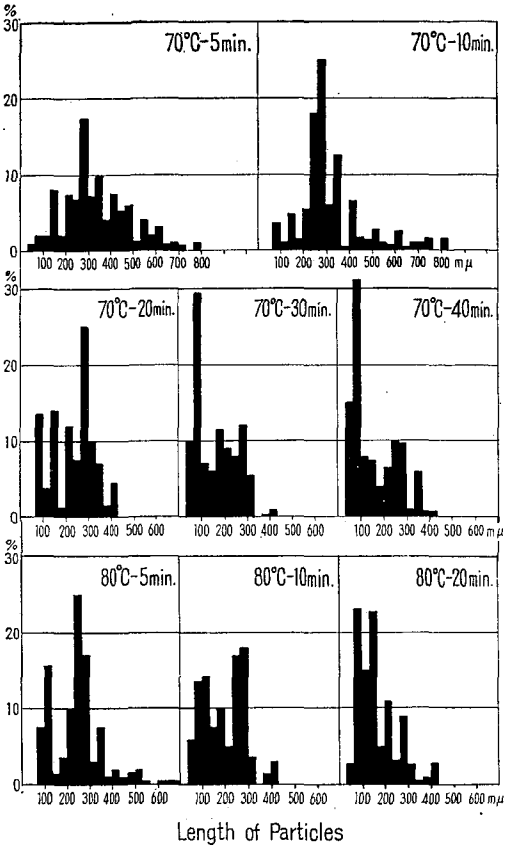

Diagram 11. Length Distribution of Virus Particles in the Dialized Suspension of Chemically Purified Tobacco Mosaic Virus, Treated by Heat

of globular deposits among virus rods. When heated at 90°C and 95°C for ten minutes, amorphous masses appeared and rod-shaped virus particles disappeared (Figs. 10 to 20). Table 16 and Diagrams 10 and 11 show the results of measurements of dispersed virus particles. Particles shorter than 233 mμ increased in number, and those around 300 mμ or longer decreased in the suspensions heated at 70°C for 30 to 40 minutes and at 80°C for 10 to 20 minutes. When heated at 80°C for 30 minutes, and at 90°C for 10 minutes, no rod-like particles remained and only amorphous or globular deposits were observed by the electron microscope.

Infectivity of virus suspension was slightly decreased when heated at

70°C for 30 or 40 minutes. There was little infectivity at 80°C for 10 to 20 minutes, but no infectivity at 90°C for 10 minutes and 80°C for 30 minutes (Table 16).

Series 2. TAKAHASHI and RAWLINS (1948), and later TAKAHASHI (1949-b) reported that tobacco mosaic virus particles scarcely showed end-to-end aggregation in a buffered solution at pH 7.0. In this experiment, consequently, purification and concentration of the virus were carried out with 1/15 M phosphate buffer at pH 7.0 instead of distilled water. Finally, the purified virus suspension was centrifuged at 10,000 rpm for 30 minutes and then the supernatant was diluted with distilled water to 1 : 10; otherwise salts in the suspension crystallized on the collodion membranes after the virus suspension was dried.

Virus particles in these preparations are dispersed uniformly and only few aggregations into long rods appear when heated. Therefore, the virus suspensions, divided into test tubes, were heated in a water bath and then rapidly cooled with tap water. These preparations were used for electron microscope examinations and inoculation experiments on leaves of *N. glutionsa* plants.

The virus in the dialyzed solution remained clear even when heated to 90°C, while the buffered solution with the virus became turbid at 70°C, more cloudy at 75° and 80°C, and filled with small flocculent aggregates at 85°C.

TABLE 17. Infectivity and Particle Length of Tobacco Mosaic Virus, Heated in a Buffered Suspension at pH 7.0

Treatment	Length of Particles					No. of Particles	Infectivity*
	Globular Particles	Shorter than 233 mμ	233–367 mμ	367–500 mμ	Longer than 500 mμ		
Untreated		18.5%	64.1%	8.8%	8.5%	340	247
70°C–10 min		56.7	41.7	1.7		288	161
75°C– "		82.0	18.0			239	38
80°C– "	(95%)						0
85°C– "	(100%)						0
90°C– "							0
Untreated		18.5	64.1	8.8	8.5	340	416
80°C–5min		63.3	33.1	3.6		390	213
" 8 "		98.5	1.5			389	86
" 10 "	(80%)	96.5	3.5			226	0
" 12 "	(95%)						0
" 15 "							0

* The same in Table 15

As shown in Figs. 21 to 27, the length of virus rods become shorter and shorter, as the virus suspension was heated at from 60°C to 80°C. When kept at 80°C for 10 minutes, most of the virus particles changed into numerous globular particles of 20 to 50 mμ in diameter and a few of them remained in the form of short rods. At 85°C there were no rod-shaped particles, and some of the globular particles appeared, aggregating into small flocculents. The infectivity of the virus solution decreased when heated at 75°C for 10 minutes, and was completely lost at 80°C for 10 minutes. The results are shown in Table 17 and Diagram 12.

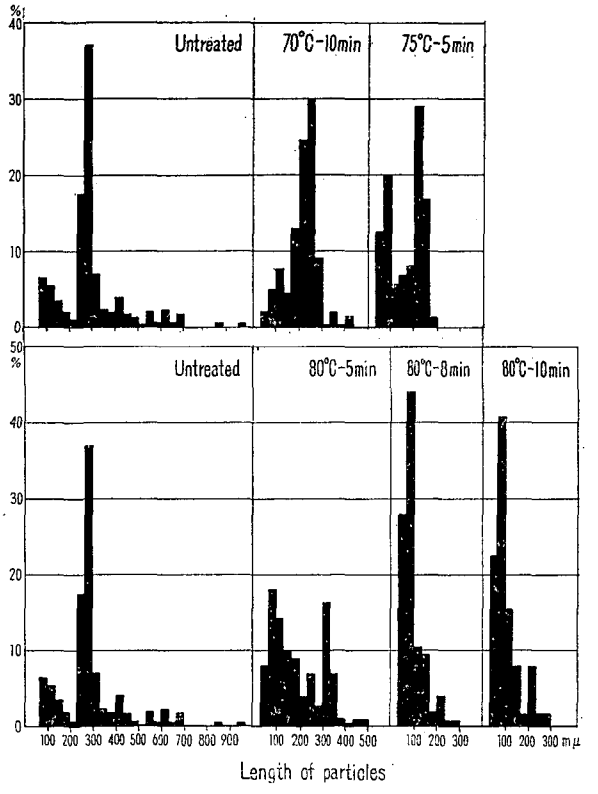

Diagram 12. Length Distribution of Virus Particles in the Buffered Suspension at pH of Chemically Purified and Heat-treated Tobacco Mosiac Virus

More detailed experiments were performed by heating the virus suspensions at 80°C for 5, 8, 10, 12, and 15 minutes to observe morphological changes of the virus particles (Table 17 Diagram 12). As the pariods of heating became

longer, the number of shortened rods gradually increased. As shown in Figs. 24 and 25, particles shorter than 100 mμ were abundant in the suspensions heated at 80°C for 8 or 10 minntes and were replaced by small globular particles of 20 to 50 mμ in diameter at 80°C for 15 minutes. The shortest rods which could be observed by the electron microscope were about 20 mμ in length and particles shorter than 100 mμ were frequently observed.

TABLE 18. Infectivity and Particle Length of Tobacco Mosaic Virus, Heated in Buffered Suspension at pH 5.2

Treatment	Length of Particles					No. of Particles	Infectivity*
	Globular Particles	Shorter than 233 mμ	233–367 mμ	367–500 mμ	Longer than 500 mμ		
Untreated							213
75°C–10min		36.5%	59.5%	4.1%		266	193
80°C– »		66.6	31.8	1.7		484	36
85°C– »	(48.0%)	64.6	23.9	11.5		209	0
90°C– »							0

* The Same as in Table 15

In Cr-shadowed particles smaller than 20 mμ, it was very difficult to determine whether the particles were rod-shaped or spherical.

When heated at 80°C for 20 or 30 minutes, the small globular particles aggregated into masses (Fig. 26).

The virus suspended in the buffered solution at pH 5.2 was used in heating tests at 75°, 80°, 85°, and 90°C for 10 minutes (Table 18, Diagram 13). These experiments also showed that the number of shorter virus particles, dispersed uniformly in the solution at pH 5.2, increased with increased temperature. Treatment at 85°C for ten minutes produced rods shorter than 100 mμ and globular particles, while treatment at 90°C for 10 minutes eliminated all rods in the virus suspension and left only small spherical particles of 20 to 50 mμ in diameter.

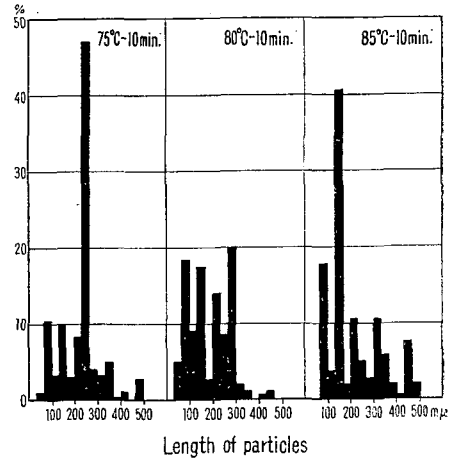

Diagram 13. Length Distribution of Virus Particles in Buffered Suspension at pH 5.2 of Chemically Purified, Heat-treated Tobacco Mosaic Virus

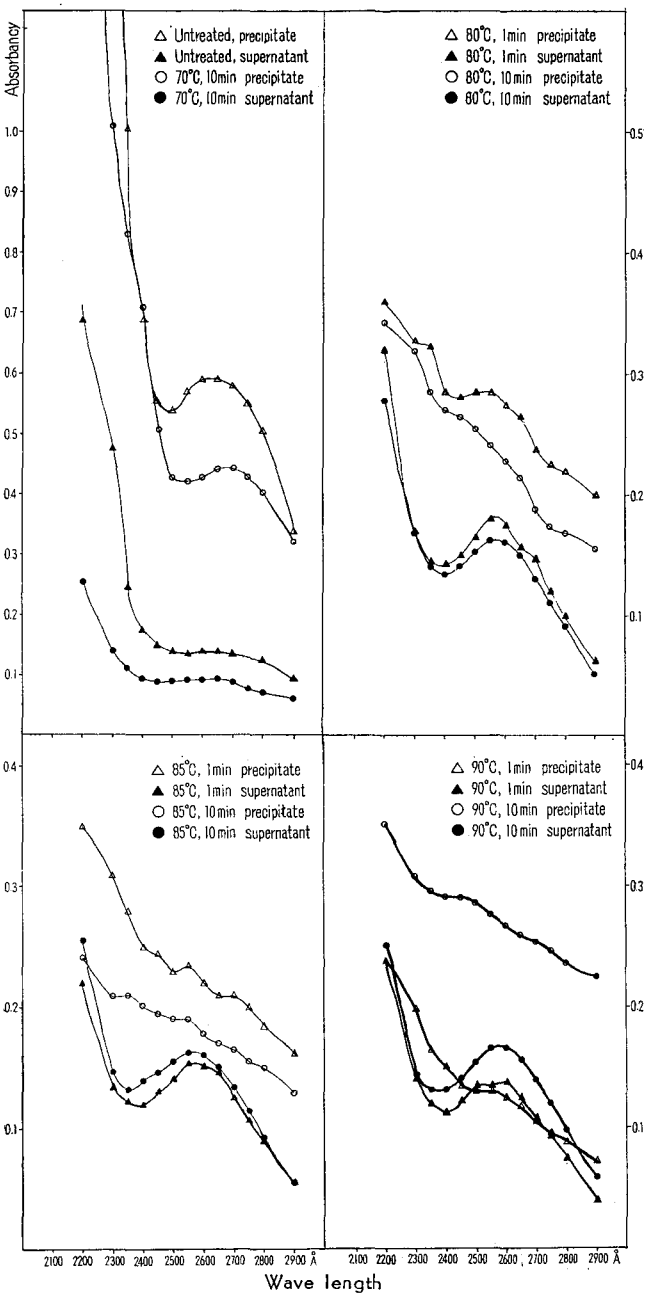

Diagram 14. UV Absorption Spectra of Heat-Treated Suspension of Tobacco Mosaic Virus. Precipitates were Obtained by Centrifugation at 40,000 rpm for 1 Hour, Following the Heat Treatment.

Series 3. 2 ml of virus preparations was suspended in a 1/15 M phosphate buffered solution at pH 7.0 and divided into test tubes and then heated in a water bath at 60°C or 70°C for 10 minutes, at 85°C for 1 or 10 minutes, at 85°C for 1 or 10 minutes, and at 90°C for 1 or 10 minutes. After heating, each preparation was cooled by running tap water, diluted 1 : 8 to 10 with distilled water and centrifuged at 40,000 rpm for 1 hour.

The measurements of ultraviolet absorption spectrum of the supernatants and pellets obtained by centrifugation were carried out with an HITACHI EPU-2 spectrophotometer. The pallets were dissolved in a buffered solution equal in volume to that of the original sap.

Diagram 14 shows that the pellets from the unheated control, from preparations heated at 60°C for 10 minutes and at 70°C for 10 minutes had disclosed similar UV absorption spectra of RNA.

When heated at 80°C for 1 minute, RNA was separated from virus protein and remained in the supernatant fluid after centrifugation. The UV absorption spectrum of the preparation heated at 80°C for 1 minute showed that some virus RNA still remained in the precipitate. Complete separation of RNA from virus protein occurred at 80°C after 10 minutes' heating, at 85°C after 1 and 10 minutes, and at 90°C after 1 and 10 minutes.

As indicated in Table 17, Diagram 22, at 70°C for 10 minutes, treated preparation contained approximately 56.7% shortened virus, while at 80° for 10 minutes most rod particles were changed into shortened rods shorter than 233 mμ. All the evidence obtained showed that separation of RNA from virus protein may occur as rod particles start breaking by heat.

Series 4. The same preparations used in series 3 were examined with precipitin reaction. After heating, virus preparations were centrifuged at 3,500 rpm for 10 minutes and the supernatants were used in the experiment.

Table 19 shows the results when antigen and antiserum mixtures were preserved for 2 hours at 37°C. The reaction was decreased after heating the virus at 80°C for 10 minutes and disappeared at 90°C for 10 minutes.

After the mixture was placed in the refrigerator at 3 to 5°C for 24 hours, numerous flocculents appeared in those preparations. When the heated virus preparations were centrifuged at 40,000 rpm for 1 hour and then mixed with antiserum, no flocculents appeared even after 24 hours' storage (Table 19). Consequently, it is likely that a little amount of shortened virus protein produced by heating could not be precipitated by centrifugation at 3,500 rpm for 30 minutes and coagulated into small precipitates after 24 hours. The results show that even the shortened rods produced by heating have serological reaction, but no serological reactions were shown in globular particles.

TABLE 19. Precipitin Reaction of the Heat-treated Tobacco Mosaic Virus Suspension

Traetment	Centrifugation	Final Concentration of Antiserum					Control
		16	32	64	128	256	
Untreated	Supernatant at 3,000 rpm for 30 min after Heating	+	+	+	+	±	−
70°C-10 min		+	+	+	+	+	−
75°C- »		+	+	±	±	−	−
80°C- »		+ (+)	± (+)	− (+)	− (±)	−	−
85°C-1 min		+ (+)	− (+)	− (+)	− (±)	−	−
» -10 min		+ (+)	− (+)	− (+)	− (±)	−	−
90°C-1 min		+ (+)	− (+)	− (+)	−	−	−
» -10 min		− (+)	− (+)	− (+)	−	−	−
Untreated	Supernatant at 3,500 rpm for 30 min after Heating	±	±	+	±	−	−
70°C-10 min		+	+	+	−	−	−
80°C-1 min		+	+	+	−	−	−
80°C-10 min		−	−	−	−	−	−
85°C-1 min		− (+)	− (±)	−	−	−	−
» -10 min		− (+)	−	−	−	−	−
90°C-1 min		− (+)	− (+)	− (±)	− (±)	−	−
95°C-10 min		−	−	−	−	−	−
Untreated	Supernatant at 40,000 rpm for 60 min after Heating	−	−	−	−	−	−
60°C-10 min		−	−	−	−	−	−
70°C- »		−	−	−	−	−	−
80°C-1 min		−	−	−	−	−	−
80°C-10 min		−	−	−	−	−	−
85°C-1 min		−	−	−	−	−	−
» -10 min		−	−	−	−	−	−
90°C-1 min		−	−	−	−	−	−
» -10 min		−	−	−	−	−	−

(±) Flocculent Appeared after 24 Hours

D. Effect of hydrogen ion concentration on tobacco mosaic virus

The purified preparations of tobacco mosaic virus suspended in a 1/15 M phosphate butter at pH 6.8 were adjusted at pH 0.5 to 12.4 by using 1N HCl and NaOH and kept at 3°to 5°C for 20 hours. Each preparation was tested for infectivity by the half-leaf method on *N. glutinosa* plants, as well as by the precipitin reaction against antiserum, and observed by the electron microscope.

There were small differences in infectivity between preparations treated at pH 4.1 and pH 6.8, as shown in Table 22. Infectivity of the preparation adjusted to pH 3.0 decreased, but at pH 2.15 the infectivity was recovered. At pH 1.1 (dialyzed for 2 hours), infectivity decreased again. There was no apparent infectivity at pH 0.5.

In alkaline solutions from pH 8.2 to pH 11.1, infectivity of the treated solution gradually decreased. At pH 11.1, 99% of the virus was inactivated.

Generally, the virus preparations in acid solution were slightly opalescent, while in the alkaline solution they became clear and transparent. Satin-like sheen appeared in the solution at pH 3.3 to 3.4, that is, at the isoelectric point of this virus.

The virus preparation, treated at pH 0.5 and 1N HCl, became turbid and a profuse white precipitation appeared after 20 hours of incubation. When prepared at pH 12.4 and 1N NaOH, the virus suspensions were clear. After dialyzing them against tap water for 2 hours, the virus suspensions became turbid.

Electron microscopic observations were made and the results are shown in Figs. 28 to 46.

In alkaline solutions the tobacco mosaic virus showed no end-to-end aggre-

TABLE 20. Particle Length of Tobacco Mosaic Virus Treated with Various Hydrogen Ion Concentration

pH of Virus Suspension	Length of Virus Particles					Number of Virus Particels Measured
	Less than 120 mμ	120–240 mμ	240–360 mμ	360–480 mμ	More than 480 mμ	
1.1	35.3%	18.2%	44.6%	1.9%		374
2.1	30.1	29.5	37.1	2.7	0.6%	630
3.0*	23.1	25.6	46.7	4.5		246
5.0	18.2	16.8	39.8	7.2	17.9	475
6.8	19.4	13.5	52.6	8.7	5.9	950
8.2	23.5	13.2	56.8	4.3	1.9	370
9.0	35.7	24.9	36.2	1.5	1.7	723
10.0	39.1	36.4	22.4	0.9	1.1	442

* Dialized Against Tap Water for 2 Hours

gation. As pH values became higher, more shorter particles, below 240 mμ in length, appeared.

In the preparation treated at pH 11.1, most of the particles had the shape

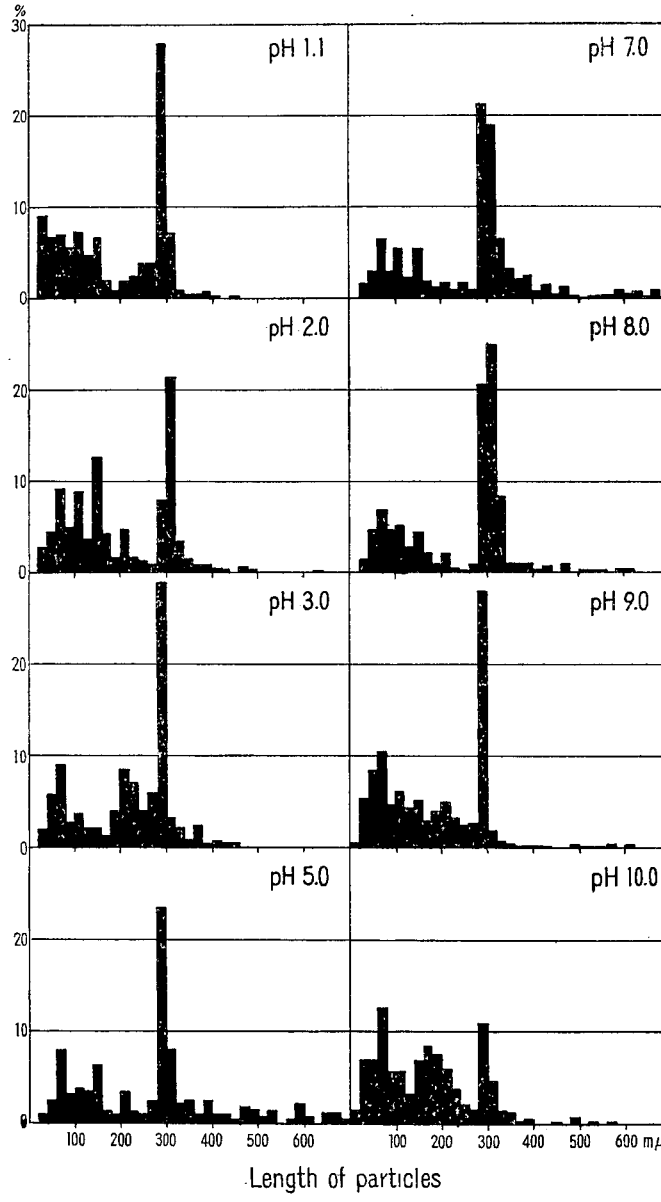

Diagram 15. Length Distribution of Virus Particles in the Suspension of Various Hydrogen Ion Concentration

of small globules of 20 to 40 mμ in diameter. Table 20 and Diagram 15 show how the long virus rods changed gradually into small rods in different buffered suspensions.

Tobacco mosaic virus particles showed a tendency toward end-to-end and side-by-side aggregations in acid solutions. At pH 5.0, the virus slightly aggregated and at pH 4.0 most of the particles showed end-to-end and side-by-side aggregation into networks (Fig. 33). At pH 3.3, which is the isoelectric point of the virus, the rod-shaped particles formed paracrystalline aggregations (Fig. 35, 36). These aggregates included either monomers of 300 mμ long or shorter ones. Therefore, it was difficult to obtain homogenous virus preparations by chemical purification through isoelectric point precipitation. In virus solution at pH 2 and pH 1.1, it was found that virus rods scattered again and those shorter than 240 mμ in length increased in number, while those equal to or longer than 300 mμ in length became sparse. At pH 0.5, virus particles were denatured and changed into an amorphous globular mass, without infectivity and no longer detectable by the precipitin reaction.

Consequently, destruction of rod particles occurred suddenly between pH 1.1 and 0.5 in acid solution, while in alkaline solution the particles gradually became shortened as pH values became higher, and they denatured completely

TABLE 21. Precipitin Reaction of the Virus Suspension Treated with Various Hydrogen Ion Concentration
(After Treating, All Materials were Diluted 1 : 5 with Dist. Water without Dializing)

pH of Virus Suspension	pH of Virus Suspension after 20 Hours	Final Concentration of Antiserum					Control
		16	32	64	128	256	
1N HCl		−	−	−	−	−	−
1.1	1.05	+	±	±	−	−	−
2.1	2.05	+	+	+	+	+	−
3.0	3.0	±	−	−	−	−	−
3.3	3.3	−	−	−	−	−	−
4.0	3.98	+	+	+	+	+	−
5.0	5.5	+	+	+	+	+	−
6.7	6.7	+	+	+	+	+	−
8.2	8.1	+	+	+	+	+	−
9.0	8.85	+	+	+	+	+	−
10.0	9.7	+	+	+	±	−	−
11.05	10.2	+	+	−	−	−	−
11.9	11.4	−	−	−	−	−	−

between pH 11.1 and 11.9.

Table 21 and 22 show the results of serological tests. A precipitin reaction appeared in the preparation treated at between pH 1.1 and 11.1.

Whenever shortened or broken rod-shaped particles were observed by the electron microscope in virus preparations at various pH values, precipitin reaction against antiserum was also demonstrated in the same preparation.

TABLE 22. Infectivity and Precipitin Reaction of the Virus Suspension Treated with Various Hydrogen Ion Concentration
(Precipitin Reaction were Tested after Adjusting the Virus Suspension at pH 7.0)

pH of Virus Suspension	pH of Virus Suspension after 20 Hours	Infectivity (1)	Final Concentration of Antiserum					Control
			32	64	128	256	512	
1N HCl (2)		0	−	−	−	−	−	−
1.5	0.5 (2)	0	−	−	−	−	−	−
1.1	1.1	134	++	+	+	+	+	−
2,15	2.25	494	++	+	+	+	+	−
3.0	3.08	141	++	+	+	+	+	−
4.1	4.08	639	++	+	+	+	+	−
6.8	6.8	618	++	+	+	+	+	−
8.2	8.15	428	++	+	+	+	+	−
9.0	8.95	373	++	+	+	+	+	−
10.1	9.9	39	+	+	+	+	+	−
11.1	10.5	0	+	+	±	−	−	−
12.4	12.3 (2)	0	−	−	−	−	−	−
1N NaOH		0	−	−	−	−	−	−

(1) Total Lesions Inoculated with the Treated Virus Suspension on 20 Leaves of *N. glutinosa*

(2) Dialized in a Cellophane Sac against Tap Water for 2 Hours

E. Effect of hydrogen peroxide on tobacco mosaic virus

Series 1. To the purified virus suspensions was added H_2O_2 solution to make a final concentration of 3, 5, 10, 20, 25, or 30% at pH 6.4 to 6.8. The concentration of the virus in those suspensions was about 0.015%. After treating for 15 hours in a cold room at 4°C, the virus suspensions, without dialyzing against tap water, were rapidly dried on the collodion film in vacuum and then observed with an electron microscope. They were also tested for infectivity on leaves of *N. glutionsa* plants and a precipitin reaction against antiserum was carried out.

The H_2O_2-treated virus solutions were all clear and transparent, including even those treated with 30% for 15 hours.

The length of the particles in the solution treated with 10 to 30% H_2O_2 for 15 hours was influenced by the treatment. The number of rod particles that were shorter than 240 mμ increased when the concentration of H_2O_2 increased. As shown in Table 23 and Diagram 16, about 72.5% of the particles

TABLE 23. Particle Length of Tobacco Mosaic Virus Treated with H_2O_2 without Dializing

H_2O_2	pH	Length of Virus Particles					No. of Particles Measured
		Shorter than 120 mμ	120–240 mμ	240–360 mμ	360–480 mμ	Longer than 480 mμ	
Untreated	6.8	7.2%	10.0%	66.4%	10.7%	5.7%	290
10%	"	2.1	19.6	70.1	4.1	4.1	297
20%	"	2.5	22.5	65.0	5.0	5.0	240
25%	"	7.3	33.1	54.3	4.0	1.3	351
30%	"	9.2	65.3	18.0	5.9	1.7	478

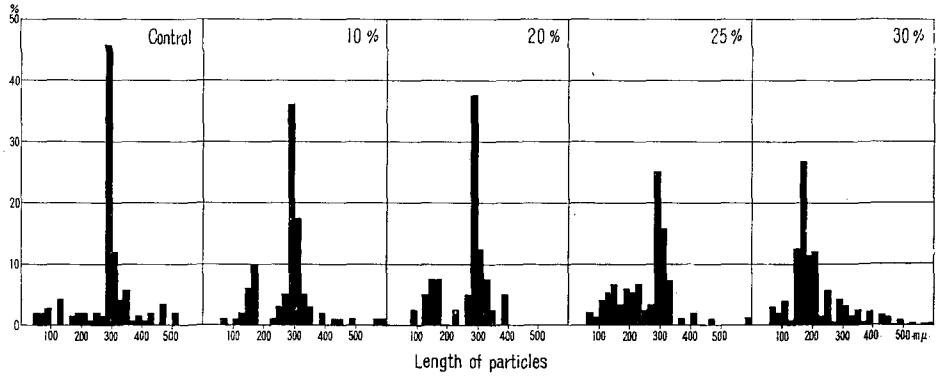

Diagram 16. Length Distribution of Tobacco Mosaic Virus Particles Treated by H_2O_2 at pH 6.8 without Dializing

were shorter than 240 mμ in the preparation treated with 30% H_2O_2 for 15 hours, while only 18.0% were of normal length.

The precipitin reaction of H_2O_2-treated virus suspensions against antiserum was not completely destroyed even in 30% H_2O_2 (Table 24). However, a small amount of flocculents similar to those that appeared in the precipitin reaction was observed in the solution of H_2O_2-antibody mixtures. Consequently, the following experiments were carried out by dialyzing against tap water to remove

TABLE 24. Precipitin Reaction of the Virus Suspension Treated with H_2O_2

Virus	H_2O_2	pH	Dializing	Final Concentration of Antiserum					Control
				16	32	64	138	256	
Virus + H_2O_2	0%	6.8	None	++	+	+	+	+	−
	3			++	+	+	+	+	−
	5			++	+	+	+	±	−
	10			++	+	+	+	±	−
	20			+	+	+	+	−	−
	30			+	±	±	−	−	−
Buffer + H_2O_2	0%	7.0	None	−	−	−	−	−	−
	3			++	+	±	−	−	−
	5			++	±	±	−	−	−
	10			++	+	−	−	−	−
	20			+	±	−	−	−	−
	30			±	±	−	−	−	−

TABLE 25. Particle Length of Tobacco Mosaic Virus Treated by H_2O_2

H_2O_2	pH after Adjusting ~ after 15 Hours	Dia-lizing	Length of Particles					No. of Particles Measured	Infectivity *	
			Shorter than 120 mμ	120–240 mμ	240–360 mμ	360–480 mμ	Longer than 480 mμ			
	6.8~6.8	5 Days	4.8%	7.0%	62.2%	18.7%	7.4%	230	220	150
3%	6.8~6.7		13.4	22.0	63.0	1.8	0	216	4	0
5	6.4~6.4								0	0
10	6.8~6.7		18.6	25.1	53.4	1.6	1.2	247	0	0
20	6.6~6.6		13.6	22.9	57.4	3.8	2.2	366	0	0
30	6.8~6.75		5.0	34.1	50.4	6.6	3.9	595		

* Total Lesions Inoculated on 10 Leaves of *N. glutinosa*

H_2O_2 comlpetely just after treating with H_2O_2.

The purified virus suspensions treated with desired H_2O_2 concentrations were taken into cellophane sacs and then dialyzed against running tap water for 5 days. As shown in electron micrographs (Figs. 47 to 49, Diagram 17, Table 25), the virus particles were not much destroyed even by exposure to 30% H_2O_2 at pH 6.8. The virus preparations treated with 30% H_2O_2 retained

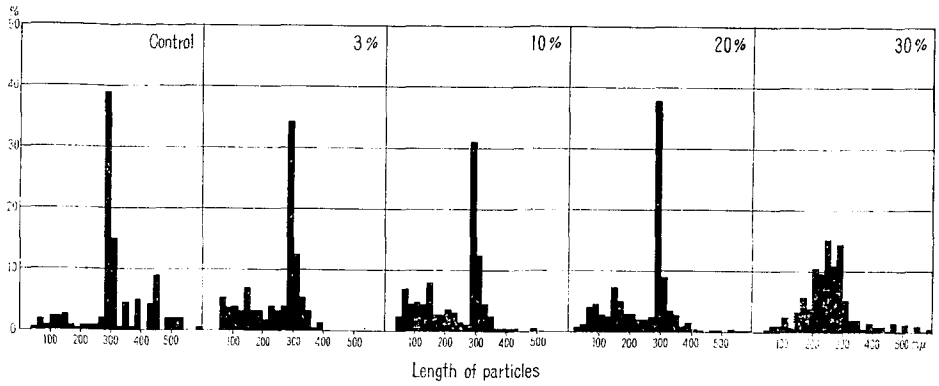

Diagram 17. Length Distribution of Tobocco Mosaic Virus Particles Treated by H_2O_2 at pH 6.8 after Dializing

TABLE 26. Precipitin Reaction of Tobacco Mosaic Virus Suspension Treated by H_2O_2

Virus	H_2O_2	pH after Adjusting ~after 15 Hours	Dializing	Final Concentration of Antiserum					Control
				16	32	64	128	256	
Virus + H_2O_2	0%	6.8~6.8	5 Days	++	++	+	+	+	−
	3	6.8~6.7		++	++	+	+	+	−
	5	6.4~6.4		++	++	+	+	+	−
	10	6.8~6.7		++	++	+	+	+	−
	20	6.6~6.6		++	++	+	+	+	−
	30	6.8~6.75		++	++	+	+	+	−
Buffer + H_2O_2	0%	6.8~6.8	None	−	−	−	−	−	−
	3	6.6~6.6		±	−	−	−	−	−
	5	6.8~6.8		+	±	−	−	−	−
	10	6.7~6.65		±	±	−	−	−	−
	20	6.8~6.7		+	±	−	−	−	−
	30	6.7~6.65		+	±	−	−	−	−
Buffer + H_2O_2	0%	6.8~6.75	5 Days	−	−	−	−	−	−
	3	6.8~6.8		−	−	−	−	−	−
	5	6.8~6.7		−	−	−	−	−	−
	10	6.7~6.8		−	−	−	−	−	−
	20	6.7~6.65		−	−	−	−	−	−
	30	6.6~6.6		−	−	−	−	−	−

their antigenicity, while infectivity tn the solution treated with 3% H_2O_2 at pH 6.8 was completely destroyed. There were no flocculents in the preparations of H_2O_2-antibody mixtures after the H_2O_2 solutions were dialyzed against tap water for 5 days (Table 26).

Series 2. H_2O_2 solutions were added to the purified virus suspensions to make the final H_2O_2 concentrations of 1, 3, 5, 10, 20, and 30% at pH 3.0 to 3.7. After preservation in a cold room for 15 hours, each preparation was dialyzed for 5 days against tap water. When the virus suspensions were treated with H_2O_2, they were clear and transparent, but after dialyzing, each solution became turbid. The results are shown in Figs. 50 and 51, Diagram. 18, and Tables 27 and 28.

TABLE 27. Particle Length of Tobacco Mosaic Virus Treated by H_2O_2 at pH 3.3

H_2O_2	pH after Adjusting ~ after 15 Hours	Dializing	Length of Particles					No. of Particles Measured
			Shorter than 120 mμ	120–240 mμ	240–360 mμ	360–480 mμ	Longer than 480 mμ	
Control	3.2~3.2	5 Days	20.5%	18.5%	56.4%	4.8%	0%	248
20%	3.3~3.7		26.0	18.9	50.9	2.5	1.7	238
30%	3.1~3.6		25.2	41.2	28.6	4.4	0.6	318

TABLE 28. Precipitin Reaction of the Virus Suspension Treated by H_2O_2 at pH 3.3

H_2O_2	pH after Adjusting ~ after 15 Hours	Dializing	Final Concentration of Antiserum					Control
			16	32	64	128	256	
Control	3.2~3.2	5 Days	++	+	+	+	+	−
1%	3.0~3.4		++	+	+	+	+	−
3	3.1~3.2		++	+	+	+	+	−
5	3.2~3.3		++	+	+	+	+	−
10	3.0~3.4		++	+	+	+	+	−
20	3.3~3.7		++	+	+	+	+	−
30	3.1~3.6		++	+	+	+	+	−

Electron micrographs of the preparation treated at pH 3.0 without treating with H_2O_2 showed that the virus particles shorter than 240 mμ increased, as compared with untreated control of pH 6.8. This indicates that the virus particles were destroyed even by the treatment of isoelectric precipitation.

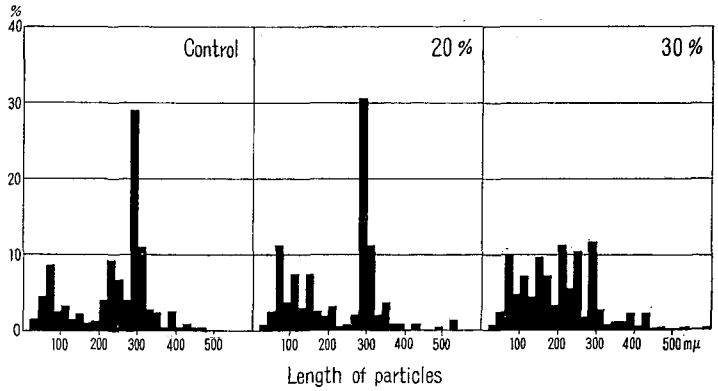

Diagram 18. Length Distribution of Tobacco Mosaic Virus Treated by H_2O_2 at pH 3.3 after Dializing for 5 Days

When treated with 20% H_2O_2, there appeared only few morphological changes, but when treated with 30% H_2O_2 about 66.4% of the virus was found in the form of rods shorter than 240 mμ. The virus preparations treated with various H_2O_2 concentrations at pH 3.0 to 3.7 retained their antigenicity.

Series 3. As shown in Table 25, tobacco mosaic virus was inactivated by treatment with 3% H_2O_2 for 15 hours at pH 6.8, but morphological changes were not very apparent.

In acid solution, H_2O_2 is rather stable, while in an alkaline solution it easily separates into water and active oxygen. Therefore, the following experiments were carried out.

The virus solutions containing 1, 3, and 5% H_2O_2 were adjusted at pH 8.9 to 9.0 with 1N NaOH, and then preserved in the refrigerator for 15 hours. The results are shown in Figs. 52 to 54, Tables 29 to 31, and Diagram. 19.

TABLE 29. Infectivity and Particle Length of Tobacco Mosaic Virus Treated by H_2O_2 at pH 8.9–9.0

H_2O_2	pH after Adjusting ~after 15 Hours	Dia-lizing	Length of Particles						No. of Particles Measured	Infecti-vity*
			Globular Particles	Shorter than 120 mμ	120–240 mμ	240–360 mμ	360–480 mμ	Longer than 480 mμ		
Control	8.9~8.9			24.1%	19.3%	50.0%	4.3%	2.3%	352	82 81
1%	8.8~8.7	5		23.5	33.9	38.6	3.2	0.8	251	0 0
3%	8.9~8.7	Days		81.8	14.6	3.5			314	0 0
5%	9.0~9.1		100%						608	0 0

* Same as Table 25

TABLE 30. Precipitin Reaction of the Virus Suspension Treated by H_2O_2 at pH 8.9-9.0

H_2O_2	pH after Adjusting ~after 15 Hours	Dializing	Final Concentration of Antiserum					Control
			16	32	64	128	256	
Cntrol	8.8~8.6	5 Days	++	++	+	+	+	−
1%	8.8~8.6		++	+	+	+	+	−
3	9.0~8.75		+	+	+	±	−	−
5	9.0~8.8		±	−	−	−	−	−
10	9.0~8.8		−	−	−	−	−	−
20	8.8~8.4		−	−	−	−	−	−
30	8.0~8.0		−	−	−	−	−	−

TABLE 31. Precipitin Reaction of the Virus Suspension Treated by H_2O_2 at pH 8.8-9.0

H_2O_2	pH after Adjusting ~after 15 Hours	Dializing	Final Concentration of Antiserum					Control
			16	32	64	128	256	
Control	8.9~8.9	5 Days	++	+	+	+	+	−
1%	8.8~8.7		++	+	+	+	+	−
3	8.9~8.7		+	+	±	±	−	−
5	9.1~9.3		−	−	−	−	−	−
10	8.8~9.0		−	−	−	−	−	−
20	8.6~8.7		−	−	−	−	−	−
30	8.3~8.4		−	−	−	−	−	−

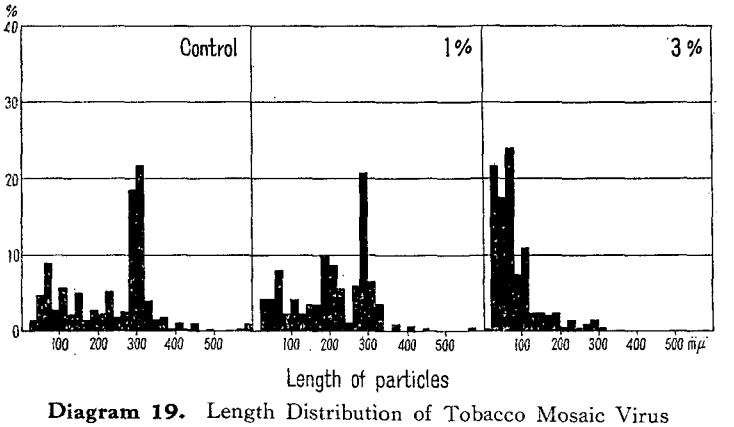

Diagram 19. Length Distribution of Tobacco Mosaic Virus Particles Treated by H_2O_2 at pH 8.9-90, after Dializing for 5 Days

When the virus particles were kept for 15 hours in the alkaline solution at pH 8.9, particles shorter than 120 mμ increased in number as compared with particles in the neutral solution.

After treating with 1% H_2O_2 for 15 hours at pH 8.9, the number of shorter particles, of 120 to 240 mμ in length, increased. In 3% H_2O_2, there were about 81.8% of particles shorter than 20 mμ in length. The precipitin reaction did not appear in the preparation treated with 3% H_2O_2. The infectivity was lost in solutions treated with 1% H_2O_2.

The following experiments were made to investigate in detail the processes of particle changes under the influence of H_2O_2 in alkaline solution.

The virus solutions treated with 10% H_2O_2 were adjusted to pH 8.2 to 8.3 and placed in a cold room for 1, 5, 10, 15, 24, and 48 hours. After treatment, the virus preparations were adjusted to pH 6.0 and then dialyzed against tap water for 3 days.

The virus preparations treated with H_2O_2 in the alkaline solutions were transparent. When these preparations were adjusted to pH 6.0 after treatment, they appeared turbid.

The results of these experiments are shown in Figs. 55 to 60, Table 32 and Diagram 20. Apparent morphological changes were not recognized in the preparations treated with 10% H_2O_2 at pH 8.3 for 1 hour, but the infectivity of the virus was completely lost. After treatment for more than 5 hours, particles shorter than 240 to 360 mμ had a tendency to increase, as the period of treatment increased. Approximately 90.9% of the particles became shorter than 240 mμ in the preparation treated for 24 hours, and after 48 hours of

TABLE 32. Infectivity and Particle Length of Tobacco Mosaic Virus Treated by H_2O_2 at pH 8.3

10% H_2O_2	pH	Dia-lizing	Length of Particles						No. of Particles Measured	Infec-tivity*	
			Globular Particles	Shorter than 120 mμ	120–240 mμ	240–360 mμ	360–480 mμ	Longer than 480 mμ			
Control	8.3	3 Days		24.6%	13.9%	56.3%	3.8%	1.4%	366	128	107
1 hour				27.9	13.8	55.3	2.4	0.6	499	0	0
5 »				33.1	38.8	23.5	3.3	1.2	510	0	0
10 »				54.0	25.6	19.6	0.8	0	679	0	0
15 »				62.5	23.3	13.8	0.4	0	472	0	0
24 »				70.7	20.2	8.6	0.5	0	559	0	0
48 »			100%						623	0	0

* Same as Table 23

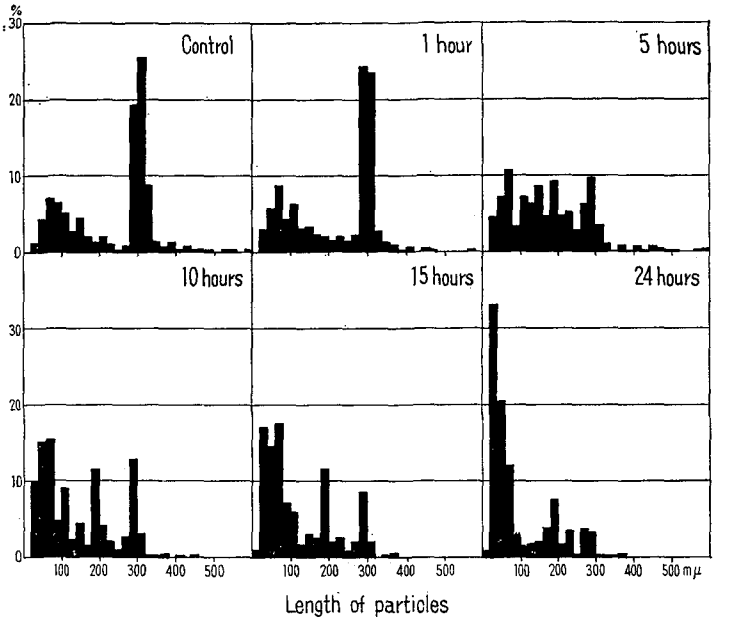

Diagram 20. Length Distribution of Tobacco Mosaic Virus Particles Treated by 10% H_2O_2 at pH 8.3

treatment virus rods changed into globular particles having 20 to 40 mμ in diameter.

Fig. 57 shows a piece of a shortened particle which seems to stand up on the supporting film. The shadow of the particle shows that this is not a globular particle but a rod having 6 sides in cross section.

Another photograph of Fig. 60 shows the rod particles cut into small

TABLE 33. Precipitin Reaction of the Virus Suspension Treated by H_2O_2

10% H_2O_2	pH	Dializing	Final Concentration of Antiserum					Control
			16	32	64	128	256	
Control	8.3	3 Days	++	+	+	+	+	−
1 hour			++	+	+	+	+	−
5 »			++	+	+	+	+	−
10 »			++	+	+	+	+	−
15 »			++	+	+	+	+	−
24 »			+	+	+	+	+	−
48 »			±	−	−	−	−	−

globular particles on a linear line.

Antigenicity of the virus preparations treated with 10% H_2O_2 at pH 8.3 was lost after 48 hours of treatment (Table 33).

F. Effect of formalin on tobacco mosaic virus

To the purified virus suspensions were added equal volumes of neutralized formalin to make concentrations of 0.5, 2, 5, 10, 50, and 100%, and these were preserved in a cold room for 20 hours.

After treating with formalin, the virus solution was poured into a cellophane sac and dialyzed against tap water for 2 or 3 days.

As shown in Table 35, the virus was inactivated in the solution treated with 10% H_2O_2, but antigenicity was not destroyed even by the 100% formalin treatment.

The virus preparations containing 50% and 100% formalin did not show the precipitin reaction but, after dialyzing, the serological reaction clearly appeared (Table 34, 35).

Figs. 61 to 64, Table 36, and Diagram 21 showed the result of the electron microscopic observation. The virus particles were not completely destroyed, even by treatment of 100% formalin. The virus solutions treated with 0.5, 2, 5, 10, 50, and 90% formalin were centrifuged at 40,000 rpm for one hour, precipitates were dissolved in an equal volume of phosphate buffer at pH 7.0

TABLE 34. Precipitin Reaction of Virus Suspension Treated by Formalin

Virus	Formalin	Dializing	Final Concentration of Antiserum					Control
			16	32	64	128	256	
	0%		+	+	+	+	+	−
	0.5		+	+	+	+	±	−
Virus	2		+	+	+	+	+	−
+	5	Non	+	+	+	+	+	−
Formalin	10		+	+	+	+	+	−
	50		−	+	+	+	±	−
	100		−	−	−	−	−	−
	1%		−	−	−	−	−	−
	4		−	−	−	−	−	−
Formalin	10	Non	−	−	−	−	−	−
	20		−	−	−	−	−	−
	100		−	−	−	−	−	−

TABLE 35. Preciptin Reacition of Virus Suspension Treated by Formalin

Virus	Formalin	Dializing	Final Concentration of Antisrum					Control	Infectivity*
			16	32	64	128	256		
	0%		+	+	+	+	+	−	197
	0.5		+	+	+	+	±	−	88
Virus	2		+	+	+	+	±	−	51
+	5	Non	+	+	+	+	±	−	36
Formalin	10		+	+	±	±	−	−	
	50		−	−	−	−	−	−	
	100		−	−	−	−	−	−	
	0%		±	+	+	+	+	−	
	0.5		+	+	+	+	±	−	
	2	2	+	+	+	+	±	−	
"	5	Days	+	+	+	+	±	−	
	10		+	+	+	+	±	−	
	50		+	+	+	+	±	−	
	100		+	+	+	+	±	−	
	0%		±	+	+	+	+	−	96
	0.5		±	+	+	+	+	−	78
	2	3	±	+	+	+	+	−	67
"	5	Days	±	+	+	+	+	−	36
	10		±	+	+	+	+	−	0
	50		±	+	+	+	+	−	0
	100		±	+	+	+	+	−	0

* The Virus Suspension were Diluted 1 : 6

TABLE 36. Particle Length of Tobacco Mosaic Virus Treated by Formalin

Formalin	Length of Particles				
	Shorter than 120 mμ	120–240 mμ	240–360 mμ	360–480 mμ	Longer than 480 mμ
	12.8%	13.8%	52.3%	9.5%	12.4%
0.5%	15.3	11.8	51.9	7.9	13.3
2	17.4	17.3	54.4	5.9	4.9
5	14.4	19.3	56.4	6.2	4.8
10	18.9	16.2	47.4	6.4	10.4
50	34.0	13.8	44.4	4.0	3.7
100	41.0	15.3	40.6	1.8	1.3

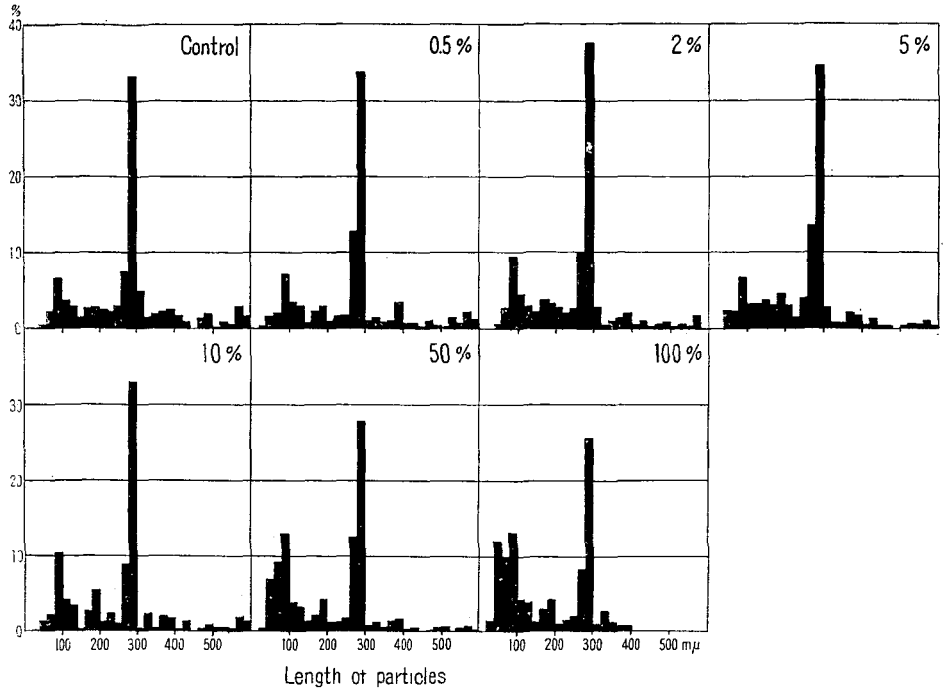

Diagram 21. Length Distribution of Tobacco Mosaic Virus Particles Treated by Formalin

and the original virus solutions, and the supernatants were dialyzed against tap water.

The ultraviolet absorption spectra of two preparations were examined by a Hitachi EPU-2 Spectrophotometer. The results showed that the nucleic acid could not be separated from virus proteins, even after treating with 100% formalin (Diagram 22).

G. Effect of sodium nitrite on tobacco mosaic virus

Purified virus solutions were precipitated at the isoelectric point of the virus at pH 3.3 and then resuspended in 5, 10, 20, and 50% $NaNO_2$ solutions for 24 hours or in 50% $NaNO_2$ for 6, 18, 24, 48, 72, and 96 hours at pH 3.3 to 4.0. These treated preparations were than dialyzed against tap water for 4 days in cellophane sacs.

As shown in Table 37 and 38, infectivity was lost in the solution treated with 10% $NaNO_2$ for 24 hours, whereas antigenicity remained, even in the

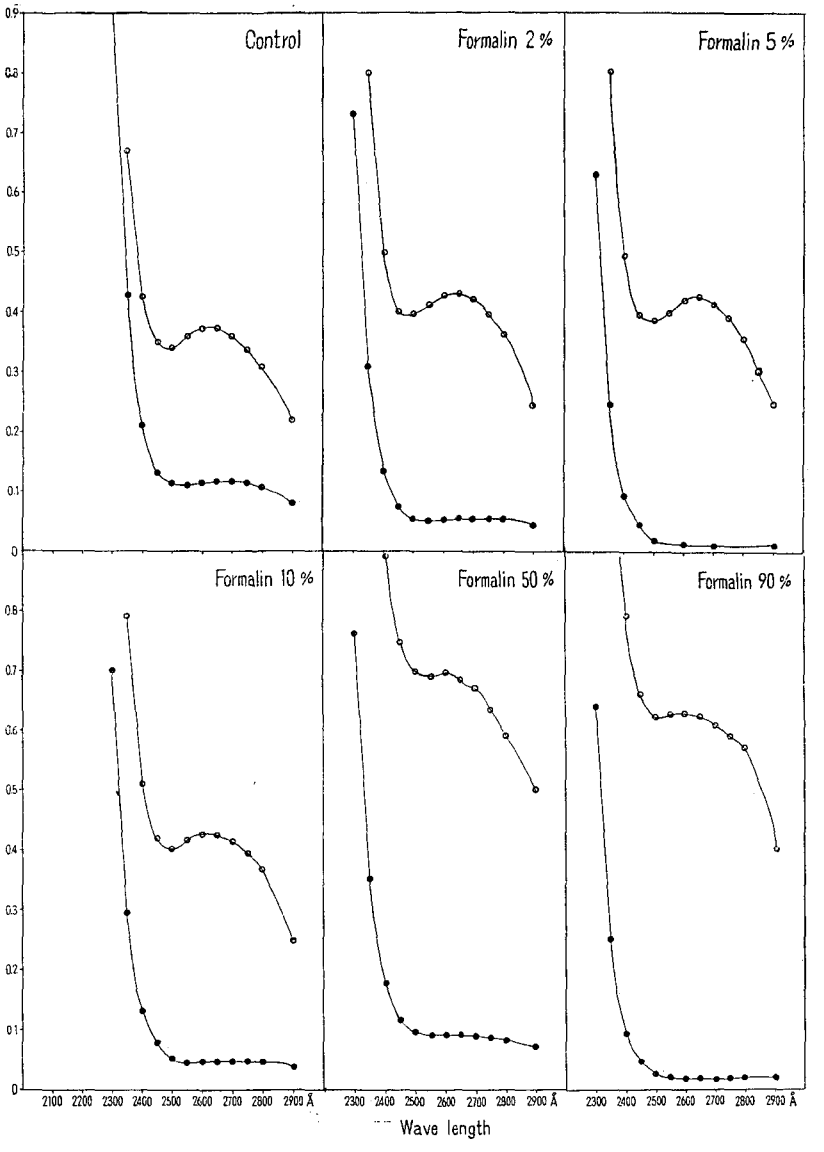

Diagram 22. UV Absorption Spectra of Tobacco Mosaic Virus Treated by Formalin

solution treated with 50% $NaNO_2$ for 7 hours.

There were only a few morphological changes in the particles in these treated solutions, except in the solution treated with 50% $NaNO_2$ for 72 hours, where a few particles were cut into short rods, as shown in Figs, 65 to 70.

TABLE 37. Precipitin Reaction of Virus Suspension Treated by $NaNO_2$

Treatment				Final Concentration of Antiserum					Control	Infectivity*
				16	32	64	128	256		
Untreated Control				++	++	+	+	+	−	606
$NaNO_2$	5%	pH 3.3	Hours 24	++	+	+	+	+	−	25
	10		"	++	+	+	+	+	−	0
	20		"	++	+	+	+	+	−	0
	50		"	++	+	+	+	+	−	0
	50		48	++	+	+	+	+	−	0
	50		72	++	+	+	+	+	−	0

* Total Lesions Inoculated by Treated Virus Suspension on 5 Leaves of *N. glutinosa*

TABLE 38. Precipitin Reaction of Virus Suspension Treated by $NaNO_2$

Treatment			Final Concentration of Antiserum					Control	Infectivity*
			16	32	64	128	256		
Untreated Control			+	+	+	+	+	−	110
Virus only	pH 4.0	Hours 6	+	+	+	+	+	−	201
		18	+	+	+	+	+	−	136
		24	+	+	+	+	+	−	100
		48	+	+	+	+	+	−	126
		72	+	+	+	+	+	−	63
Virus + 50% $NaNO_2$	pH 4.0	Hours 6	+	+	+	+	+	−	0
		18	+	±	±	−	−	−	0
		24	+	+	±	±	−	−	0
		48	+	+	+	+	±	−	0
		72	+	+	±	±	−	−	0
		96	−	−	−	−	−	−	0

* Same as Table 37

H. Effect of ultraviolet light on tobacco mosaic virus

Purified virus suspensions were diluted 1 : 10, to make a final concentration of 0.00015%, and then used for the experiment. 10 ml of virus suspensions were poured into petri dishes and were shaken under a sterilizing lamp (MATSUDA 15 W sterilizing lamp) and irradiated by UV light from 10 minutes to 20 hours at a distance of 10 cm.

After UV irradiation, the infectivity of virus suspensions was tested on leaves of *N. glutinosa* plants.

The virus suspension retained some of its infectivity after 10 minutes' exposure to UV irradiation, and was completely inactivated after 20 minutes' exposure (Table 39), while morphological changes of particles were not detectable on these preparations. Therefore, further exposures for 1 to 20 hours were made and the precipitin tests and electron microscopic observations were carried

TABLE 39. Infectivity of Tobacco Mosaic Virus Suspension Irradiated by UV. Numbers in the Columms Shows Total Local Lesions on 10 Leaves of *N. glutinosa*

UV Treatment		No. of Experiment			Total
		I	II	III	
10 cm	10 min	2	0	1	3
〃	20	0	0	0	0
〃	30	0	0	0	0
〃	45	0	0	0	0
〃	60	0	0	0	0
Control		26	19	35	80

TABLE 40. Precipitin Reaction of Virus Suspensions Irradiated by UV

UV Irradiation		Final Concentration of Antiserum						Control
		16	32	64	128	256	512	
	Hours							
	1			++	++	++	++	−
	4			++	+	+	±	−
	5	++	++	+	+	+	+	−
	6	+	+	+	+	+	+	−
10 cm	7	+	+	±	±	+	+	−
	8	−	−	−	−	−	−	−
	10			−	−	−	−	−
	20			−	−	−	−	−
Control		++	++	++	++	++	++	−

TABLE 41. Particle Length of Tobacco Mosaic Virus Irradiated by UV

UV Irradiation	Length of Particles						No. of Particles Measured
	Glolular partciles	Shorter than 125 mμ	125~ 250 mμ	250~ 350 mμ	350~ 475 mμ	Longer then 475 mμ	
Control		2.3%	6.9%	58.8%	15.9%	16.2%	234
10 cm 1 Hour		16.9	21.3	44.5	10.2	6.4	497
" 3 Hours		20.8	14.9	55.9	7.5	0.9	442
" 4 "		44.7	23.8	30.8	0.6		172
" 5 "		68.0	22.7	9.3			334
" 6 "		88.5	10.2	0.9			226
" 7 "	Mostly						
" 8 "	100%						
" 10 "	"						
" 15 "	Coagulation						
" 20 "	"						

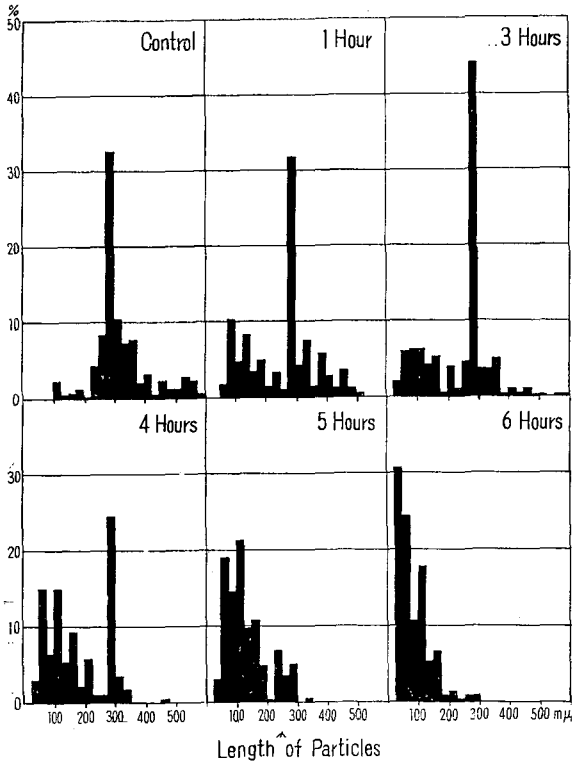

Diagram 23. Length Distributions of Tobacco Mosaic Virus Particles Irradiated by UV

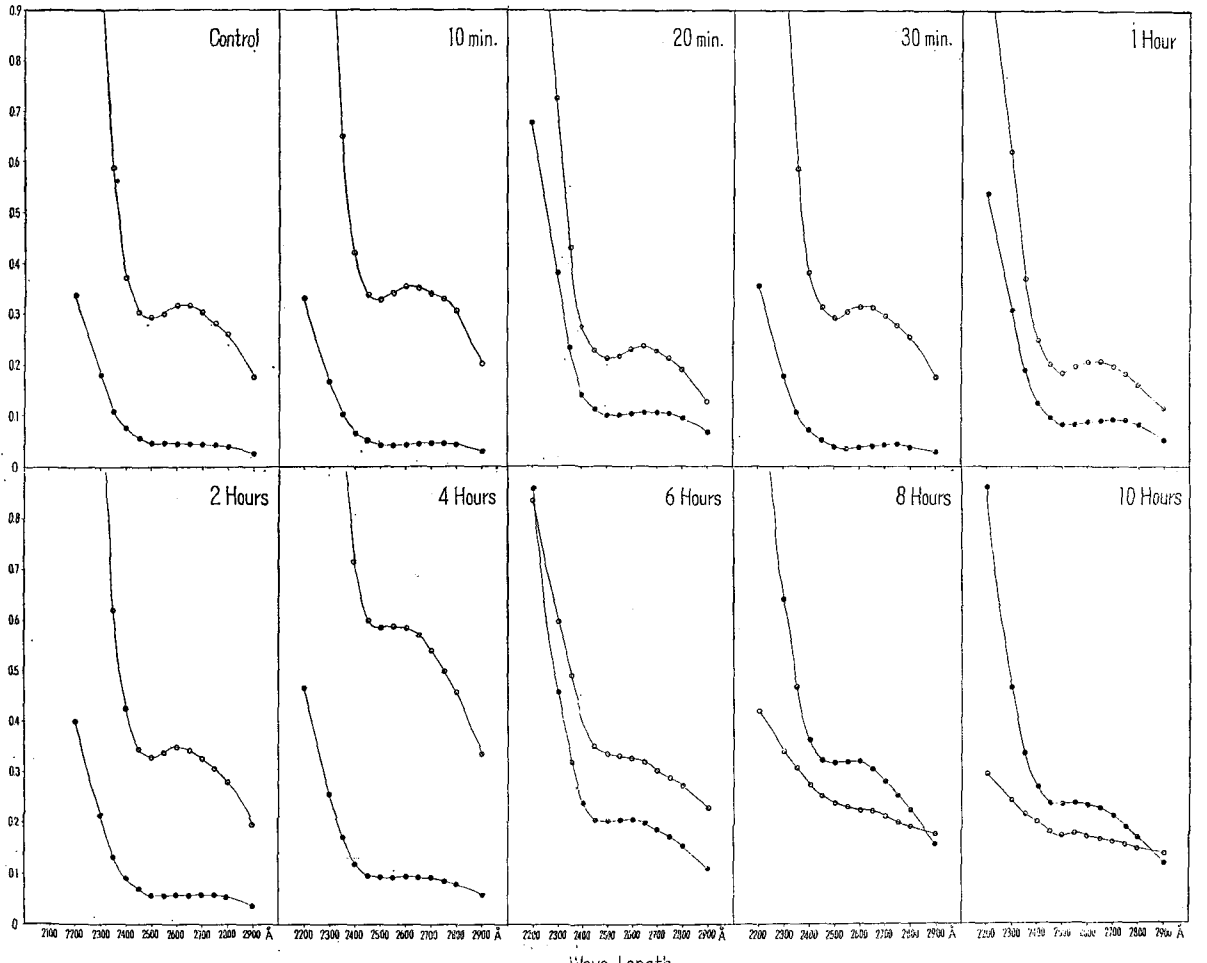

Diagram 24. UV Absorption Spectra of Tobacco Mosaic Virus Irradiated by UV
○ Precipitates after 40,000 rpm Centrifugation for 60 min.
● Supernates after 40,000 rpm Centrifugation for 60 min.

out on these preparations.

After 4 hours of exposure, the virus solutions became more and more turbid. Numerous coagulated amorphous deposits were seen in the virus suspensions irradiated for 10 hours.

In precipitin tests, it was found that the virus preparations irradiated for 1, 3, 4, 5, 6, or 7 hours retained serological activity. This activity was destroyed after 8, 10, or 20 hours' exposure (Table 40). No significant morphological change was observed in the virus rods irradiated for 3 hours. The number of virus particles shorter than 300 mμ increased in the virus suspension irradiated for 4 hours, while the number of particles of about 300 mμ or longer decreased (Table 41, Diagram. 23).

After 5 to 6 hours' exposure, 90.7 to 98.7% of the virus rods were in the form of particles shorter than 250 mμ. In the virus preparation irradiated for 7 hours, rod-shaped particles with a length of 25 mμ were found intermingled with spherical particles of about 20 mμ in diameter. The aggregation of these spherical particles occurred after 8 hours of irradiation, and after 10, 15, or 20 hours' irradiation the particles aggregated to precipitates, which were visible to the naked eye in the test tube (Figs. 71 to 76).

The UV treated virus suspensions were separated by centrifugation at 40,000 rpm for 1 hour, and UV absorption spectra of the supernatants and precipitates were examined.

As shown in Diagram. 24, a UV absorption spectrum showed that no RNA was liberated by 4 hours of UV irradiation, after 6, 8, or 10 hours of exposure, the inactivated rods in the precipitates failed to show a UV absorption spectrum for RNA.

I. Effect of X-ray on tobacco mosaic virus

Purified virus suspensions with concentrations of about 0.005% were diluted 1 : 10 or 1 : 300 with pH 6.8 phosphate buffer solution and then divided into petri dishes that measured about 4.5 cm. in diameter. Every Petri dish was covered with paraffin paper to prevent evaporation, and placed at a distance of 5.5 cm from an X-ray bulb. Doses of X-ray irradiation were 794 r/min. or 1115 r/min. and the total doses on the virus suspensions were $2\text{–}80 \times 10^4\, r$. After irradiation, the virus suspensions were diluted 1 : 2 with distilled water and then tested for infectivity on leaves of *N. glutinosa* plants. Morphological changes of the particles were studied by electron microscopy. When 10-fold diluted virus suspensions were irradiated at 2, 4, 6, 8, 10, and $20 \times 10^4\, r$, the infectivities of the irradiated suspensions decreased as doses of X-ray irradiation increased. Only 3.0% of the infectivity of the unirradiated control was retained

TABLE 42. Infectivity and Precipitin Test of Virus Suspension Irradiated by X-ray

Virus	Doses	Final Concentration of Antiserum					Control	Infectivity	
		16	32	64	128	256			
×10 Diluted	Control	+	+	+	+	+	−	435*	100%
	$2\times10^4\gamma$	+	+	+	+	+	−	355	81.6
	4 "	+	+	+	+	+	−	246	56.5
	6 "	+	+	+	+	+	−	221	50.8
	8 "	+	+	+	+	+	−	160	36.7
	10 "	+	+	+	+	+	−	125	28.7
	20 "	+	+	+	+	+	−	13	3.0

* Total Numbers of Local Lesions on 4 Leaves of *N. glutinosa*

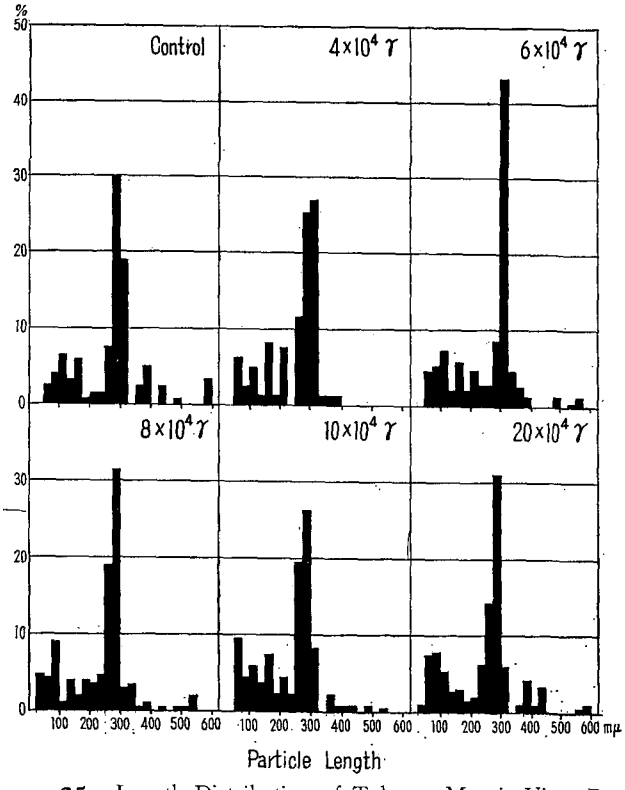

Diagram 25. Length Distribution of Tobacco Mosaic Virus Particles Irradiated by X-ray (× 300 Dilution)

after $2\times10^4\gamma$ irradiation, while neither the precipitin reaction nor the morphology of the particles was affected (Table 42, Diagram 25).

Therefore, the following experiments were carried out. The virus suspensions were diluted 300-fold and then irradiated by X-ray at 25, 30, 35, 40, 50, 60, 70, 75, and $80\times10^4\gamma$.

When the virus suspensions were subjected to more than $65\times10^4\gamma$ irradiation, they became turbid. As shown in Table 43 to 46, infectivity of the virus solution irradiated by X-ray at $25\times10^4\gamma$ was completely lost, but the precipitin reactions were detected even at $40\times10^4\gamma$ irradiation.

Electron micrographs of the virus particles are shown in Figs. 77 to 87, and length distributions of these particles are shown in Table 45 to 46 and Diagram 26.

As the doses of X-ray irradiation increased, particles shorter than 240 mμ in length became more numerous. When the virus suspension was irradiated by X-ray with more than $30\times10^4\gamma$ the virus particles were cut linearly into

TABLE 43. Precipitin Reaction of Virus Suspension Irradiated by X-ray

Virus	Doses	Final Concentration of Antiserum					Control
		16	32	64	128	256	
× 300 Diluted	Control	+	+	+	+	±	−
	$2\times10^4\gamma$	+	+	+	+	±	−
	4 "	+	+	+	+	±	−
	6 "	+	+	+	+	−	−
	8 "	+	+	+	±	−	−
	10 "	+	+	+	±	−	−
	20 "	+	+	+	±	−	−

TABLE 44. Precipitin Reaction of Virus Suspension Irradiated by X-ray

Virus	Doses	Final Concentration of Antiserum					Control
		16	32	64	128	256	
× 300 Diluted	Control	+	+	+	+	±	−
	$25\times10^4\gamma$	+	+	+	±	±	−
	30 "	+	+	+	+	±	−
	35 "	+	+	+	±	±	−
	40 "	+	+	+	±	±	−

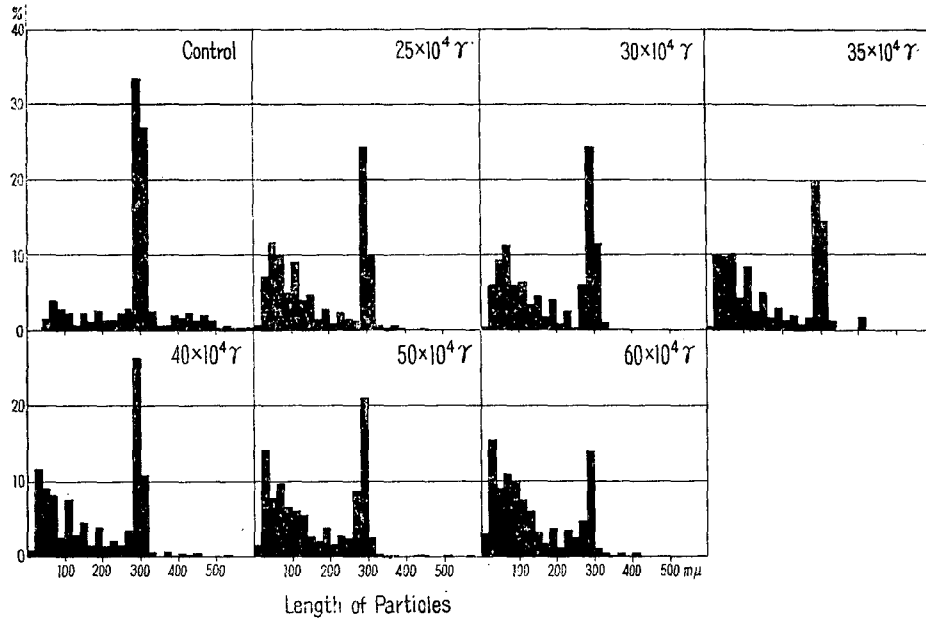

Diagram 26. Length Distribution of Tobacco Mosaic Virus Particles Irradiated by X-ray (× 300 Dilution)

TABLE 45. Infectivity and Particle Length of Tobacco Mosaic Virus Irradiated by X-ray

Virus	Doses	Length of Particles					No. of Particles Measured	Infectivity	
		Shorter than 125 mμ	125–250 mμ	250–375 mμ	375–500 mμ	Longer than 500 mμ			
× 300 Diluted	Control	13.3%	13.3%	59.2%	8.3%	5.8%	240	304*	100%
	2×10⁴γ							91	30.0
	4 »	15.2	17.2	65.2	2.5		158	76	25.0
	6 »	18.9	17.9	60.3	1.3	1.7	306	62	20.4
	8 »	18.8	18.8	57.6	2.1	2.6	191	28	9.2
	10 »	20.0	20.3	56.4	3.0	0.3	266	9	3.0
	20 »	21.5	16.0	52.2	8.7	1.4	209	1	0.3

* Total Lesions on 15 Leaves of *N. glutinosa*

several shorter rods. Most of these particles were cut into about 4 to 5 pieces and the total length of each shortened piece for each line was about 300 mμ.

Small globular particles intermingled with shortened rods were observed in the virus suspensions irradiated at more than 70, 75, and 85 × 10⁴γ. When

TABLE 46. Infectivity and Particle Length of Tobacco Mosaic Virus Irradiated by X-ray

Virus	Doses	Length of Particles					No. of Particles Measured	Infectivity*
		Shorter than 120 mμ	120–240 mμ	240–360 mμ	360–480 mμ	Longer than 480 mμ		
×300 Diluted	Control	10.6%	9.2%	6.76%	9.7 %	3.3%	360	93
	25×10⁴γ	44.0	16.5	38.3	1.3		316	0
	30 »	39.4	17.4	43.0	0.2		505	0
	35 »	43.2	15.9	38.6	1.8		747	0
	40 »	39.7	15.9	42.5	1.7		471	0
	50 »	45.9	18.2	35.2	0.4	0.3	918	0
	60 »	56.4	19.6	23.2	0.9		863	

* Total Lesions on 5 Leaves of *N. glutinosa*

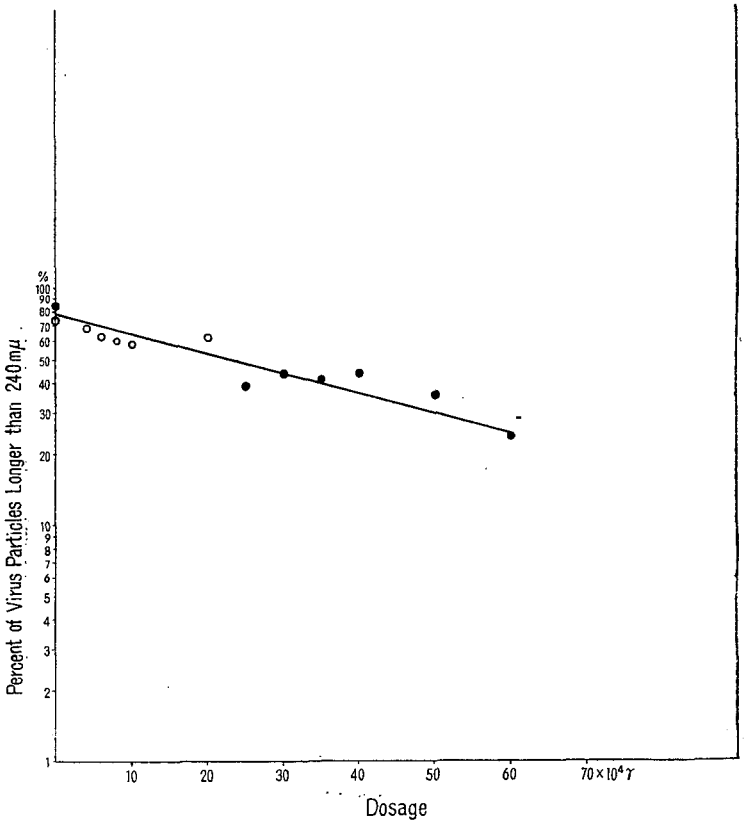

Diagram 27. Relationship between Particles Longer then 240 mμ and X-ray Dosage

○ 4–20×10⁴ Irradiation ○ 20–60×10⁴ Irradiation

the logarithm of the total ratio of particles longer than 240 mμ was plotted against the dosage of X-ray irradiation, the survival curve of the normal, or longer, length was a straight line (Diagram. 27).

J. Effect of detergent on tobacco mosaic virus

To the purified virus suspension was added sodium laurylsulfate (SLS) ($NaC_{12}H_{25}SO_4$) to make a 0.001% or 0.0001% solution. A drop of SLS containing virus suspension was heated in saturated vapor on the collodion film supported by the copper grids for 2 minutes at 70°C or 1 minute at 85°C and then dried rapidly in a vacuum chamber.

As shown in Figs. 87 to 91, the virus particles treated with 0.01% SLS for 1 hour without heating were shortened in length and those treated at 85°C for 1 minute liberated fine thread-like particles. Some of these fine particles were about 300 mμ in length. In these preparations, almost all virus particles were shortened in length. When 0.0001% ribonuclease was added to the suspension and preserved at 37°C for 1 hour, these fine threads almost disappeared (Figs 90).

This result showed that these fine threads composed of the ridonucleic acid, as reported by Hart (1955).

K. Ultrathin sectioning

Diseased leaves of tobacco plants infected with tobacco mosaic virus 30 days after inoculation were cut into small pieces, fixed with 1% osmium tetroxide for 24 hours, dehydrated with ethanol, and then embedded in methacrylate resins.

Four or 7 days after inoculation with tobacco mosaic virus, portions of local necrotic lesions were excised from leaves of *N. glutionsa* plants and embedded in the resins.

Ultrathin sections were cut by using JUM-4 or JUM-5 microtomes equipped with glass knives.

Accumulations of tobacco mosaic virus particles most frequently appeared in the mesophyll cells and also in the epidermis of infected tobacco plant (Figs. 92 and 93).

In some cases, infected cells seemed to be filled with virus particles (Fig. 94) without any regular arrangement, and in the other cases the virus particles were arranged regularly in a belt or a band. These bands were usually surrounded by a membranous structure which consisted of dense, small particles.

As shown in Fig. 95, virus particles were aggregated end-to-end or side-to-side. No morphological changes appeared in the nuclei and the chloroplasts

of the diseased cells.

Various morphological changes were recognized in the cell components of cells in local lesions of *N. glutionsa* plants infected with tobacco mosaic virus. Figs. 96 to 101 show the ultrathin sections from healthy and infected *N. glutinosa* plants. The ultrathin sections through the young local lesions on the leaves of diseased *N. glationsa* showed that the cell nuclei were not affected but the chloroplasts and the mitochondria seemed to be disintegrated. Fig. 98 shows disintegrated mitochondria in a cell of a local lesion of a diseased leaf in which crystae in the mitochondria were not developed and seemed to be affecteld by the virus. In the chloroplasts of local lesion cells, grana could not well be recognized (Fig. 99, 100). No virus particles were observed in the cells of these necrotic portions. Cells in such partions were destroyed and large electron dense materials were frequently observed. The electron dense materials usually appeared around the chloroplasts. Virus-like particles were only recognized around the cell walls in the varcular bundle (Figs. 102 to 104).

L. Discussion and conclusions

It is concluded that the most effective method to determine the size and shape of virus particles is by the electron microscope. This method was also occasionally used for identifying or diagnosing virus diseases (DE BRUYN OUBOTER, BEIJER and VAN SLOGTEREN 1951).

As mentioned in Chapter III, the measurements of virus particles by the electron microscope might contain various kinds of errors. Consequently, workers have differed in their reported definite values of sizes of the virus particles. For example, the length of tobacco mosaic virus particles previously reported is summarized in Table 47. This shows that the length of tobacco mosaic virus particles had been reported as 280 mμ or 300 mμ. In 1946, RAWLINS, ROBERTS, and UTECH discussed in detail several methods of measurement of tobacco mosaic virus. They concluded that the length of tobacco mosaic virus was between 280 and 320 mμ and the average length of the particles was about 300 mμ. WILLIAMS and STEERE (1951) reported that the tobacco mosaic virus particle has an average length of 298 ± 1 mμ as compared with Dow latex particles. HALL (1958) also showed that the particle length was 300 mμ by the electron microscopic measurements. As mentioned in Chapter IV, A, the tobacco mosaic virus particles had an average length of 300 ± 0.5 mμ. Consequently, it is most likely that tobacco mosaic virus particles have an uniform length, and an average length of 300 mμ, as determined by the electron microscopic measurements.

TABLE 47. The Size of Tobacco Mosaic Virus Particles Reported by Various Workers

Worker	Year	Size of TMV
KAUSCHE, PFANKUCH & RUSKA	1939	150~300×15 mμ
STANLEY & ANDERSON	1941	280×15 mμ
RAWLINS, ROBERTS & UTECH	1946	300 mμ (280~320 mμ)
KNIGHT & OSTER	1947	280±8.6×10.2 mμ (6 strains) Cucumber Virus 3 & 4 297±8.6×130±0.6 mμ
OSTER, KNIGHT & STANLEY	1947	280±8.6×15.2 mμ (3 strains)
TAKAHASHI & RAWLINS	1947	280~340 mμ (2 strains)
SIGURGEIRSON & STANLEY	1947	280×15 mμ
OSTER	1947	280 mμ
TAKAHASHI	1949	300 mμ
KAHLER & WOODS	1949	280×15 mμ
KAHLER & LLAYD	1950	150±3.6 Å in diameter
WILLIAMS & STEERE	1951	298±1 mμ
HIDAKA & MURANO	1952	280 mμ
FUKUSHI & SHIKATA	1952	280 mμ
PAUL u. BODE	1956	293 mμ
WETTER u. BRANDES	1956	286 mμ
WILLIAMS	1957	299×18 mμ
HALL	1958	300 mμ
WILLIAMS	1959	300×18 mμ

Most of the authors who reported the width of the particles measured by the electron microscope gave the value of 15 mμ (STANLEY and ANDERSON, 1941; KAHLER and WOODS, 1949). Initially, it was difficult to determine exactly the shape and the width of the tobacco mosaic virus particles because of the poor resolving power of the electron microscope.

BERNAL and FANKUCHEN (1941) reported the result of their measurement by X-ray diffraction patterns and showed the model of tobacco mosaic virus particle having a hexagonal cross section of 152 Å in width and its longest diameter as 174 Å. Upon considering the resolving power of the electron microscope used in this experiment and the difference of the result of measurements between shadowed and unshadowed particles, the width of the tobacco mosaic virus particles is about 15 to 20 mμ in diameter. A few years ago, WILLIAMS (1957, 1959) reported that the width of the virus is 180 Å in

diameter when measured by the electron microscope. FRANKLIN *et al.* (1959) showed the particle diameter was 180 Å by X-ray diffraction.

HALL (1955) reported that PTA is effective for the electron staining of viruses, and HUXLEY (1957) pointed out that KCl can also be used for the electron staining of tobacco mosaic virus particles.

Experiments reported in this paper showed that PTA is more effective than KCl for staining, as shown in Figs. 6 to 9.

There are many reports concerning inactivation of tobacco mosaic virus particles by physicochemical procedures. BARTELS (1955) has summarized the results of these experiments.

PRICE (1933), LAUFFER and PRICE (1940), reported that tobacco mosaic virus particles were inactivated by heat treatment. HIDAKA and KIRIYAMA (1953) observed that the tobacco mosaic virus particles changed into short rods after heating, and HART (1956) showed by electron micrographs that one or both ends of tobacco mosaic virus particles swelled as the result of heating.

In the present report it has been demonstrated that morphological changes in heated tobacco mosaic virus particles depend upon the condition of the solution in which the virus particles were suspended. When the virus solutions were dialyzed against tap water to remove the salts completely, and then heated at 60°C to 70°C, tobacco mosaic virus particles had a tendency to coagulate, and to disintegrate into small globular particles when heated at more than 70°C. When virus particles suspended in a buffered solution at pH 7.0 or 5.2 were heated, no aggregations appeared and the particles changed into small shortened rods or globular particles of uniform size and shape of about 20 mμ in diameter.

Infectivities of virus suspensions decreased as the particles of middle length (SIGURGEIRSON *et al.*, 1947) or normal length (BRANDES and WETTER, 1959) decreased in number and the proportion of the short rods in the virus suspensions increased. Infectivities were lost completely by heating at 80°C for 10 minutes in the pH 7.0 buffered solution, at 85°C for 10 minutes in the pH 5.2 buffered solution, and at 90°C for 10 minutes in the dialyzed solution. It has been reported by many workers that infectivity of tobacco mosaic virus particles was affected or destroyed by treatment with various hydrogen ion concentrations (FUKUSHI, 1933; STANLEY, 1935; THORNBERRY, 1935; BEST and SAMUEL, 1936; BEST, 1936; BAWDEN and PIRIE, 1937, 1940).

As mentioned in Chapter IV, the morphological changes of tobacco mosaic virus particles caused by heating were affected by hydrogen ion concentrations of the suspension. WYCKOFF (1937), WYCKOFF, BISCOE and STANLEY (1937), SCHRAMM (1954), and SCHRAMM, SCHUMACHER und ZILLING (1955 a, b) studied by electron microscopy or ultracentrifugation the morphological changes of

tobacco mosaic virus particles suspended in various hydrogen ion concentrations.

It is desirable that the length of virus particles in the virus suspensions used for the electron microscopic studies is kept homogeneous during the experiment. Homogeneity of chemically purified tobacco mosaic virus particles used in this experiment was not always satisfactory for the electron microscopic work.

Homogeneity depends upon the procedure of purification and on the effects of salts in the suspension during preservation. RAWLINS, ROBERTS, and UTECH (1946) and TAKAHASHI and RAWLINS (1946) reported that the proportion of the shortened particles in the infective sap increased as the periods that elapsed between infection and symptom appearance on plants were getting loner.

Accordingly, it is necessary to choose the proper growing stage of infected host plants.

As mentioned in the experiment, increase of shortened particles was taking place in the suspension of tobacco mosaic virus particles purified by the isoelectric point precipitation. Therefore, repeated precipitation in the isoelectric point and dissolving in the buffered solution for isolation of the tobacco mosaic virus particles caused inhomogeneity of the virus paraticles. Inhomogeneity of the particles was caused more abundantly in the alkaline solution than in acid solution.

As shown in Table 21 22, denaturation of the virus particles took place in alkaline solutions. Tobacco mosaic virus particles did not aggregate and remained scattered in the alkaline solution. They were not cut into short rods even in a solution at pH 8.2. They were split into small particles at pH 11.0 (Fig. 46).

SCHRAMM, SCHUMACHER und ZILLIG (1955 a, b) and SCHRAMM (1955) observed the fine thread-like structure of RNA between shortened rods, but the author could not observe the same structure in this experiments. They also reported the tobacco mosaic virus denaturation by ultracentrifugation in alkaline solution. The virus particles were composed of small protein particles having a molecular weight of 1×10^6, and the size of 150×70 Å. It was impossible to observe such small particles in detail because of the low resolving power of the electron microscope, JEM-4B, used in the present experiments.

In the acid direction, the virus particles have a tendency to aggregate, with small paracrystalline formations at pH 3.3, the isoelectric point of tobacco mosaic virus. At pH 2.15 or 3.0, aggregation of the particles became a net-like structure on the collodion film. This showed that the small aggregated particles in the suspensions could not develop a large crystalline structrue and consequently they dried in different directions.

STANLEY (1936) briefly reported the effect of H_2O_2, formalin, nitrous acid,

and ultroviolet light on tobacco mosaic virus. The virvs particles did not lose their antigenicity but their infectivity was lost upon treatment with these chemicals or UV light. WYCKOFF, BISCOE, and STANLEY (1937) also reported that when the virus particles were treated with H_2O_2, formalin, and nitrous acids, no remarkable changes in sedimentation constant occurred.

In this paper, the tobacco mosaic virus susponsion lost its infectivity after 5% H_2O_2 treatment, while no morphological change took place. Denaturation of the particles did not occur with treatments of 30% H_2O_2 in acid solutions. The particles completely denatured with treatments of 5% H_2O_2 for 15 hours at pH 8.9, 10% H_2O_2 for 48 honrs at pH 8.3. In those samples, rod-shaped particles could not be observed by the electron microscope and antigenicity of the treated suspensions was completely lost. It is probable that the alkaline solution easily resolved H_2O_2 into H_2O and O, and tobacco mosaic virus particles were severely oxidized. WILLIMS (1952) observed by the electron microscope that tobacco mosaic virus particles, broken by ultrasonic waves, had a hexagonal cross section. The short rods treated with H_2O_2 also showed a six-sided cross section, as seen in Fig. 57.

STANLEY (1936), WYCKOFF, BISCOE, and STANLEY (1937), ROSS and STANLEY (1938), and KASSANIS and KLECZKOWSKI (1944) reported that tobacco mosaic virus particles were inactivated by treatment with formaldehyde but that formaldehyde did not change their structure. HIDAKA and KIRIYAMA (1953) confirmed this by the electron microscope. The author observed in this paper that morphology or antigenicity of the tobacco mosaic virus particles could not be destroyed by treatment with 5% formalin while infectivity was completely lost. The shortened particles were sometimes found in the specimens of 50% formalin treatment.

Loss of infectivity of tobacco mosaic virus by $NaNO_2$ has been reported by STANLEY (1936), BAWDEN and PIRIE (1937), and JOHNSON (1941). The morphological changes were hardly apparent after treatment with 50% $NaNO_2$ or 72 hours at pH 4.0 and antigenicity was not lost.

The effects of UV on tobacco mosaic virus have been studied by F. F. SMITH (1926), MULVANIA (1926), ARTHUR and NEWELL (1929), DUGGER and HOLLAENDER (1934 a, b), HOLLAENDER and DUGGER (1936), PRICE and GOWEN (1937), and LEA and SMITH (1940). STANLEY (1936) reported that the tobacco mosaic virvs particles lost their infectivity after UV irradiation but that this treatment did not cause chemical or antigenic changes.

In the present experiments, tobacco mosaic virus particles lost their infectivity after irradiation for 20 minutes, while no morphological changes appeared after 3 hours' exposure. As previously reported by STANLEY (1936),

the tobacco mosaic virus particles were shortened after 4 to 6 hours' exposure and then homegeneity of the particles in the suspensions was reduced. LEA (1955) pointed out that the intrinsic nature of ionizing and nonioning radiation was quite different.

GOWEN and PIRIE (1936), LEA and SMITH (1940), and MIYAMOTO and KAWAMURA (1954) pointed out that an exponential relation existed between infectivities and X-ray doses. The experiment by the author showed that the same relation was recognized between the length of tobacco mosaic virus particles and radiation dosages.

BAWDN (1950 a) and FUKUSHI (1952) discussed the fact that inactivation of viruses consists of three types of changes in the particles, such as (1) loss of infectivity, (2) partial inactivation, and (3) denaturation.

The author proved by electron microscopy that heat treatments and pH changes caused the denaturation of tobacco mosaic virus. The action of H_2O_2, formalin, $NaNO_2$, UV or X-ray irradiation produced partial inactivation, but the particles were broken by further treatments.

GIERER and SCHRAMM (1956 a, b) and FRAENKEL-CONRAT (1956) confirmed that the infectivity of tobacco mosaic virus particles depends on RNA itself but not on the outer protein sheath. In this paper, an attempt was made to examine RNA liberation from particles by treatment with heat, formalin, and UV irradiation.

Virus RNA seemed to be freed from the virus protein when the virus particles were cut into small rods and then further changed into small globular particles.

HART (1955), SCHRAMM, SCHUMACHER and ZILLIG (1955 a), and STAHMANN and KAESBERG (1955) observed the fine structure of RNA which joins each of the shortened rods or projects out of the ends of the virus protein.

A similar structure of RNA was seen in the preparations treated with heat, formalin, freeze-drying (Fig. 88) and detergents. SCHRAMM (1955) also observed that the RNA strands, which join the shortened rods, appeared in the alkaline treated particles. Shortened particles in a linear line were seen in the preparations treated with $NaNO_2$ and X-ary irradiation, but the RNA strands which join the shortened rods could not be found in the experiments.

Tobacco mosaic virus was easily observed in cells of the epidermis and parenchyma, where it formed masses of parallel rods, as reported by BLACK, MORGAN, and WYCKOFF (1950), LEYON (1953), TSUJITA and TSUDA (1954), SKOTLAND, HAGEDORN, and STAHMANN (1955), BRANDES (1955, 1956 a), and MATSUI (1956). Fig. 95 shows a long band of a virus mass which is similar to the crystal-like mass observed by BRANDES (1955 a, 1956). Virus particles,

filling a cell, are shown in Fig. 94. BRANDES considered that after the X-body burst, the virus particles in the X-body flew out and scattered in a cell. But MATSUI (1958 c) and MATSUI and YAMADA (1958) confirmed that no virus particles could be observed within X-bodies of the diseased tobacco plants.

No virus particles were seen in the cells of the portions of local lesions or around local lesions of *N. glutinosa* plants inoculated with tobacco mosaic virus. Similar findings were already reported by SHALLA (1959 a, b).

However, in the present study, a few regularly arranged virus particles were found attached to the cell wall of a cell within a vascular bundle. The cells near the vascular bundle contained disintegrated chloroplasts surrounded by a mass of electron dense particles. These masses of dense small particles sometimes filled a plant cell. YOSHII and KAWAMURA (1947) mentioned that the corky layers observed around the local lesions are not for preventing the spread of the virus in the leaf. They reported that when necrosis appared in the infected cells, corky layers were produced in consequence. The dense material shown in Figs. 100 and 101 seems to be a portion of such a corky layer, formed when tobacco mosaic virus attacked the cells of *N. glutionsa*. Electron micrographs proved that cells in local lesions of *N. glutionsa* were more severely damaged than those in *N. tabacum*.

V. Potato virus X

A. Size and shape of potato virus X

Series 1. The expressed juice from young leaves of diseased tomato plants infected with potato virus X, strains X-c_1, X-5, X-I_{43}, and X-68, were frozen at -20 to -30°C for 15 to 20 hours. After thawing, the juice was centrifuged at 16,000 rpm for 30 minutes and diluted 1 : 100 or 1 : 500 with distilled water. The crude sap virus was mixed with either Dow latex 580 G or tobacco mosaic virus and then dried on the supporting films. The preparations were shadowed with a small amount of chromium or platinum and examined by the electron microscope.

Potato virus X in crude sap showed a flexible thread-like structure (Figs. 106 to 108), as previously reported by TAKAHASHI and RAWLINS (1946). The average length of the virus particles was compared with Dow latex 580 G and tobacco mosaic virus particles, and the results are shown in Tables 48 and 49 and Diagram 28.

There were small differences in length among various strains of potato virus X. When compared with tobacco mosaic virus particles of 300 mμ long, the average lengths of each strain were 526 mμ in X-c_1, 541 mμ in X-I_{43}, 541 mμ

in X-5, and 530 mμ in X-68.

TABLE 48. Particle Length of 4 Strains of Potato Virus X in Crude Sap as Compared with Latex 580-G

Length	No. of Particles				Length	No. of Particles			
(mμ)	X-I_{43}	X-68	X-5	c_1	(mμ)	X-I_{43}	X-6	X-5	c_1
20					640	1	4		
40	1				660	3			
60					680		2		
80	2				700				
100	2		3		720			2	
120	1	3	1		740	1			
140	3		2	2	760			2	1
160	1			5	780	1	2		
180	3	2	2	3	800			1	
200		1		2	820	1			
220			3	3	840				
240	1			5	860			1	
260	1	3	3	2	880			1	
280	2	1		2	900			1	
300	1	2		1	920				
320	1		2	2	940			2	
340	3			1	960	1			
360	3		2		980				
380	1	1		1	1000				
400		1		6	1020			2	
420	3	1	5	1	1040				
440	1	2	1	4	1060	1			1
460	1	1	2	1	1080				1
480	5	8	3	5	1100				1
500	6	10	2	8	1120	4			
520	13	45	14	18	1140	2			
540	56	80	30	49	1160	2			
560	71	77	102	27	1180	1			
580	32	19	22	3	1200	1			
600	21	6	4	6	Total	251	275	216	163
620	1	4	1	1					

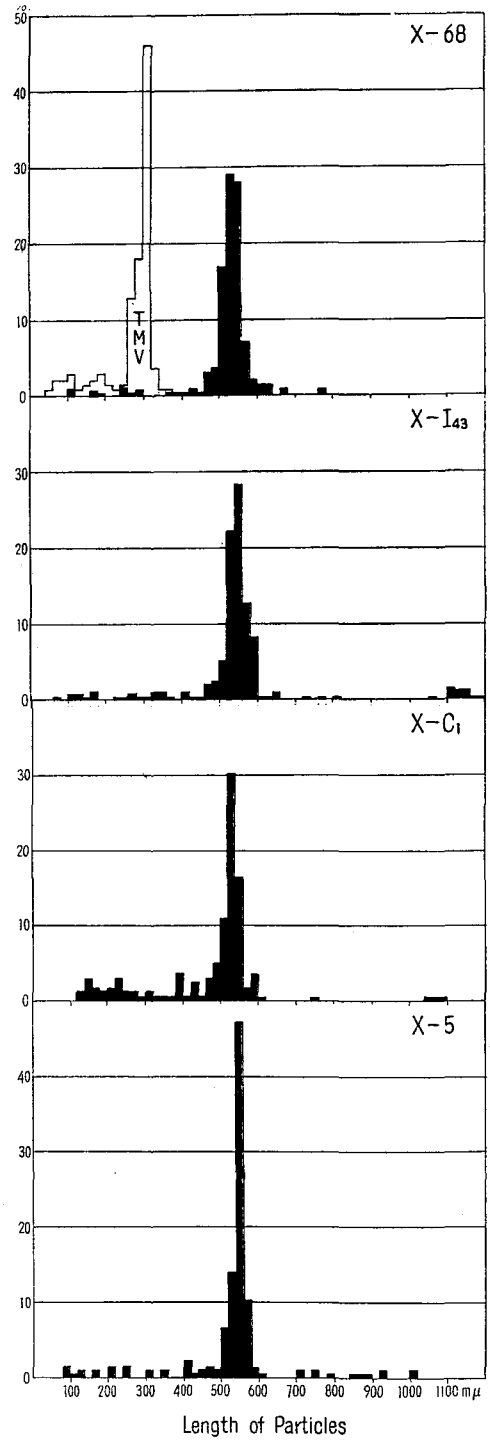

Diagram 28. Length Distribution of 4 Strains of Crude Sap Potato Virus X and Tobacco Mosaic Virus as Compared with Dow Latex 580-G

TABLE 49. Particle Length of Four Strains of Potato Virus X in Crude Sap as Compared with Tobacco Mosaic Virus and Dow Latex 580-G

Virus Strain	X-c_1	X-I_{43}	X-68 (TMV)	X-5
No. of Particles	116	204	245 (226)	177
Average Length (mμ) (1)	530	545	534 (302)	545
Standard Deviation	26	27	24 (15)	20
Standard Error	2.4	1.9	1.5	1.5
Length of the Virus (2)	(526)	(541)	(530) (300)	(541)

(1) Average Length as Compared with Dow Latex 580-G
(2) Average Length as Compared with Tobacco Mosaic Virus

Series 2. Isolation or purification of potato virus X, strains X-I_{43}, X-68, and X-5, was carried out by the modified procedure of BAWDEN and PIRIE (1938). Young diseased leaves of tomato or tobacco plants preserved in a cold room at -20 to -40°C were macerated and then thawed. The virus in the expressed sap was purified by precipitation with ammonium sulfate. Whenever the final suspension contained impurities in large quantities, further purification was carried out by precipitating at pH 4.5.

To the purified virus preparations was added Dow latex 580 G or tobacco mosaic virus particles and then dried on the collodion films.

The morphology of the purified virus was the same as the crude sap virus (Fig. 105). The length of the virus was compared with Dow latex 580 G and tobacco mosaic virus particles. The results are shown in Table 50, Diagram 29. The average length of the virus is calculated in Table 51.

There were no apparent differences in length among strains of potato virus X. When compared with tobacco mosaic virus of 300 mμ in length, the average lengths of respective strains were 520 mμ in X-I_{43}, 528 mμ in X-68, and 537 mμ in X-5.

Series 3. To the crude sap virus of strains X-5 and X-68 were added Dow latex samples 15 N-8, 15 N-7, and 580 G, and the preparations examined by the electron microscope. The length distribution of the virus particles is shown in Table 52 and Diagram 30. Table 53 shows that the average lengths of the viruses, as comared with Dow latexes, were 527 mμ in X-5 for Dow latex 15 N-8, 521 mμ in X-5 for 15 N-7, 522 mμ in X-68 for 580 G.

The results indicated that there was no apparent difference between particle length of 4 strains of potato virus X. The average of particle lengths of 4

TABLE 50. Particle Length of 3 Strains of Potato Virus X in a Purified Suspension as Compared with Dow Latex 580–G

Length	No. of Particles			Length	No. of Particles		
(mμ)	X-I_{43}	X-68	X-5	(mμ)	X-I_{43}	X-68	X-5
20				640	2		
40			1	660	3		4
60	2		4	680	2		
80			7	700	2		
100			11	720	2		
120	1	1	7	740			
140	4		13	760			1
160	1	3	8	780			1
180			9	800			
200		1	4	820	1		1
220	4		7	840			2
240			4	860	2		
260	4	1	6	880			
280	1		1	900			1
300	4	3	3	920			
320	1	2	2	940			
340	4	2	4	960	1		
360	2	1	4	980	1		
380	3		1	1000			1
400	1	1	1	1020	1		
420	2		3	1040			
440	7	1	3	1060	2		
460	10		1	1080			
480	12	1	3	1100			
500	33	3	10	1120			
520	83	3	8	1140			
540	92	22	47	1160			
560	52	6	73	1180			
580	9	5	21	1200	1		
600	4		3	Total	359	61	282
620	3	1	2				

TABLE 51. Particle Length of 3 Strains of Purified Potato Virus X as Compared with Tobacco Mosaic Virus and Dow Latex 580-G

Virus Strains	X-I_{43}	X-68 (TMV)	X-5
No. of Particles	285	40 (226)	165
Average Length (mμ) (1)	523	532 (302)	541
Standard Deuiation	24	23 (15)	23
Standard Error	1.4	3.7	1.8
Length of the Virus (2)	(520)	(528) (300)	(537)

(1) Average Length as Compared with Dow Latex 580-G
(2) Average Length as Compared with Tobacco Mosaic Virus

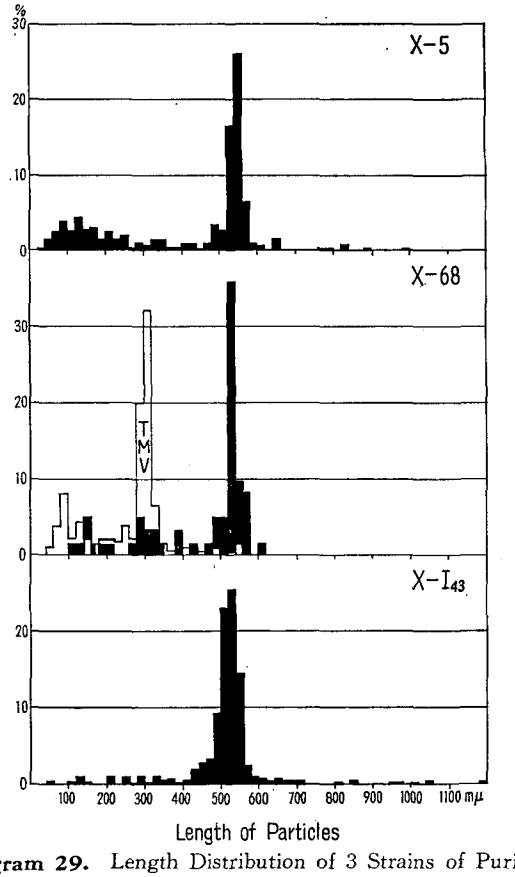

Diagram 29. Length Distribution of 3 Strains of Purified Potato Virus X and Tobacco Mosaic Virus as Compared with Dow Latex 580-G

TABEL 52. Particle Length of 3 Strains of Potato Virus X in Crude Sap as Compared with Dow Latex 580-G, 15 N-7, 15 N-8

Particle Length (mμ)	No. of Particles			Particle Length (mμ)	No. of Particles		
	X-68 (580G)	X-5 (15 N-7)	X-5 (15 N-8)		X-68 (580G)	X-5 (15 N-7)	X-5 (15 N-8)
20				640	4	1	
40				660	2	4	
60				680	4	4	
80		1		700	1	6	
100		2		720		2	1
120	3	2		740	2	1	
140	1	2		760		3	
160		2		780	2	1	
180	2	5		800		2	1
200	2	4		820		1	
220		2		840			
240	2	8		860	1	3	
260	5	7		880		1	
280	1	3		900			
300	4	3		920		2	
320	2	3		940	1	3	
340	2	5		960		7	2
360	3	2		980		8	
380	2	4		1000	1	7	1
400	2	8		1020		8	
420	5	12		1040	3	1	
440	6	9		1060	8	4	2
460	2	13	2	1080	1	3	1
480	26	24	1	1100		1	2
500	50	66	14	1120	1	3	2
520	228	130	26	1140		1	
540	166	126	56	1160		1	1
560	94	42	25	1180		3	1
580	22	23	6	1200			
600	6	14		Total	672	607	145
620	5	4	1				

TABLE 53. Particle Length of 3 Strains of Potato Virus X in Crude Sap as Compared with Dow Latex 580-G, 15 N-7, 15 N-8

Strains of Potato Virus X	X-5	X-5	X-68
Dow Latexes	15 N-8	15 N-7	580 G
No. of Potato Virus X Particles	128	425	592
Average Length ($m\mu$)	527	521	522
Standard Deviation	21	28	23
Standard Error	1.9	1.4	0.87

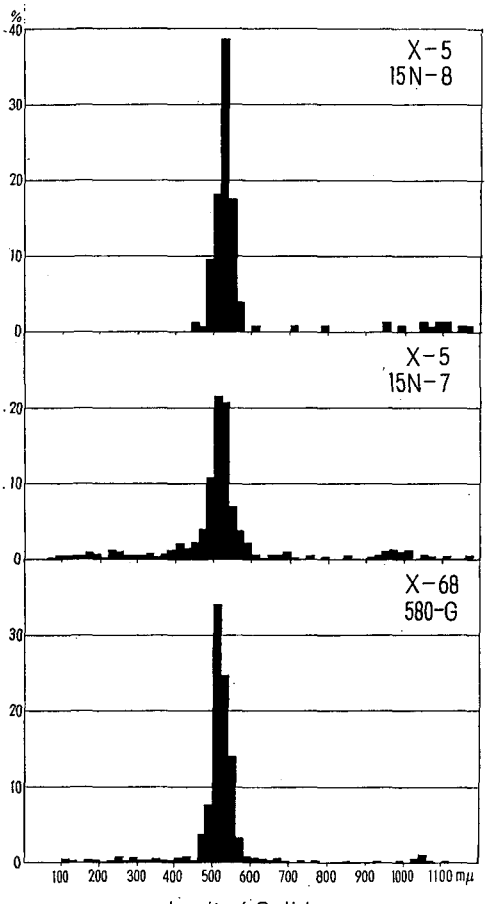

Diagram 30. Length Distribution of 3 Strains of Potato Virus X in Crude Sap as Compared with Dow Latex 580-G, 15 N-7, 15 N-8

TABLE 54. Average Length of 4 Strains of Potato Virus X

As compared with	Lengte of particles (mμ)				Average length
	X-c_1	X-I_{43}	X-68	X-5	
15 N-8				527 ± 1.9	
15 N-7				521 ± 1.4	
580 G			522 ± 0.9		
TMV (crude)	526	541	530	541	
TMV (purified)		520	528	537	
Average length	526	530.5	526.6	531.5	528.65

strains was 529 mμ in length, as shown in Table 54.

The width of potato virus X, as compared with tobacco mosaic virus particles, was 10 mμ to 15 mμ.

B. Effect of hydrogen ion concentration on potato virus X

The suspensions of chemically purified potato virus X, adjusted at various pH values, were kept in a cold room at 1 to 3°C for 16 hours. After readjusting to pH 6.0, the treated virus was observed by the electron microscope, its infectivity was tested on *D. stramonium* or *N. glutinosa* plants, and its precipitin reactions were checked against antiserum.

Figs. 109 to 115 show the results of morphological changes observed by the electron microscope when the virus suspensions were treated at pH 1.0, 2.0, 4.0, 6.0 8.0, 10.0, 11.0, and 12.0 for 16 hours. The chemically purified

TABLE 55. Infectivity and Precipitation Reaction of Potato Virus X in Various Hydrogen Ion Concentrations

pH Adjusted	pH after 16 Hours	Final Concentration of Antiserum					Control	Infectivity*	
		16	32	64	128	256		*D. stramonium*	*N. glutinosa*
2.1	2.1	−	−	−	−	−	−	0/5	0/5
3.0	3.1	+	+	+	±	±	−	0/5	0/5
4.1	3.92	+	+	±	±	−	−	0/5	0/5
6.0	5.98	+	+	+	+	+	−	5/5	5/5
8.25	8.2	+	+	+	±	±	−	5/5	5/5
10.0	9.7	+	+	+	±	±	−	5/5	5/5
12.06	11.8	−	−	−	−	−	−	0/5	0/5
6.3	6.3	+	+	+	+	+	−	5/5	5/5

* Denominator: Number of Plants inoculated
Numerator : Number of Plants infected

virus particles in a solution at pH 6.0 and pH 4.0 showed end-to-end aggregation. At pH 3.0 these aggregated particles were dispersed into short rods. They changed into small globular particles intermingled with a few shortened rods of about 20 to 30 mμ long at pH 2.5 or 2.0. The virus was completely disrupted at pH 1.0. In alkaline solutions the virus particles were shortened at pH 10.0 and 11.0 and changed into small globular particles at pH 12.0.

As shown in Tables 55 and 56, loss of infectivity appeared at pH 2.26 and 11.1, while antigenicity of the virus was lost completely at pH 2.1 and 11.1.

TABLE 56. Infectivity and Precipitin Reaction of Potato Virus X in Various Hydrogen Ion Concentration

pH Adjusted	pH after 16 Honrs	Final Concentration of Antiserum					Control	Infectivity*	
		16	32	64	128	256		*D. stramonium*	*N. glutinosa*
1.0	1.1	−	−	−	−	−	−	0/5	0/5
2.1	2.1	−	−	−	−	−	−	0/5	0/5
2.26	2.28	+	±	−	−	−	−	0/5	0/5
3.0	3.0	+	+	±	±	±	−	1/5	0/5
4.1	4.8	+	+	+	+	+	−	5/5	4/5
6.2	6.1	+	+	+	+	+	−	5/5	5/5
7.0	7.0	+	+	+	±	±	−	5/5	5/5
9.0	9.1	+	+	±	±	−	−	5/5	5/5
9.9	9.9	+	±	±	±	−	−	5/5	5/5
11.1	10.75	+	±	−	−	−	−	0/5	0/5
12.15	11.9	−	−	−	−	−	−	0/5	0/5

* Same as Table 55

C. Effect of ultraviolet light on potato virus X

Chemically purified virus suspended in a buffered solution of equal volume of original sap was used in the experiment. The ultraviolet irradiation was carried out in Petri dishes at a distance of 10 cm from the surface of the specimen fluid. The virus suspensions irradiated for 2.5, 3, 3.5, 4, 4.5, 5, and 6 hours were dried on collodion films and observed by the electron microscope. The treated specimens were also inoculated into leavs of *Datura stramonium* plants in order to examine their infectivity and they were used for precipitin reactions.

The virus particles irradiated for 2.5 and 3 hours were cut by this treatment into rods shorter than 100 mμ (Fig. 122). Most of the rods became small particles of 10 to 20 mμ long after irradiating for 3.5 to 4.5 hours, and after

5 hours of exposure the virus rods became completely denatured.

In order to investigate the more detailed morphological changes of potato virus X, the following experiments were carried out. The chemically purified virus preparations were diluted 1 : 10 with distilled water and then irradiated for 5, 10, and 30 minutes, 1, 1.5, 2, 2.5, 3, 3.5, and 4 hours. As shown in Figs. 116 to 121, there occurred no apparent morphological changes in virus particles in a suspension irradiated for 10 minutes. After 30 minutes' exposure, the particles were cut into short rods. Most of the particles changed into small rods of 50 mμ or less, after 60 minutes' exposure; small globular particles appeared in the virus suspension irradiated for 90 minutes. After 2 hours of exposure, these globular particles aggregated to amorphous deposits. Table 57 shows the results of infectivity and antigenicity tests of the treated virus. The infectivity was destroyed after 10 minutes' irradiation, while the antigenicity was completely lost after 1.5 hours of exposure.

TABLE 57. Infectivity and Precipitin Reaction of Potato Virus X after UV Irradiation

UV Irradiation	Final Concentration of Antiserum					Control	Infectivity*	
	16	32	64	128	256		Tomato	*D. stramonium*
Control	+	+	+	+	+	−	5/5	5/5
10 cm, 5 min.							0/5	1/5
1 » 10 »							0/5	0/5
» 30 »	+	+	+	+	±	−		
» 1 hour	+	±	−	−	−	−		
» 1.5 »	−	−	−	−	−	−		
» 2 »	−	−	−	−	−	−		
» 2.5 »	−	−	−	−	−	−		
» 3 »	−	−	−	−	−	−		
» 3.5 »	−	−	−	−	−	−		
» 4 »	−	−	−	−	−	−		

* Same as Table 55

D. Ultrathin sectioning

Leaves of *N. glutionsa* plants infected with potato virus X, strain X-5, were used in the experiment. About 10 days after inoculation, the diseased leaves, cut into pieces of about 2 × 4 mm., were fixed with 1% osmium tetroxide at pH 7.0 for 24 hours, dehydrated with graded ethanol solution, and then embedded in methacrylate resin.

Fig. 123 shows one of the cross sections of a diseased leaf of a *N. glutinosa* plant. No remarkable morphological changes in the nuclei or chloroplasts were seen in the cells of diseased leaves. Virus particles were detected in the cytoplasm, but could not be found in the cell nuclei or chloroplasts, as shown in Figs. 123 to 128. They were usually surrounded by some membranous substances which seemed to consist of granular, electron dense materials, as shown in Fig. 125. Most of the virus particles showed end-to-end aggregation (Fig. 127).

Fig. 128 shows that a virus mass burst and the particles were freed into the cytoplasm of the cell. At the end of virus threads, the particles scattered and they were of uniform length of about 530 mμ.

E. Discussion and conclusions

The previously reported results of measurements of potato virus X are summarized in Table 58. As can be seen, there were small differences between the average length of potato virus X, according to earlier investigators.

TABLE 58. Length of Potato Virus X

Authors	Year	Length of PVX
TAKAHASHI & RAWLINS	1946	500–600 mμ X 14–18 mμ
BODE u. KÖHLER	1952	600–620 mμ (X^N strain)
		560–580 mμ (X^E strain)
BODE	1954	525 mμ
BODE u. PAUL	1955	500–525 mμ
WETTER u. BRANDES	1956	513 mμ
REICHMANN	1958	540 mμ

TAKAHASHI and RAWLINS (1947 b) and BODE and KÖHLER (1952) concluded that there were significant differences in length between particles of two strains of the virus. However, the experiment in this paper shows that there were little differences in length between the four tested strains of potato virus X, which is in line also with previous reports concerning tobacco mosaic virus (KNIGHT and OSTER, 1947; OSTER, KNIGHT, and STANLEY, 1947; TAKAHASHI and RAWLINS, 1946).

BAWDEN and PIRIE (1936) and BAWDEN (1939) stated that infectivity of potato virus X was affected by various hydrogen ion concentrations and the author also examined in detail the effect of hydrogen ion concentration on tobacco mosaic virus in Chapter IV.

When potato virus X was treated at pH 2.2 and 11.1, the virus particles were cut into short rods intermingled with small globular particles. Slight antigenicity remained, while infectivity was completely destroyed.

BAWDEN and PIRIE (1938) as well as BAWDEN (1950 a) reported that potato virus X lost its infectivity by ultraviolet irradiation without loss of antigenicity. MURAYAMA (1959) confirmed their results. He found that the antigenicity of potato virus X was destroyed after continuous exposure to ultraviolet light. Loss of antigenicity of potato virus X was recognized after disappearance of the shortened rods.

The findings, that exposure to ultraviolet light denatured potato virus X particles, are reminiscent of the results reported in Chapter IV; they parallel the findings with tobacco mosaic virus exposed to UV irradiation.

BRANDES (1957) as well as KIKUMOTO and MATSUI (1960) observed by the electron microscope potato virus X particles in ultrathin sections of leaves of diseased plants. The author also observed masses of filamentous particles of potato virus X in the cytoplasm of diseased cells of *N. glutionsa* plants.

The nuclei, chloroplasts, and mitochondria in diseased cells seemed to be unaffected and no virus particles could be found in them.

KIKUMOTO and MATSUI (1960) reported that a membranous or fine granular organelle was observed around the virus masses. Similar membranes were seen surrounding the virus mass, as shown in Fig. 125.

Additional photographs of Figs. 126 to 128 show that the virus particles were liberated from these membranes. The end of the virus filaments appeared to be separated into particles corresponding with the normal length of the virus.

VI. Barley stripe mosaic virus

A. Isolation and purification of barley stripe mosaic virus

Diseased leaves of barley or of sweet corn plants were macerated in 1/15 M phosphate buffer at pH 7. The expressed juice was centrifuged at 3.500 rpm for 30 minutes and the suspernatant was frozen overnight. After thawing, the juice was centrifuged at 3,500 rpm for 30 minutes. The virus was purified by alternate differential centrifugation at 8,000 rpm for 30 minutes and at 30,000 rpm for 2 hours.

The precipitates containing the virus were dissolved in phosphate buffer solutions. These preparations were used for electron microscopic examinations and were found to contain impurities.

Therefore, further, purifications were carried out using density gradient centrifugation with graded concentrations of sucrose solutions. The gradient

columns were formed from 1 cm layers of buffered solutions containing 100, 200, 300, and 400 gm sucrose per liter. The concentrated virus solutions were placed on the top of the sucrose solutions and then centrifuged at 20,000 rpm for 60 minutes using RP 40 Rotor of Hitachi's preparative ultracentrifuge Model 40 P.

Visible virus zones were obtained between 2.5 to 3.1 cm from the bottom.

From the results of infectivity tests and electron microscopic observations, it was determined that the virus particles were concentrated in the visible zone between 2.5 and 3.1 cm. from the bottom.

B. Size and shape of barley stripe mosaic virus

It was observed that the barley stripe mosaic virus had the shape of short rods, of uniform size, as shown in Figs. 129 to 132.

Length distribution of the virus isolated from diseased barley and corn plants is shown in Tables 59 to 62 and Diagram 31 and 32. An average length of the particles was calculated as 126 mμ and 129 mμ from diseased braley and corn plants, respectively.

TABLE 59. Particle Length of Barley Stripe Mosaic Virus Isolated from Diseased Barley Plants

Length (mμ)	No. of Particles			Total	Length (mμ)	No. of Particles			Total
	I	II	III			I	II	III	
20					340		1		1
40		2	1	3	360	1	2		3
60	17	29	14	60	380	1			1
80	22	38	15	75	400				
100	51	71	16	138	420				
120	76	73	21	170	440				
140	109	97	37	243	460				
160	44	56	30	130	480				
180	39	44	20	103	500				
200	33	23	12	68	520				
220	15	24	7	46	540				
240	12	18	3	33	560				
260	6	16	5	27	580				
280	5	7	4	16	600				
300	4	6	3	13	Toatl	436	508	188	1132
320	1	1		2					

TABLE 60. Average Length of Barley Stripe Mosaic Virus Particles Isolated from Diseased Barley Plants

No, of Experiments	I	II	III	Total
No. of Particles	406	455	172	1033
Average Length (mμ)	128	124	128	126
Standard Deviation	38.3	41.4	41.4	41.0
Standard Error	1.9	1.9	3.2	1.3

TABLE 61. Particle Length of Barley Stripe Mosaic Virus Isolated from Diseased Corn Plants

Length (mμ)	No. of Particles	Length (mμ)	No. of Particles
0		320	3
20		340	5
40		360	1
60	4	380	3
80	10	400	
100	16	420	
120	14	440	2
140	20	460	
160	15	480	
180	18	500	
200	8	520	
220	3	540	2
240	10	560	
260	4	580	
280	2	600	
300	3	Total	143

TABLE 62. Average Length of Barley Stripe Mosaic Virus Isolated from Diseased Corn Plants

No. of Particles	108
Average Length (mμ)	129
Standard Deviation	41.4
Standard Error	3.9

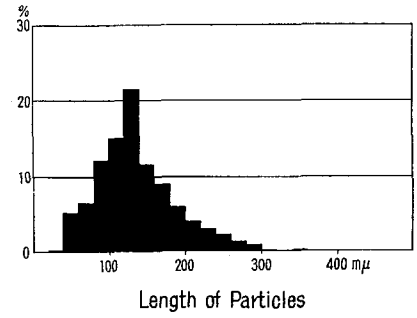

Diagram 31. Length Distribution of Barley Stripe Mosaic Virus Particles from Diseased Barley Plants.

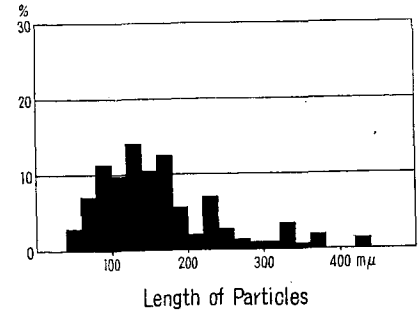

Diagram 32. Length Distribution of Barley Stripe Mosaic Virus Particles Isolated from Diseased Corn Plants.

Measurements of the particle diameter were carried out on chromium-shadowed particles. Particles, placed parallel to the shadowing direction, were used for measurements. When compared with Latex LS-075-A, the average diameter of 44 shadowed particles was 28 mμ.

Fig. 132 showed that some of the shortened particles seemed to stand up on the supporting film. The diameter of these standing particles was also 28 mμ. In cross section the particles were found to be hexagonal in shape, having a small hole in the center. This was reminiscent of tobacco mosaic virus particles.

C. Barley stripe mosaic virus stained by phosphotungstic acid and potassium chloride

Series 1. Phosphotungstic acid

Equal volumes of 20% phosphotungstic acid were added to purified virus solution and then preserved at 0° to −5°C for 2 to 10 hours. The supernatant solution was diluted 1 : 10 and 1 : 100 with distilled water and then dried on the supporting films.

As shown in Figs. 133 to 135, stained virus particles were more clearly distinguishable than unstained particles. Fine dense threads of 5 to 8 mμ in diameter running along the axis were found in the center of the particles.

When the PTA stained particles were washed with distilled water on the grids, the thread-like structure in the virus core disappeared (Fig. 136).

Measurements of the diameter of the particles were carried out from the PTA stained materials using scattered particles, as well as those of side-by-side aggregation. An average diameter of 55 side-by-side aggregated particles was calculated as 23.5 mμ, while by measuring 73 single scattered particles a diameter of 23.64 $\pm$ 0.31 mμ was obtained.

Series 2. Potassium chloride

To the purified virus solution was added potassium chloride to make a 0.1 *M* solution, and this was preserved at 0° to 5°C for 15 hours.

The preparations were diluted 1 : 100 and 1 : 1,000 and then dried on the supporting films.

Potassium chloride stained virus particles had less contrast than those stained with PTA. A central thread-like structure was also recognized although it was not so clear as shown in Fig. 137. When stained by potassium chloride, the average diameter of the virus particles was about 25 mμ.

D. Effect of detergent on barley stripe mosaic virus

To the purified virus suspension was added sodium laurylsulfate (SLS) to

make a 0.001% solution. A drop of the mixture was heated at 60°C for 1 minute and 85°C for 1 minute in saturated vapor on the collodion film supported by the copper grids.

Figs. 138 to 140 showed that the virus particles were broken into short rods by SLS treatment. The virus particles, as shown in Fig. 140, which seemed to reveal surface structure, were found in the suspension treated with 0.001% SLS at 85°C. for 1 minute.

Figs. 141 and 142 showed an electron micrograph with a fine thread-like structure, connected to a broken rod. Similar fine threads from broken rods were sometimes observed in purified suspensions.

E. Discussion and conclusions

Regarding the size of barley stripe mosaic virus, several workers had reported different values, as shown in Table 63; GOLD *et al.* (1954) reported an average size of the virus as 130×30 mμ. KLINKOWSKI *et al.* (1958) agreed with their results. But PAWLITSCHEK (1958) measured 600 particles and concluded that the average length was 125 mμ and the diameter was 28 to 30 mμ.

TABLE 63. Size of Barley Stripe Mosaic Virus Particles

Workers	Year	Size
GOLD *et al.*	1954	130×30 mμ
KLINKOWSKI *et al.*	1958	130×30 mμ
PAULITSCHEK	1958	125×28–30 mμ (25–27 mμ)
KASSANIS *et al.*	1959	$135 \sim 175 \times 20$ mμ
BRANDES	1950	126×20 mμ

The length of the virus particles calculated by the author was 126 ± 1 mμ. This confirmed closely the results reported by BRANDES (1959).

As mentioned in Chapter III, apparent differences concerning the diameter of shadowed and unshadowed Dow latex particles have also been recognized by electron microscopic measurements of barley stripe mosaic virus. In fact, the diameter of shadowed barley stripe mosaic virus was apparently larger than the diameter of unshadowed virus particles in actual measurements.

HALL (1955) and HUXLEY (1957) considered that PTA did not cause appreciable morphological changes of the virus, and the author agreed with them, as observed in Chapter IV on tobacco mosaic virus.

Accordingly, the author confirms that the diameter of barley stripe mosaic virus is 24 mμ and the length is 126 mμ.

HUXLEY (1957) reported that a fine dense thread was observed in the centers of tobacco mosaic virus particles stained by PTA. The author agreed with this statement (Chapter IV.).

These dense thread-like structures were also seen in the center of barley stripe mosaic virus particles stained by both PTA and potassium chloride.

After washing the stained particles, this dense structure disappeared. This proved that the virus particle has a central hole of 5 to 8 mμ in diameter.

VII. Rice dwarf virus.

A. Isolation of rice dwarf virus from diseased rice plants

a) According to KIMURA (1962), chlorotic portions of diseased leaves had higher infectivity than green portions of the same leaves. This showed that the virus particles may be accumulated in the chlorotic portion of the diseased leaves. Therefore, the following experiments were carried out.

A chlorotic portion of a diseased rice leaf was cut out and macerated on a slide glass with a drop of 1/30 *M* phosphate buffer at pH 7.0. One loop of clear supernatant from macerated juice was diluted with drop of distilled water. After several successive dilutions, the final supernatant was dried on collodion films supported by copper grids, and then examined by an electron microscope.

The characteristic electron dense globular particles having 80 to 90 mμ in diameter were found in final diluted materials, as shown in Fig. 143. These particles could not be found either in macerated juice from green portions of diseased leaves or healthy leaves.

b) 0.05 gm of chlorotic portion of diseased rice leaves were cut out, macerated in 0.5 ml of 1/30 *M* phosphate buffer at pH 7.0, and centrifuged at 8,000 rpm for 30 minutes. The supernatant fluid was diluted 1 : 1000 with distilled water and dried on the collodion membranes. Under the electron microscope, a number of electron dense globular particles of about 80 mμ in diameter were found. Such particles could not be found in the preparation from green portions of the same leaves and also from the healthy leaves.

c) 10 gm of diseased leaves of rice plants were macerated in an equal volume of 1/30 *M* phosphate buffer at pH 7.0 and homogenized for 5 minutes. The expressed sap was centrifuged at 10,000 rpm for 30 minutes to remove the debris. The supernatant fluid was then centrifuged at 10,000 rpm for 2 hours. The supernatant from the 10,000 rpm centrifugation was centrifuged at 20,000 rpm for 2 hours, and the resulting supernatant was then centrifuged again at 30,000 rpm for 2 hours. The precipitates from each high speed centrifugation were dissolved in the phosphate buffers, respectively, and clarified

by centrifugation at 10,000 rpm for 30 minutes, and then examined by the electron microscope.

The electron dense globular globular particles, 60 to 90 mμ in diameter, were found most frequently in the preparation from the precipitates of 10,000 rpm centrifugation for 2 hours. The precipitates from 20,000 rpm centrifugation included few of these particles (Fig. 144), while there were no particles in the 30,000 rpm precipitates.

KIMURA (1962) had carried out infectivity tests by injecting the same materials into healthy leafhoppers. The experiments reported by KIMURA showed that most infective agents were sedimented by the centrifugation at 10,000 rpm for 2 hours. These characteristic particles were not seen in the juice from healthy rice leaves.

d) The expressed sap from diseased rice leaves was centrifuged at 3,000 rpm for 30 minutes, the supernatant was centrifuged at 5,000 rpm for 30 minutes, and then the resulting supernatant was centrifuged again at 10,000 rpm for 30 minutes. Each of the precipitates from 3,000, 5,000, and 10,000 rpm centrifugation was clarified by 3,000 rpm for 20 minutes.

The materials from each precipitate and supernatant were placed on the collodion film and examined by the electron microscope. A few virus particles were seen in the preparation from the precipitates at 10,000 rpm for 30 minutes, and a large number of particles appeared in the supernatant from 10,000 rpm for 30 minutes.

e) Expressed juice from diseased rice leaves, clarified at 5,000 rpm for 30 minutes, was centrifuged at 10,000 rpm for 30 minutes. The resulting supernatant was centrifuged at 10,000 rpm for 60 minutes, 90 minutes, and 120 minutes. Each precipitate was clarified at 5,000 rpm for 30 minutes. The virus particles were found most frequently in the preparation at 10,000 rpm for 90 minutes and 120 minutes, as shown in Figs. 145 to 147. Few virus particles appeared in the supernatant from 10,000 rpm for 120 minutes (Fig. 148).

f) Repeated precipitation was carried out by alternating high and low centrifugation at 10,000 rpm for 120 minutes. and 5,000 rpm for 30 minutes. As shown in Figs. 149 and 150, the virus particles isolated after two precipitations were morphologically unchanged. The particles were remarkably flattened after 5 times' precipitation.

The result showed that rice dwarf virus particles were concentrated at the yellowish-white portion of diseased rice leaves and most of the particles were precipitated and concentrated by the high speed centrifugation at 20,000 rpm for 120 minutes, but not precipitated by centrifugation at 10,000 rpm for 30 minutes. Suitable preparations of rice dwarf virus for electron microscopic study were

made by alternating high and low speed centrifugation at 10,000 rpm for 120 minutes and 30 minutes, respectively. Poor yield of the virus particles by this method was unavoidable. After several experiments, chloroform treatment was introduced for clarifying the plant juice and it was found successful in purifying the final product (Fig. 151). The final rice dwarf virus purification was as follows. All procedures were carried out in a cold room at 2° to 4°C.

Diseased rice dwarf leaves, 10 mgm
+
1/30 *M* phosphate buffer at pH 7.0, 50 ml
↓
Macerate
↓
Expressed juice through cheesecloth
↓
Add chloroform of 1/10 volume of expressed sap
↓
Homogenize for 5 minutes
↓
Centrifuge 3,500 rpm for 30 minutes
↓
Remove aqueous layer and centrifuge at 20,000 rpm for 60 minutes
↓
Dissolve the precipitates in a buffered solution with an equal volume of original sap
↓
Clarify the supernatants at 8,000 rpm for 30 minutes
↓
Repeat high and low centrifugation two times.

Similar particles could not be isolated from healthy rice leaves by the same isolation procedure.

B. Isolation of rice dwarf virus from diseased *Echinochloa crus-galli* Beauv

The virus was isolated by two alternating cycles of centrifugation at 10,000 rpm for 120 minutes and 30 minutes. Similar particles as those from diseased rice plants were seen by the electron microscope, as shown in Fig. 152. No such particles were found in healthy plants.

C. Isolation of rice dwarf virus from viruliferous leafhoppers

To macerated sap of 37 viruliferous leafhoppers (110 mgm) or 34 healthy insects (110 mgm) were added 5.5 ml phosphate buffer at pH 6.8 and then centrifuged to isolate the virus particles according to the same procedure as

described in Chapter VII A c. Characteristic particles similar to those isolated from diseased rice plants were also frequently found in precipitates from 10,000 rpm for 2 hours, obtained from infective leafhoppers (Figs. 153 to 155). A few of those particles were also shown in the preparation centrifuged at 20,000 rpm for 2 hours. No such particles were isolated from the sap of the 34 healthy insects.

The experiments described above were carried out in our laboratory from 1958 to 1961, parallel with the infectivity tests by the artificial injection technique wihch has been reported previously by KIMURA (1962). The results obtained in infectivity tests by KIMURA showed that the characteristic electron dense particles isolated from both rice dwarf diseased plants and infective leafhoppers were correlated to the infectivity.

It was therefore concluded that the particles isolated by differential centrifugation from diseased plants and from infective leafhoppers are the causative agent of rice dwarf disease.

D. Size and shape of rice dwarf virus particles

The chromium-shadowed virus particles isolated from diseased rice leaves by ultracentrifugation are shown in Fig. 151. The particles seen under the electron microscope were globular in shape and seemed to have an internal fine structure (Fig. 151). It is interesting to note that the shape of the shadow from the virus particles was wider than the diameter of virus particles themselves (Figs. 151 to 163). The particles isolated from diseased *Echinochloa crus-galli* and from infective leafhoppers were of similar size and shape, as shown in Figs. 152 to 155.

Unshadowed particles revealed hexagonal shape having a central darker area, surrounded by relatively transparent regions and outer envelopes (Figs. 156 to 159). Virus particles isolated by differential centrifugation were always associated with these envelopes. An accumulation of isolated particles (Figs. 156 and 166) was also accompanied with thin membranous structures which seemed to be of cytoplasmic origin of diseased cells. The envelopes were obscured by heavily shadowed particles (Figs. 160 and 161). Light shadowing, and double shadowing of particles from two sides clearly showed these envelopes (Figs. 162 to 164). A series of electron micrographs of virus particles shadowed by varying amounts of platinum revealed that the envelopes were very thin membranous structures surrounding virus particles (Figs. 166 to 168). Therefore, the width of the shadow from the particles covered with envelopes always appeared wider than the diameter of virus particles the mselves (Fig. 162 to 164). Attempts to remove envelopes from the virus particles by repeated

centrifugations were unsuccessful.

There has been substantial evidence that the virus particles have a polyhedral form, as shown in Figs. 163 to 165, by shadowed particles. PTA staining of the isolated virus particles also clearly revealed the polyhedral form but failed to show any inner structures (Fig. 169). To the purified virus suspensions was added ammonium carbonate to make a 2% solution, and then the mixture was sprayed on the collodion film using a Vaponephrin nebulizer. After drying in a vacuum chamber for 4 to 5 hours, the specimen grids were placed at 60°C for 1 hour to remove the ammonium carbonate. As shown in Fig. 170, the virus particles from ammonium carbonate suspensions also showed hexagonal shape. No envelopes were detected surrounding those particles.

The virus particles stained by 10 to 20% PTA solution for 2 to 24 hours were dried on collodion film. After washing the grids, each specimen was examined by the electron microscope with, or without, shadowing. Electron micrographs of PTA-stained particles without shadowing (Fig. 169) showed the hexagonal particles having central well-stained areas and outer, less dense regions. No clear envelopes were found around particles stained with PTA. Some of the particles isolated by centrifugation were empty with a less dense central core. Such empty particles were also revealed in the specimen of shadowed virus particles stained by PTA (Figs. 171, 172), Electron micrographs of particles shadowed with chromium (Figs. 171, 172) clearly revealed the polyhedral shape of particles, particularly well defined by the shape of the shadow of some particles (Figs. 172, 181), which seemes to suggest that the rice dwarf virus particles are icosahedron in shape, as reported for some insect viruses by SMITH and WILLIAMS (1958). No envelopes were detected in those particles. Virus particles negatively stained by 1% sodium phosphotungstate are shown in Fig. 174. Hexagonal particles with no outer projection were detected.

Table 64 shows results of diameter measurements of the rice dwarf virus particle, isolated from plant and insect hosts and prepared by various methods for electron microscopy.

As mentioned in Chapter III, the shadowed particles measured by electron microscopy were positively larger than unshadowed particles. Therefore it was concluded that the actual size of rice dwarf virus particles is approximately 70 mμ in diameter.

It was not possible to demonstrate the three-dimensional structure by freeze-drying, using the apparatus described by NEI, SAKAI and SHIKATA (1956). It is of interest that the particles from freeze-dried preparations had

TABLE 64. Sizs of Rice Dwarf Virus Particles Isolated from Three Different Hosts

	Sample	Number of Particles Measured	Diameter
Isolated from Rice Leaves	Unshadowed Particle	132	68 mμ
	Unshadowed Particle (Central Core)	47	42
	Cr-shadowed (Diameter)	349	89
	Cr-shadowed (Height)	50	70 *
	Soft Cr-shadowed	37	69
	Aggregated Particles	29	73
	Right Angle Double Shadowed	73	87
	Opposite Direction Double Shadowed (Heavy)	16	92
	Opposite Direction Double Shadowed (Soft)	77	75
	PTA Stained Particles	231	75
Isolated from Echinochloa Crus-galli	Cr-shadowed Particles	17	84
	Aggregated Particles	10	67
	Aggregated Particles (Central Core)	10	42
Isolated from Leafhoppers	Cr-shadowed Particles	34	88

* Compared by Shadow Length from Dow Latex Particles.

narrower shadows than the diameter of virus particles (Fig. 175).

In an attempt to remove the envelopes surrounding the virus particles, isolated virus suspensions were treated by repeated freeze-thawing, formalin, ethanol, ether, phenol, acid solution, alkaline solution, preservation for several days in a cold room, heating, and sodium lauryl sulphite. All of these treatments failed to remove the envelopes without destroying the particles. However, some morphological changes, showing the inner structure of the particles, were observed in those treated in purified suspensions.

When the virus suspension was heated at 74°C for 10 minutes, most particles were distorted into smaller globular particles and fine thread-like particles were frequently observed over the supporting films (Fig. 176). Similar small granules were also found in the preparation of 50% ethanol precipitation (Figs. 177, 178), after repeated centrifugation (Figs. 179 to 183), and with 50% ether precipitation (Figs. 184 to 185). The virus particles were precipitated from 25, 33, and 50% ethanol solutions without noticeable morphological changes. Some particles seemed to be destroyed by 50% ethanol precipitation,

revealing an inner structurel. There were a few particles that remained in the supernatants of 25% ethanol precipitation. In a 50% cold ether suspension of rice dwarf virus, most particles were precipitated by 5,000 rpm centrifugation without significant morphological changes. However, some of the particles showed their internal structure,

In an attempt to observe the fine structure of the particles, negative staining was employed, using a purified virus suspension obtained by a slightly modified chloroform emulsion technique (SCHNEIDER, 1953) and by hot ether treatment. The isolated virus suspension was treated with twice its volume of ether at 70°C for 40 at 60 minutes. The aqueous phase was then removed and dilyzed against 1% ammonium acetate solution for 2 hours at 5°C. The virus suspension treated with hot ether was mixed with equal volume of 1% PTA at pH 7 and then placed on the collodion films. As shown in Figs. 186 and 187, individual particles showed a hexagonal outline and appeared clearly to have outer projections, which were not seen in partially purified preparations. A lot of empty capsids with capsomeres, which probably were destroyed by hot ether treatment, were revealed in the preparation.

Another sample of negatively stained virus particles, prepared by the chloroform emulsion technique, also revealed the fine structure of the virus particles, as shown tn Figs. 188 to 193. The diameter of the negatively stained particles is 70 mμ, with capsomeres 9.5 mμ long and 5.5 mμ in diameter. Figs. 194 to 196 show the virus particles somewhat destroyed during preparation, with capsomeres seemingly flattened on the supporting membrane. High magnification electron micrographs suggest that the capsomere has a hexgonal cross section of approximately 6 mμ in diameter (Figs. 197 to 199). Within a negatively stained preparation of purified virus some disrupted particles were sometimes seen, as shown in Figs. 200 and 201, releasing a long band from the disrupted particles. The width of the band was 10 mμ, which corresponds with the length of the capsomeres of rice dwarf virus particles. It seems likely that a capsomere is built up from smaller fine rods, as revealed in Figs. 198 and 201.

A pellet of partially purified virus particles was fixed with 1% osmic acid and then embedded in methacrylate. Utrathiln sections of these partially purified pellets were cut and then stained by 2% uranyl acetate. Electron micrographs of the sections revealed loose scattered virus particles within pellets. The size of the particles embedded in methacrylate resin are somewhat elongated and considerably smaller than isolated virus particles. Electron micrographs of the sections of partially purified virus pellets revealed membranous structures intermingled with the particles; these resembled envelopes, associated with the

virus particles within thin sections. The diameter of the rice dwarf virus particles in thin sections is approximately 60×40 mμ. The particles have a central darker core and a less dense surrounding area (Figs. 202 to 204). Some internal structure was also discernible in the particles of ultrathin sections stained by uranyl acetate, as shown in Fig. 202.

E. Ultrathin sections of diseased rice leaves

Yellowish-white portions of the diseased leaves of rice plants were cut into pieces of 7 to 8×2 to 3 mm. and then fixed with 1% osmic acid in 1/100 *M* phoshate buffer at pH 7.0 with 0.1 *M* sucrose for 24 to 48 hours at 4°C. After dehydration with graded alcohol, the materials were embedded in methacrylate resin and then cut into ultrathin sections of about 25 to 50 mμ thick, using a UM-4 or UM-5 ultramicrotome equipped with glass knives. Pieces of healthy rice leaves were also embedded in methacrylate and cut into thin sections. In an ultrathin section from a healthy rice leaf, as shown in Fig. 218, the epidermis has a thick silicaceous layer. There were many chloroplasts in the palisade cells and in mesophyll cells. Large vacuoles usually developed in parenchymatous cells so that the cytoplasm of the cells was limited to a narrow area around the cell wall. There were abundant intracellular spaces in the healthy leaves. In the leaves infected with rice dwarf virus, there appeared some cells with disintegrated chloroplasts or without chloroplasts (Figs. 219 to 220). Such chlorotic cells were usually found near vascular bundles of the diseased leaves.

Accumulations of particles having the characteristic size and shape of rice dwarf virus were frequently found in the chlorotic cells, as shown in Fig. 205. Sometimes the virus masses were found beside the nuclei of the cell (Fig. 206). Except for virus masses in the cells of diseased leaves, there were no virus particles found in the nuclei, chloroplasts, or mitochondria of infected cells. There were no particular organelles found, having similar size to nuclei, that would resemble X-bodies or inclusion bodies. The size of virus particles found in the cells of diseased rice leaves embedded in metacrylate resin was 40 to 60 mμ in diameter, which corresponds to the size of the particles from purified pellets embedded in methacrylate.

In young leaves, approximately 10 to 20 days aftter infection, it was found that the virus particles were loosely arranged or scattered throughout the cytoplasm of infected cells (Fig. 207). In old diseased leaves, more than 30 days after infection, there were accumlations of compactly or regularly arranged virus particles in the infected cells (Fig. 208).

Figs. 209 to 213 show chromium-shadowed sections as they appeared after methacrylate resin was dissolved by xylene. The virus particles enclosed by

thin membranes were clearly seen in these pictures. Such shadowed particles are very similar to those shown in isolated virus particles. Regularly arranged virus particles were also found in the diseased cells, as shown in Fig. 212.

Tubular structures which contained strings of virus particles were sometimes observed in the diseased plant cells, as shown in Figs. 214 and 215. The diameter of these tubular structures was about 60 to 80 mμ. The virus particles were arranged inside of these structures. Several layers of tubular structures including virus particles are also shown in Fig. 217.. A figure in Fig. 216 seems to represent across section of the tubular structures with the virus particles inside. It was also interesting to note that the virus particles seem to be arranged within some thin membranous structures in the cytoplasm of diseased cells, as indicated in Fig. 217, in the group of scattered virus particles below the tubular structures.

Some cytological changes were observed in the yellowish-white partion of young infected leaves removed 10 to 15 days after infection. When the sections were cut in the direction from a green portion to a chlorotic portion, there appeared some disordered cell arrangements. The palisade cells were shortened, while the parenchyma cells were somewhat larger in size, being filled with cytoplasmic substances, as compared to healthy rice leaves (Figs. 218 and 219). There were no virus particles in the cells shown in Fig. 219. A few sections further from those shown in Fig. 219, a loose accumulation of virus particles was found in one of the parenchyma cells (Figs. 220 and 221). Numerous virus particles were encountered in the defined area surrounded by a thin membrane. In the young infected leaves, virus particles were usually scattered loosely or accumulated in small masses, arranged in some cytoplasmic structure, as shown in Figs. 222 and 223. Figs. 224 and 225 show the cytoplasmic changes which were found in the cell of a green portion of a diseased leaf of a young infected plant (Fig. 224) and also very close to infected cells of the chlorotic portion of the same specimen (Fig. 225).

F. Ultrathin sections of infective leafhoppers

Viruliferous leafhoppers which were maintained on diseased rice plants were examined for their infectivity individually on young rice seedlings. After symtom appeared on the test plant, the infective insects were dissected. Salivary glands, ovarian tubules, and abdomens were cut and fixed with 1% osmium tetroxide in 1/100 *M* phosphate buffer solution for 24 hours at 4°C.

The size and shape of virus particles of rice dwarf disease were found in the cells of fathody, Malpighian tubules, epithelial cells of the intstine, salivary grand, and ovarian tubules.

In the cells of the fatbody, the virus particles were usually found in a defined structure, with accumulation of virus particles in the cytoplasm of the cells. Individually scattered virus particles were also found in rare cases in the cytoplasm of fatbody cells, as shown in Fig. 226. Electron micrographs of shadowed thin sections revealed clearly charcteristic particles similar to those found in purified suspensions and in ultrathin sections from diseased rice leaves (Fig. 227). These virus clusters were usually encountered in the cytoplasm of fatbody cells from infective leafhoppers (Fig. 228), but not in nuclei or mitochondria. Virus particles were also frequently found in cells which were considered to be blood cells, as shown in Figs. 229 and 231. In such cells there appeared accumulations of virus particles, or scattered particles. Regularly arranged virus particles are shown in Figs. 232 to 235, prepared from thin sections of an abdomen. Virus clusters were usually encountered in defined structures surrounded by membranes. Fig. 232 shows the crystalline aggregation of virus particles encountered in the thin sections of the abdomen. High magnification of the crystalline virus arrangment is shown in Fig. 233. Single particles in the electron micrographs revealed the hexagonal structure of the particles, having a central darker area and a less dense outer part. The size of the virus particles was measured and determined as 40 to 60 mμ in diameter, by center-to-center measurement and by single particle measurements. Such crystalline arrangments of virus clusters surrounded by membranes were also found in the cells of Malpighian tubules (Figs. 233, 234). The virus cluters usually appeared in the cytoplasm of cells, but not in the vesicles including brochosomes (DAY and BRIGGS 1958), nuclei, and mitochoondria.

As shown in Figs. 236 to 238, an abundance of vacuolated cells were observed in the infected fatbody tissues. It was hard to identify cell membranes separating individual cells. The size of the defined structures including virus particles approximately corresponds to the size of mitochondria, as shown in Figs. 236, 237.

Virus particles, intermingled with smaller dense particles, approximately 10 to 20 mμ in diameter, were surrounded by several layers of fine membranes. Such membranes seemed to represent smooth endoplasmic reticulum, as shown in Fig. 239. Usually these membranes were enclosing the virus clusters (Fig. 238), but sometimes they did not completely enclose them (Fig. 239). Virus particles in the infected fatbody, associated with well developed smooth endoplasmic reticulum, are also shown in Figs. 240 to 242. Strings of virus particles arranged within tubular structures were also found in those areas. The diameter of those tubular structures was about 60 to 70 mμ, which was similar to tubular structures found in plant cells infected with rice dwarf virus. Virus

clusters with crystalline array were also found in the cytoplasm of epithelial cells of the intestine (Figs. 243, 244).

In salivary glands, virus particles were encountered in defined vesicles within the cytoplasm of cells, as shown in Fig. 245. However, virus particles were not detected in all lobes of a salivary gland from an infected leafhopper. Figs. 246, 247 showed the virus accumulations enclosed by dense substances or scattered in defined vesicles surrounded by a membrane. Other accumulations found in the salivary gland cells were compact, containing many virus particles in a particular vesicle, which seemed to be a salivary product (Figs. 248, 249, 252). Strings of virus particles arranged within tubular structures were also observed in those vesicles (Figs. 250, 251, 253). The rice dwarf virus particles were also found in the thin sections from ovarian tubules of infected female insects, as shown in Figs. 254, 255. No virus particles were detetced in muscle cells, trachea, and the nervous system of infective insects.

G. Discussion and conclusions.

BRANDES and WETTER (1959) have attempted the classification of rod-shaped and elongated plant viruses from a morphological point of view. No proposal has been made until now for a classification of globular-shaped plant viruses. Recently, the study of the fine structure of virus particles has been developed by the application of negative staining and the help of the improved high resolution electron mitroscope. This may enable us to study in more detail the morphology of globular virus particles for the purpose of classification.

Amonug the globular plant viruses as shown in Table 65, wound tumor virus is one of the most throughly studied, and first in which the virus particles were recovered from both plant and insect hosts, (BRAKKE, VATTER and BLACK, 1954). There has been no information available regarding the size and shape of persistent leafhopper borne plant viruses other than wound tumor virus. In addition, no paper has been reported concerning the site of virus multiplication and accumulation in the plant host and in insect vectors, not even for wound tumor virus.

In an attempt to find the rice dwarf virus particles in cells of its plant host and insect vector, the author carried out the following experiments: 1) Isolation of virus particles from diseased plants, 2) Isolation of virus particles from viruliferous leafhoppers, 3) Ultrathin sections of the leaves of diseased rice plants, and 4) Ultrathin sections of viruliferous leafhoppers.

As described in this report, the polyhedral particles of 70 mμ in diameter were isolated from both diseased rice leaves and diseased *Eichinochloa crus-galli*, and from infective leafhoppers. In addition, by means of ultrathin

sections, particles of the same size and shape as purified virus were found in the cells of diseased leaves of rice plants as well as in the fat body, epithelial cells of the intestine, blood cells, Malpighian tubules, ovarian tubules, and salivary glands of infective leafhoppers. The infectivity of isolated virus suspensions was examined and found to be high (KIMURA, 1962). Thus, all the evidence mentioned above leads to the conclusion that the particles isolated from both diseased rice leaves and infective insects, and found in ultrathin sections from both hosts, are the causative virus of rice dwarf disease. It is worthy to mention that these are the first electron micrographs of a leafhopper borne plant virus *in situ* in its plant and insect hosts.

SMITH and WILLIAMS (1958) showed for the first time by the double shadowed technique that particles of *Tipula iridescent* virus have the shape of an icosahedron. Recent experiments also showed that some of the plant viruses have the same structure (KAESEBERG 1956, HARRISON and NIXON 1960). The electron micrographs of rice dwarf virus taken by chromium-shadowing, PTA staining and ammonium carbonate suspension indicate that the particles also have an icosahedron structure.

Among the spherical plant viruses, tomato spotted wilt virus (BLACK, 1955), potato yellow dwarf virus (BRAKKE, BLACK and WYCKOFF, 1951), wound tumor virus (BLACK, 1955) and rice dwarf virus belong to the group of larger viruses being more than 60 mμ in diameter. Their size and shape bear close resemblance to some of the insect viruses (SMITH and WILLIAMS, 1958; WILLIAMS and SMITH, 1957).

As pointed out by FUKUSHI, SHIKATA and KIMURA (1962), it is most likely that crystalline arrangement of virus particles in their host cells showed the actual mode and site of virus multiplication *in situ*. Therefore, it is possible to say that finding of rice dwarf virus particles either in accumulations or in a crystalline array within the vector strongly confirm the fact of virus multiplication of rice dwarf virus in its insect vector which has been demonstrated experimentally by FUKUSHI (1940).

According to FUKUSHI (1931, 1934), intracelular bodies could be detected in diseased leaves of rice plants, while no particular organelles which would be inclusion bodies could be found in the insect vectors. In spite of the huge number of examined thin sections from diseased leaves, numbering into the hundreds, the author failed to find the particular structure which could be interpreted as the so-called X-body or inclusion body as MATSUI (1958 c, d) reported in the cells of tobacco mosaic virus infected tobacco leaves. Only virus clusters appeared in the diseased leaves, almost similar in size to nuclei, and sometimes found close together.

TABLE 65, Diameter of Spherical Virus Particles

Virus	Size (mμ)	Shape	Workers
Alfalfa Mosaic Virus	50×20		BANCROFT (1958)
Arabis Mosaic Virus	29 - 30	Polyhedron	HARRISON & NIXON (1960)
Aster Yellows Virus	30×50 ?	Globular ?	PROTSENKO (1958)
Broad Bean Mosaic Virus	25 - 30	Polyhedron	PAUL, BRANDES u. QUANTZ (1958)
Carnation Mosaic Virus	31	Globular	AMES & THORNBERRY (1952)
Cucumber Mosaic Virus	35	"	SILL, BURGER, STAHMANN & WALKER (1952)
	40	"	TOMLINSON, SHEPHERD & WALKER (1959)
Potato Stolbur Virus	65 ± 11	"	BLATTNY (1958)
Potato Yellow Dwarf Virus	110		BRAKKE, BLACK & WYCKOFF (1951)
Prune Dwarf Virus	22	Globular	FULTON (1959)
Raspberry Ring Spot Virus	29 - 30	Polyhedron	HARRISON & NIXON (1960)
Rothamsted Tobacco Necrosis Virus	14.6	Globular	LABAW (1959)
Sunn Hemp Mosaic Virus	62 - 40	"	DAS GUPTA (1951)
	37.4+6	"	DE (1951)
Sourcherry Necrotic Ring Spot Virus	23	"	FULTON (1959)
Southern Bean Mosaic Virus	25	"	PRICE, WILLIAMAS & WYCKOFF (1946)
	24.5	"	LABAW & WYCKOFF (1957)
Tobacco Leaf Curl Virus	39	"	SHARP & WOLF (1951)

Tobacco Necrosis Virus	20	Globular	STANLEY & ANDERSON (1941)
	25	"	LABAW (1958)
Tobacco Ring Spot Virus	25	Polyhedron	WILLIAMS (1953)
	25	"	STEERE (1953)
Tomato Black Ring Virus	29 - 30	"	HARRISON & NIXON (1960)
Tomato Bushy Stunt Virus	30 ± 1	"	WILLIAMS (1953)
Tomato Ring Spot Virus	43～13.5 Average 27	"	SENSENEY, KAHN & DESJARDINS (1954)
Tomato Spotted Wilt Virus	85	"	BLACK (1955)
Turnip Y ellow Mosiac Virus	26	Globular	COSENTINO, PAIGEN & STEERE (1956)
		Polyhedron	KAESBERG (1956)
Wild Cucumber Mosaic Virus	28	"	SINCLAIR, GEIL & KAESBERG (1957)
Wound Tumor Virus	80	"	BRAKKE, VATTER & BLACK (1954)
	75	"	BLACK (1955)

Observations carried out on thin sections from young diseased leaves showed that the site of virus multiplication probably was in the cytoplasm of the infected cells. The virus particles appeared in the cells of the chlorotic portion next to cells of a green portion from infected leaves, usually scattered in the cytoplasm or as small masses associated with some membranous structures. When the diseased leaves were cut in the direction from a green portion to a chlorotic portion, larger virus accumulations were usually encountered in the cells of the chlorotic portion. Almost the same arrangements were also found in sections from chlorotic portions of infected leaves after shorter and longer periods of infection. In the leaves after less than 20 days of infection, the virus particles filled the cytoplasm of infected cells, forming loose masses, while after 2 months of infection most of the virus clusters were crystalline in arrangement or forming compact masses. No particular structures except virus clusters, often as large as the nuclei, could be found in young and old infected leaves.

It is most likely that the inclusion bodies reported by FUKUSHI (1931 and 1934) are the same as the virus inclusions detected by electron microscopy. There has been no evidence to suspect that rice dwarf virus multiplies in defined cell organelles, such as nucleus or mitochondria and plastids.

Crystalline arrangements of virus clusters were also detected in the thin sections from various organs of infected leafhoppers, mostly in fatbody, Malpighian tubules and gut. Usually the size of virus clusters was smaller than that of a nucleus, and more similar in size to that of mitochondria in insects. Therefore, the virus mass occupied a relatively small area within insected cells, causing neither death nor appreciable damage, as would be the case if they filled the whole area in a cell. In plant cells, on the other hand, large masses of virus particles accumulated within the infected plant cells. The rice dwarf virus particles seem to bear a morphological resemblance to some of the insect viruses rather than to plant viruses. Yet there has been no evidence to indicate that rice dwarf virus would completely destory the cell structure of an infected insect and consequently kill the insect.

LITTAU and MARAMOROSCH (1956 and 1960) have reported the first evidence that histological changes may take place in the infected fat body of leafhoppers transmitting aster yellows virus. As far as the author could determine, most infected fatbodies from diseased leafhopper vectors of rice dwarf virus showed an extremely vacuolated structure. It was very difficult to identify each cell in the infected fat body tissue, because infected cells seemed to combine, joining together, and the cytoplasm of these cells was squeezed against the cell wall by extensive vacuoles. While many vacuoles were occasionally

observed in some cells of the fatbodies of healthy insects, their size and numbers were considerably smaller than those of infective leafhoppers. In addition, the cell walls usually were cleary visible in the fatbody of healthy insects. The results clearly confirmed the first finding on aster yellows infected vectors by LITTAU and MARAMOROSCH (1956) and the light microscope study on rice dwarf virus infected vectors by NASU (1963).

FUKUSHI did not find inclusion bodies or X-bodies in infective leafhoppers of rice dwarf virus disease. Electron micrographs through the thin sections of infective leafhoppers revealed the presence of abundant crystalline arrangements of virus particles. It is possible to say that the crystalline inclusions of the rice dwarf virus were found in the various organs of diseased leafhoppers, although their size and shape were too small to identify under the light microscope.

Tubular structures including or surrounding a string of virus particles are a new finding. They seem to be comprised of smooth endoplastic reticulum on which virus particles were arranged. Further observations will be carried out to determine the nature and role of those structures.

Electron microscopic studies of ultrathin sections form diseased rice leaves and infective insects and of isolated virus particles strongly support the fact that rice dwarf virus belongs to the group of viruses closely linking insect viruses and plant viruses. (MARAMOROSCH, 1955).

Similar to wound tumor virus (BRAKKE, VATTER and BLACK, 1954), rice dwarf virus particles of identical size and morphology were also isolated from both plant and insect hosts.

The evidence obtained through thin sections from infective insects may explain the circulation of virus particles in the insect vector. The virus particles acquired by vectors from diseased leaves may infect gut cells and multiply in them. The virus particles may infect blood cells and fatbody cells. Salivary gland cells may obtain virus particles from blood cells. A supply of virus for the blood and salivary gland cells may come from fatbody cells which appear to be the main organ of virus multiplication in insects. The abundance of virus in the salivary gland cells may explain the rather high infectivity record of rice dwarf vectors. However, questions still remain unanswered whether the virus can multiply in the blood cells and in salivary gland cells. So far as the author could determine through ultrathin sections, the location and structure of virus accumulations in those organs were quite similar to those found in other infected organs from diseased insects. This may suggest that the virus particles multiply in blood cells and also in the salivary gland. Further experiments should be carried out regarding multiplication of virus particles in

blood cells and in the salivary gland.

The author failed to find virus particles in eggs of viruliferous female insects, but detected numerous virus particles in ovarian tubules, probably in nurse cells. No virus could be found in follicle cells of ovarian tubules. The accurate localization of rice dwarf virus particles in the ovarian tubules and ovary can help in the understanding of the mechanism of transovarial transmission of this virus.

VIII. Summary

1. Morphological studies were carried out on tobacco mosaic virus, potato virus X, barley stripe mosaic virus, and rice dwarf virus by means of electron microscope.

2. In regard to the calculation of the size of virus particles, it was shown that the magnification of the electron microscope can be determined using grating replica and Dow latex particles, provided careful attention is given to errors caused by shrinkage of replica films, contamination on Dow latex particles in the electron microscope, and differences between the diameters of shadowed and unshadowed particles.

3. The chemically purified tobacco mosaic virus particle is rod-shaped, 300 mμ long, and 15 to 20 mμ wide.

4. Tobacco mosaic virus particles stained by 10% phospotungstic acid clearly contrasted with the background and revealed their fine thread-like structure in the center of the rods.

5. When tobacco mosaic virus particles were heated after dialyzing against tap water, rod-shaped particles were getting shorter and shorter as temperature increased. Finally the rods changed into globular particles and settled together with amorphous precipitates. When tobacco mosaic virus particles were suspended in a buffered solution at pH 7.0 and heated, no aggregation of particles was observed. However, the particles also became shorter by treatment at higher temperature, and then changed into globular particles. Loss of infectivity and antigenicity of the virus suspensions at pH 7.0 took place at 80°C for 10 minutes, at which temperature most of the particles in the suspension were changed to globular deposits. UV absorption spectrum showed that the viral RNA was freed from the virus protein at 80°C after 1 minute heating.

6. Tobacco mosaic virus particles have a tendency to aggregate in acid solution from pH 7.0 to 3.3. At pH 3.3, paracrystalline aggregates of virus particles were seen in the suspension after drying on collodion films. Below pH 3.3, the rod-shaped particles were changed into globular particles and they lost their infectivity and antigenicity.

As the pH of the virus suspension went up, the rod-shaped particles became shorter and finally changed into globular particles at pH 11.1 and pH 12.4, being inactivated at the same time and losing their antigenicity.

7. Tobacco mosaic virus particles lost their infectivity without morphological changes of particles after treating by H_2O_2. The virus rods became shortened after treatment with high concentrations or longer pariods of H_2O_2 treatments. The effect of H_2O_2 on tobacco mosaic virus particles was more severe in alkaline solution than in acid solution. After treatment with 5% H_2O_2 at pH 9.0 for 15 hours and 10% H_2O_2 at pH 8.3 for 48 hours, only globular particles were present in the virus suspension, and their antigenicity was lost.

8. Formalin destroyed the infectivity of tobacco mosaic virus suspension without affecting particle morphology or virus antigenicity.

9. $NaNO_2$ treatment of tobacco mosaic virus did not cause any morphological changes nor affect antigenicity, in spite of loss of infectivity after treatment with 5% $NaNO_2$ at pH 3.3 for 24 hours.

10. Loss of infectivity occurred in UV irradiated virus suspension without morphological and antigenetic changes. Longer irradiation by UV light on tobacco mosaic virus particles caused destruction of particles and denatured the rods into globular particles. No antigenicity was retained in the suspension of globular particles. Virus RNA was not liberated from virus protein by UV irradiation.

11. X-ray treatments caused loss of infectivity of tobacco mosaic virus particles and breaking of rods, without loss of antigenicity. The shortened rod particles gradually changed into globular particles as dosage of X-ray increased.

12. Fine thread-like structures which seemed to be RNA threads were released from the tobacco mosaic virus particles after treatmemt with sodium lauryl sulfate.

13. Electron micrographs of ultrathin sections from tobacco leaves infected with tobacco mosaic virus revealed bands of virus aggregation in epidermal cells and parenchyma cells. No virus particles were found in the cells of necrotic portions of *N. glutinosa* except in vascular bundles.

14. There were no differences in morphology between 4 strains of potato virus X. The average size of the virus is 529 mμ in length and 10 to 15 mμ in width.

15. Potato virus X particles have a tendency to aggregate into long threads in an acidic suspension, while in alkaline solution the particles are cut into short rods and changed into globular particles that lose their infectivity and antigenicity.

16. Following UV irradiation infectivity of potato virus particles was lost without morphological changes. However, continuous irradiation caused breaking of rod-shaped particles and appearance of globular particles. Antigenicity was also lost after rod particles disappeared in the suspension.

17. Ultrathin sections from *N. glutinosa* plants infected with potato virus X revealed masses of potato virus X being embedded in dense granular substances in the cells.

18. The size of barley stripe mosaic virus particles was calculated as 126 mμ long and 24 mμ in diameter. Electron microscopy of phosphotungstic acid stained particles clearly showed their rod structure without shadowing, and a fine thread-like structure in the center of the rods, parallel to the long axis, was observed.

20. Successful isolation of rice dwarf virus particles from diseased rice plants, *Echinochloa crus-galii*, and from viruliferous leafhoppers was carried out by differential centrifugation.

21. The size and shape of rice dwarf virus particles isolated from diseased plants and from infective insects were similar, 70 mμ in diameter, with surrounding envelopes. It was also shown by means of an electron microscope that the particles have a polyhedral structure. Negative staining of the virus particles showed their fine structure, with projected subunits and a central core.

22. Similar particles were also found in ultrathin sections of cells of infected rice leaves. Regular arranged particles were encountered in the cytoplasm of chlorotic portions of the cells. No virus particles were found in the nucleus and mitochondria of such cells.

23. Rice dwarf virus particles were also found in the cells of fatbody, Malpighian tubules, gut, blood cells, salivary gland, and ovarian tubules of the infected leafhoppers. Their size and shape did not differ from that of the infected plants. Crystalline inclusions of virus particle were encountered in some of the insect orgasns.

IX. Literature

1. AKASHI, K., T. MASUDA and S. OGAWA: A method for precise determination of size of small materials by using replica films. Electron Micorscopy 5: 79–82, 1956 (in Japanese)
2. AMES, R. W. and H. H. THORNBERRY: Carnation mosaic virus: Properties and electron microscopy. Phytop. 42: 289–291, 1952
3. ANDERSON, T. E.: Techniques for the preservation of three dimentional structure in preparing specimens for the electron microscope. Trans. N. Y. Acad. Sci. Ser. 2, 13: 130–134, 1951

4. ANDERSON, T. E.: Stereoscopic studies of cells and viruses in the electron microscope. Amer. Nat. 86: 91-100, 1952
5. ANDERSON, T. E.: Electron microscopy of microorganisms. in Oster and Pollister; Physical techiques in biological research 3: 177-240, Academic Press N. Y. 1956
6. ARTHUR, J. M. and J. M. NEWELL: The killing of plant tissue and the inactivation of tobacco mosaic virus by ultraviolet radiation. Amer. J. Bot. 16: 338-353, 1929
7. BACKUS, R. C. and R. C. WILLIAMS: Some use of uniform sized spherical particles. J. Appl. Phys. 19: 1186-1187, 1948
8. BACKUS, R. C. and R. C. WILLIAMS: Small spherical particles of exceptionally uniform size. J. Appl. Phys. 20: 224-225, 1949
9. BANCROFT, J. B. and P. KAESBERG: Size and shape of alfalfa mosaic virus. Nature 181: 720-721, 1958
10. BARTELS, W.: Der gegenwärtige Stand der Forschung auf dem Gebiet der Inaktivierung Pflanzenpathogener Viren, insbesondere des Tabakmosaikvirus. Phytop. Z. 24: 117-178, 1955
11. BAWDEN, F. C.: Plant viruses and virus diseases. Leiden, Chronica Botanica 272 pp. 1939
12. BAWDEN, F. C.: Plant viruses and virus diseases. 3rd ed. Waltham Mass. 335 pp. 1950
13. BAWDEN, F. C. and N. W. PIRIE: Experiments on the chemical behaviour of potato virus 'X'. Brit. J. Exp. Path. 17: 64-74, 1936
14. BAWDEN, F. C. and N. W. PIRIE: The isolation and some properties of liquid crystalline substances from Solanaceous plants infected with three strains of tobacco mosaic virus. Proc. Roy. Soc. London S-B, 123: 274-320, 1937
15. BAWDEN, F. C. and N. W. PIRIE: Liquid crystalline preparations of potato virus 'X'. Brit. J. Exp. Path. 19: 66-82, 1938
16. BAWDEN, F. C. and N. W. PIRIE: The effects of alkali and some simple organic substances on three plant viruses. Biochem. J. 34: 1278-1292, 1940
17. BERNAL, J. D. and I. FANKUCHEN: X-ray and crystallographic studies of plant virus preparations. I. II. III. J. Gen. Phys. 25: 111-165, 1941
18. BEST, R. J.: The relationship between the activity of tobacco mosaic virus suspensions and hydrogen-ion concentration over the pH range 5 to 10. Aust. J. Exp. Biol. Med. Sci. 14: 323-328, 1936
19. BEST, R. T. and G. SAMUEL: The reaction of the viruses of tomato spotted wilt and tobacco mosaic to the pH value of media containing them. Ann. Appl. Biol. 23: 509-537, 1936
20. BLACK, L. M.: Concept and problems concernig purification of labile insect-transmitted plant viruses. Phytop. 45: 208-216, 1955
21. BLACK, L. M., C. MORGAN and R. W. G. WYCKOFF: Visualisation of tobacco mosaic virus within infected cells. Proc. Soc. Exp. Biol. Med. 73: 119-122, 1950
22. BLATTNY, C.: Bemerkungen zur Epidemiologie des Stolburs und der verwandten Krankheiten. Proc. 3rd. Conf. Potato Virus Diseases, 1957: 255-263, 1958

23. BODE, O. und E. KÖHLER: Elektronmikroskopische Untersuchungen am Kartoffel-X- und Tabakmosaik-Virus. Z. Naturf. 7 b: 598–600, 1952
24. BODE, O. und H. L. PAUL: Elektronenmikroskopische Untersuchungen über Kartoffel-Viren. I. Vermessungen an Teilchen des Kartoffel-X-Virus. Biochem. Biophys. Acta 16: 343–345, 1955
25. BRADFORD, E. B. and J. W. VANDERHOFF: Electron microscopy of monodisperse latexes. J. Appl. Phys. 26: 864–871, 1955
26. BRAKKE, M. K., L. M. BLACK and R. W. G. WYCKOFF: The sedimentation rate of potato yellow-dwarf virus. Amer. J. Bot. 38: 332–342, 1951
27. BRAKKE, M. K., A. E. VATTER and L. M. BLACK: Size and shape of wound tumor virus. Abnormal and pathological plant growth. Brookheven symposia in Biology No. 6: 137–156, 1954
28. BRANDES, J.: Elektronmikroskopischer Nachweis von Pflanzenviren in ihren Wirtszellen. Naturwiss. 42: 101, 1955
29. BRANDES, J.: Über das Aussehen und die Verteilung des Tabakmosaikvirus im Blattgewebe: Elektronenmikropische Untersuchungen an ultradünen Mikrotomschnitten. Phytop. Z. 26: 93–106, 1956
30. BRANDES, J.: Eine elecktronenmikroskopische Schnellmethods zum Nachweis faden- und stäbchenförmiger Viren insbesondere in Kartoffeldunkelkeimen. Nachr Bl. Dtsch. Pflschdienst 9: 151–152, 1957
31. BRANDES, J.: Elektronenmikroskopische Grössenbestimmung von acht stäbchen- und fadenförmigen Pflanzenviren. Phytop. Z. 35: 205–210, 1959
32. BRANDES, J. and C. WETTER: Classification of elongated plant viruses on the basis of particle morphology. Virology 8: 99–115, 1959
33. BRENNER, S. and R. W. HORNE: A negative staining method for high resolution electron microscopy of viruses. Biochem. Biophys. Acta 34: 103–110, 1959
34. CONSENTINO, V., K. PAIGEN and R. L. STEERE: Electron microscopy of turnip yellow mosaic virus and the associated abnormal protein. Virology 2: 139–148, 1956
35. DAS GUPTA, N. N., M. L. DE and S. P. RAYCHAUDHRI: Structure of sunn hemp (Crotalaria juncea Linn.) mosaic virus with the electron microscope. Nature 168: 114, 1951
36. DAY, M. F. and M. BRIGGS: The origin and structure of brochosomes. J. Ultrastr. Res. 2: 239–244, 1958
37. BRUYN OUBOTER, M. P., J. J. BEIJER and E. VAN SLOGTEREN: Diagnosis of plant diseases by electron-microscopy. Antonie van Leeuwenhoek J. Microbiol. Serol. 17: 189–208, 1951
38. DE M. L.: Electron microscopic determination of size and shape of a new plant virus (Sunn hemp mosaic). Indian J. Phys. 24: 525–529, 1951
39. DUGGAR, B. M. and A. HOLLAEDER: Irradiation of plant viruses and of microorganisms with monochromatic light 1. The virus of typical tobacco mosaic and serratia marcescens as influenced by ultra violet and visible light. J. Bact. 27: 219–239, 1934-a
40. DUGGAR, B. M. and A. HOLLAEDER: Irradiation of viruses and of microorganisms

with monochromatic light II. Resistance to ultraviolet radiation of a plant virus as contrasted with vegetative and spore stages of certain bacteria. J. Bact. 27: 241-256, 1934-b

41. FRAENKEL-CONRAT, H.: The role of the nucleic acid in the reconstitution of active tobacco mosaic virus. J. Amer. Chem. Soc. 78: 882, 1956
42. FRANKLIN, R. E., D. L. D. CASPAR and A. KLUG: The structure of viruses as determined by X-ray diffraction. Plant Pathology—Problems and Progerss 1908-1958: 447-461, 1959
43. FUKAMI, A.: Studies on replica method (III). Filmy replica system. Electron Microscopy 4: 36-40, 1955 (in Japanese)
44. FUKUSHI, T.: On some properties of the tobacco mosaic virus 1. Japanese J. Bot. 6: 381-392, 1933
45. FUKUSHI, T.: On the intracellular bodies associated with the dwarf disease of rice plant. Trans. Sapporo Nat. Hist. Soc. 12: 35-41, 1931
46. FUKUSHI, T.: Studies on the dwarf disease of rice plant. J. Fac. Agr. Hokkaido Imp. Univ. 37: 41-164, 1934
47. FUKUSHI, T.: Further studies on the dwarf disease of rice plant. J. Fac. Agr. Hokkaido Imp. Univ. 45: 83-154, 1940
48. FUKUSHI, T.: Plant viruses. Asakura-Shoten, 286 pp. 1952 (in Japanese)
49. FUKUSHI, T. and E. SHIKATA: Electron microscopic studies on plant viruses. Ann. Phytop. Soc. Japan 16: 173, 1952 (in Japanese)
50. FUKUSHI, T., E. SHIKATA and I. KIMURA: Some morphological characters of rice dwarf virus. Virology 18: 192-205, 1962
51. FULTON, R. W.: Puriffcation of sour cherry necrotic ringspot and prune dwarf viruses. Virology 9: 522-535, 1959
52. GEROULD, C. H.: Use of Polystyrene Latex 580 G, Lot 3584 in electron microscopy. J. Appl. Phys. 21: 71, 1950-a
53. GEROULD, C. H.: Comments on the use of Latex spheres as size standards in electron microscopy. J. Appl. Phys. 21: 183-185, 1950-b
54. GIERER, A. und G. SCHRAMM: Die Infektiosität der Nucleinsäure aus Tabakmosaikvirus. Z. Naturf. 11 b: 138-142, 1956-a
55. GIRER, A. und G. SCHRAMM: Infectivity of ribonucleic acid from tobacco mosaic virus. Nature 177: 702-703, 1956-b
56. GOLD, A. H., C. A. SUNESON, B. R. HOUSTON and J. W. OSWALD: Electron microscopy of seed and pollen transmission of rod shaped particles associated with the false stripe disease of barley. Phytop. 44: 11-117, 1954
57. GOWEN, J. W. and N. W. PIRIE: Inactivation of tobacco mosaic virus by X-rays. Science 84: 536-537, 1936
58. HALL, C. E.: Electron densitometry of stained virus particles. J. Biophys. Biochem. Cytology 1: 1-11, 1955
59. HALL, C. E.: Lengths of tobacco mosaic virus from electron microscopy. J. Amer. Chem. Soc. 80: 2556-2557, 1958
60. HARRISON, B. D. and H. L. NIXON: Purification and electron microscopy of three soil borne plant viruses. Virology 12: 104-117, 1960

61. HART, R. G.: Electron-microscopic evidence for the localization of ribonucleic acid in the particles of tobacco mosaic virus. Proc. Nat. Acad. Sci, 41: 261-264, 1955
62. HART, R. G.: Morphological changes accompanying thermal denaturation of tobacco mosaic virus. Biochim. Biochys. Acta 20: 388-389, 1956
63. HART, R. G.: The nucleic acid fiber of the tobacco mosaic virus particle. Biochim. Biophys. Acta 28: 457-464, 1958
64. HIDAKA, J. and K. KIRIYAMA: Studies on the types of inactivation of purified tobacco mosaic virus (TMV). Virus 3: 39-50, 1953 (in Japanese)
65. HIDAKA, J. and H. MURANO: The size and shape of tobacco mosaic virus particles. Ann. Phytopath. Soc. Japan 16: 32, 1952 (in Japanese)
66. HOLLAENDER, A. and B. M. DUGGER: Irradiation of plant viruses and of micro-organisms with monochromatic light III. Resistance of the virus of typical tobacco mosaic and Escherichia coli to radiation from λ 3000 to λ 2250 Å. Proc. Nat. Acad. Aci. 22: 19-24, 1936
67. HUXLEY, H. E.: Some observation on the structure of tobacco mosaic virus. Electron microscopy. Proc. Stockholm Conf. 1956: 260-261, 1957
68. JOHNSON, J.: Chemical inactivation and the reactivation of a plant virus. Phytop. 31: 679-701, 1941
69. KAESBERG, P.: Structure of small spherical viruses. Science 124: 626-628, 1956
70. KAHLER, H. and B. J. LLOYD: Metallic evaporation and the diameter of tobacco mosaic virus with the electron microscope. J. Appl. Phys. 21: 699-704, 1950
71. KAHLER, H. and M. W. WOODS: Electron microscopic and electrophoretic study of the strain of tobacco mosaic virus. Arch. Biochem. 22: 393-401, 1949
72. KASSANIS, E. and A. KLECZKOWSKI: The effect of formaldehyde and mercuric chloride on tobacco mosaic virus. Biochem. J. 38: 20-24, 1944
73. KAUSCHE, G. A., E. PFANKUCH und H. RUSKA: Die Sichtbarmachung von pflanzlichen Virus in Ubermikroskop. Naturwiss. 27: 292-299, 1939
74. KERN, S. F. and R. A. KERN: The apparent size of objects as observed in the electron microscope. J. Appl. Phys. 21: 705-707, 1950
75. KIKUMOTO,T. and C. MATSUI: Electron microscopic study on potato virus X. Ann. Phytop. Soc. Japan 25: 19, 1960 (in Japanese)
76. KIMURA, I.: Further studies on the rice dwarf virus-I, II. Ann. Phytop. Soc. Japan 27: 197-213, 1962
77. KLINKOWSKI, M. und G. KREUTZBERG: Vorkommen und Verbreitung von Gramineen Virosen in Europa. Phytop. Z. 32: 1-24, 1958
78. KNIGHT, C. A. and G. OSTER: The size of the particles of some strains of tobacco mosaic virus as shown by the electron microscope. Arch. Biochem. 15: 289-294, 1947
79. LABAW, L. W.: An electron microscopic determination of the Rothamsted tobacco necrosis protein crystal structure. J. Ultrastr, 3: 58-69, 1959
80. LABAW, L. W. and R. W. G. WYCKOFF: The structure of southern bean mosaic virus protein crystals. Arch. Biochem. Biophys. 67: 225-236, 1957
81. LABAW, L. W. and R. W. G. WYCKOFF: The electron micrsscopy of tobacco mosaic

virus crystals. J. Ultrastr. Res. 2: 8–15, 1958

82. LAUFFER, M. A. and W. C. PRICE: Thermal denaturation of tobacco mosaic virus. J. Biol. Chem. 133: 1–15, 1940
83. LEA, D. E.: Actions of radiation on living cells. 2nd ed. Cambridge 416 pp. 1955
84. LEA, D. E. and K. M. SMITH: The inactivation of plant viruses by radiations. Prasitology 32: 405–416, 1940
85. LITTAU, V. C. and K. MARARMOROSCH: Cytological effects of aster-yellows virus on its insect vector. Virology 2: 128–130, 1956
86. LITTAU, V. C. and K. MARAMOROSCH: A study of the cytological effects of aster yellows virus on its insect vector. Virology 10: 483–500, 1960
87. LEYON, H.: Virus formation in chloroplasts. Exp. Cell Res. 4: 362–370, 1953
88. MARAMOROSCH, K.: Multiplication of plant viruses in insect vectors. Adv. Virus Res. 3: 221–249, 1955
89. MATSUI, C.: The electron microscopic observations of tobacco mosaic virus-infected tissue by ultrathin sectioning. Virus 6: 357–362, 1956
90. MATSUI, C.: Pathological cytology of tobacco leaf infected with tobacco mosaic virus III. J. Biophys. Biochem' Cytol. 4: 831, 1958-a
91. MATSUI, C: Fine structure of X-body. Ann. Phytop. Soc. Japan 23: 28, 1958-b (in Japanese)
92. MATSUI, C. and M. YAMADA: Mechanism of plant virus infection VII. Ann. Phytop. Soc. Japan 23: 76–78, 1958 (in Japanesə)
93. MIYAMOTO, Y. and F. KAWAMURA: Effect of X-ray on the infectivity and antigenicity of tobacco mosaic virus. Ann. Phytop. Soc. Japan 19: 53–57, 1957 (in Japanese)
94. MORITO, N. and T. KOMODA: On some problems on high power observation by means of electron microscope. Electron Microscopy 5: 76–79, 1956 (in Japanese)
95. MULVANIA, M.: Studies on the nature of the virus of tobacco mosaic. Phytop. 16: 853–871, 1926
96. MURAYAMA, D.: Immunological studies on potato virus X. 307 pp. 1959 (in Japanese)
97. NASU, S.: Studies on some leafhoppers and planthoppers which transmit virus diseases of rice plant in Japan. Bull. Kyushu Agr. Exp. Station 8: 153–349, 1963
98. NEI, T., Y. SASAKI and E. SHIKATA: The breaking of tobacco mosaic virus by freeze-drying. Low Temperature Science, Ser. B. 14: 75–85, 1956 (in Japanese)
99. OSHIMA, N.: Studies on potato virus X. Report of the Hokkaido Exp. S'ation 53: 1–159, (in Japanese)
100. OSTER, G.: Size distribution of tobacco mosaic virus in the early stages of infection. J. Appl. Phys. 18: 272, 1947
101. OSTER, G., C. A. KNIGHT and W. M. STANLEY: Electron microscope studies of Dahlem, Rothamsted, and Princeton sample of tobacco mosaic virus. Arch. Biochem. 15: 279–288, 1947

102. PAUL, H. L. und O. BODE: Elektronenmikroskopische Untersuchungen über Kartoffelviren IV. Vermessungen an Teilchen des Kartoffel-A-Virus. Phytop. Z. 27: 211-214, 1956

103. PAUL, H. L., J. BRANDES und L. QUANTS: Versuche zur Reinigung und Darstellung des Echten Ackerbohnenmosaikvirus. Phytop. Z. 31: 441-443, 1958

104. PAWLITSCHEK, W.: Gestalt und Längenvermessung des Streifenmozaik-Virus der Gerste. Biochim. Biophys. Acta 28: 650-651, 1958

105. PEASE, D. C. and R. F. BAKER: Sectioning techniques for electron microscopy using a conventional microtom. Proc. Soc. Exp. Biol. Med. 67: 470-474, 1948

106. PRICE W. C.: The thermal death rate of tobacco mosaic virus. Phytop. 23: 749-769, 1933

107. PRICE, W. C. and J. W. GOWEN: Quantitative studies of tobacco mosaic virus inactivation by ultra-violet light. Phytop. 27: 267-282, 1937

108. PRICE, W. C., R. C. WILLIAMS and R. W. G. WYCKOFF: Electron micrographs of crystalline plant viruses. Arch. Biochem. 9: 175-185, 1946

109. PROTSENKO, A. E.: (Electron micrography of phytopathogenic viruses. I. Aster yellows virus. Microbiology, Moscow 27: 131-132, 1958-a)

110. PROTSENKO, A. E.: (Electron micrography of phytopathogenic viruses. II. Bull. Acad. Sci. U. S. S. R. Ser. Biol., 1958: 451-455, 1958-b)

111. RAWLINS, T. E., CATHERINE ROBERTS and NEDRA M. UTECH: An electron microscope study of tobacco mosaic virus at different stages of infection. Amer. J. Bot. 33: 356-363, 1946

112. ROSS, A. F. and W. M. STANLEY: The partial reactivation of formalized tobacco mosaic virus protein. J. Gen. Phys. 22: 165-191, 1938

113. SCHNEIDER, I. R.: Solution of tobacco mosaic virus in the aquous phase of a chloroform-water emulsion and application of this phenomenon in virus assay. Science 117 (3028): 30-31, 1953,

114. SCHRAMM, G.: Die Biochemic der Viren. Springer. Berlin 276 S. 1954

115. SCHRAMM, G.: Neuere Untersuchungen über die Strukture des Tabakmosaikvirus und ihre biologische Bedeutung. Zentralbl. Bakteriol. II. Abt. 158: 229, 1955

116. SCHRAMM, G., G. SCHUMACHER and W. ZILLIG: An infectious nucleoprotein from tobacco mosaic virus. Nature 175: 549-550, 1955-a

117. SCHRAMM, G., G. SCHUMACHER and W. ZILLIG: Über die Strukture des Tabakmosaikvirus III. Mitt.: Der Zerfall in alkalischer Lösung. Z. Naturf. 10: 481-492, 1955-b

118. SENSENEY, C. R., R. P. KAHN and P. R. DESJARDINS: Particle size and shape of purified tomato-ringspot virus. Science 120: 456-457, 1954

119. SHALLA, T. A.: A method for increasing the electron density of tobacco mosaic virus in ultrathin tissue sections. Virology 7: 150-160, 1959-a

120. SHALLA, T. A.: Relation of tobacco mosaic virus and barley stripe mosaic virus to their host cells as revealed by ultrathin tissue sectioning for the electron microscope. Virology 7: 193-219, 1959-b

121. SHARP, D. G. and F. A. WOLF: The virus of tobbacco leaf-curl II. Phytop. 41: 94-98, 1951
122. SIGURGEIRSON. T. and W. M. STANLEY: Electron microscope studies on tobacco mosaic virus. Phytop. 37: 26-38, 1947
123. SILL, W. H. JR., W. C. BURGER, M. A. STAHMANN and J. C. WALKER: Electron microscopy of cucumber virus I. Phytop. 42: 19-20, 1952
124. SINCLAIR, J. B., P. H. GEIL and P. KAESBERG: Biophysical studies of wild cucumber. mosaic virus. Phytop. 47: 372-377, 1957
125. SKOTLAND, C. B., D. HAGEDORN and M. A. STAHMANN: Electron microscopy of tobacco mosaic virus in situ. Phytop. 45: 603-607, 1955
126. SMITH, F. F.: Some cytological and physiological studies of mosaic diseases and leaf variegation. Ann. Missouri Bot. Gard. 13: 425-484, 1962
127. SMITH, K. M. and R. C. WILLIAMS: Insect viruses and their structure. Endeavour 17: 12-21, 1958
128. STAHMANN, M. A. and P. KAESBERG: Concepts and probems concerning the eletron microscopy of plant virus. Phytop. 45: 187-194, 1955
129. STANEY, W. M.: Chemical studies on the virus of tobacco mosaic 111. Rates of inactivation at different hydrogen-ion concentration. Phytop. 25: 475-492, 1935
130. STANLEY, W. M.: The inactivation of crystalline tobacco mosaic virus protein. Science 83: 626-627, 1936
131. STANLEY, W. M. and T. E. ANDERSON: A study of purified viruses with the electron microscope. J. Biol. Chem. 139: 325-338, 1941
132. STEERE, R. L.: Tobacco ring-spot virus, a polyhedron, purified with the use of butanol. Phytop. 43: 485, 1953
133. TAKAHASHI, W. N.: The effect of PH on the linear aggregation of tobacco mosaic virus. Ibid. 36: 646-645. 1949
134. TAKAHASHI, W. N. and T. E. RAWLINS: An electron mecroscope study of two strains of potats X virus. Amer. J. Bot. 33: 740-742, 1946
135. TAKAHASHI, W. N. and T. E. RAWLINS: An electron micoscope study of mutation in tabacco mosaic virus. Phytop. 37: 73-76, 1947
136. TAKAHASHI, W. N. and T. E. RAWLINS: An electron microscope study of tobacco mosaic virus extracted from pulp and juice after various periods of infection. Ibid, 38: 279-282, 1948
137. THORNBERRY, H. H.: Effect of phosphate buffers on infectivity of tobacco mosaic virus. Ibid. 25: 618-627, 1935
138. TODD, C.: On the electrical behavior of the bacteriophage. Brit. J. Exp. Path. 8: 369-376, 1927
139. TOMILINSON, J. A., R. J. SHEPHERD and J. C. WALKER: Purification, properties and serology of cucumber mosaic virus. Phytop. 49: 293-299, 1959
140. TSUJITA, M. and S. TSUDA: Formation of tobacco mosaic virus in plastids. Ann. Rept. Nat. Inst. Genetics. Japan No. 4: 51-54, 1954
141. WETTER, C. and J. BRANDES: Untersuchungen über das Kartoffel-S-Virus. Phytop. Z. 26: 81-92, 1956

142. WILLIAMS, R. C.: High-resolution electron microscopy of the particles of tobacco mosaic virus. Biochem. Biophys. Acta. 8: 227–244, 1952

143. WILLIAMS, R. C.: The shapes and sizes of purified viruses as determined by electron microscopy. Cold Spring Harbor Symposia on Quantitative Biol. 18: 185–196, 1953

144. WILLIAMS, R. C.: Electron microscopic studies of tobacco mosaic virus and of nucleic acid. Special publications of the New York Academy of Sciences V. Cellular Biology, Nucleic acids and Viruses. 207–215, 1957

145. WILLIAMS, R. C.: The structure of viruses as determined by electron microscopy. Plant Pathology-Problems and Progress 1908–1958: 437–445, 1959

146. WILLIAMS, R. C. and R. C. BACKUS: The electron micrographic structure of shadow cast films and surfaces. J. Appl. Phys. 20: 98–106, 1949

147. WILLIAMS, R. C. and K. M. SMITH: A crystallizable insect virus. Nature 179: 119–120, 1957

148. WILLIAMS, R. C. and R. L. STEERE: Electron microscopic observations on the unit of length of the particles of tobacco mosaic virus. J. Amer. Chem. Soc. 73: 2057–2061, 1951

149. WYCKOFF, R. W. G.: An ultracentrifugal study of pH stability of tobacco mosaic virus protein. J. Biol. Chem. 122: 239–247, 1937

150. WYCKOFF, R. W. G., J. BISCOE and W. M. STANLEY: An ultracentrifugal analysis of the crystalline virus proteins isolated from plants diseased with different strains of tobacco mosaic virus. J. Biol. Chem. 117: 57–71, 1937

151. YOSHII, K.: Electron microscopy for phytopathology. Ann. Phytopath. Soc. Japan 12: 231–245, 1943 (in Japanese)

152. YOSHII, H. and E. KAWAMURA: Anatomy of plant diseases. Asakura-shoten 281 pp. 1947 (in Japanese)

Explanation of Plates

Fig. 1. Silica covered carbon replica of difraction grating (960 lines/mm).

2. ditto, (1200 lines/mm).

3, 4. Dow latex particles 15 N–7 (340 mμ) and 15 N–23 (138 mμ).

3. exposured shortly after elctron bombardment.

4. Same area of plate 3, taken after 20 min. The latex particles became larger by contamination.

5. Tobacco mosaic virus particles in crude sap. Dow latex 15 N–8. Cr shadowed × 62,000.

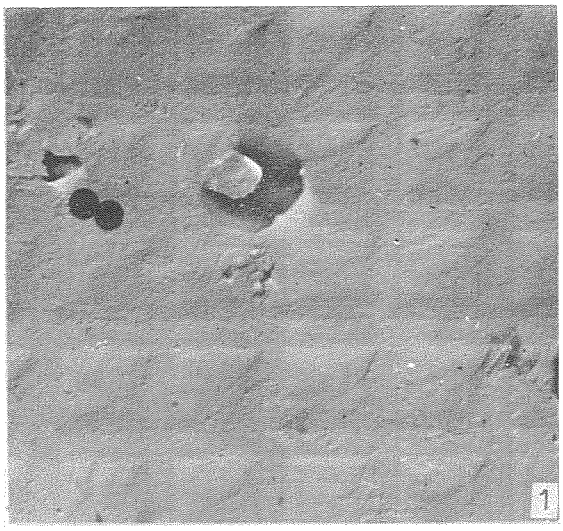
1

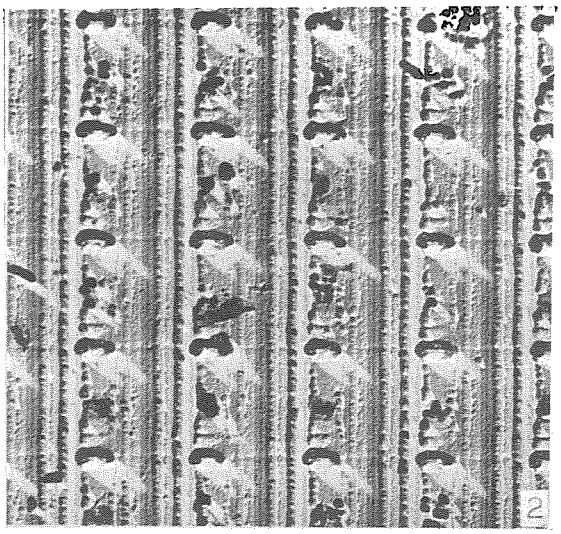
2

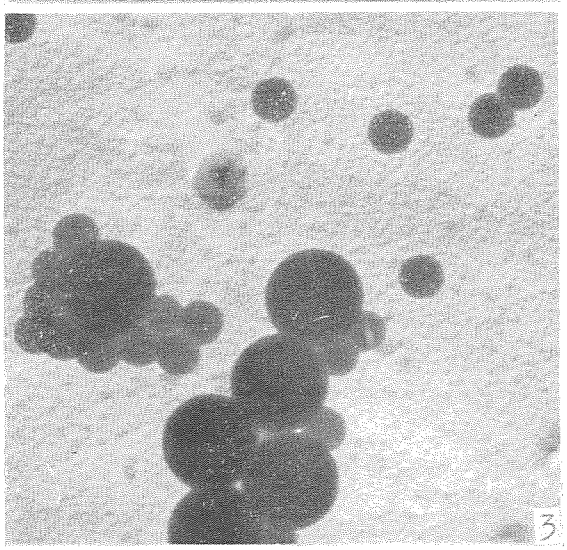
3

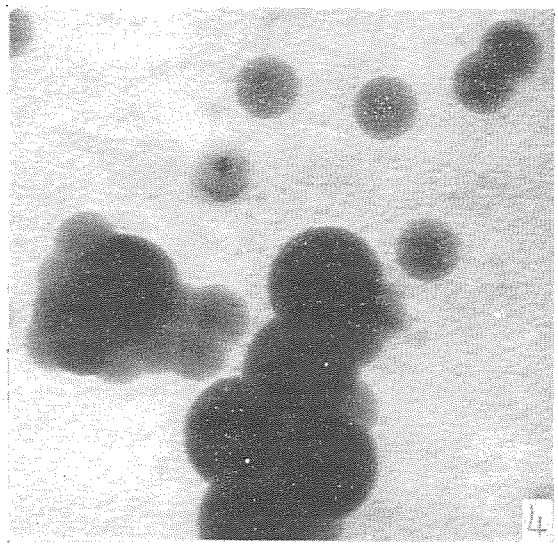
4

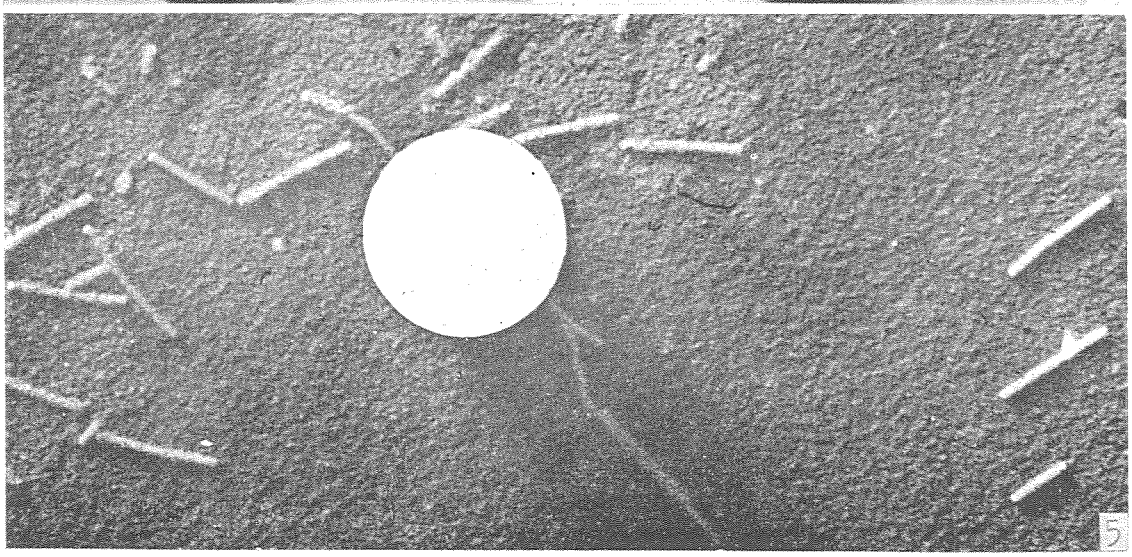
5

Fig. 6. Tobacco mosaic virus particles, unshadowed, × 100,000

7. ditto, KCl stained, × 117,000

8, 9. ditto, PTA stained, × 117,000 an arrow shows a cross section of the virus particle. A fine thread is visible in the center of the particle.

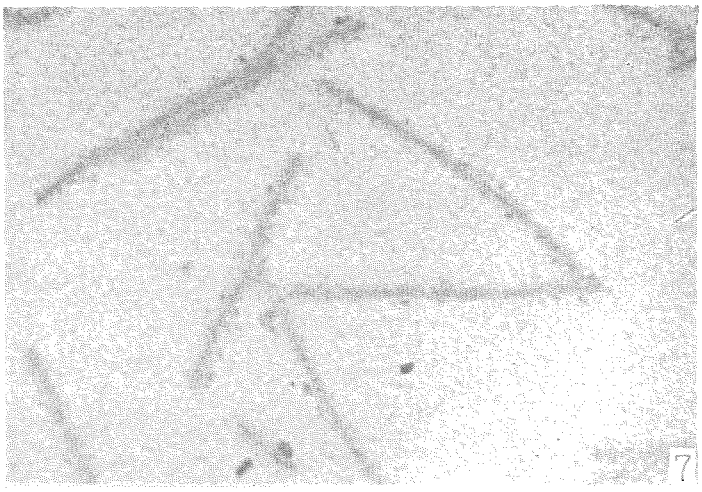

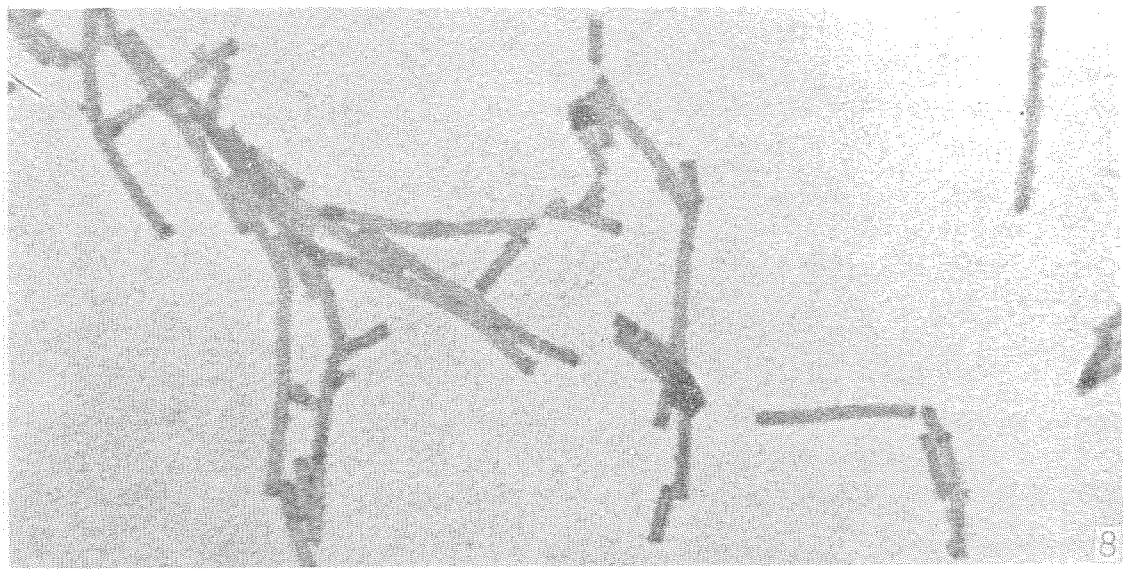

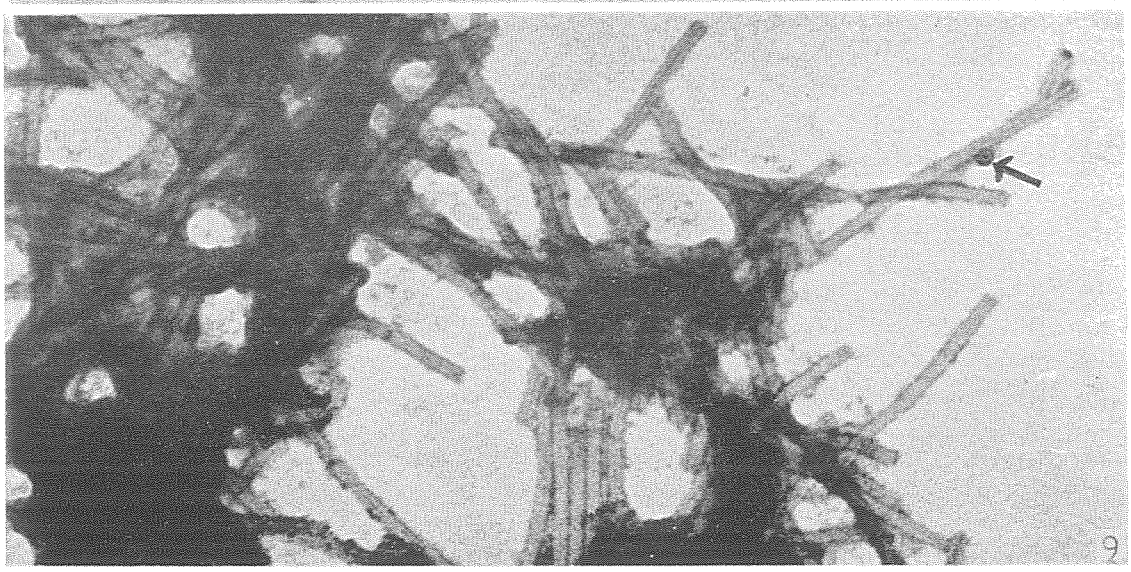

Fig. 10. Purified tobacco mosaic virus particles heated at 60°C for 10 min. after dialyzing. Cr shadowed, × 30,000.

11. ditto, heated at 70°C for 5 min.

12. ditto, heated at 70°C for 10 min.

13. ditto, heated at 70°C for 20 min.

14. ditto, heated at 70°C for 30 min.

15. ditto, heated at 70°C for 40 min.

16. ditto, heated at 80°C for 5 min.

17. ditto, heated at 80°C for 10 min.

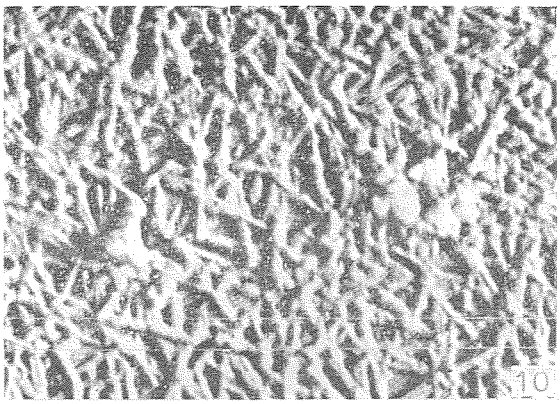
10

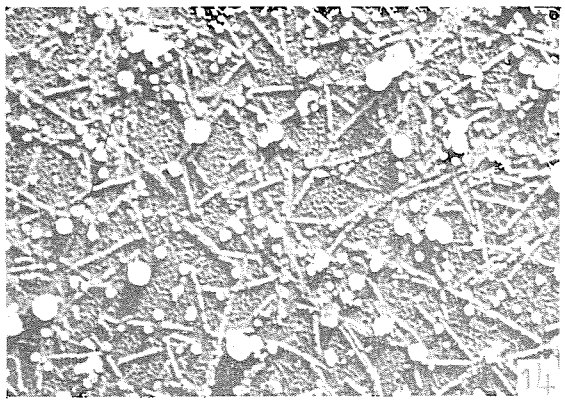
14

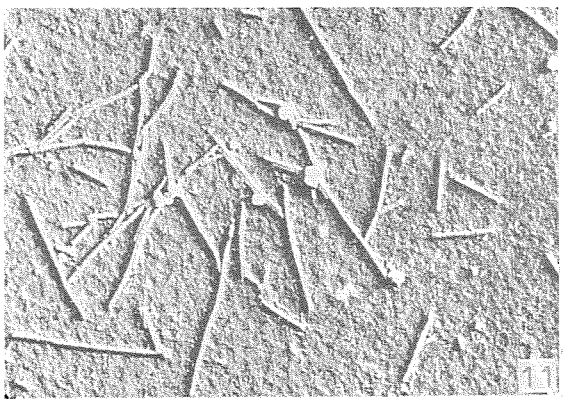
11

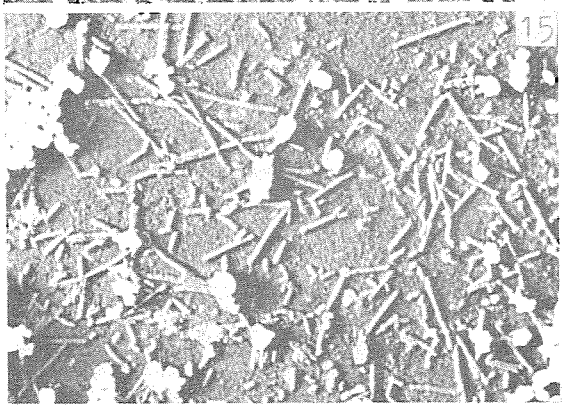
15

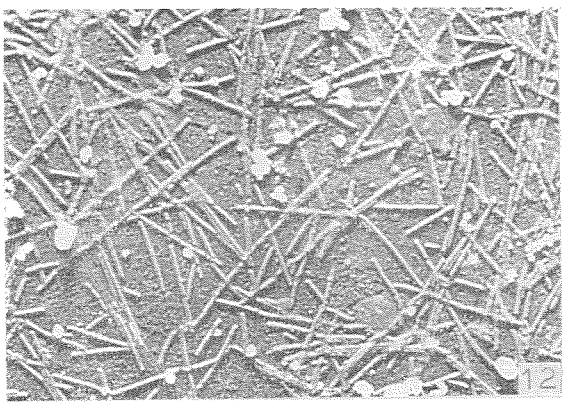
12

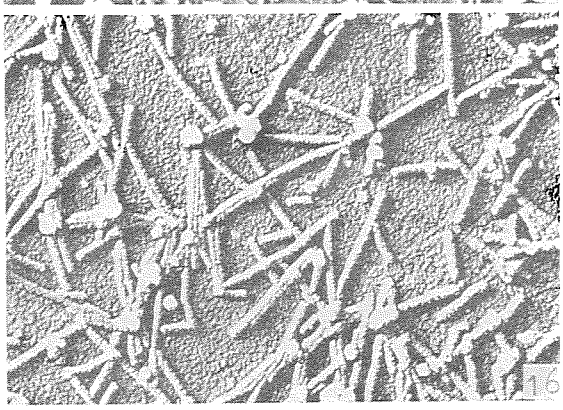
16

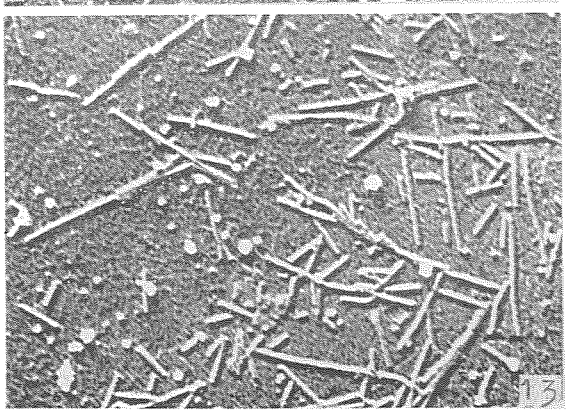
13

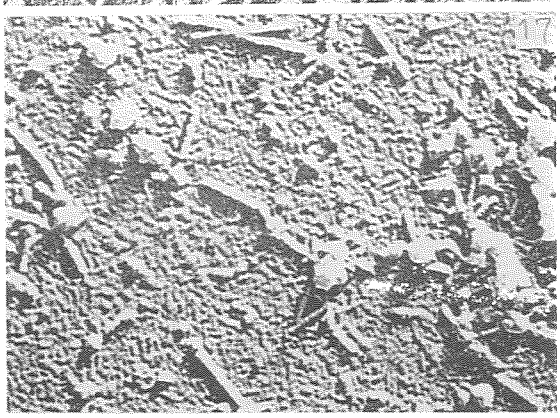
17

Fig. 18, 19. ditio, heated at 80°C for 20 min. Some parts of the dried preparation revealed shortened particles as in plate 18,another part revealed globular particles.

20. ditto, heated at 90°C for 10 min.

21. Purified virus particles suspended in a bufferred solution at pH 7. Cr shadowed, × 30,000.

22. ditto, heated at 70°C for 10 min.

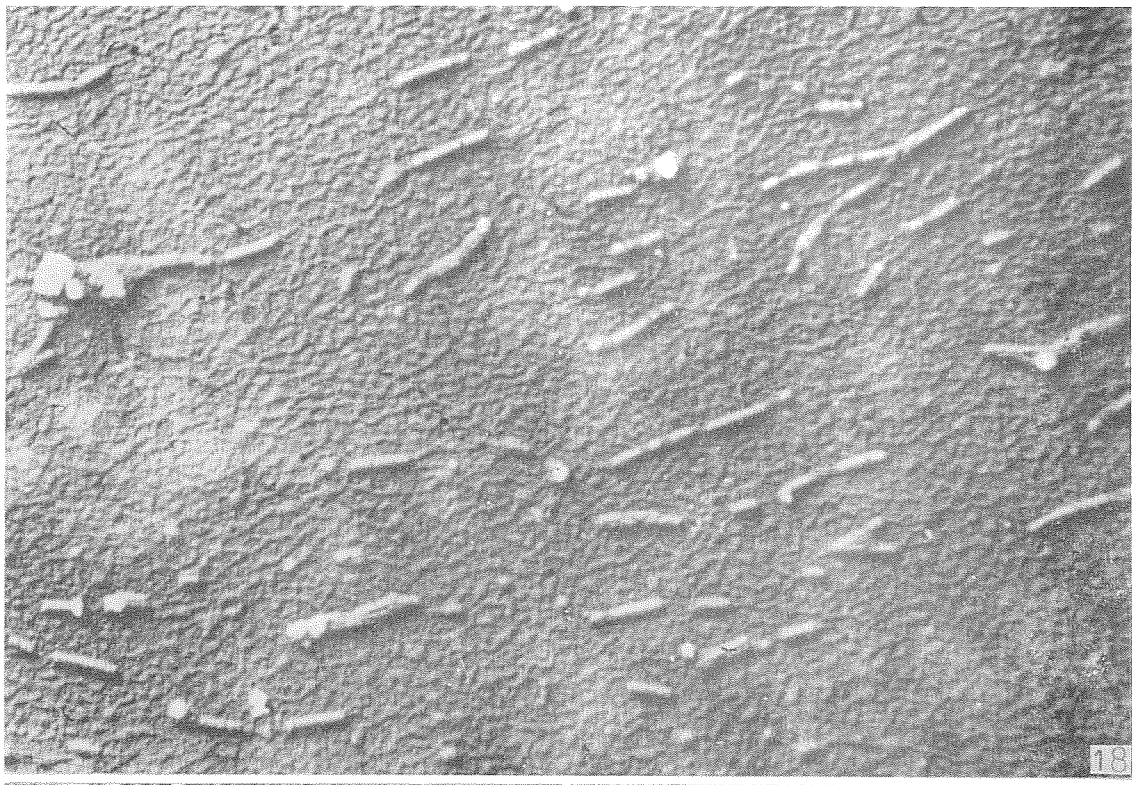
18

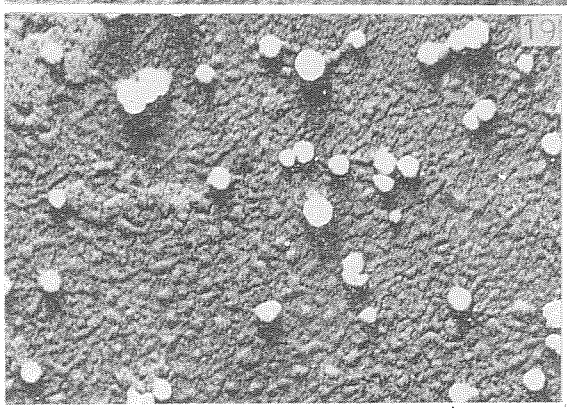
19

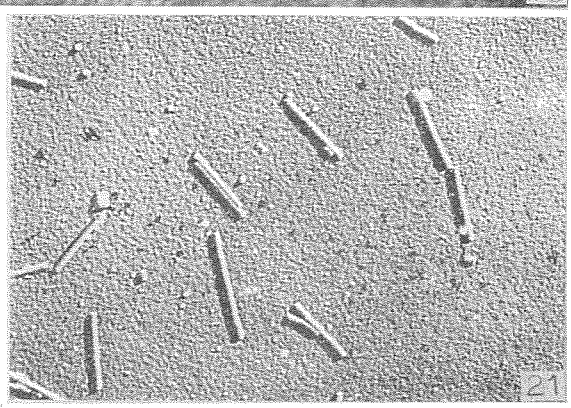
21

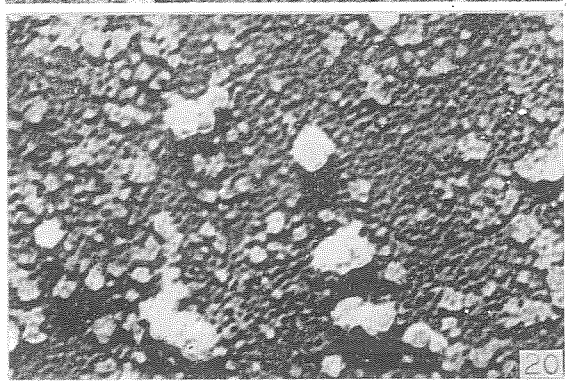
20

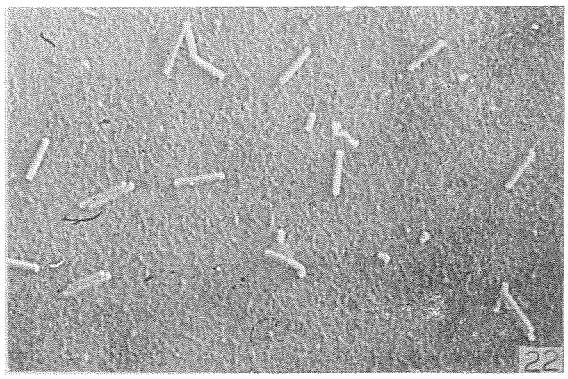
22

Fig. 23. ditto, heated at 75°C for 10 min.

24. ditto, heated at 80°C for 8 min.

25. ditto, heated at 80°C for 12 min.

26. ditto, heaten at 80°C for 20 min.

27. ditto, heated at 80°C for 30 min.

28. Tobacco mosaic virus particles treated with pH 0.5 for 20 hours. Cr shadowed, × 30,000.

29. ditto, at pH 1.1.

30. ditto, at pH 2.15.

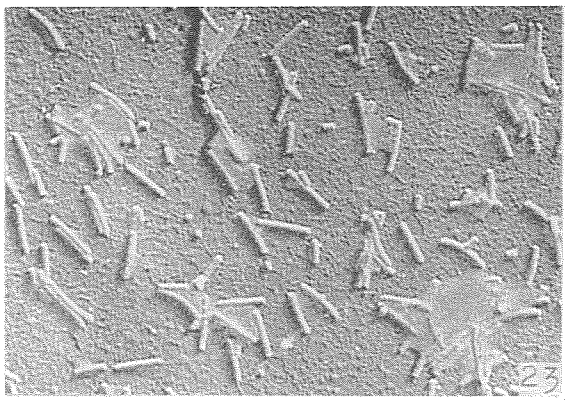
23

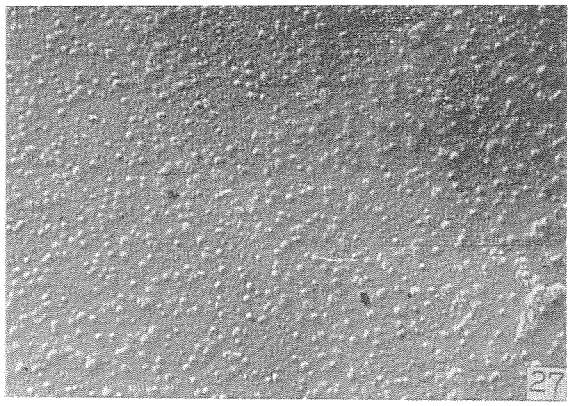
27

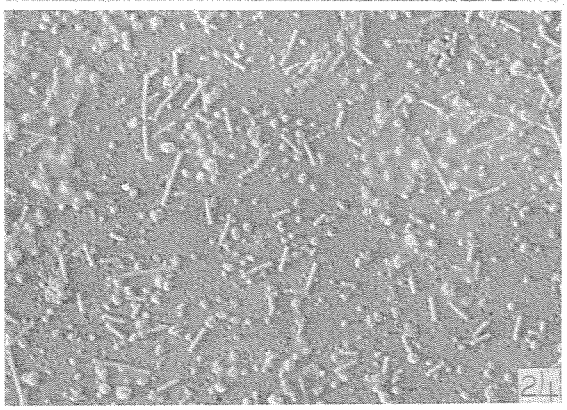
24

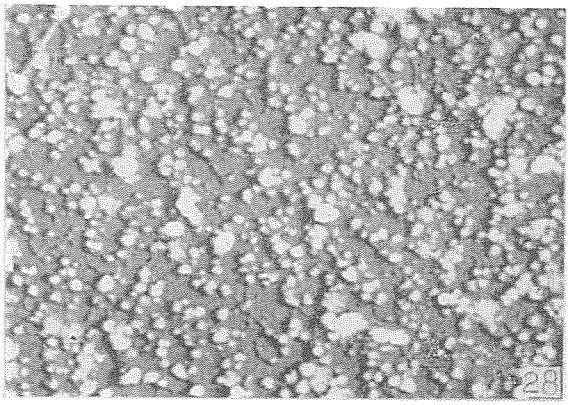
28

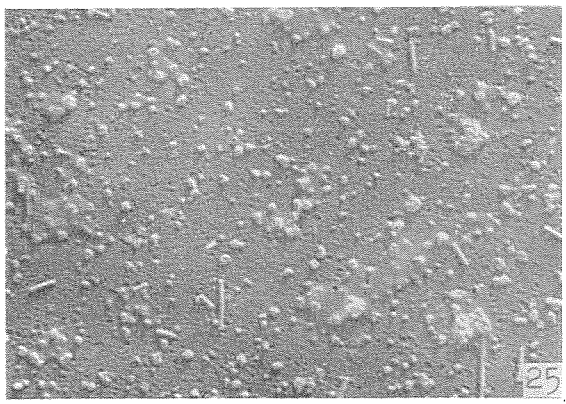
25

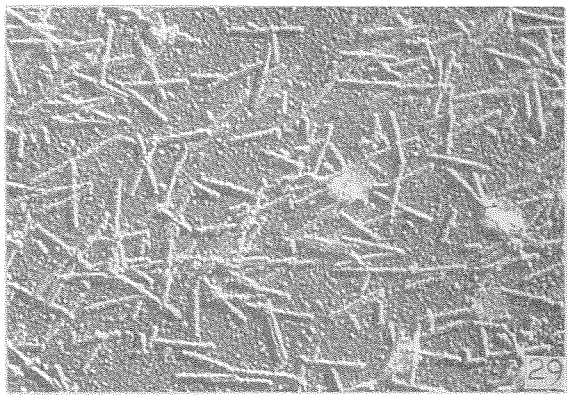
29

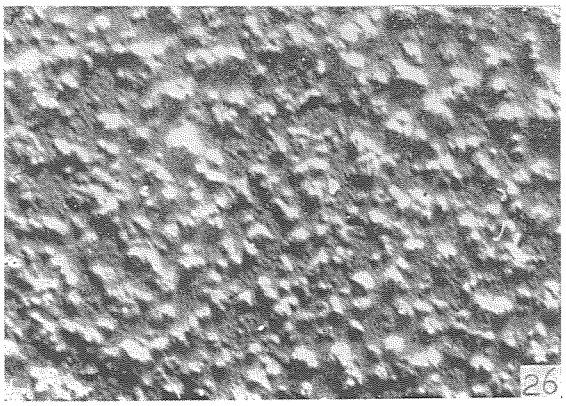
26

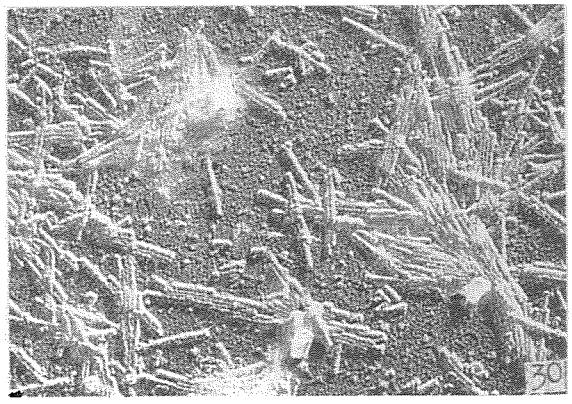
30

Fig. 31. ditto, at pH 2.1.

32. ditto, at pH 2.1, × 71,000.

33. ditto, at pH 3.0

34. ditto. at pH 3.0 Suspension was dried on the collodion film after dialyzing.

35. ditto, at pH 3.3 Paracrystalline aggregate of tobacco mosaic virus particles.

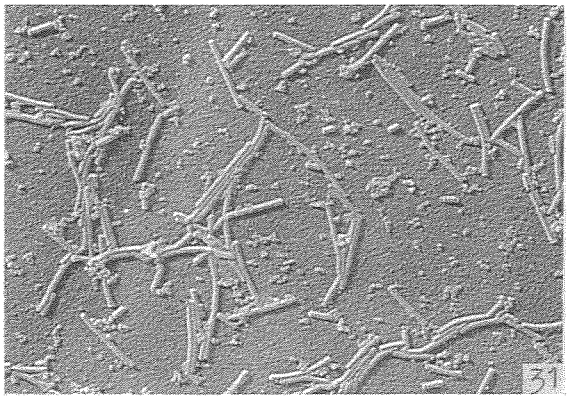
31

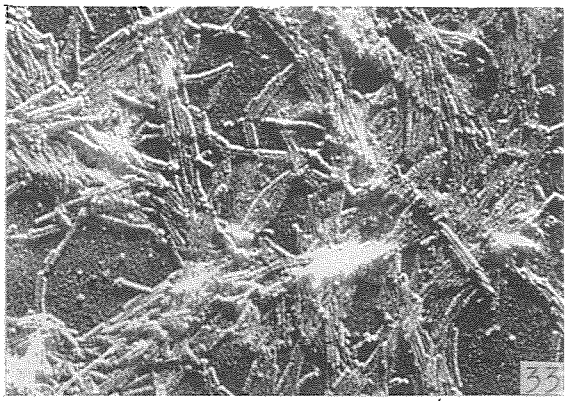
33

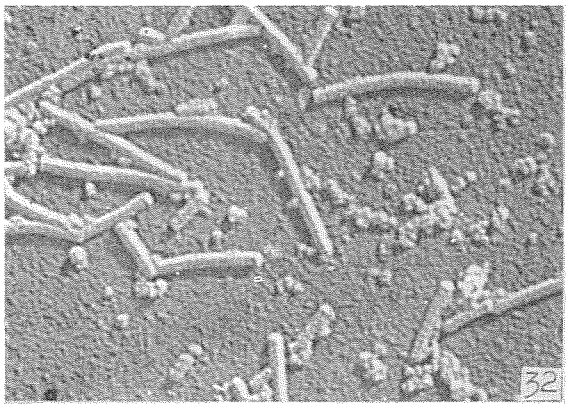
32

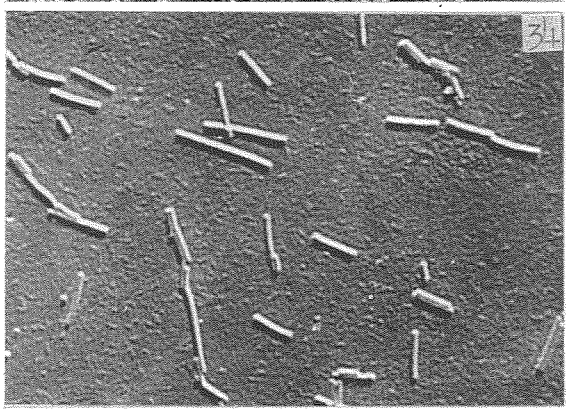
34

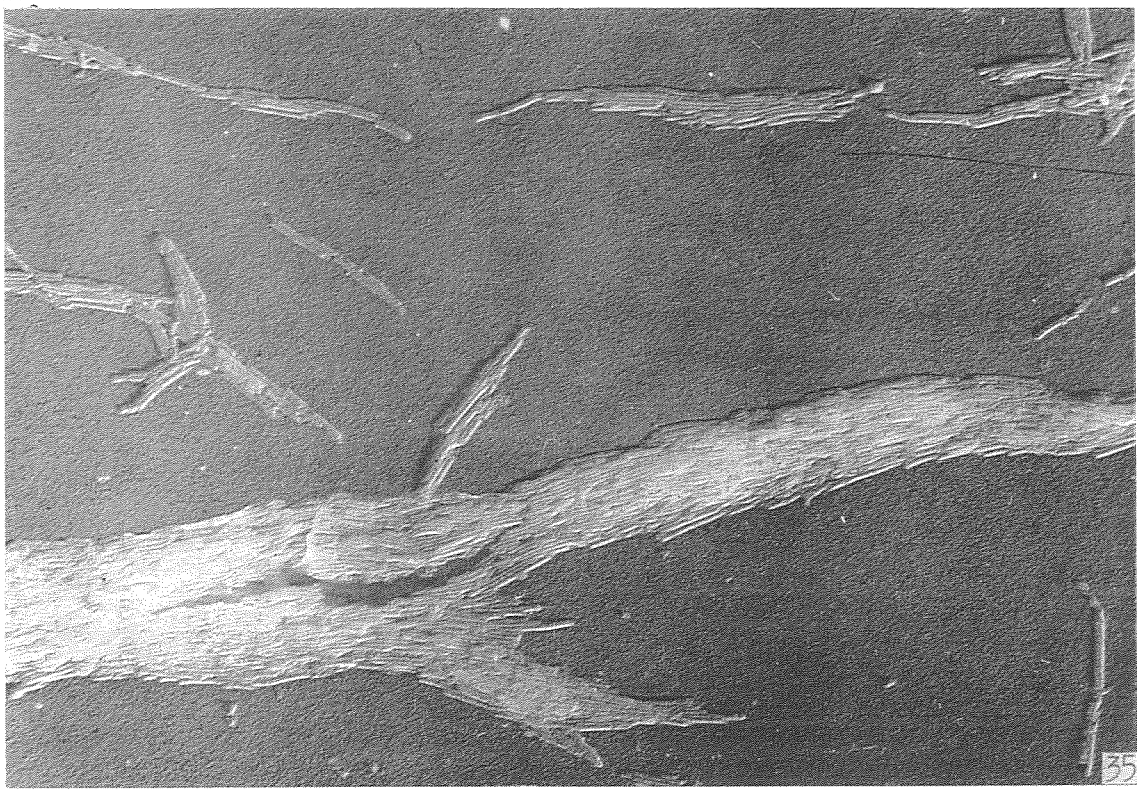
35

Fig. 36. ditto at pH 3.3 Low magnification of Plate 35. × 8,000.

37. ditto, at pH 4.0

38. ditto, at pH 4.2

39, 40. ditto, at pH 5.0

41. ditto, at pH 6.8

42. ditto, at pH 8.2

43. ditto, at pH, 9.0

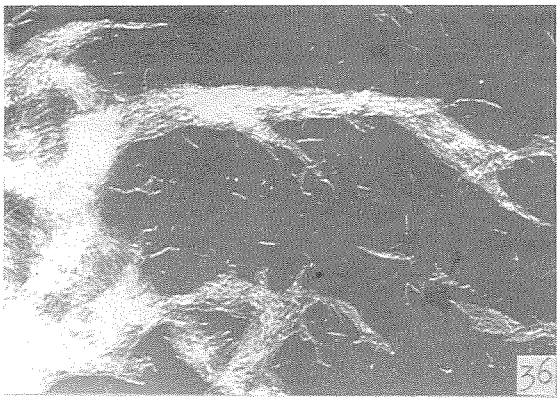
36

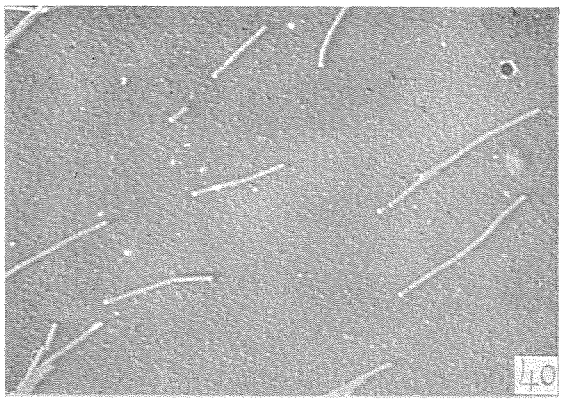
40

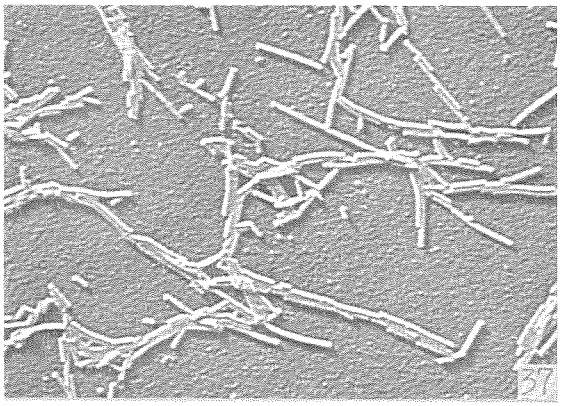
37

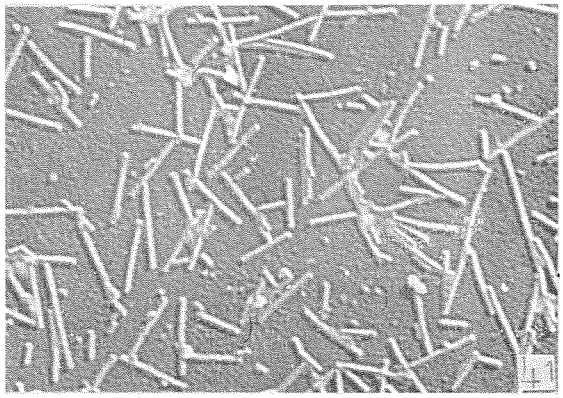
41

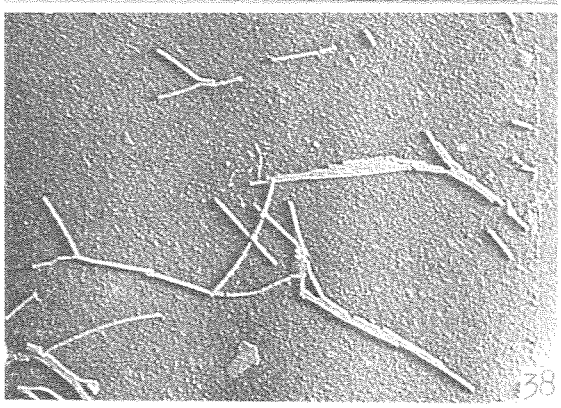
38

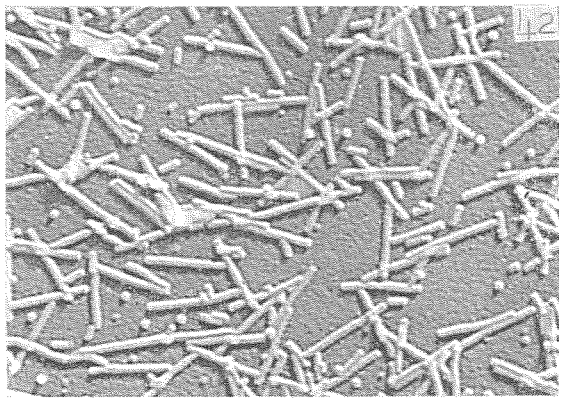
42

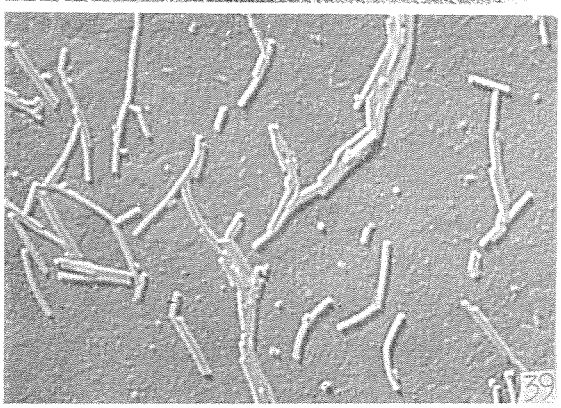
39

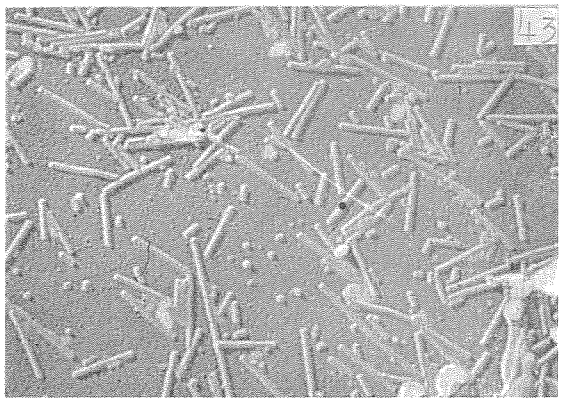
43

Fig. 44. ditto, at pH 9.0, high magnification of Plate 43. Some of the shortened particles seem to stand up on the grid. × 70,000.

45. ditto, at pH 10.1

46. ditto, at pH 11.05

47. Tobacco mosaic virus particles treated with 20% H_2O_2 at pH 6.8 for 15 hours. Sepcimen was dried on the grids after dialyzing. Cr shadow, × 30,000.

48. ditto, 30% H_2O_2

49. ditto, 30% H_2O_2 without dialyzing.

50. Tobacco mosaic virus particles preserved at pH 3.2 for 15 hours. A drop of the suspension was dried on the grids afther dialyzing. Cr shadowed, × 30,000.

51. ditto, 30% H_2O_2 at pH 3.1 for 15 hours.

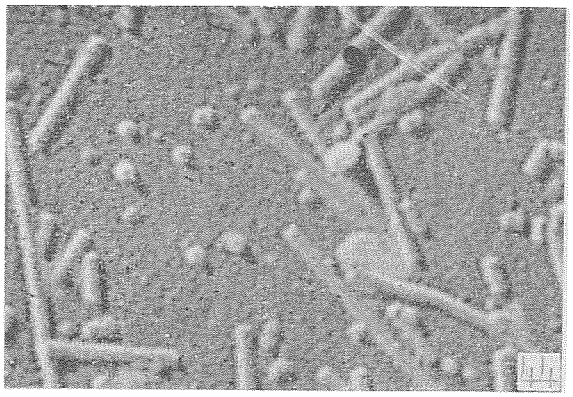
44

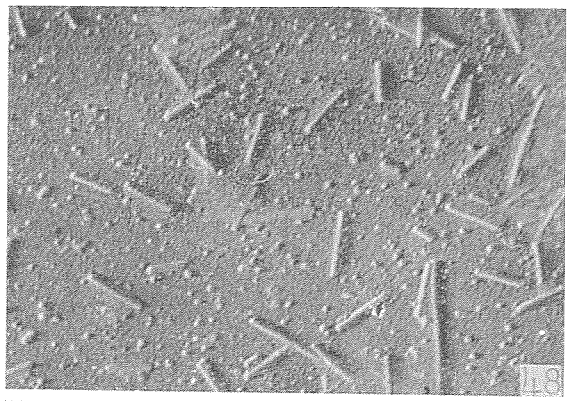
48

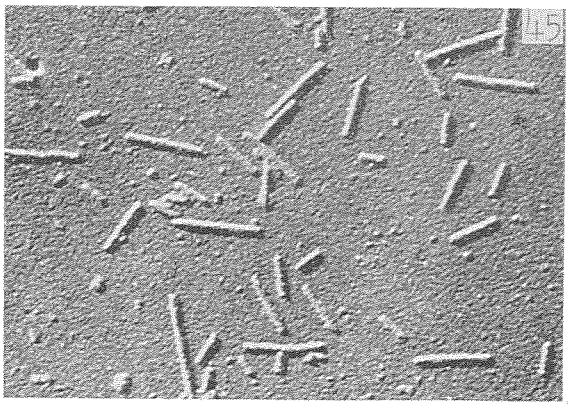
45

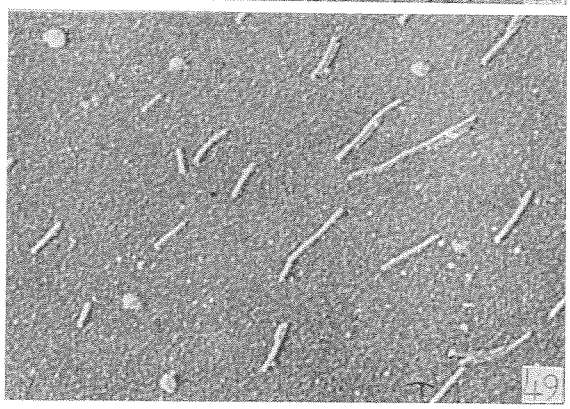
49

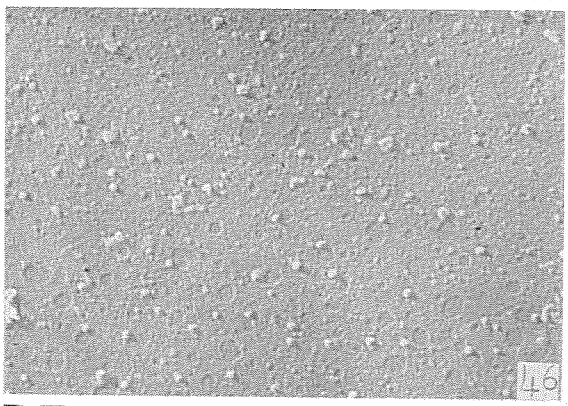
46

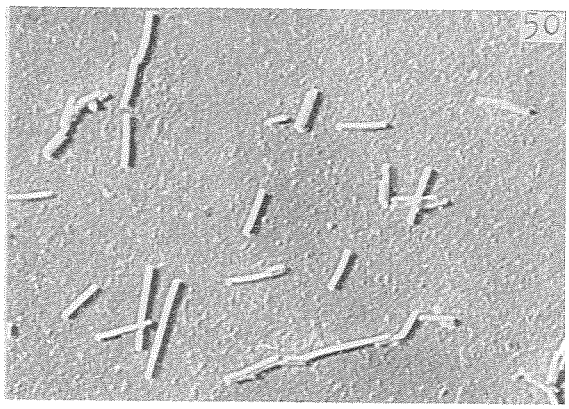
50

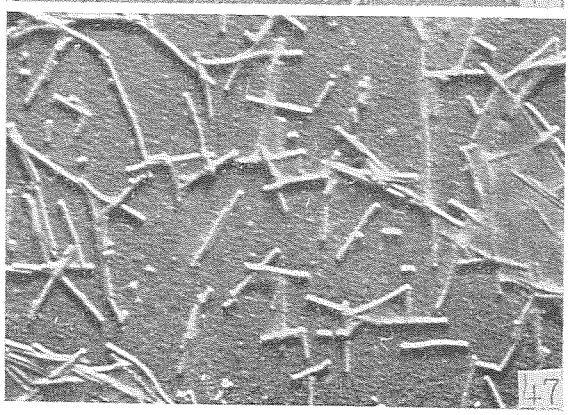
47

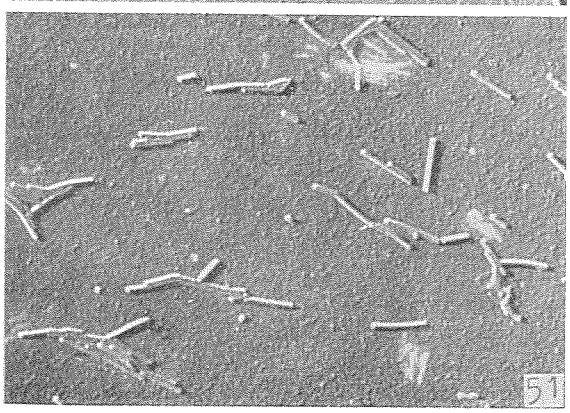
51

Fig. 52. Tobacco mosaic virus particles preserved at pH 8.9 for 15 hours. Specimen was dried on the grids after dialyzing Cr shadowed, × 30,000.

53. ditto, 3% H_2O_2

54. ditto, 5% H_2O_2

55. Tobacco mosaic virus particles treated with 10% H_2O_2 at pH 8.3 for 1 hour. Cr shadowed, × 30,000

56, 57. ditto, for 10 hours. An arrow in Fig. 57 represents the hexagonal cross section of shortened rods. × 65,000.

58. ditto, for 15 hours.

59. ditto, for 24 hours.

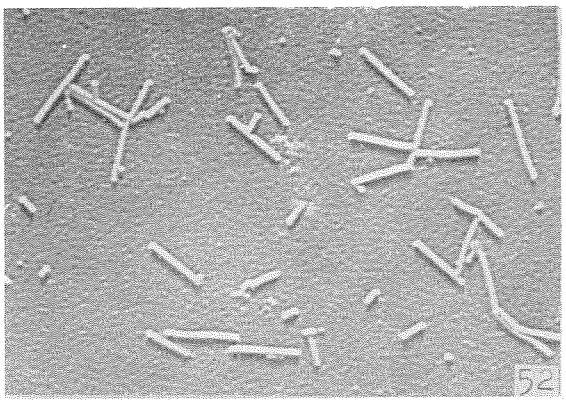
52

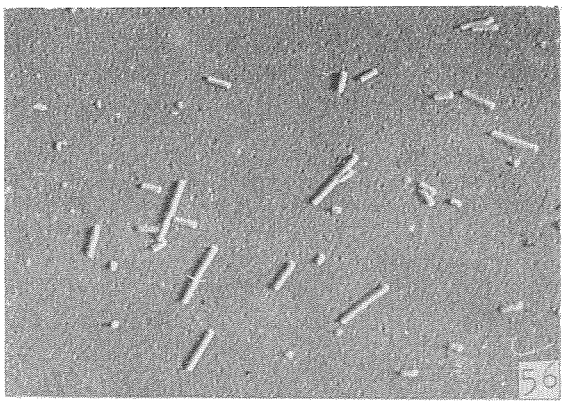
56

53

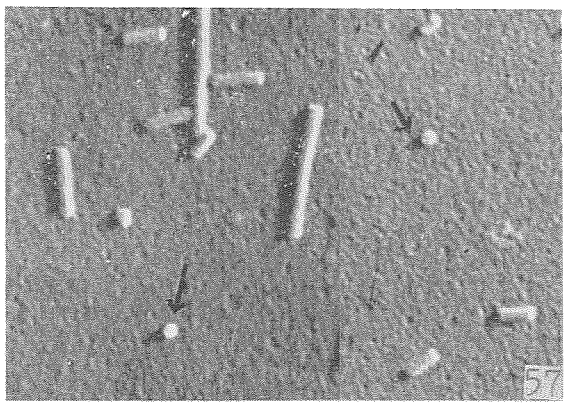
57

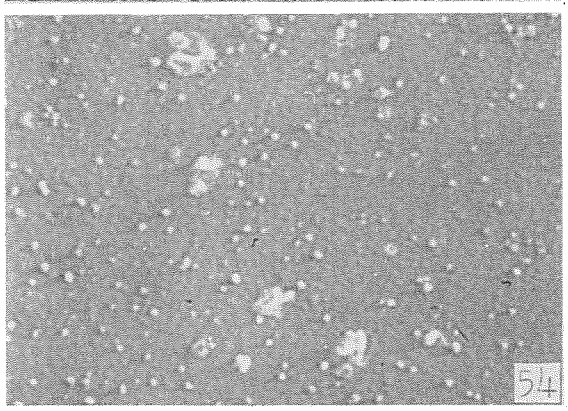
54

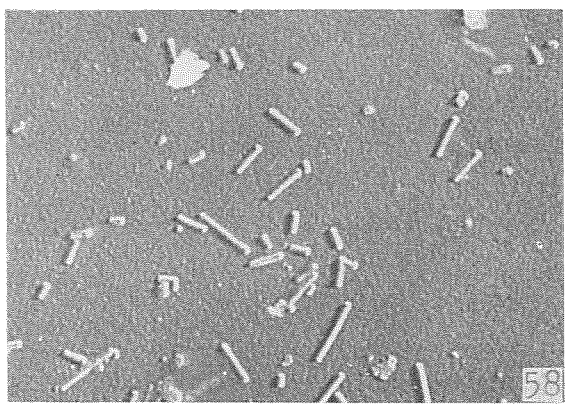
58

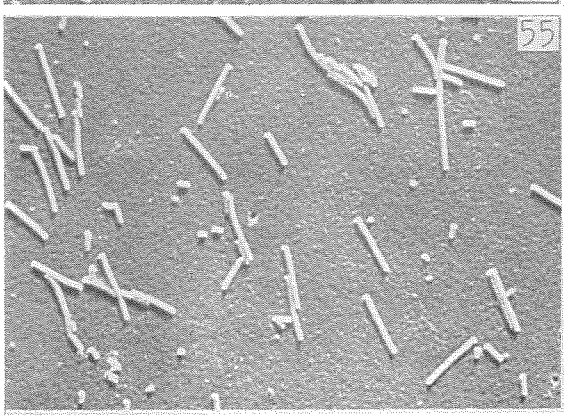
55

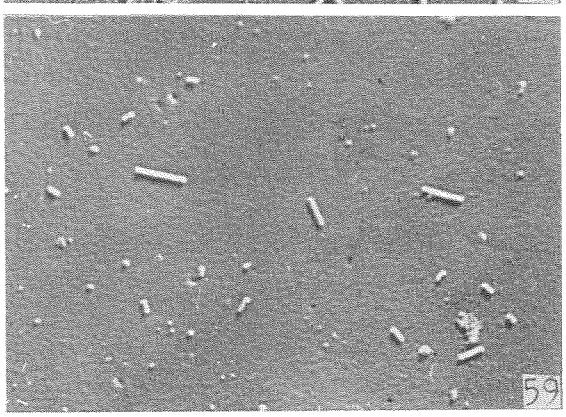
59

Fig. 60. ditto, for 48 hours.

61. Tobacco mosaic virus particles treated with 5% formalin solution for 20 hours. Cr shadowed, × 30,000.

62. ditto, 50% formaline.

63, 64. ditto, 100% formalin. High magnification of shortened particles on a line was shown in Fig. 64. × 86,400.

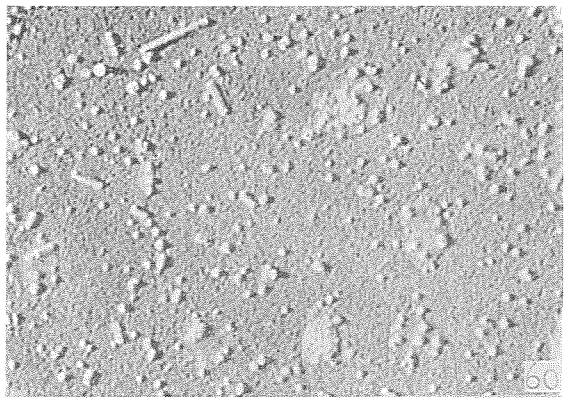
60

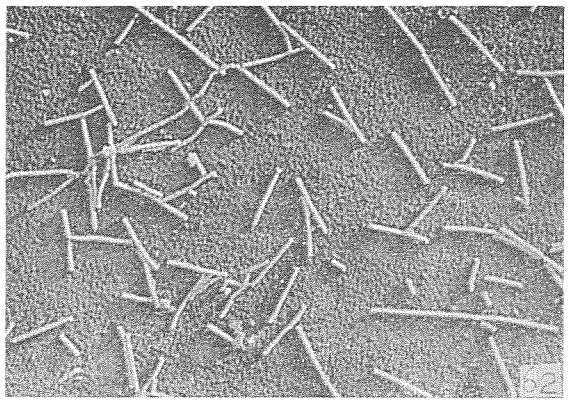
62

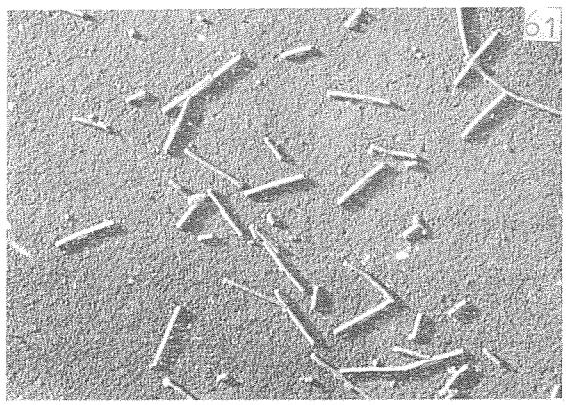
61

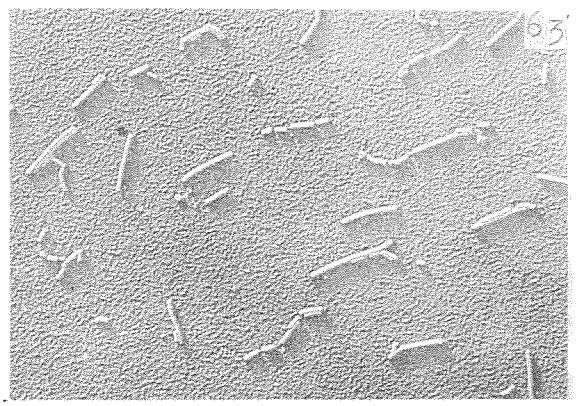
63

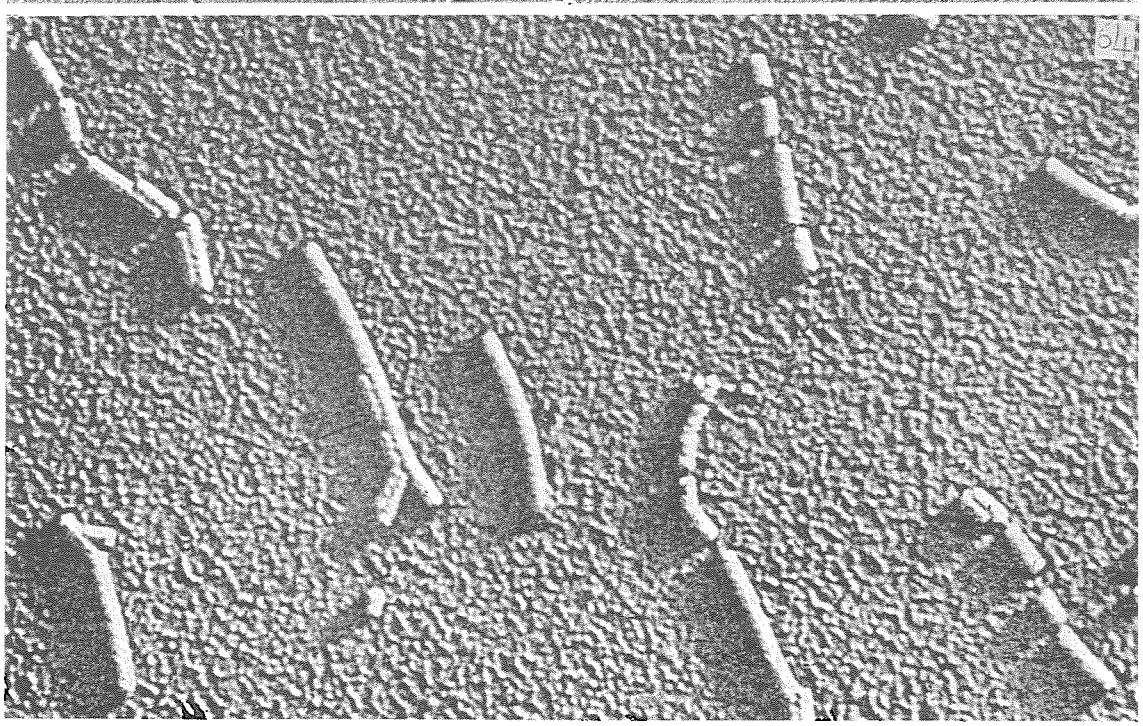
64

Fig. 65. Tobacco mosaic virus particles preserved at pH 3.3 for 24 hours, and then dialyzed for 4 days. Cr shadowed, × 30,000.

66. ditto, for 4 days.

67. Tobacco mosaic virus particles treated with 20% $NaNO_2$ for 24 hours. Cr shadowed, × 30,000.

68, 69. ditto, 50% $NaNO_2$ for 24 hours. High magnification of shortened particles are shown in Fig. 69. × 86,000.

70. ditto, 50% $NaNO_2$ for 3 days.

71. Tobacco mosai cvirus particles irradiated by ultraviolet light for 1 hour. Cr shadowed, × 30,000.

72. ditto, UV irradiation for 5 hours.

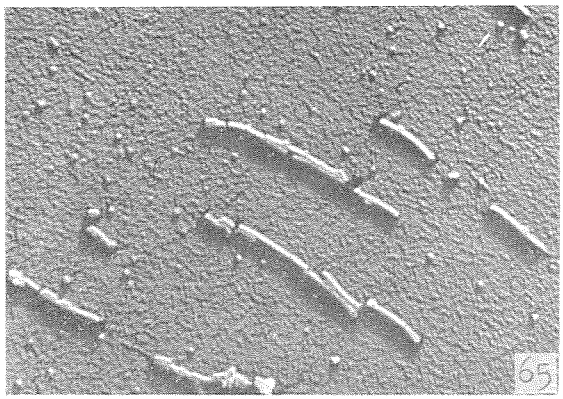
65

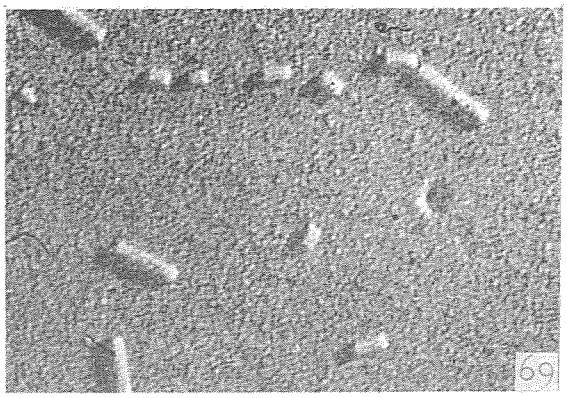
69

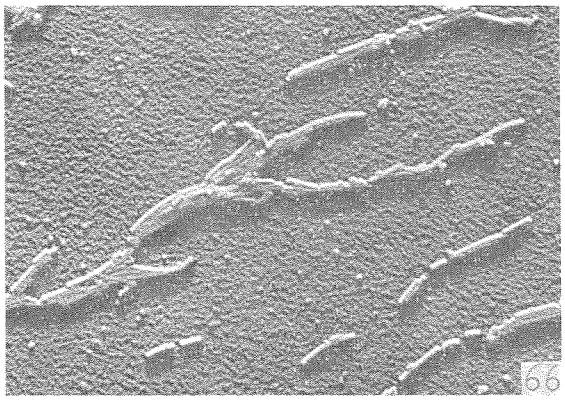
66

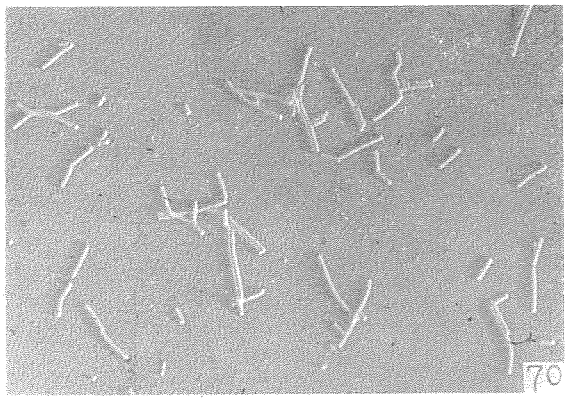
70

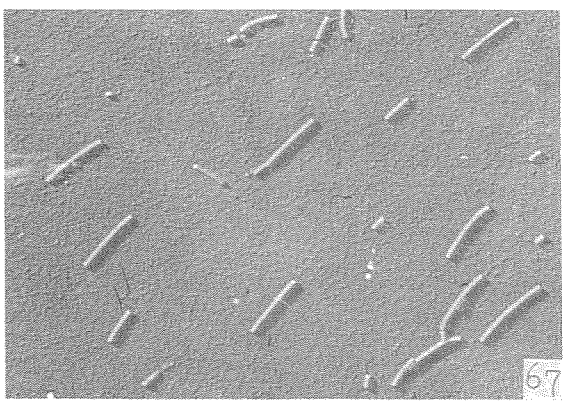
67

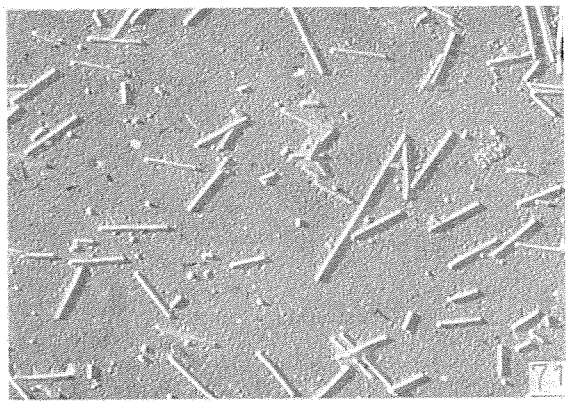
71

68

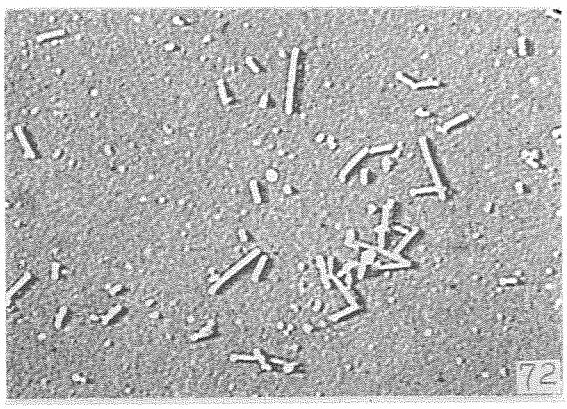
72

Fig. 73. ditto, for 6 hours

74. ditto, for 7 hours

75. ditto, for 8 hours

76. ditto, for 10 hours

77. Tobacco mosaic virus particles exposed by X-ray at $6\times10^4\,r$ Cr shadowed, $\times$ 30,000.

78. ditto, at $10\times10^4\,r$

79. ditto, at $30\times10^4\,r$

80. ditto, at $35\times10\,r$

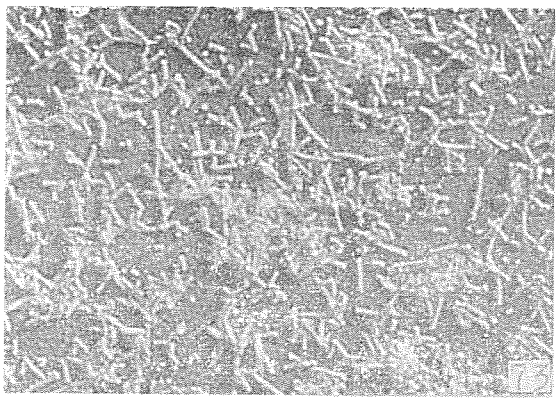
75

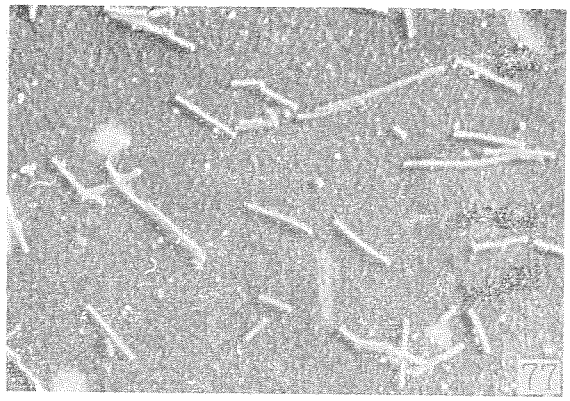
77

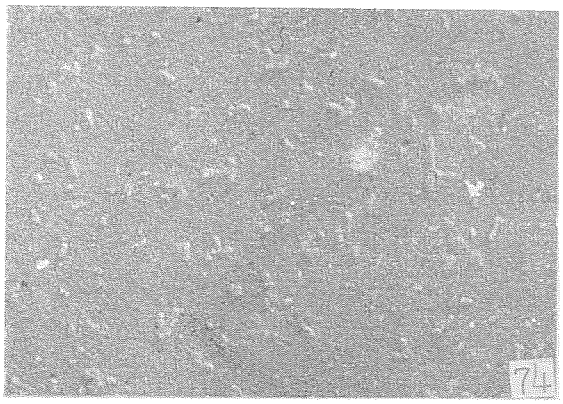
74

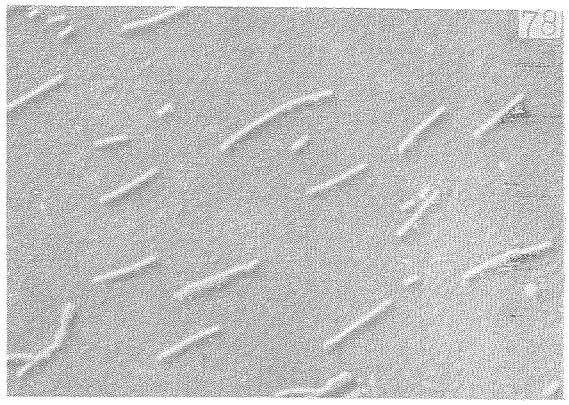
78

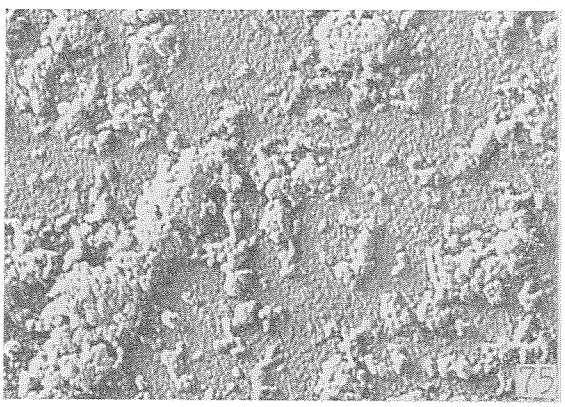
75

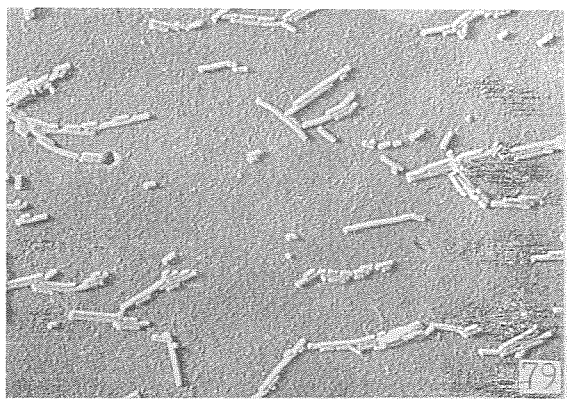
79

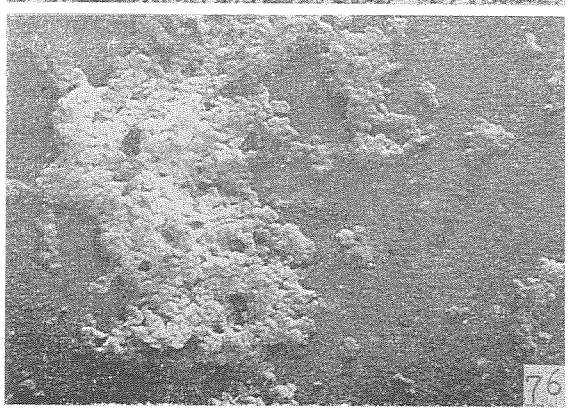
76

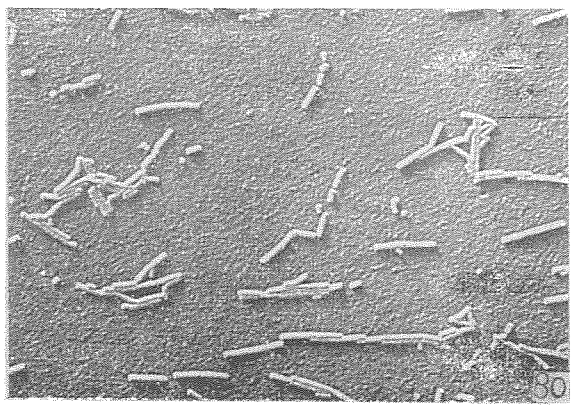
80

Fig. 81. ditto, $35\times10^4\,\gamma$ × 50.000.

82, 83. ditto, $50\times10^4\,\gamma$ High magnification of shortened particles is shown in Plate 83. × 80,000.

84. ditto, $60\times10^4\,\gamma$

85. ditto, $70\times10^4\,\gamma$

86. ditto, $75\times10^4\,\gamma$

87. ditto, $80\times10^4\,\gamma$

88. Disrupted tobacco mosaic virus particles after freeze-drying on collodion film by liquid nitrogen. Cr shadowed, × 66,000.

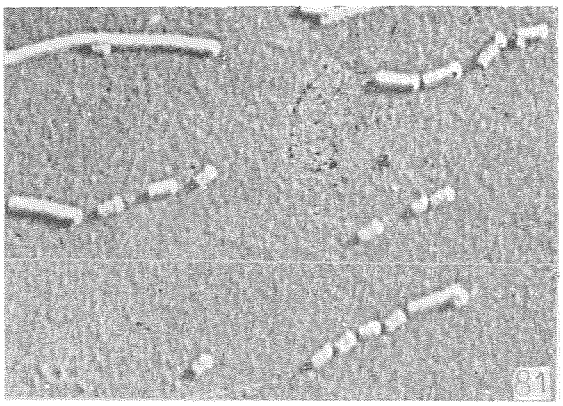
81

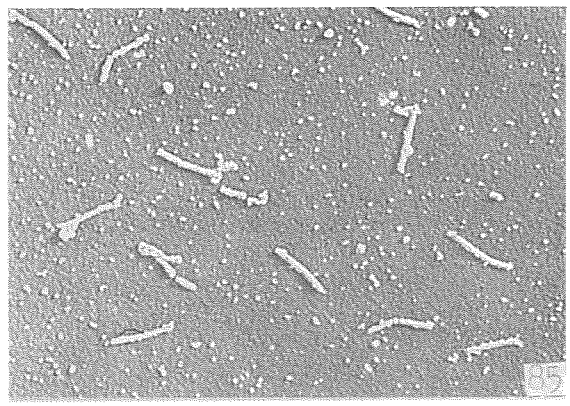
85

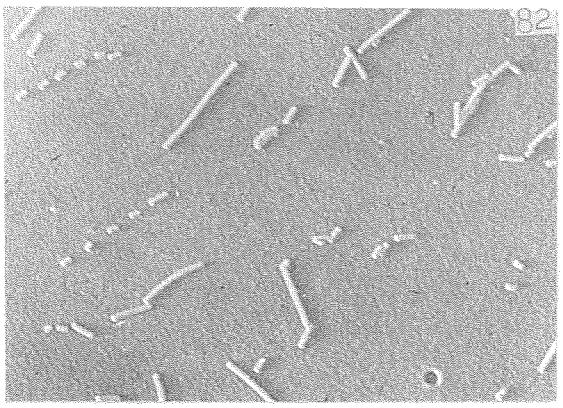
82

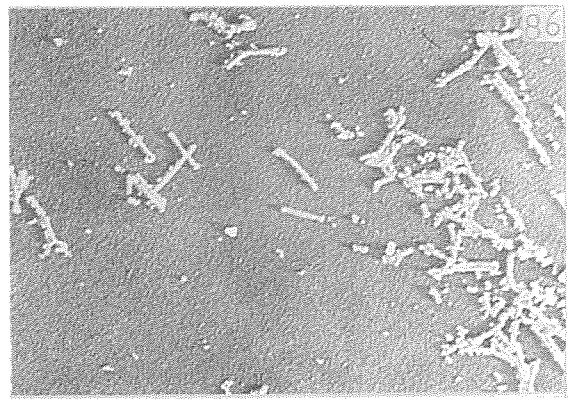
86

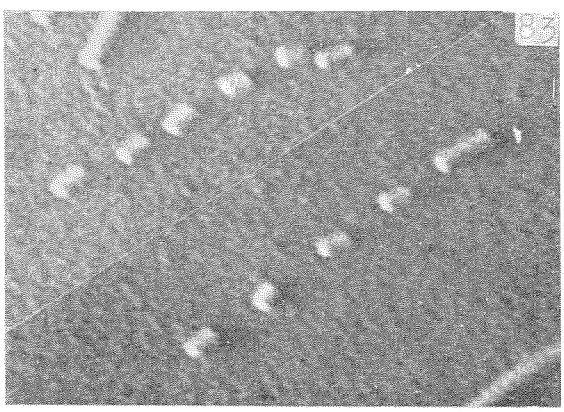
83

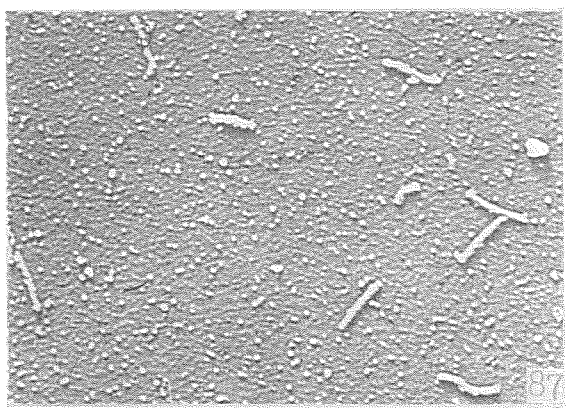
87

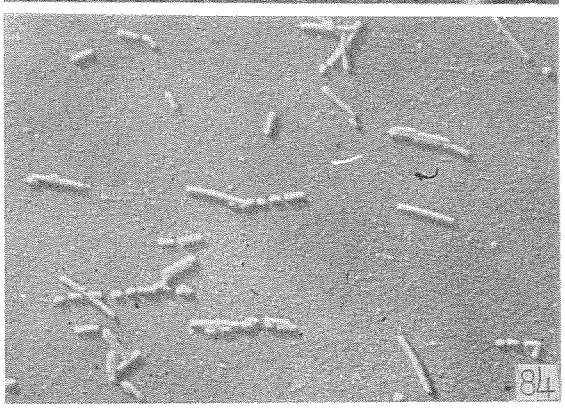
84

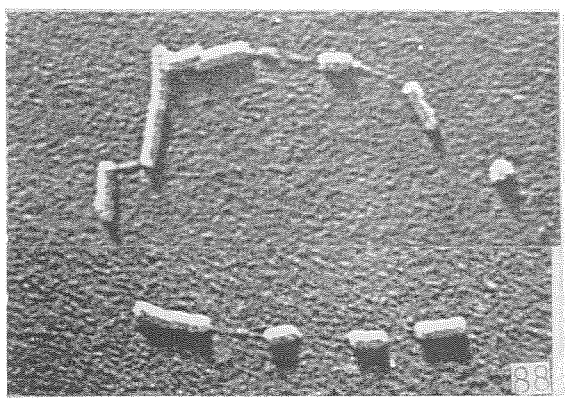
88

Fig. 89. Tobacco mosaic virus particles treated by 0.001% sodium lauryl sulfate at 85°C for 1 min. Pt shadowed, × 55,000. Fine threads were released from the shortened particles.

90. ditto, after treated by ribonuclease (0.0001%). Fine threads disappeared. Pt shadowed, × 55,000.

91. Tobacco mosaic virus particles treated by 0.01% SLS for 1 hour without heating the mixture. Pt shdowed, × 55,000.

89

90

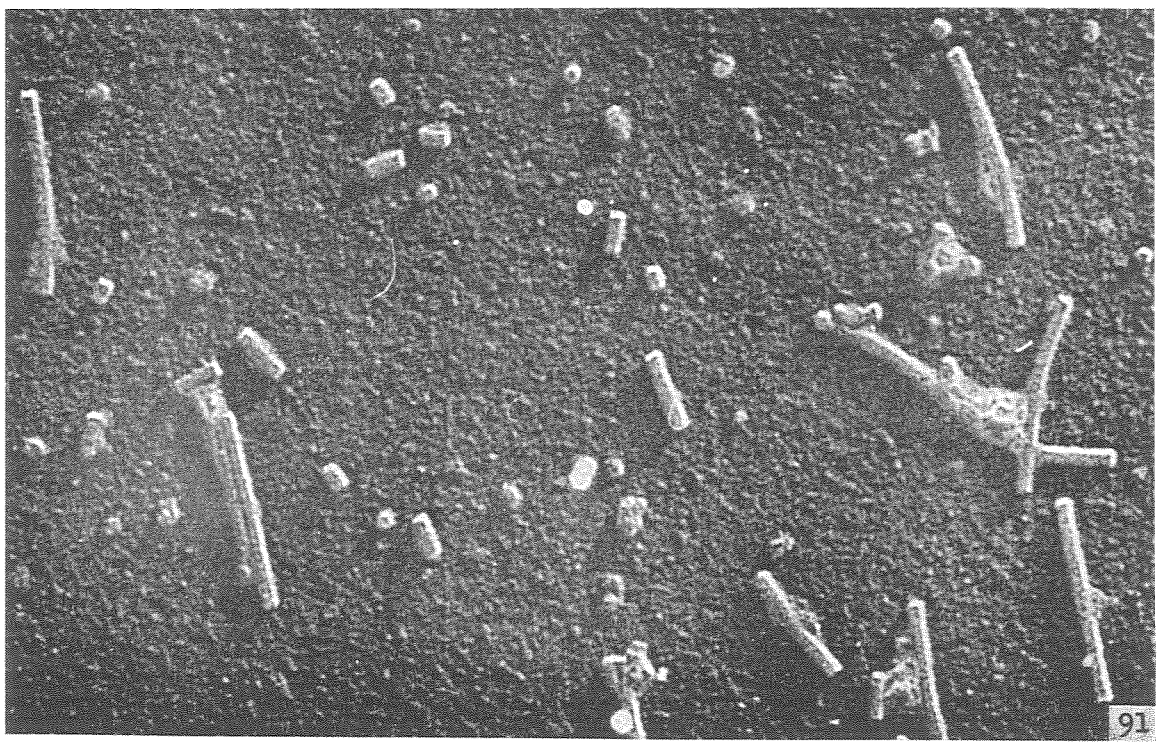

91

Fig. 92. A ultrathin section of *N. tabacum* plant infected with tobacco mosaic virus. N; Nucleus, Ch; Chloroplast, V; Virus particles. × 2,000.

93. ditto, × 1,500.

94. ditto, A mass of virus particles filled in a cell, × 3,25.

95. ditto, Two layers of virus bands, × 5,600.

92

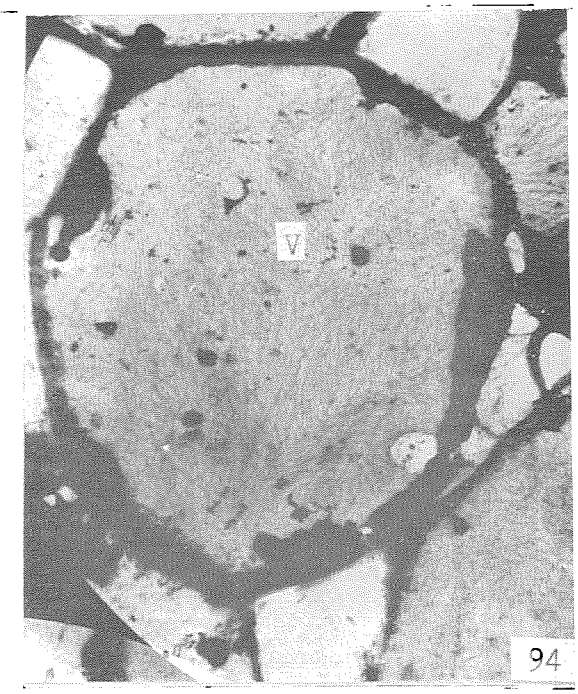

94

93

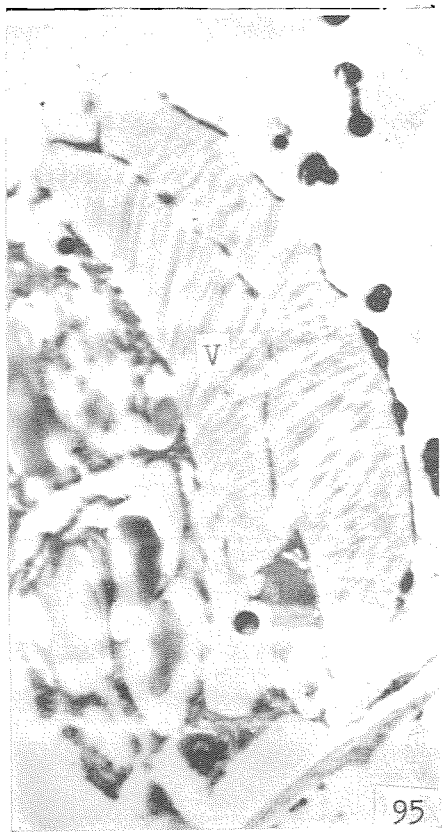

95

Fig. 96. A ultrathin section of healthy *N. glutinosa* leaf. N; Nucleus, Ch; Chloroplast. × 2,000.

97. A disintegrated chloropalst appeared in a cell of local nectrotic potten on *N. glutinosa*. Cr. shadowed, × 18,000.

98. A ultrathin section of a cell of local necrotic portion of infected *N. glutinosa*. N; Nucleus, M; Mitochondrium. × 12,000.

99, 100. The disinegrated chloroplasts appeared in the cell of local necrotic portion of *N. glutinosa*. Electron dense substances surrounding chloroplasts are shown. Fig. 99. × 16,800, Fig. 100 × 15,000.

101. Deposition of elctron dense substances in a necrotic cell of *N. glutinosa*. × 15,000.

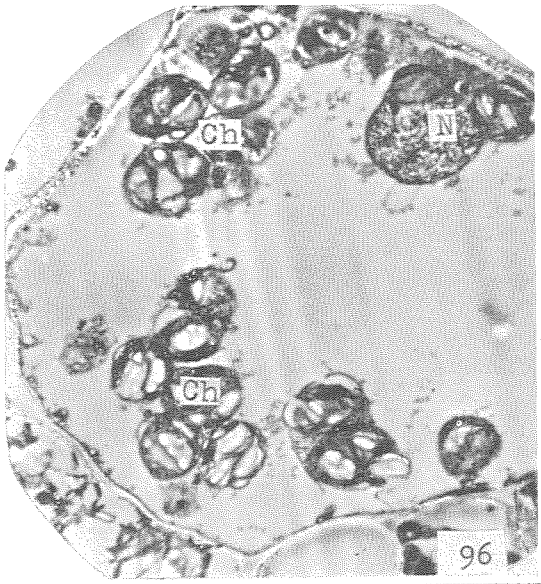

96

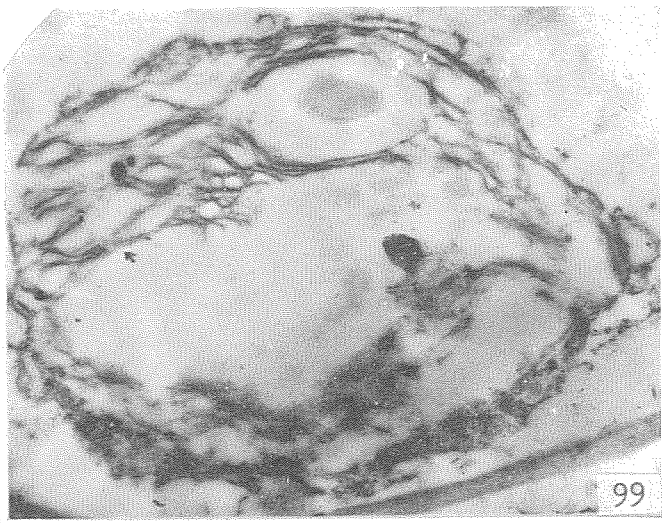

99

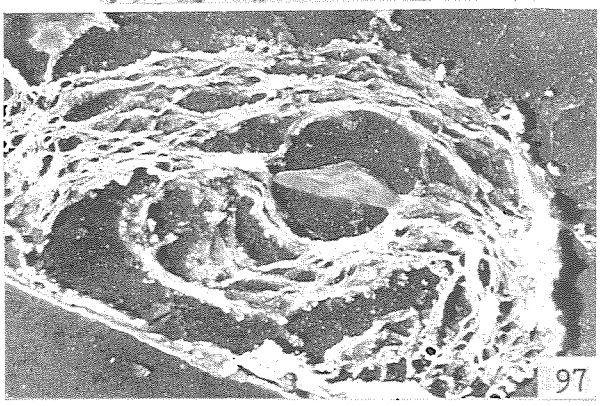

97

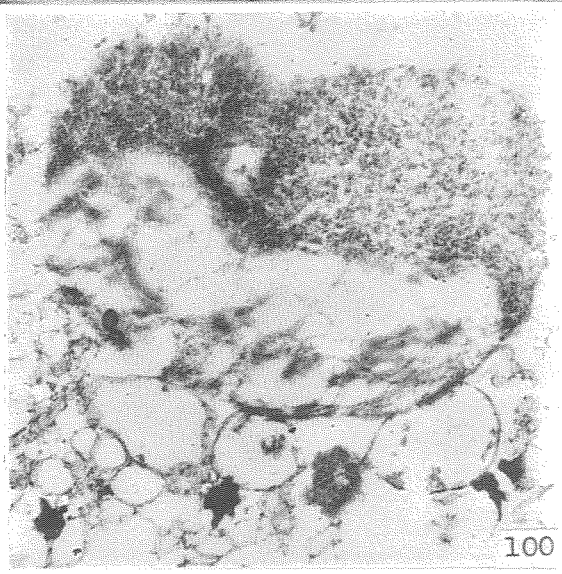

100

101

98

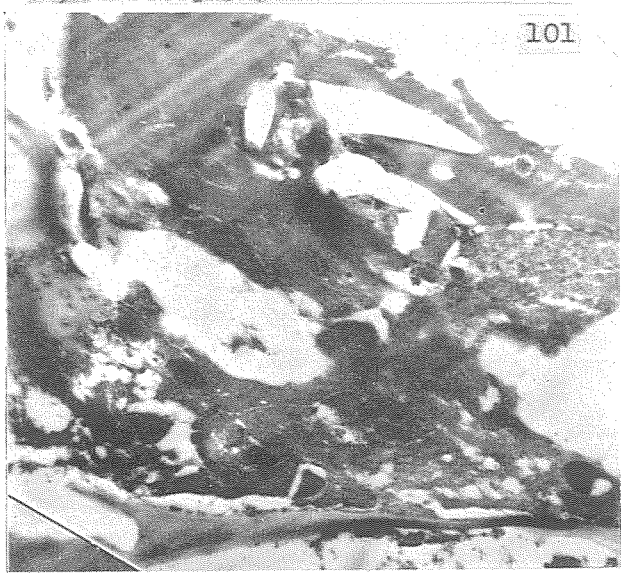

Fig. 102. Ultrathin sections of the vascular bundle in local necrotic portion of *N. glutinosa*. Ch; Chloroplast V; Virus particles encountered in the phloem. × 7,200.

V
102
Ch
Ch

Fig. 103. High magnification of a phloem cell from Fig 102. Cr shadow. × 32,000.

104. A cell next to the phloem cell, no virus particles could be found. × 24,000.

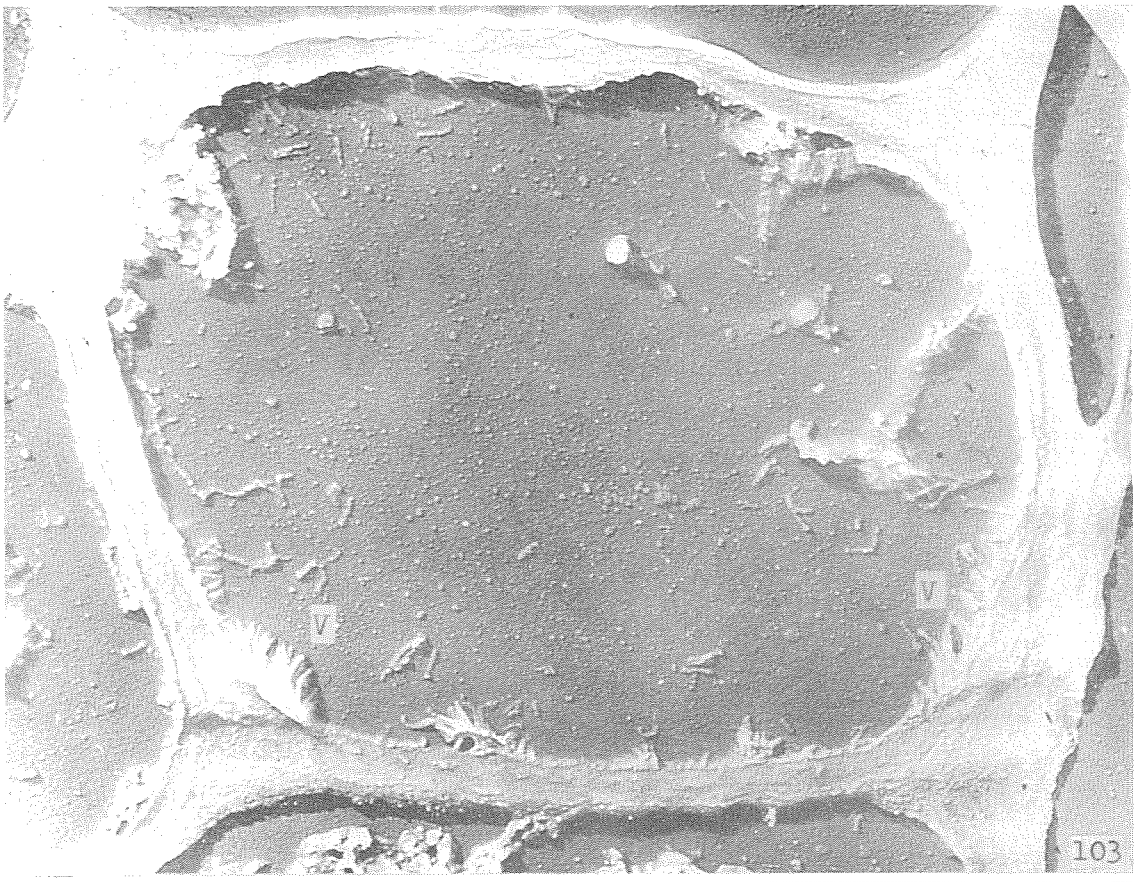
V
V
103

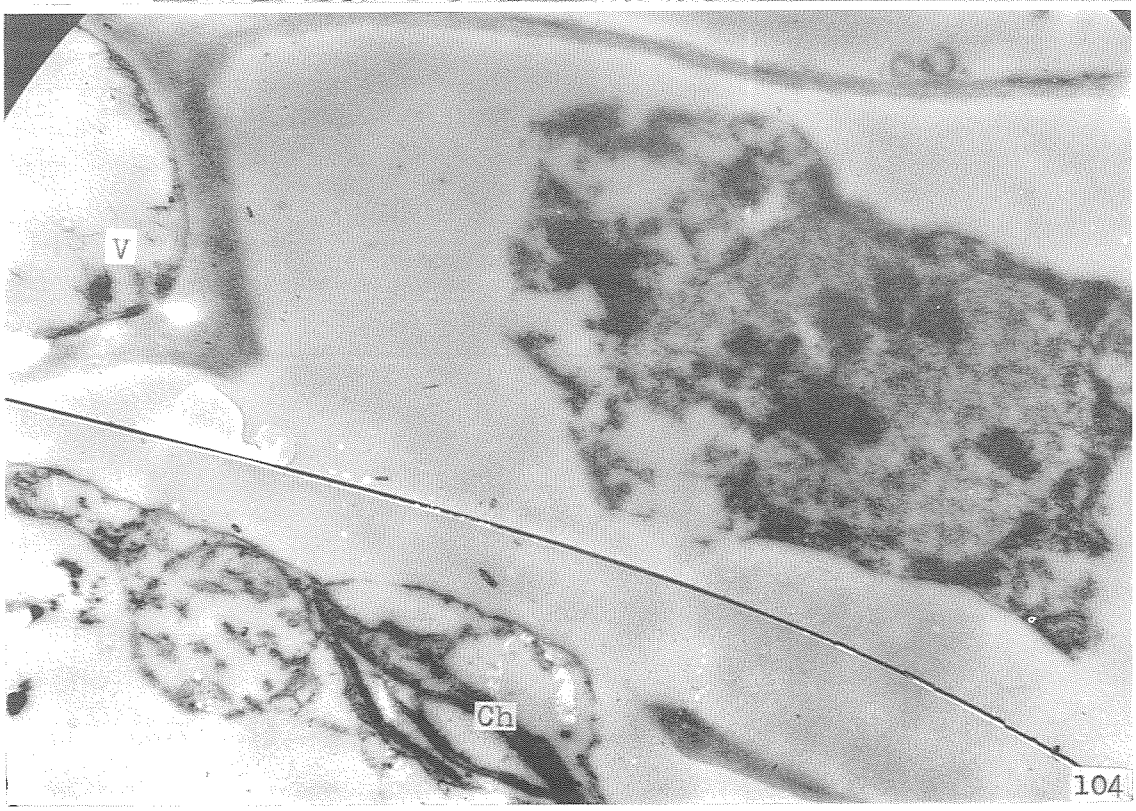
V
Ch
104

Fig. 105. Potato virus X, strain X-68 particles in purified suspension. Cr shadowed, × 95,000.

106. Potato virus X, strains X-5 in crude sap. Cr shadowed, × 30,000.

107. Potato virus X, strain I-43 in crude sap. Cr shadowed. × 30,000.

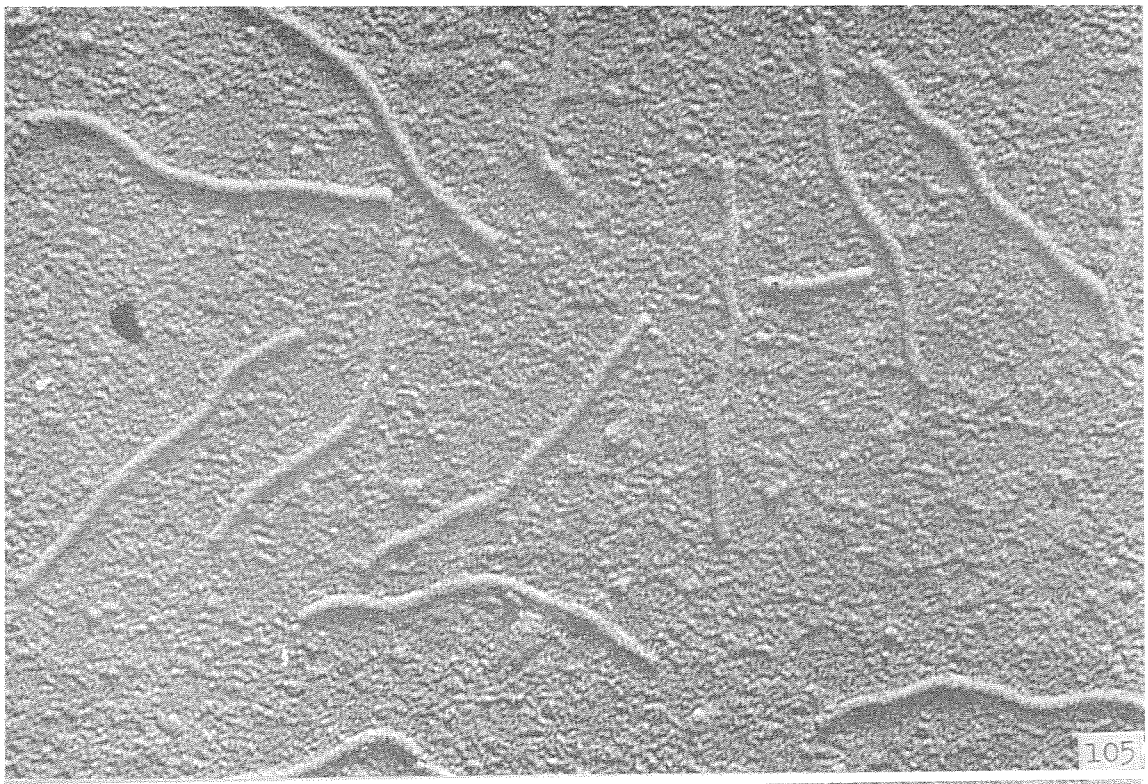

105

106

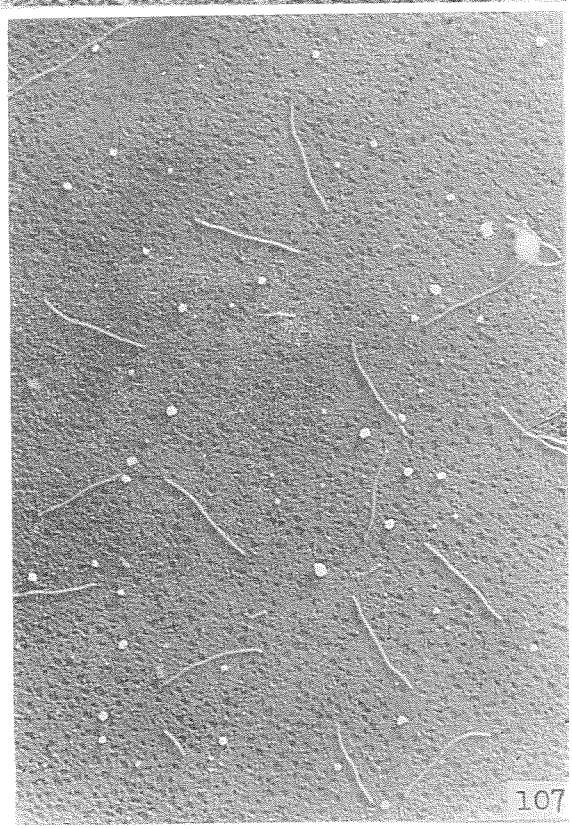

107

Fig. 108. Potato virus X, strain C-1 in crude sap. Cr shdowed, × 30,000.

109. Potato virus X particles in various hydrogen-ion concentration at pH 2.0. Cr shadow, × 30,000.

110. ditto, at pH 3.0.

111. ditto, at pH 4.6.

112. ditto, at pH 6.8.

113. ditto, at pH 10.0.

114. ditto, at pH 11.0.

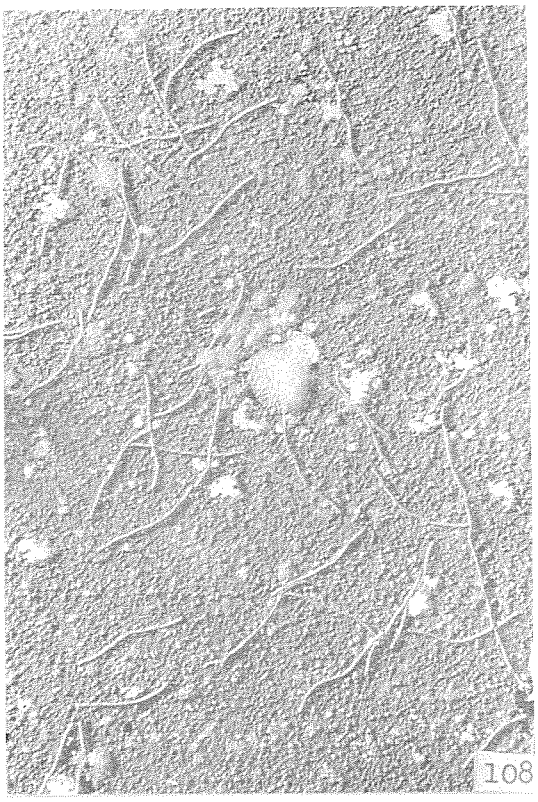
108

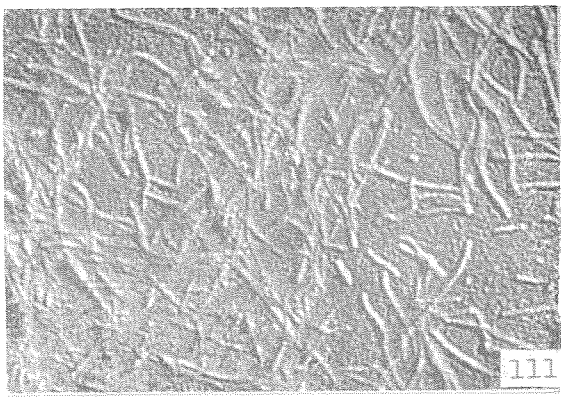
111

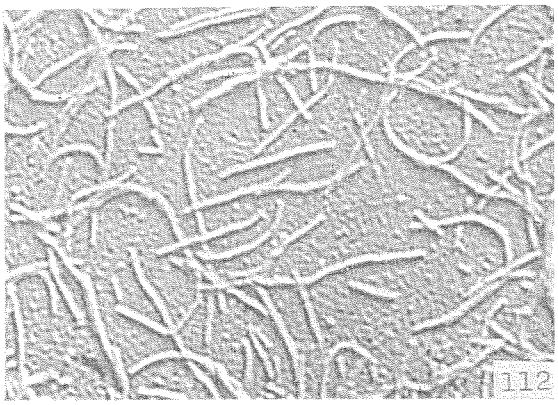
112

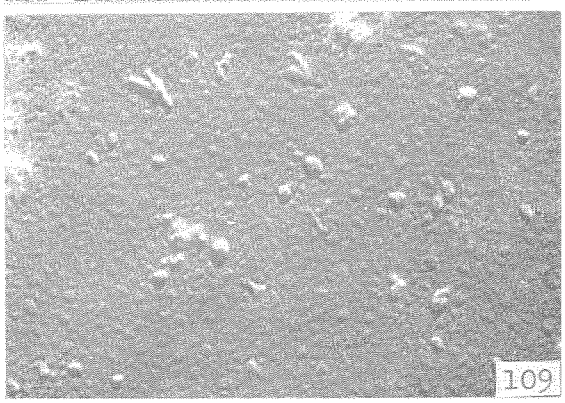
109

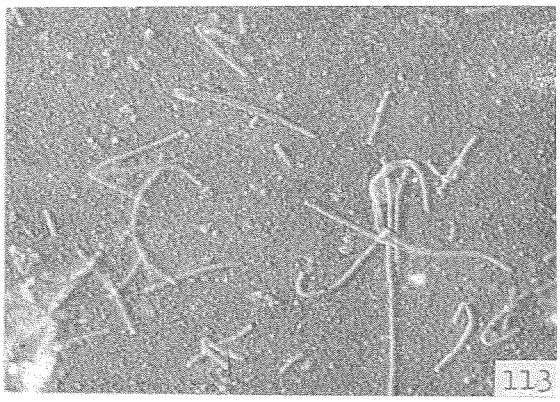
113

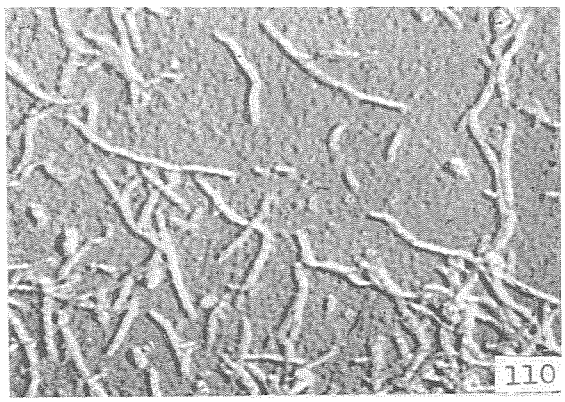
110

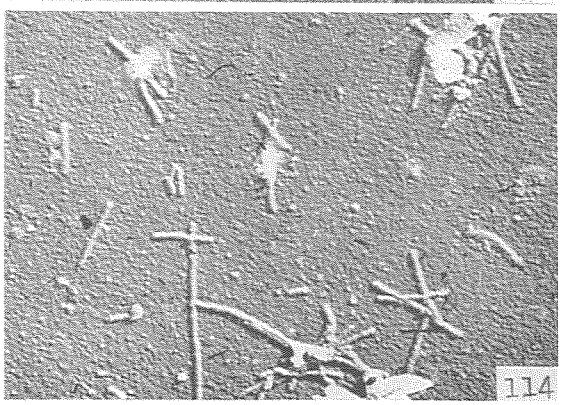
114

Fig. 115. ditto, at pH 12.0.

116. Potato virus X particles irradiated by ultraviolet light, untraeted control. Cr shadowed, × 30,000.

117. ditto, for 10 min.

118. ditto, for 30 min.

119. ditto, for 60 min.

120, 121. ditto, for 90 min.

122. ditto, for 3 hours, in ten times concentrated solution.

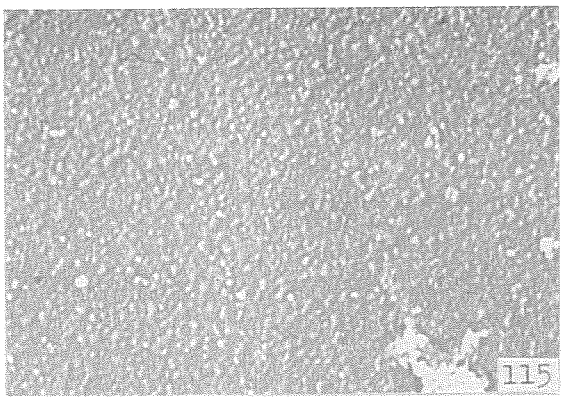
115

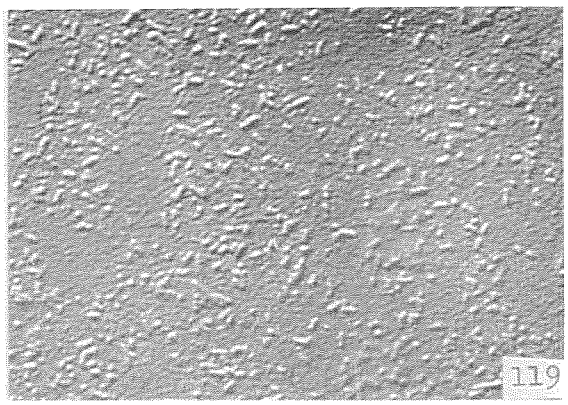
119

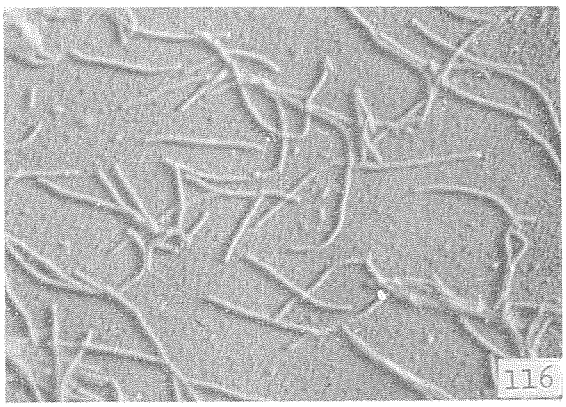
116

120

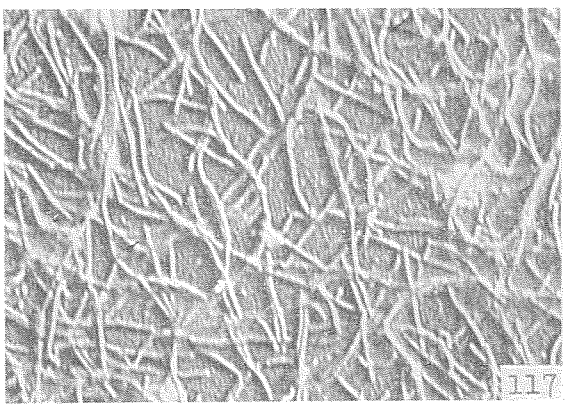
117

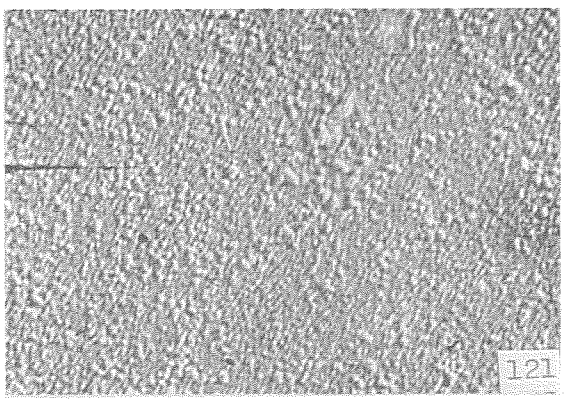
121

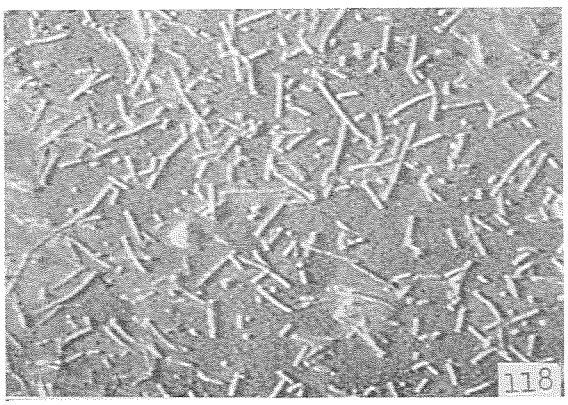
118

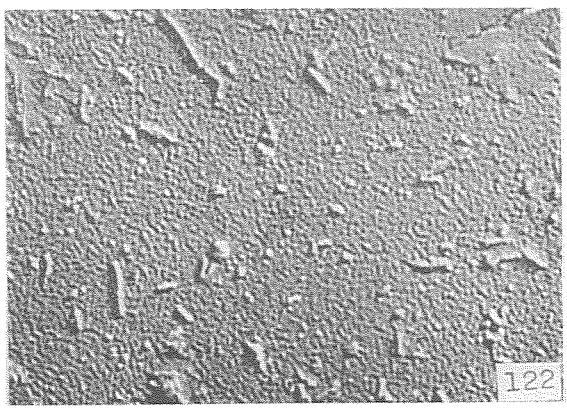
122

Fig. 123, 124, 125. Potato virus X particles encountered through ultrathin sections from *N. glutinosa* plants infected with potato virus X. Ch; chloroplast, V; potato virus X particles. Fig. 123, 124 show masses of virus particles encountered in the cytoplasm of the cell. ×16,000 & 20,000. Fig. 125 represents a dense mass of the virus surrounded by dense membraneous granules. × 16,500.

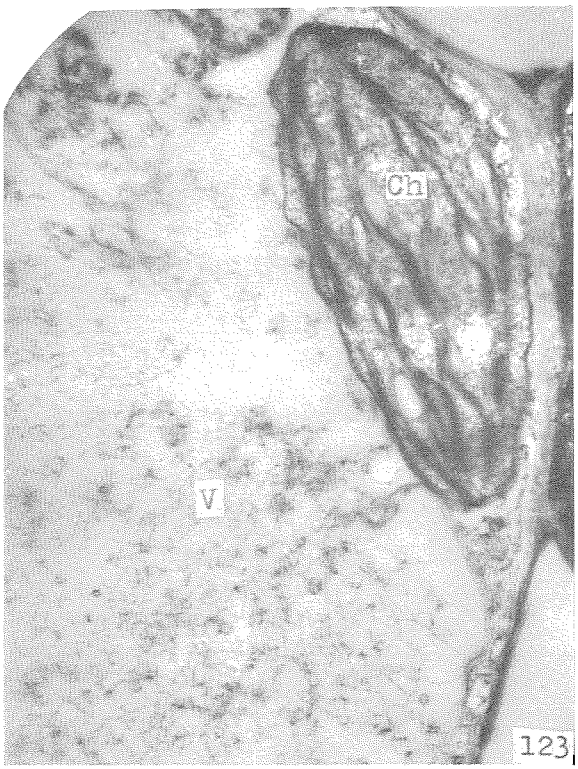

123

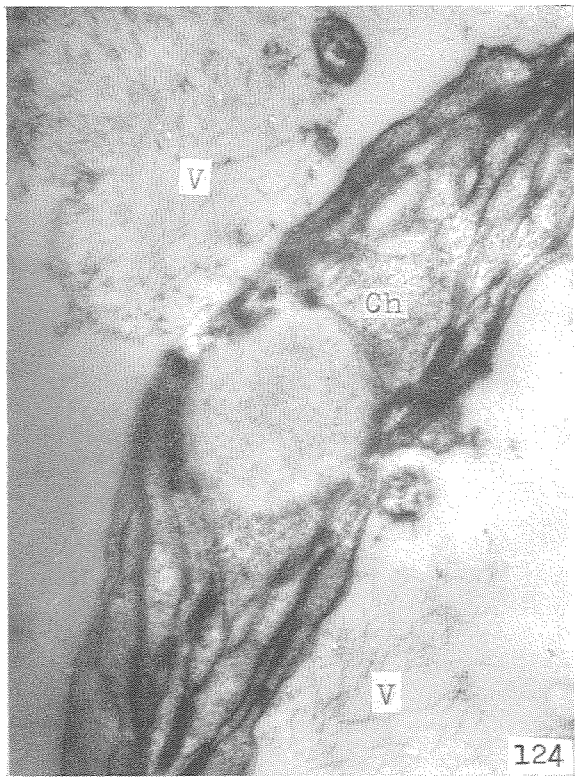

124

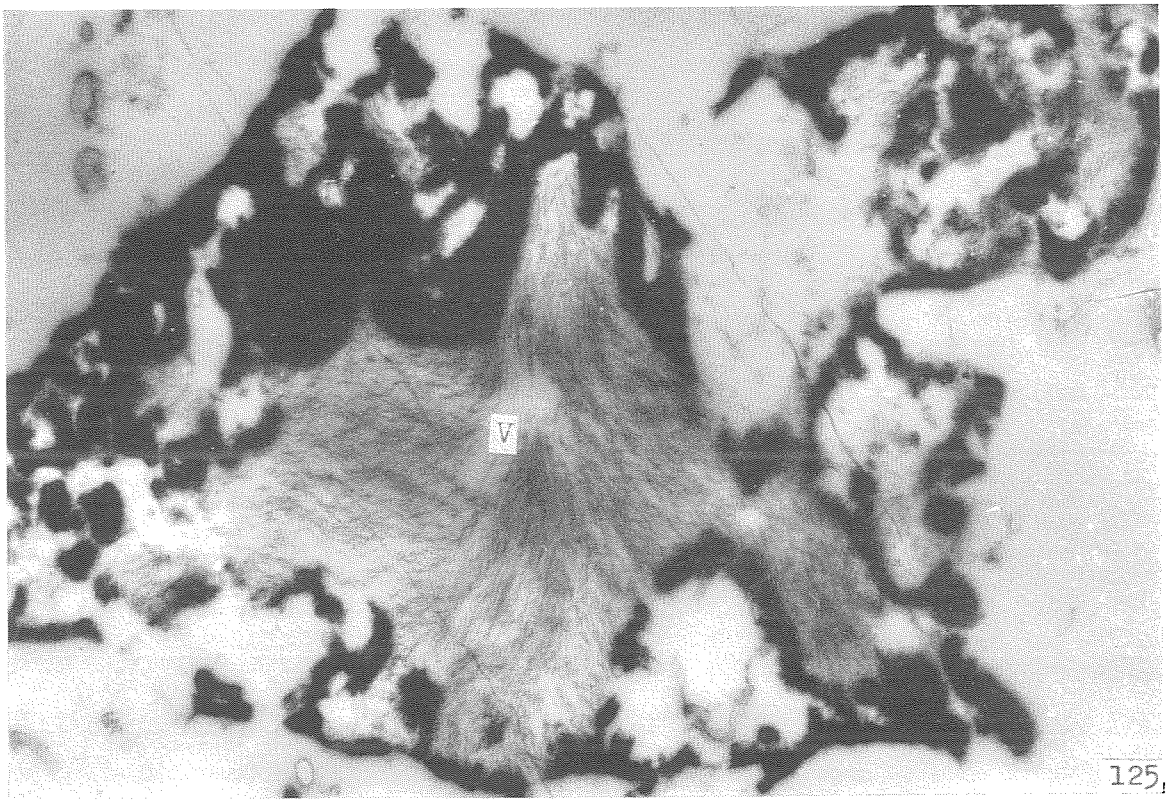

125

Fig. 126, 127, 128. ditto, virus particles seem to be liberated from a dense virus mass. × 2,300, 60,000 & 80,000.

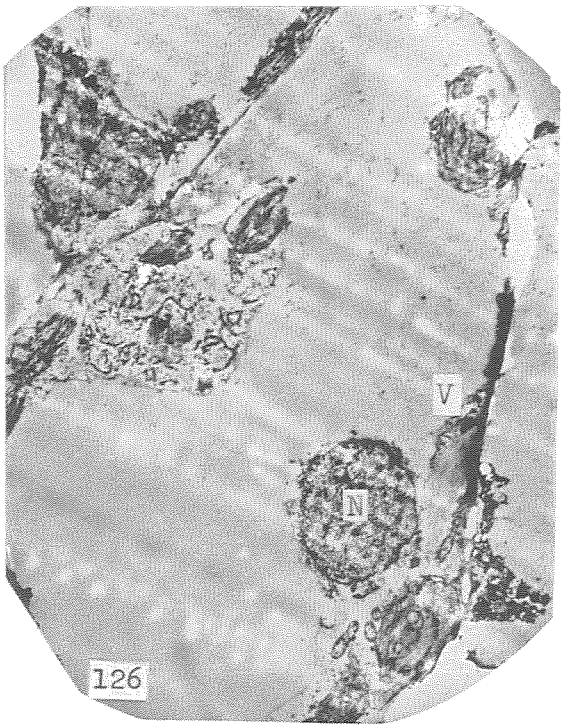
V
N
126

127

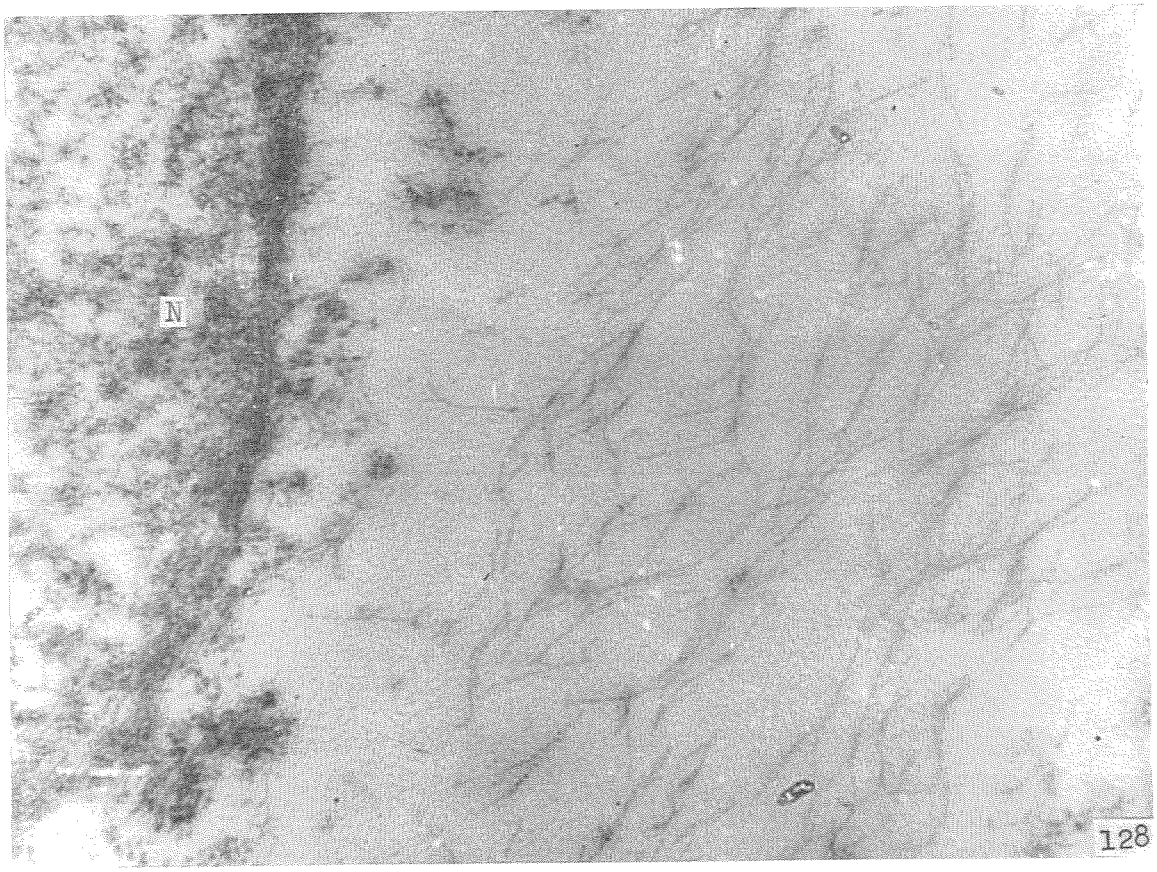
N
128

Fig. 129. Barley stripe mosaic virus particles isolated from diseased barley plants. Cr shadowed, × 80,000.

130. ditto, isolated from diseased corn plants. × 72,500.

131, 132. Barley stripe mosaic virus particles purified by sucrose density gradient centrifugation. Cr shadowed, × 40,000 & 80,000. Cross section of the virus rods with central hole were visible in Fig. 132.

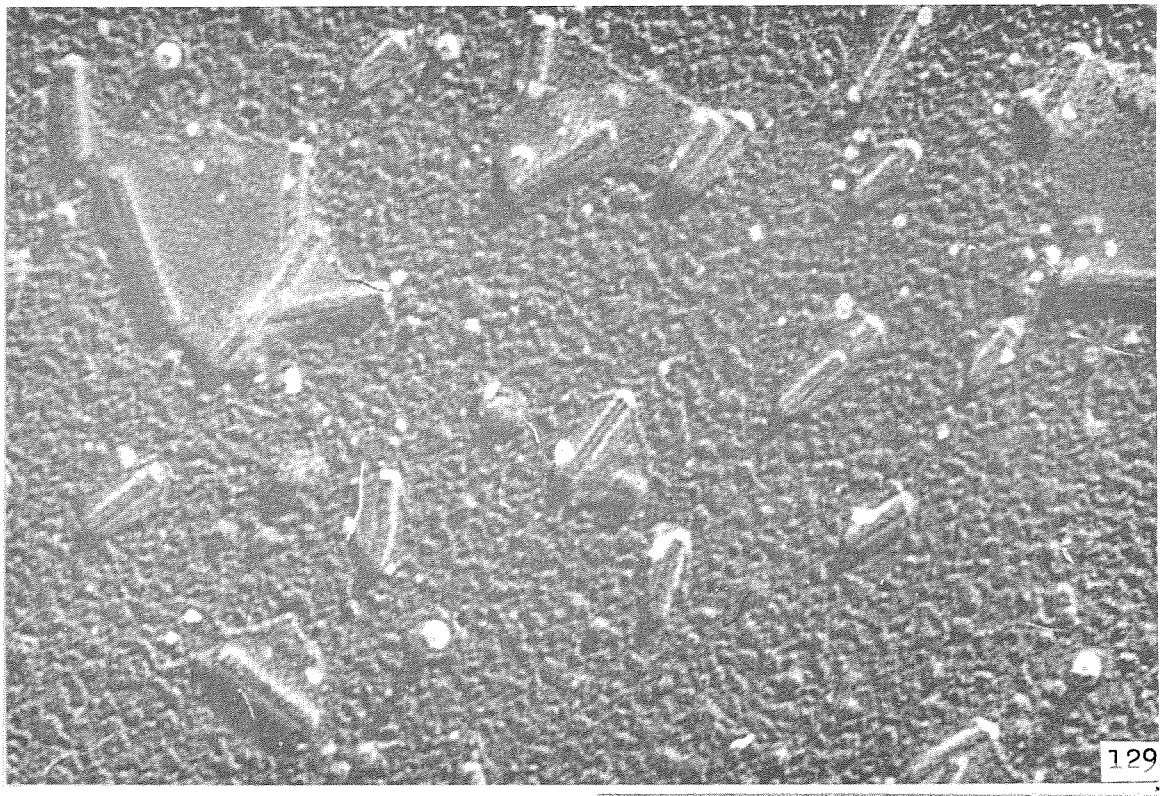
129

130

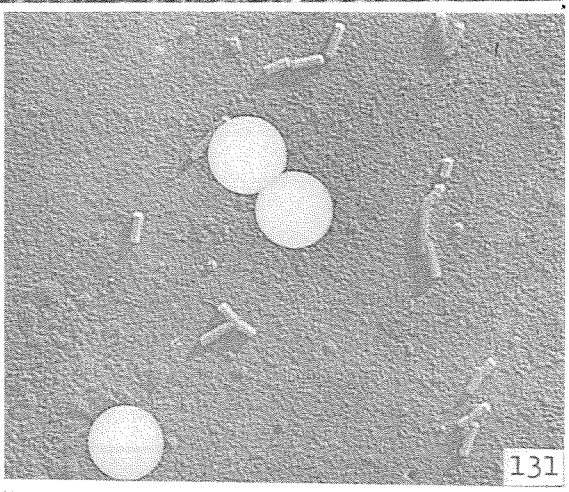
131

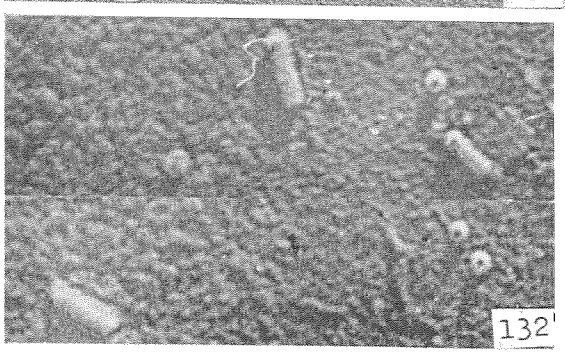
132

Fig. 133. Barley stripe mosaic virus particles. Unshadowed, × 80,000.

134, 135. ditto, PTA stained, fine thread like structure were visible in the center of the virus rods. ×80,000

136. ditto, washed with dist. water after PTA staining. No thread like structures are seen in the center of the virus rods.

137. ditto, KCl stained. ×80,000

138, 139. Barley stripe mosaic virus particles treated with 0.001% SLS at 60°C for 1 min. Cr. shadowed, × 61,000.

140. ditto, at 85 °C for 1 min.

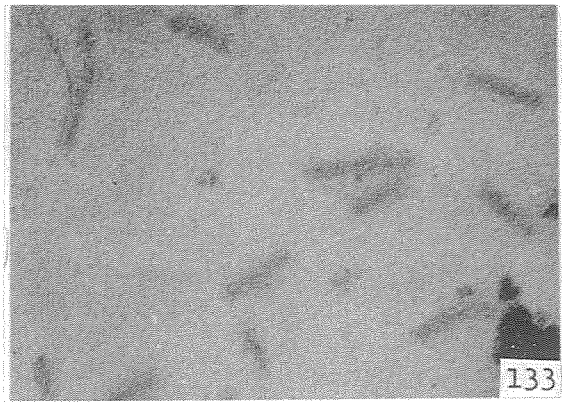
133

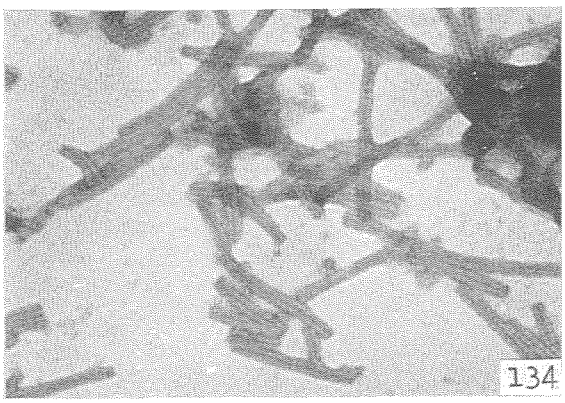
134

135

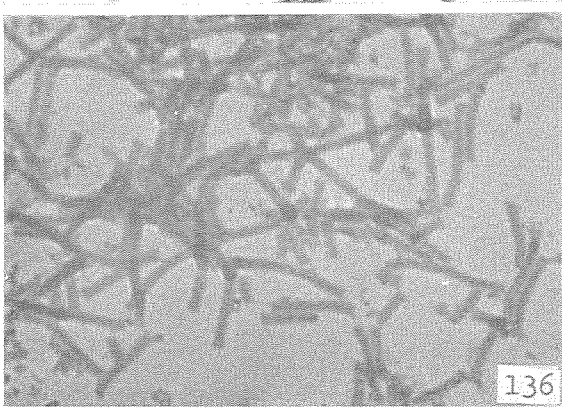
136

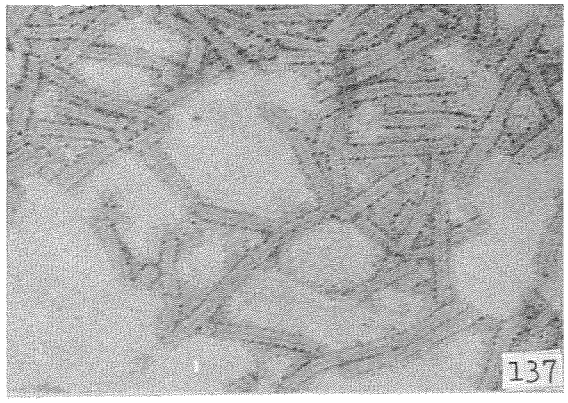
137

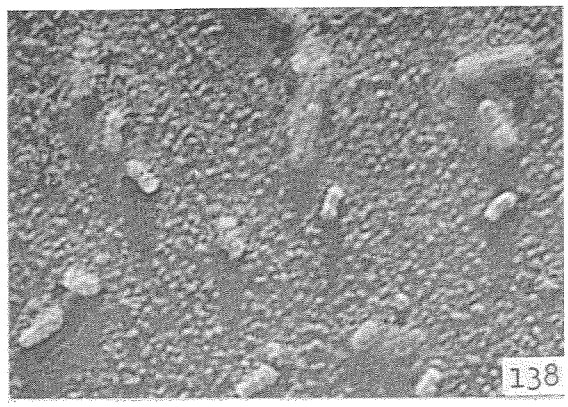
138

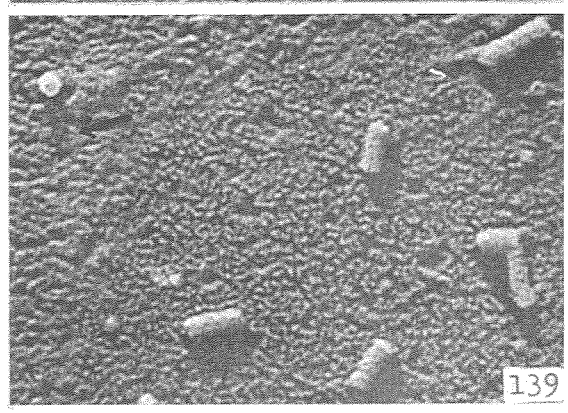
139

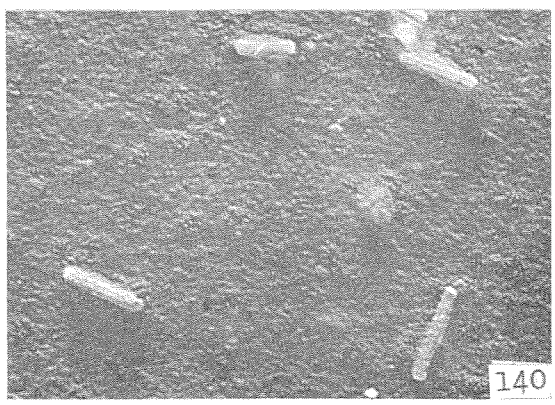
140

Fig. 141. Purified barley stripe mosaic virus particles. A fine thread between broken rods is visible. Cr shadowed, × 40,000.

142. Barley stripe mosaic virus particles treated with 0,001% SLS at 85°C for 1 min. A fine thread is projected from shortened rods. Cr shadowed, × 55,000.

141

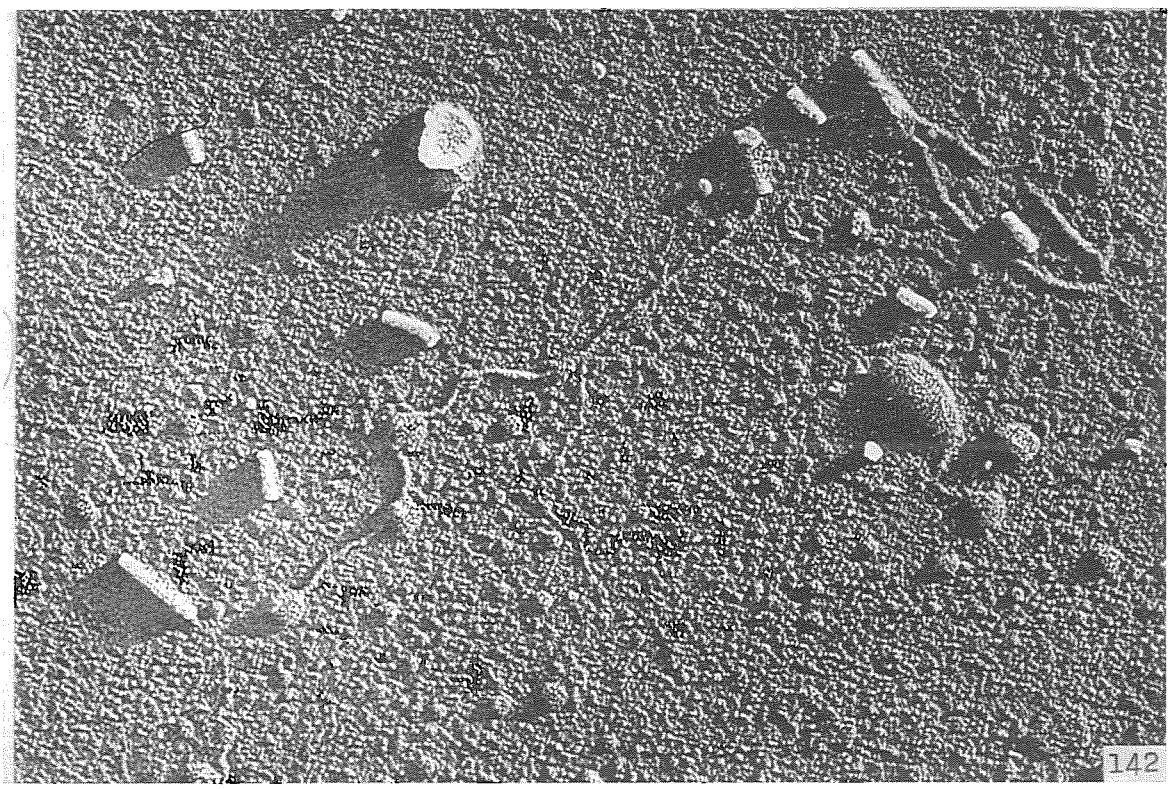
142

Fig. 143. Rice dwarf virus particles from diluted sap of chlorotic portion of diseased leaves of rice plants. Cr shadowed, × 46,000.

144. Isolation of rice dwarf virus particles from diseased rice plants. Precipitates of 20,000 rpm for 2 hours centrifugation. Cr shadowed. × 83,000.

145. ditto, precipitates at 10,000 rpm for 60 min. centrifugation. Cr shadowed, × 50,000.

146. ditto, precipitates at 10,000 rpm for 90 min.

147. ditto, precipitates at 10,000 rpm for 120 min.

148. ditto, supernates at 10,000 rpm for 120 min.

149, 150. Repeated precipitation at 10,000 rpm for 120 min.
3 times. Cr. shadowed, × 50,000 in Fig. 149.
5 times. in Fig. 150.

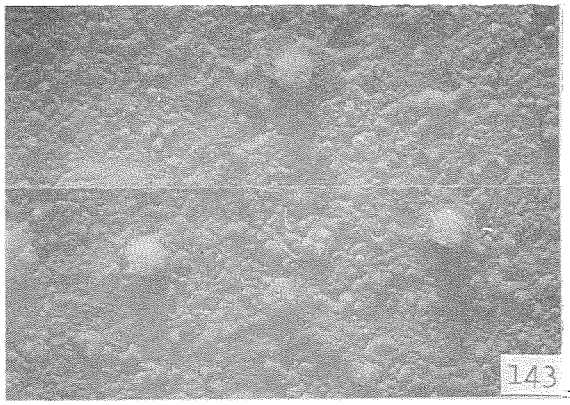
143

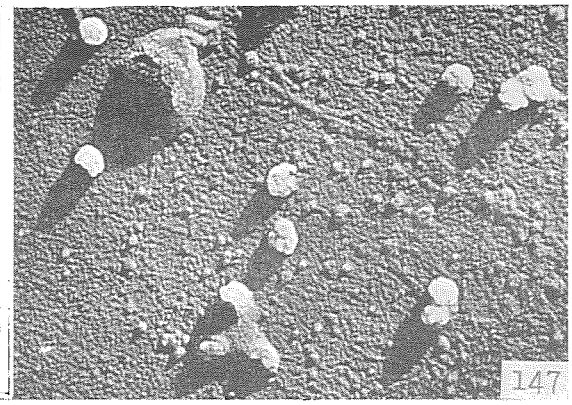
147

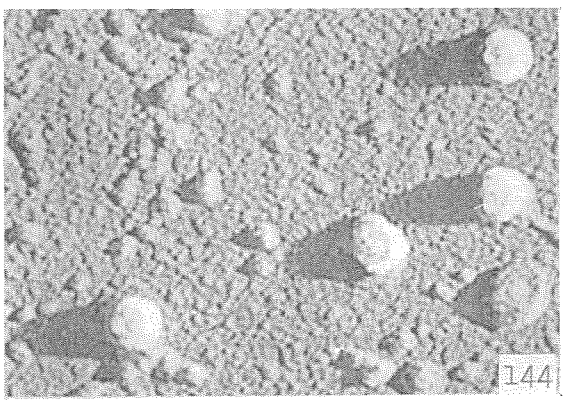
144

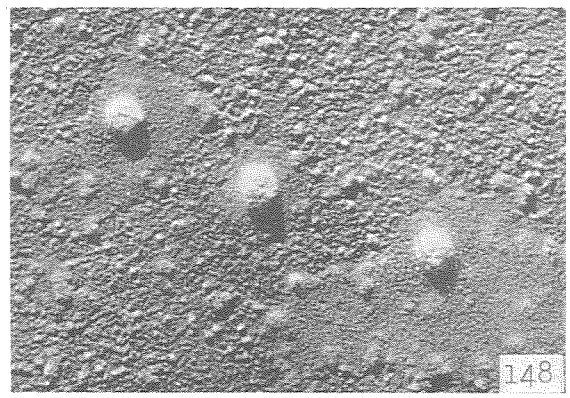
148

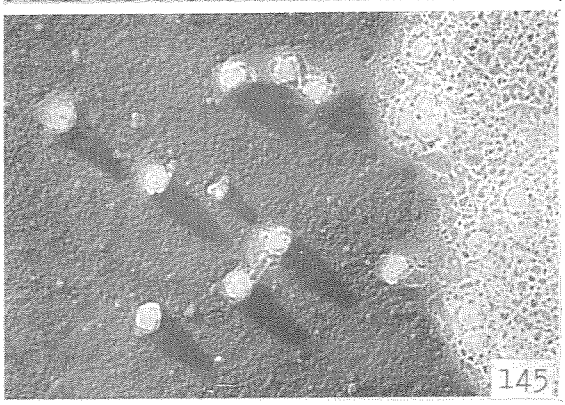
145

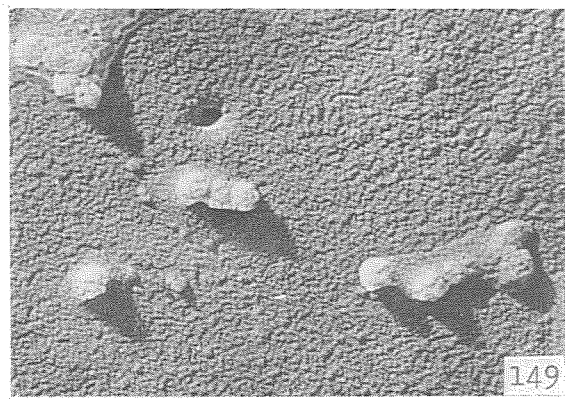
149

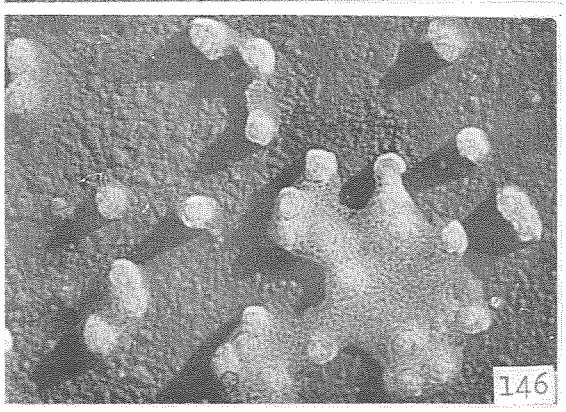
146

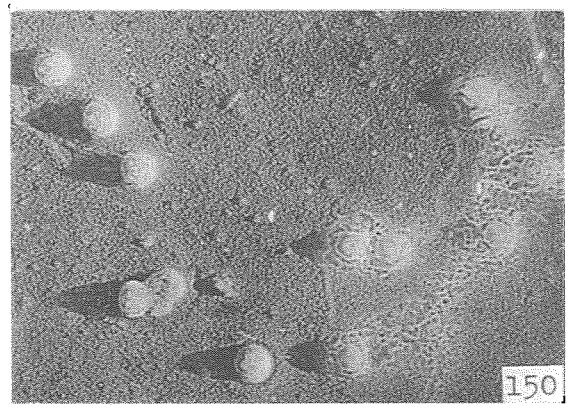
150

Fig. 151. Rice dwarf virus particles isolated from diseased rice plants by Centri fugation at 20,000 rpm for 1 hour. Cr shadowed, × 85,500.

152. Rice dwarf virus particles isolated from diseased Echinochloe crus-galii. Cr shadowed, × 76,500.

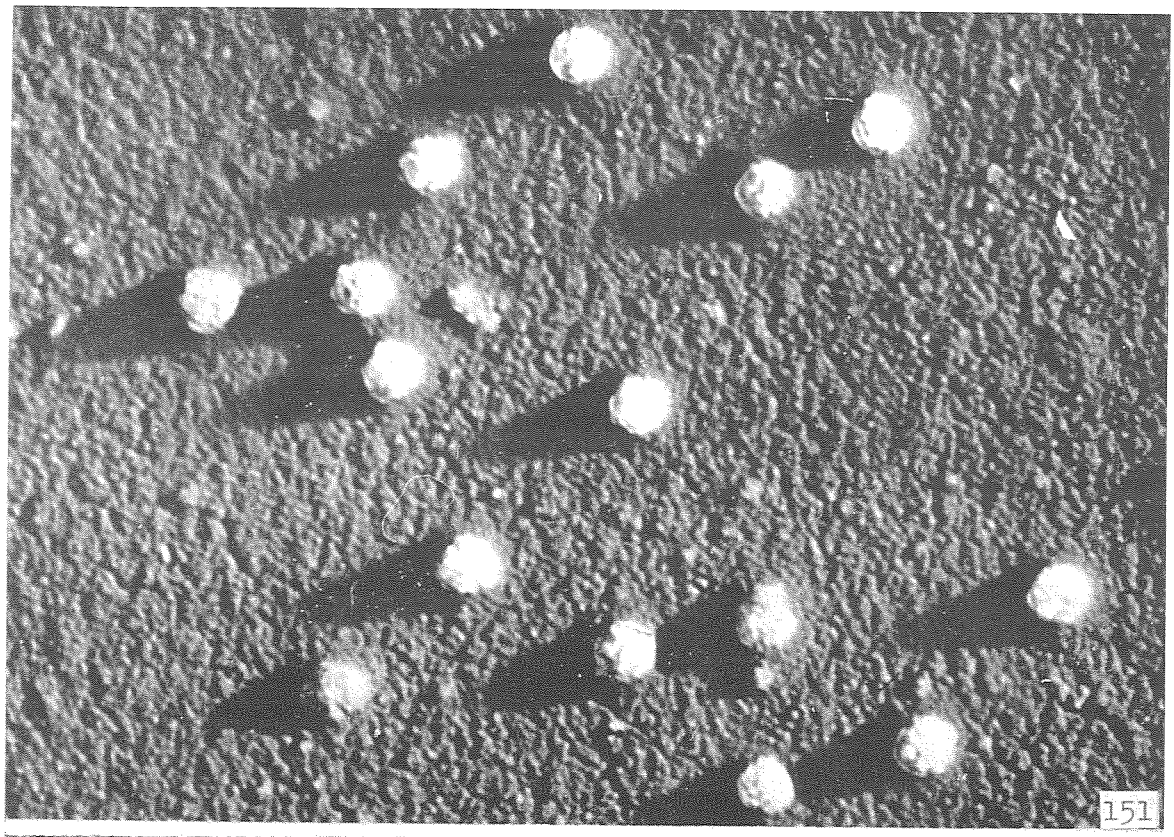

151

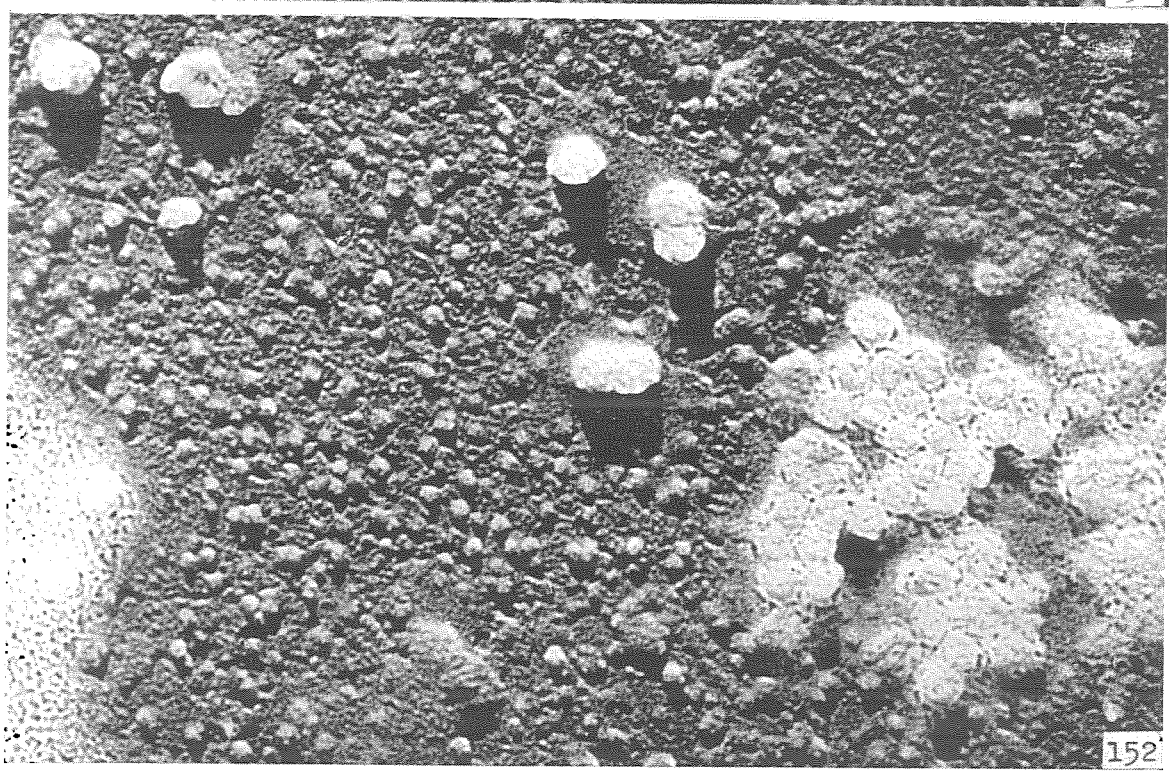

152

Fig. 153, 154, 155. Rice dwarf virus particles isolated from viruliferous leafhoppers. Cr shadowed, × 80,000 in Fig. 153, 154; × 76,500 in Fig. 155.

156–159. Unshadowed rice dwarf virus particles isolated from diseased plants. Fig. 156. × 72,000; Fig. 157, 158. × 351,000; Fig. 159. × 210,000.

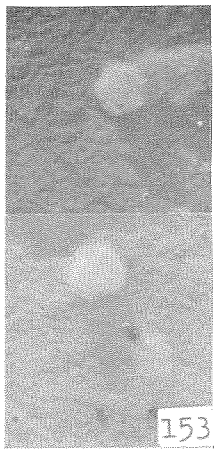
153

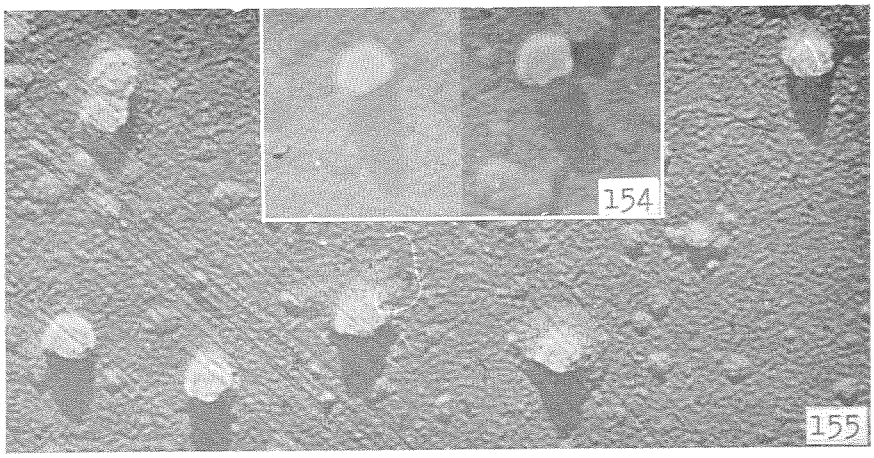
154

155

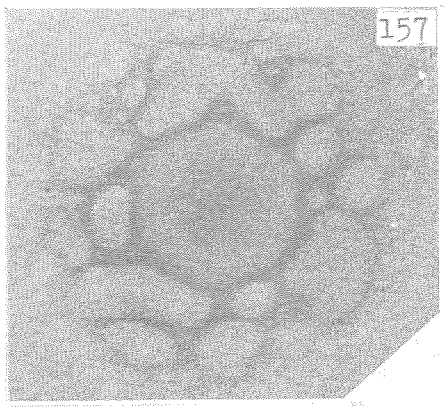
157

156

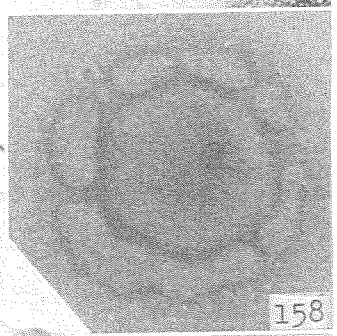
158

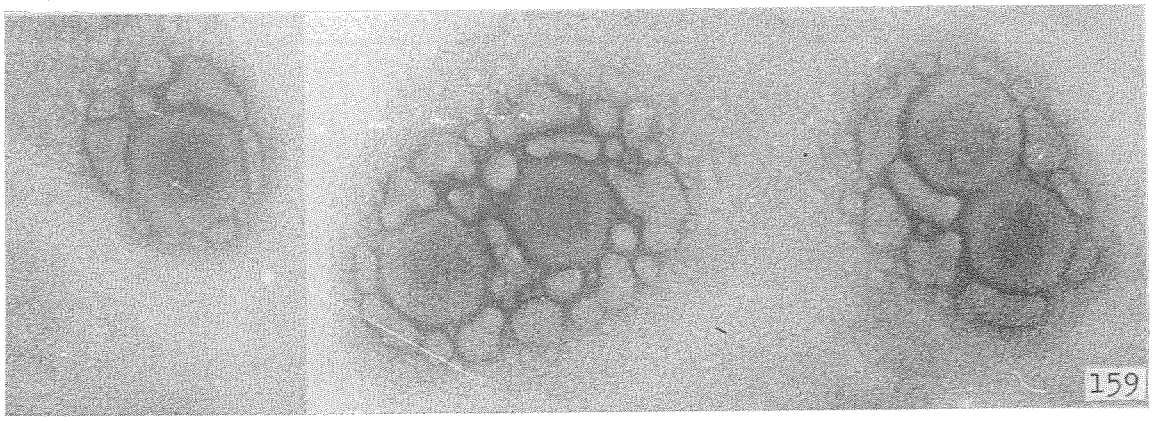
159

Fig. 160, 161. Rice dwarf virus particles showing particular form of shadow shape. Cr shadowed, × 76,500.

162–164. ditto, showing hexagonal structure of virus particles, surrounded by envelopes. The width of shadow is wider than virus particle diameter. Pt-Pd shadowed, × 90,000 in Fig. 162; × 170,000 in Fig. 163, 164.

165. ditto, double shadowed from opposite direction revealed clearly hexagonal contour of the partilces. Pt-Pd shadowed, × 80,000.

166. ditto, Soft shadowed particles show envelopes surrounding the particles. Pt-Pd shadowed, × 80,000.

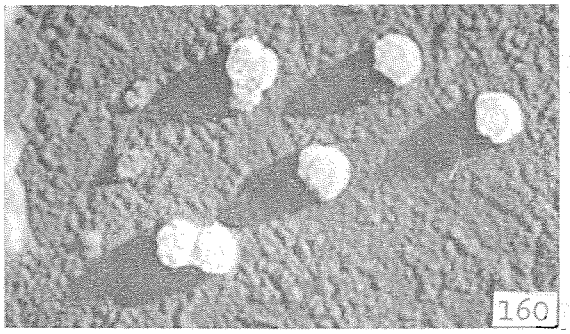
160

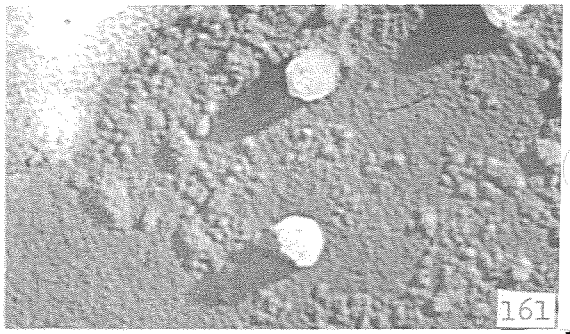
161

163

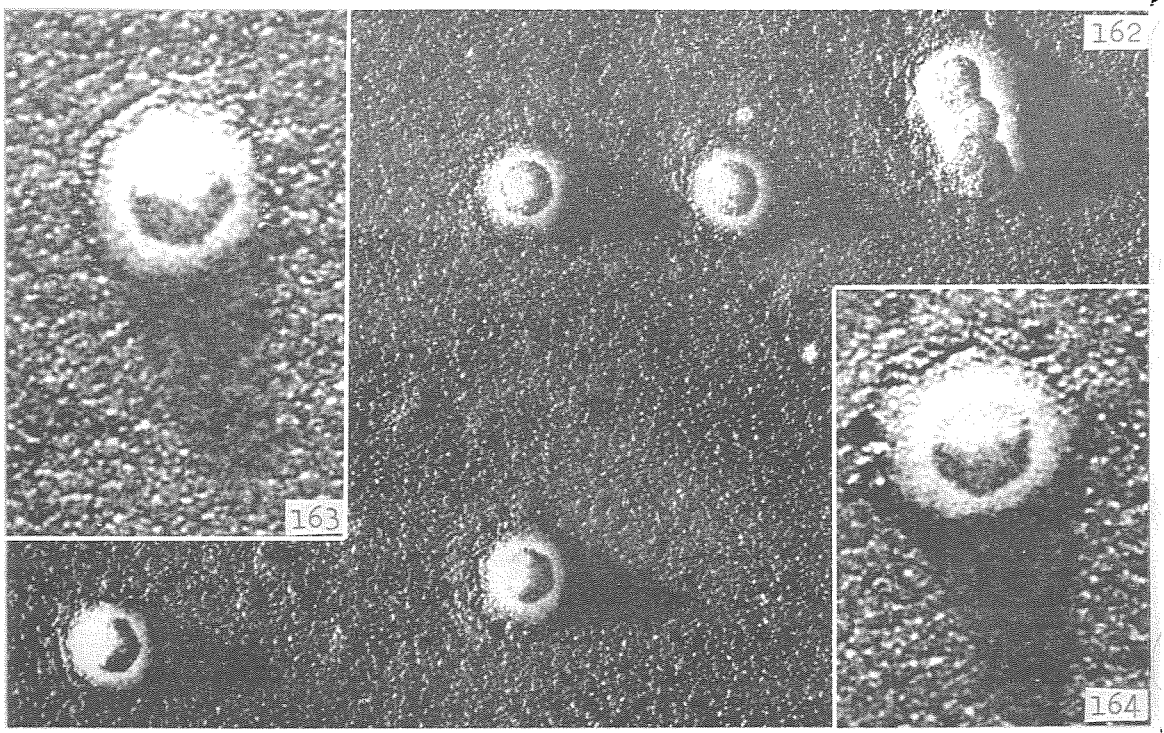
162

164

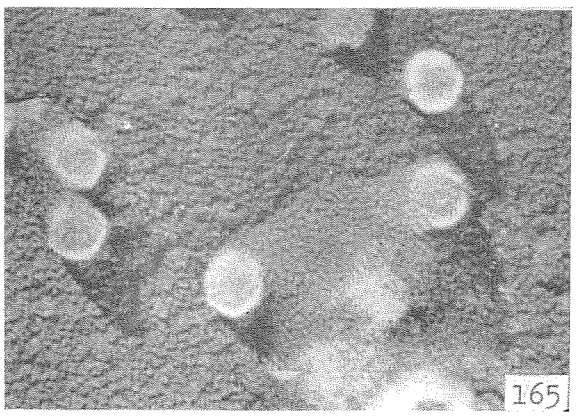
165

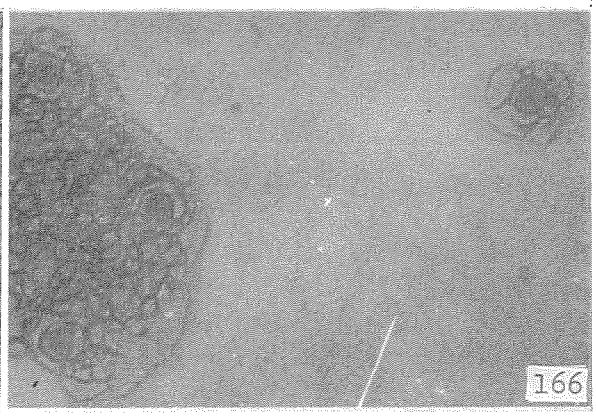
166

Fig. 167. ditto, Soft shadowed, but slight heavier than Fig. 166, Pt-Pd shadowed, × 80,000.

168. ditto, shadowed particles, envelopes surrounding the particles are not seen. Pt-Pd shadowed, × 80,000.

169. PTA stained rice dwarf virus particles, after washing in dist. water. × 80.000.

170. Rice dwaf virus particles suspended in 2% ammonium carbonate, and then dried on the grids, shows hezagonal contour or the particles. Cr shadowed, × 72,000.

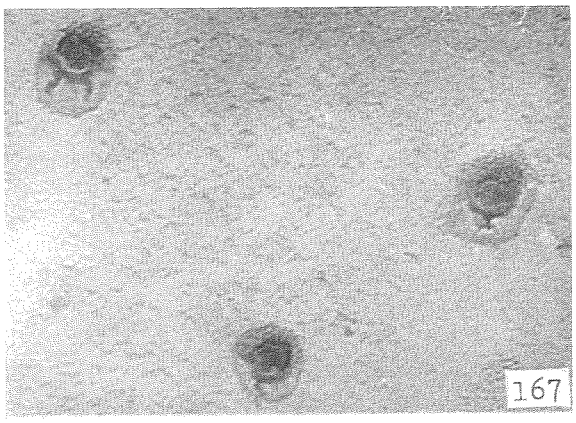
167

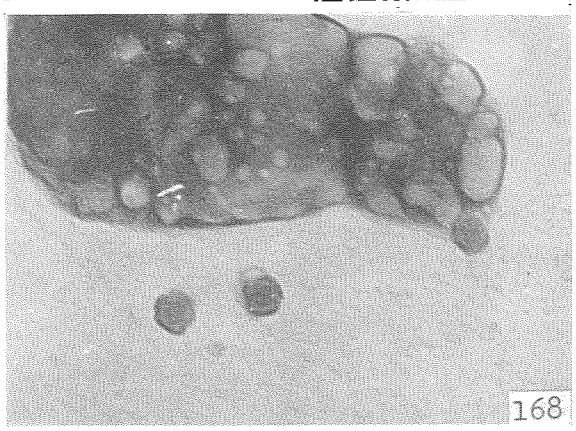
168

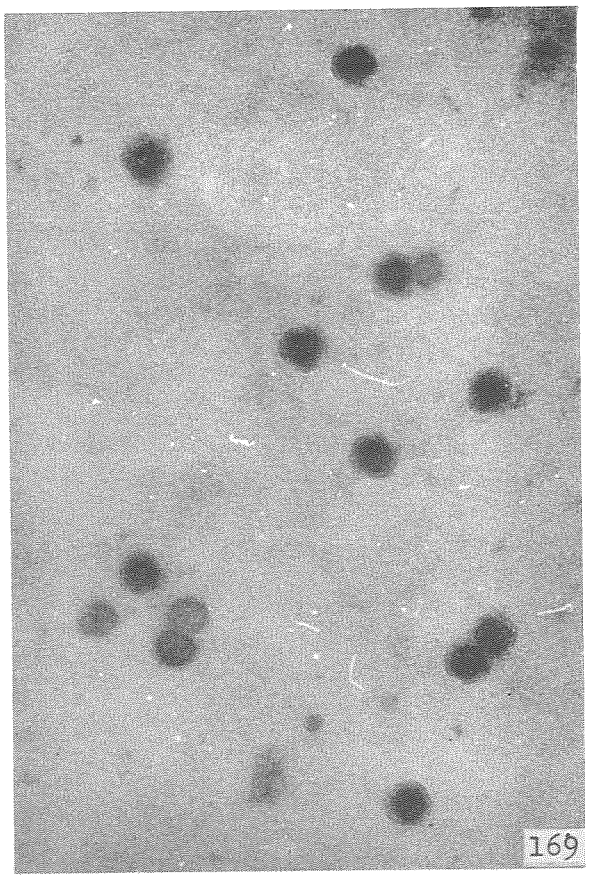
169

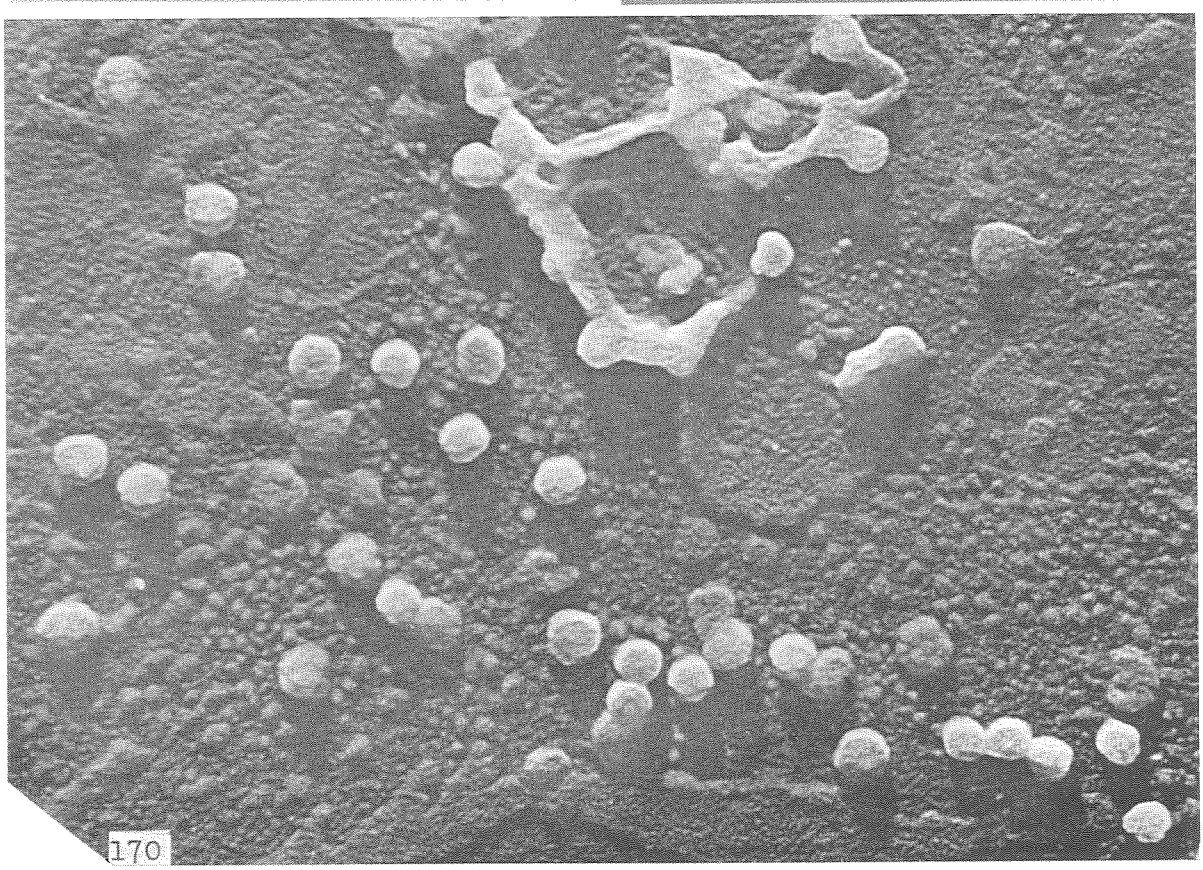
170

Fig. 171. 172. Rice dwarf virus particles stained by PTA. After washing the grids with dist, water, the specimens were shadowed by Cr. The particles showing hexagonal shape were seen. A lot of empty particles were also encountered in Fig. × 54,000 in Fig. 171. Characteristic shadow shape from the particles suggest that the particles may have polyhedral form. × 72,000 in Fig. 172.

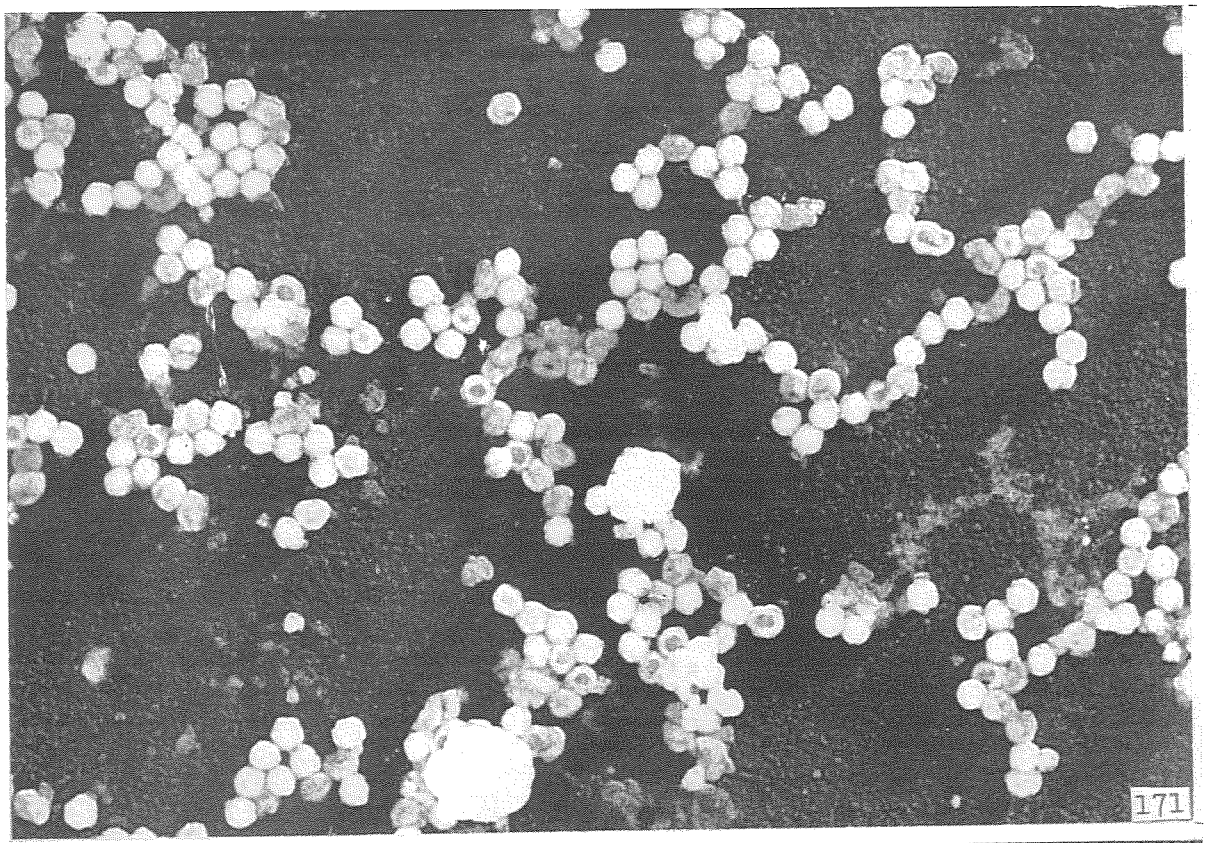
171

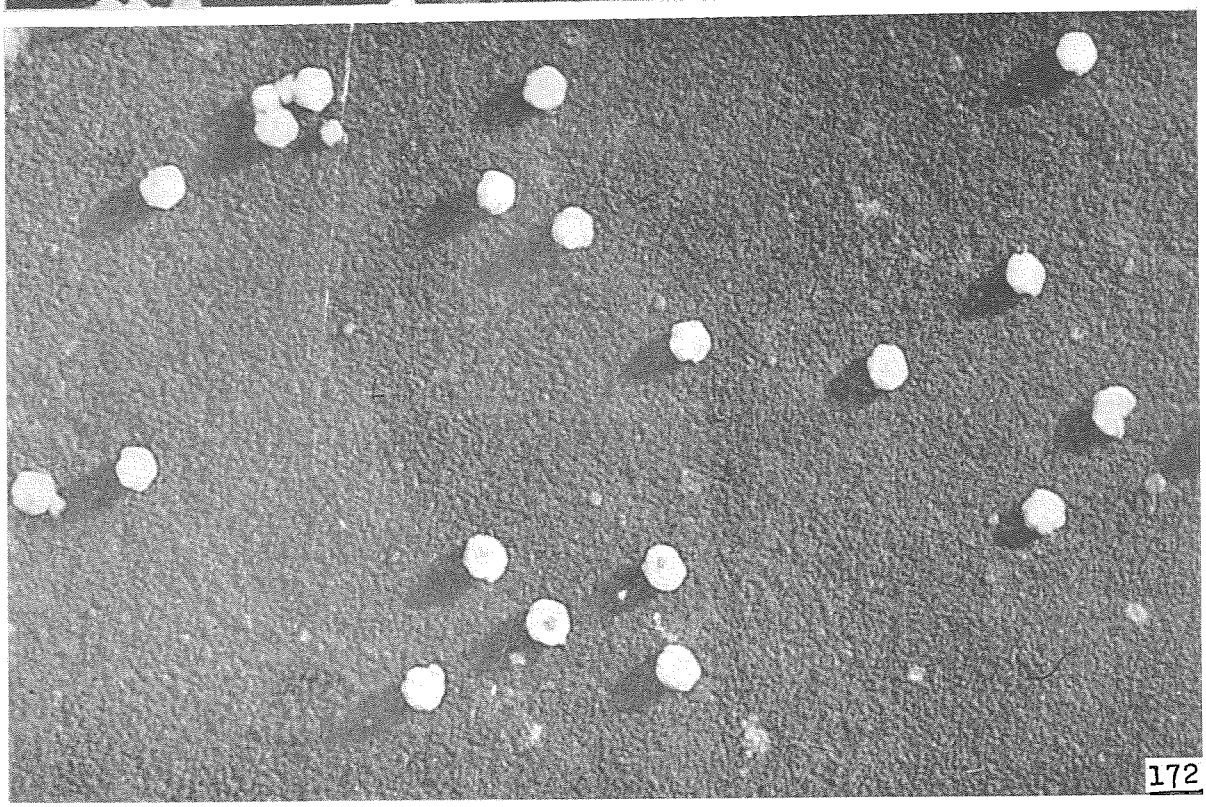
172

Fig. 173. ditto, Pt-Pd shadowed, × 85,500.

174. Negatively stained rice dwarf virus particles by 1% sodium phosphotungstate revealed hexagonal pattern without showing inner structure. × 240,000.

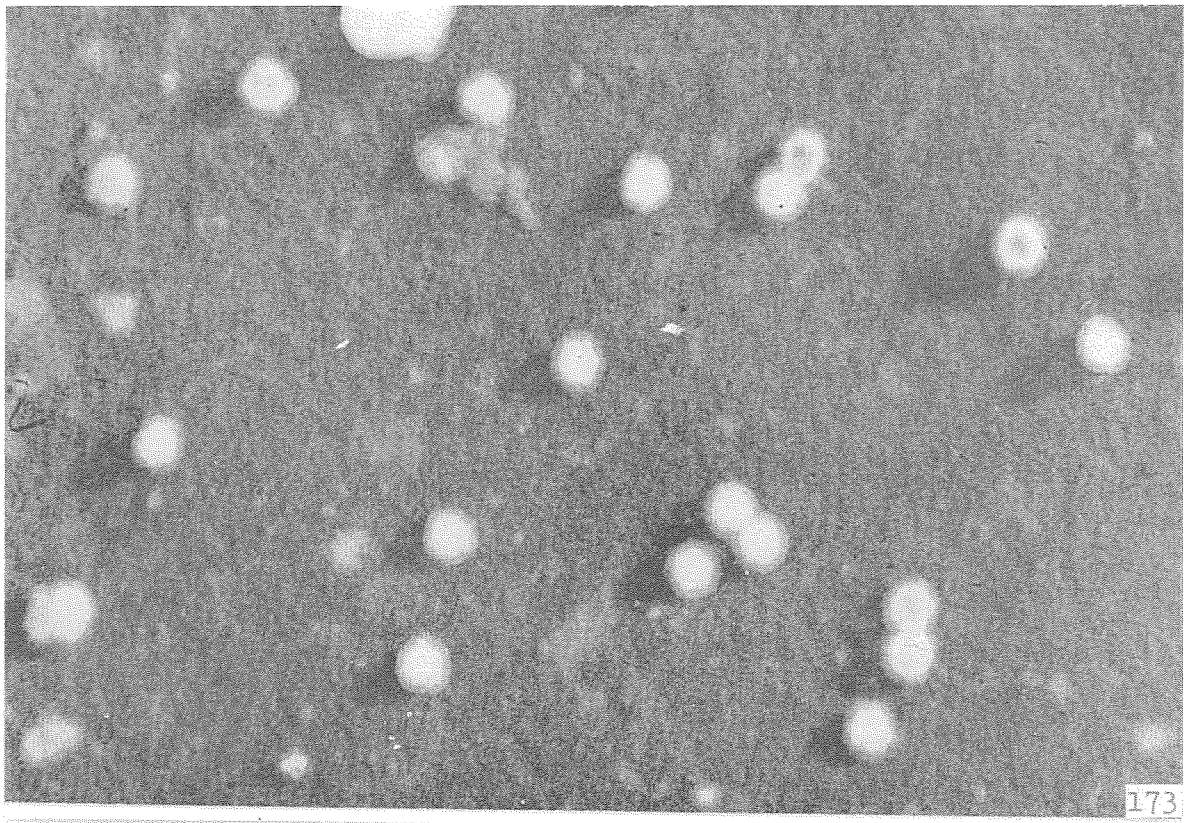

173

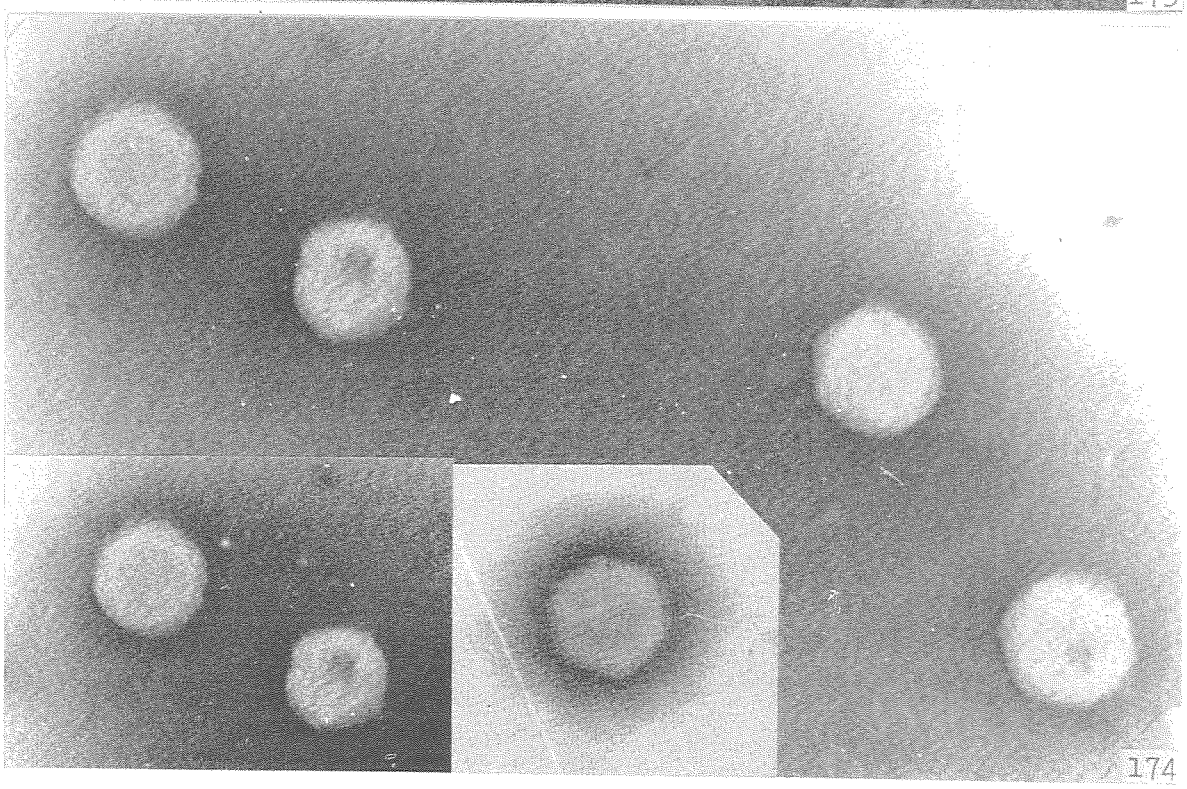

174

Fig. 175. Rice dwarf virus particles after freeze-drying by liquid nitrogen. Cr shadowed, × 72,000.

176. Rice dwarf virus particles after heating at 74°C for 10 min. A lot of fine threads appeared from the disrupted particles. Cr shadowed, × 54,000.

177, 178. Rice dwarf virus particles precipitated from 50% ethanol solution. Some inner structure is visible. Cr shadowed, × 80,000.

179, 180. Rice dwarf virus particles purified by differential centrifugation. Some inner structure is visible. Cr shadowed, × 76,500.

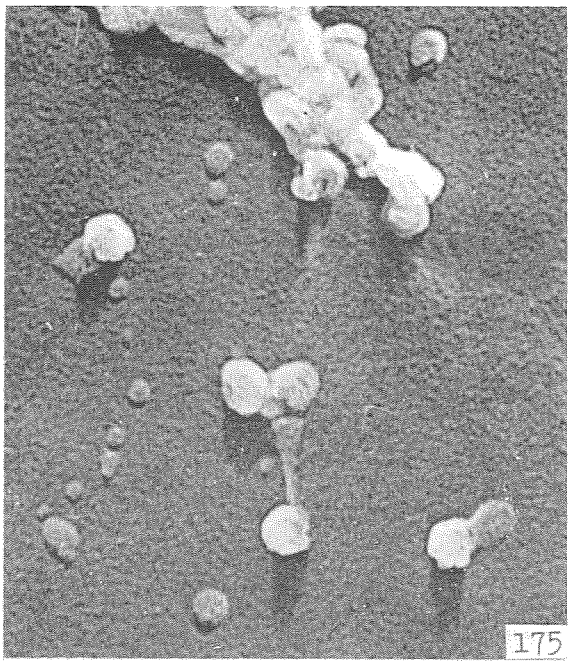
175

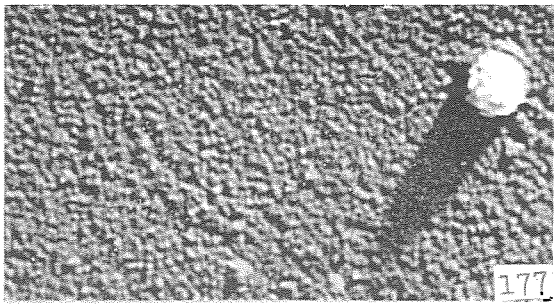
177

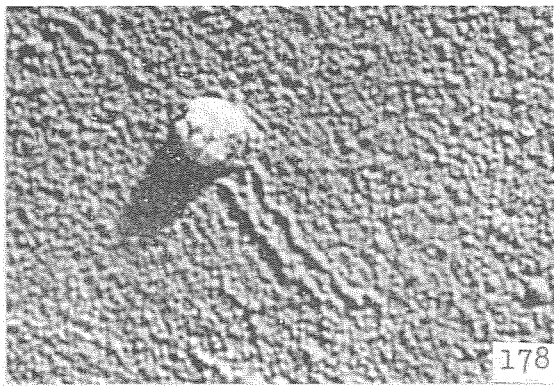
178

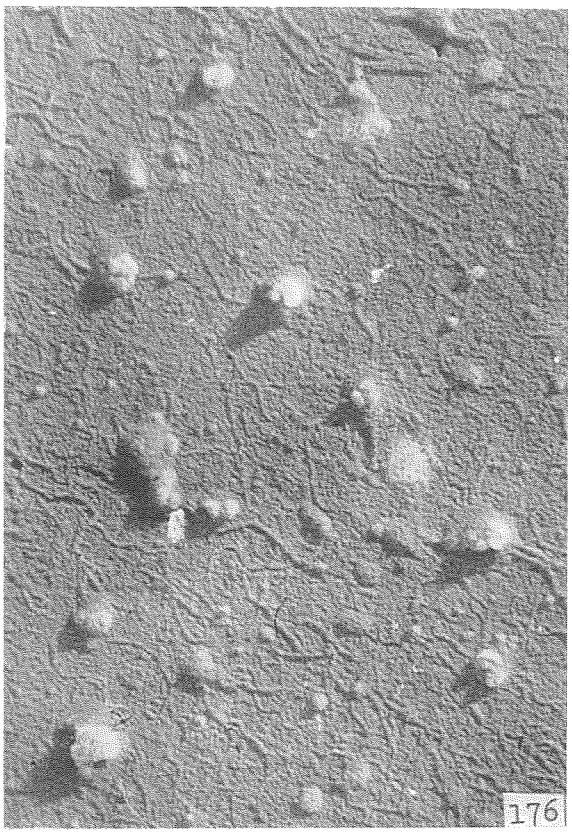
176

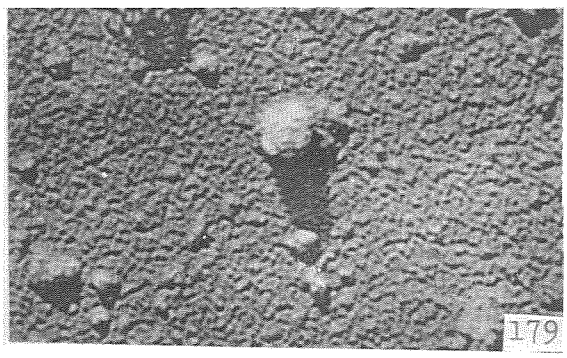
179

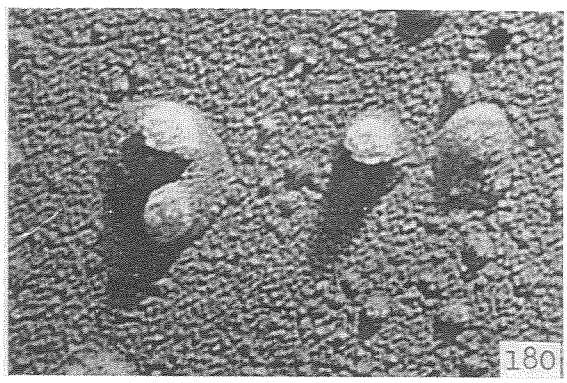
180

Fig. 181–183. Purified rice dwarf virus particles, showing inner structure. Cr shadowed, × 76,500.

184, 185. Rice dwarf virus particles precipitated from 50% ether solution, at 5°C. Cr shadowed, × 80,000.

186. Rice dwarf virus particles treated with hot ether at 37°C for 60 min. After dialyzing against 1% ammonium acetate, the virus was stained negatively with 0.5% PTA. Numerous capsomeres projected from the central cores are identical. × 210,000.

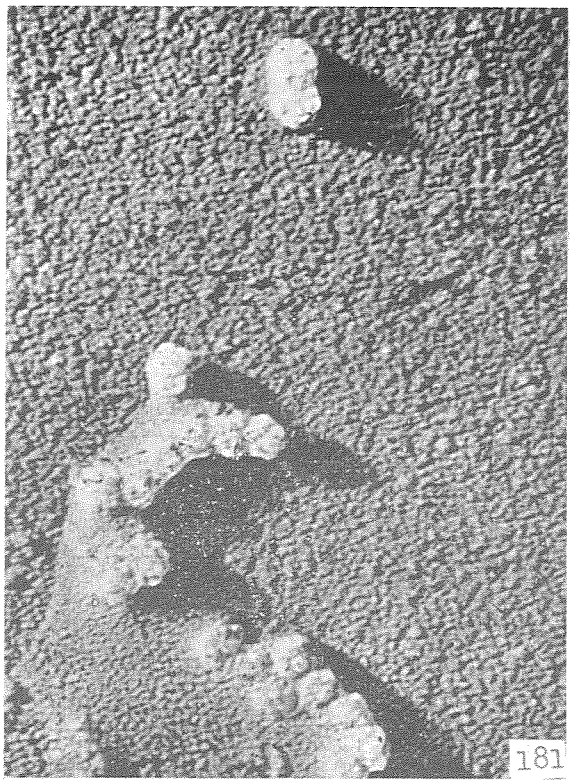

181

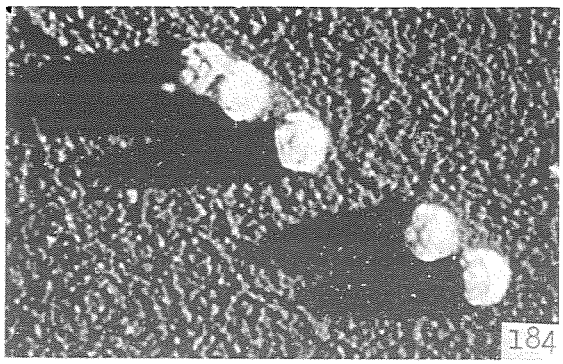

184

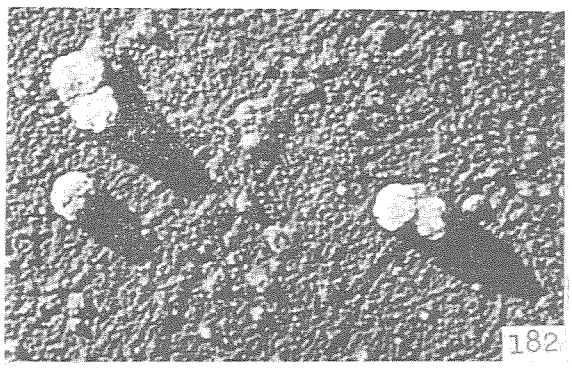

182

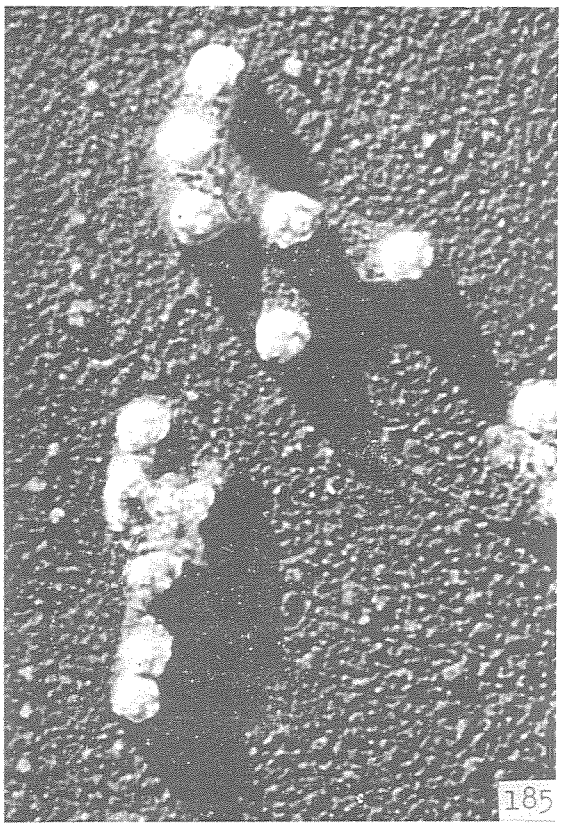

185

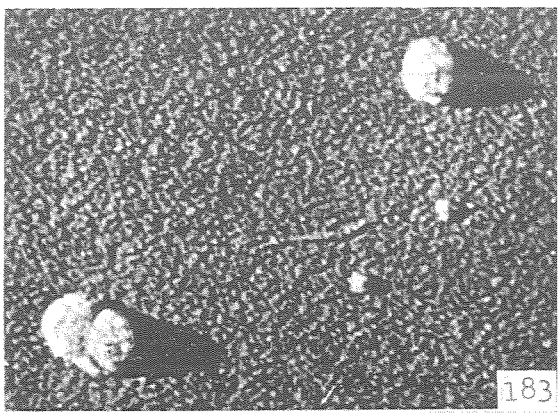

183

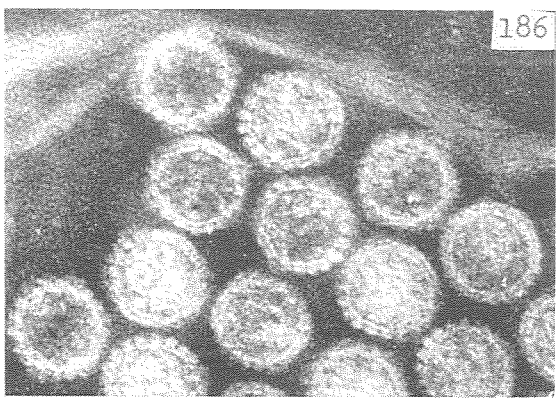

186

Fig. 187. ditto, a lot of empty capsides are seen.

188-191. Negatively stained rice dwarf virus particles purified by chloroform emulsion technique. Stained by 1% PTA. × 550,000 in Fig. 188; × 20,000 in Fig. 189, 190; × 250,000 in Fig. 191.

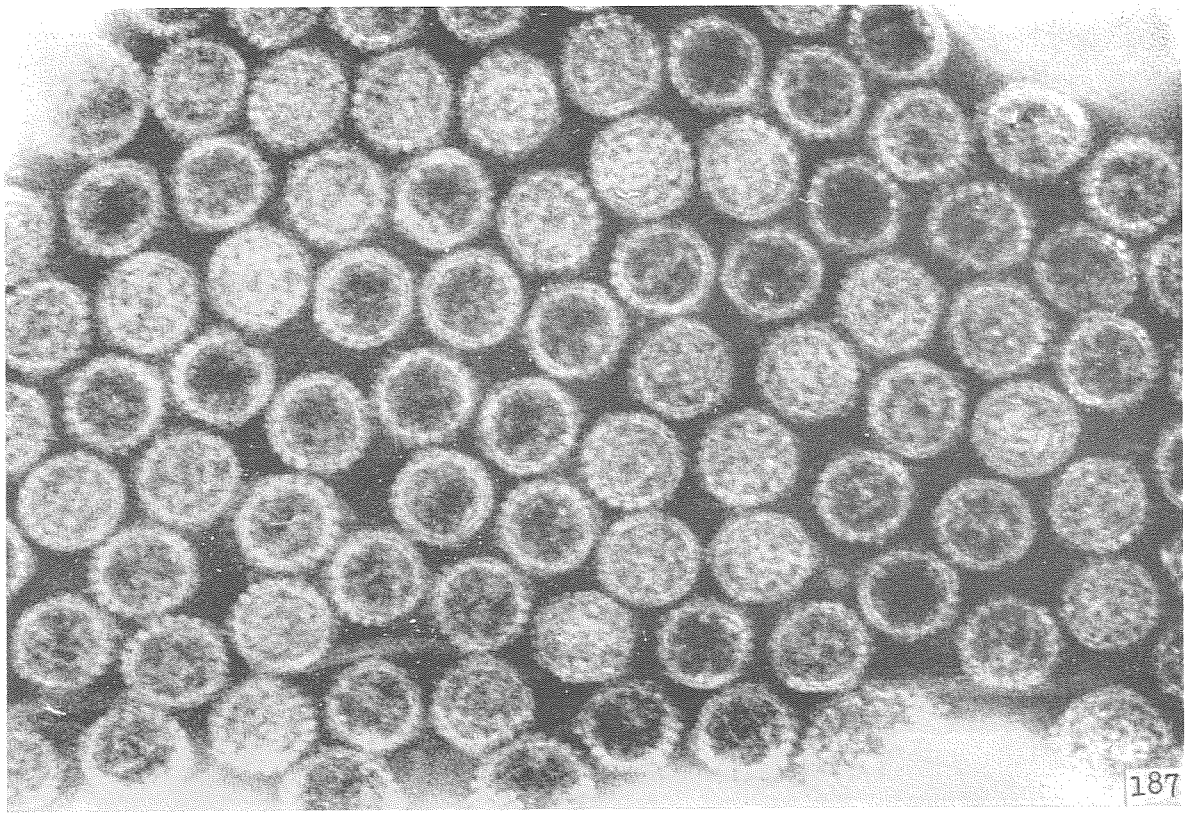
187

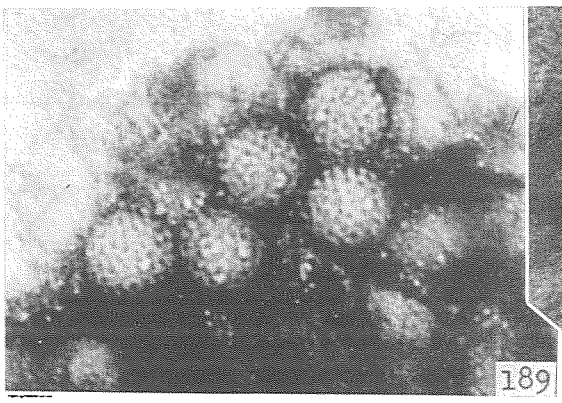
189

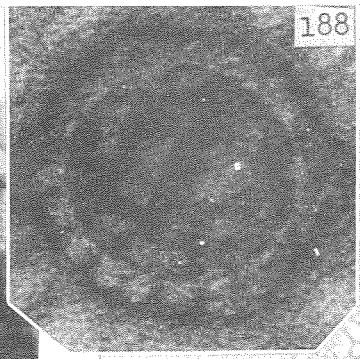
188

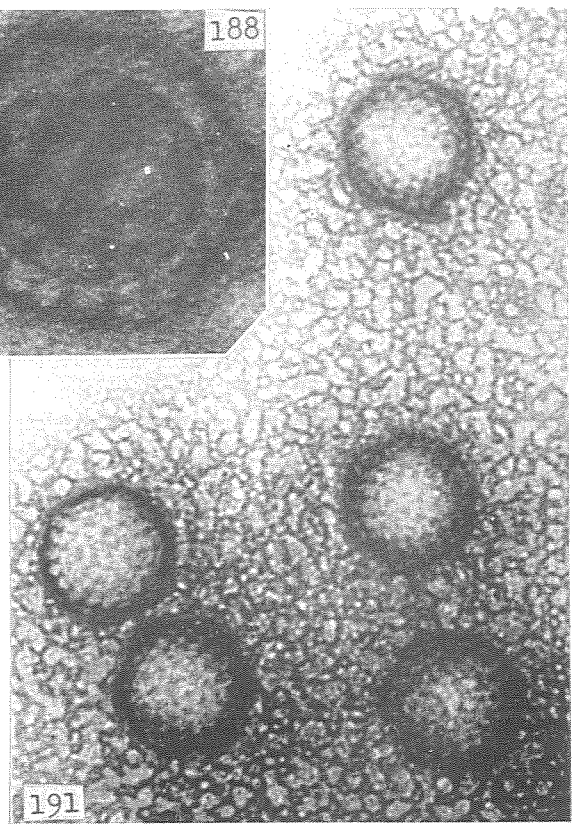
191

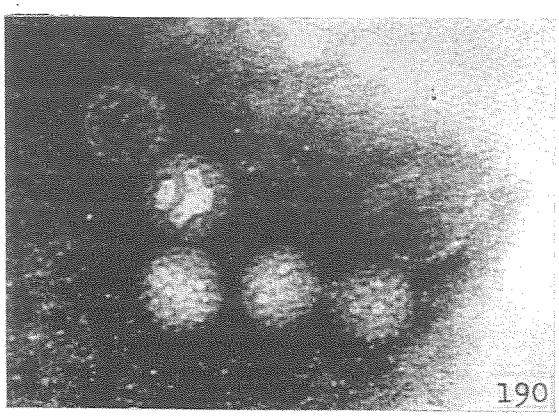
190

Fig 192, 193. ditto, ×300,000 in Fig. 192; × 550,000 in Fig. 193.

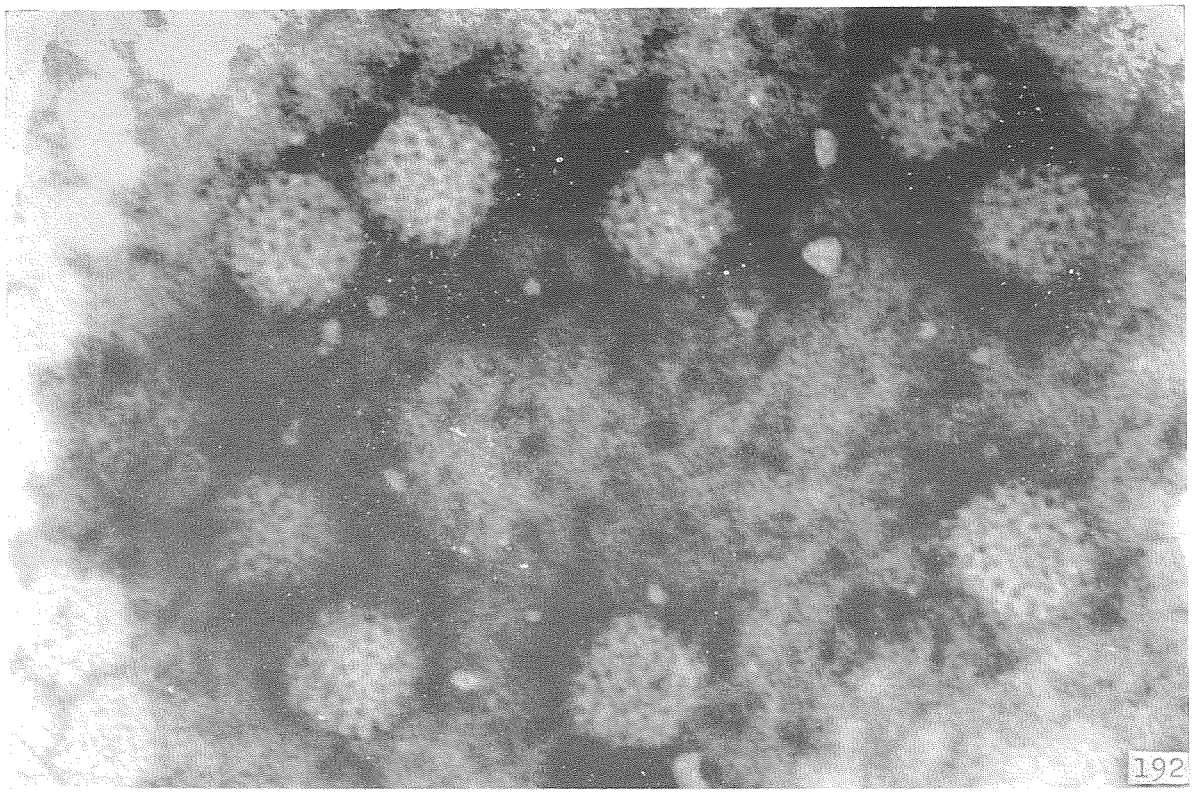

192

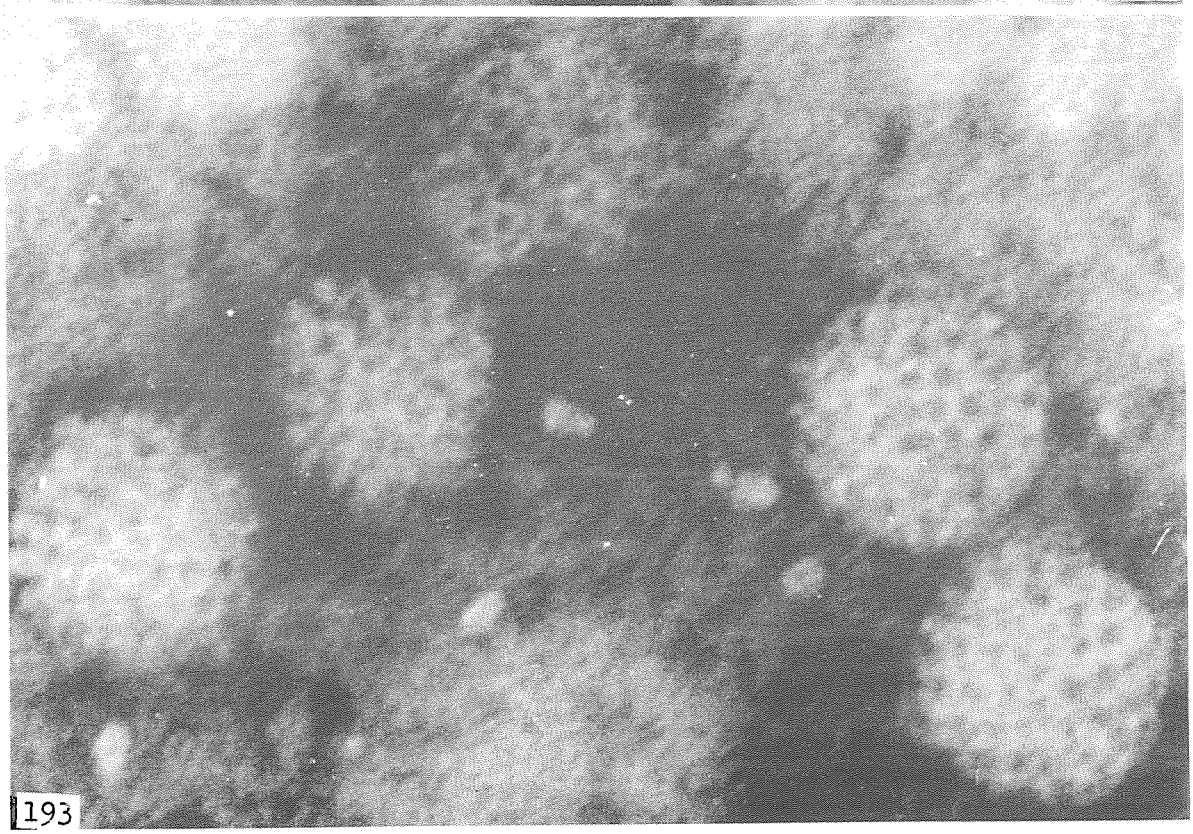

193

Fig. 194, 195. ditto, Several disrupted particles revealed expanded surface structures of the particles. 1% PTA stained, × 180,000 in Fig. 194. After washing the grids, the virus particles were shadowed by Pt-Pd as to Fig. 195. × 170,000.

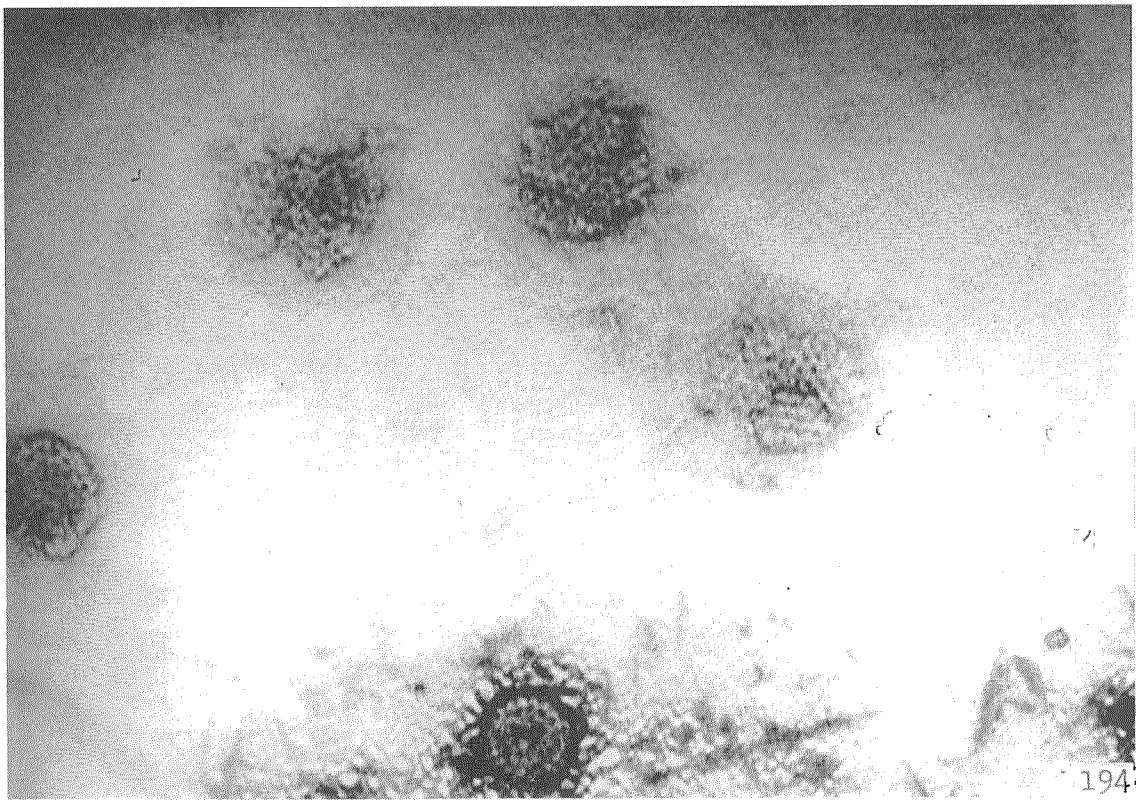

194

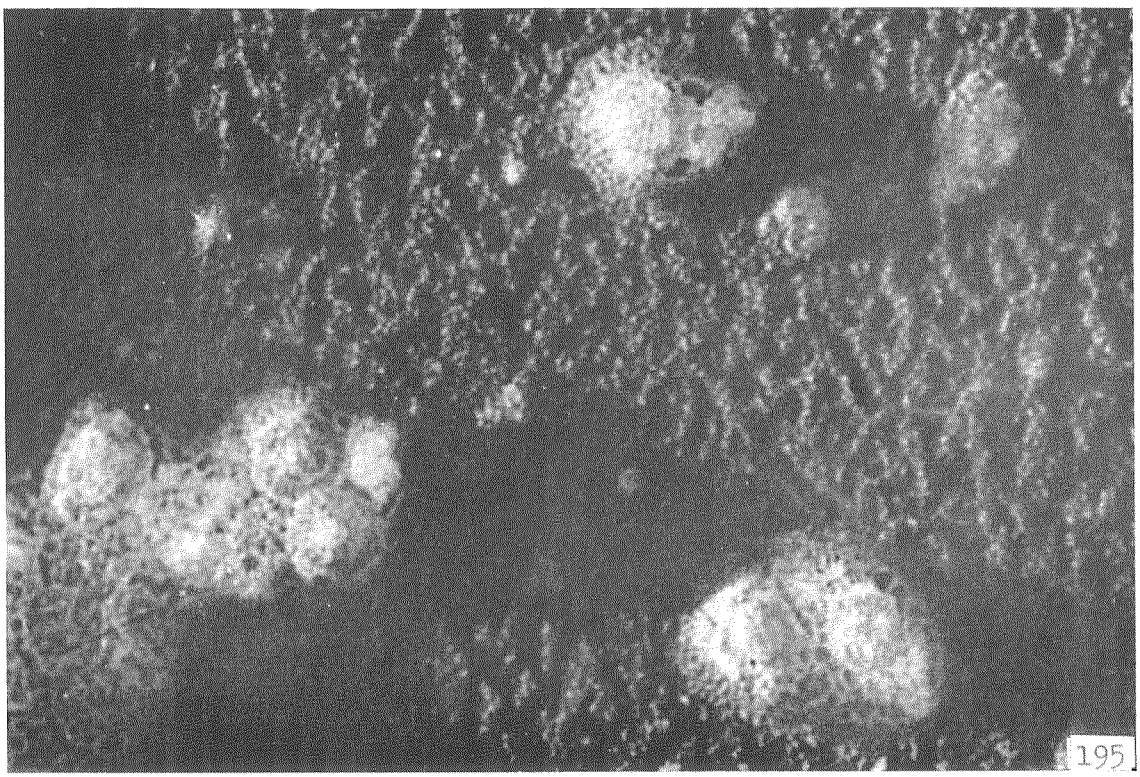

195

Fig. 196, 197. Negatively stained rice dwarf virus particles by 1% PTA. Regular pattern of surface structure of the particles were visible. × 150,000 in Fig. 196. High magnification of these capsomeres are shown in Fig. 197. × 250,000.

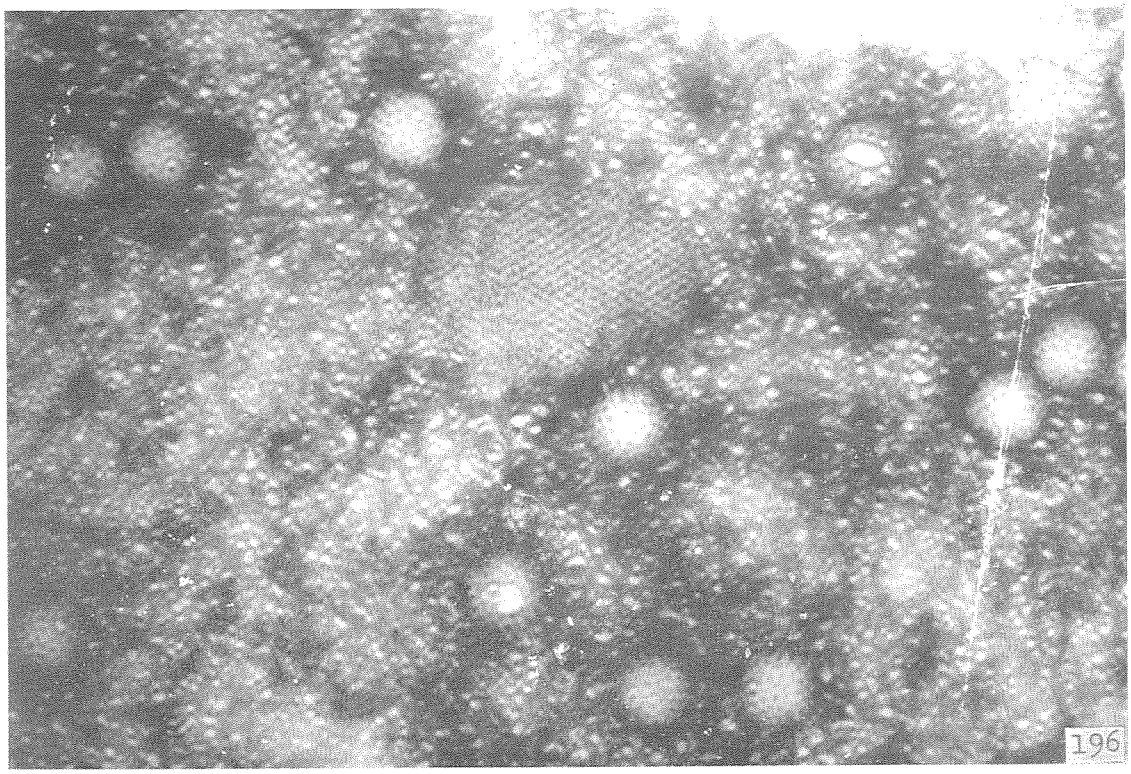
196

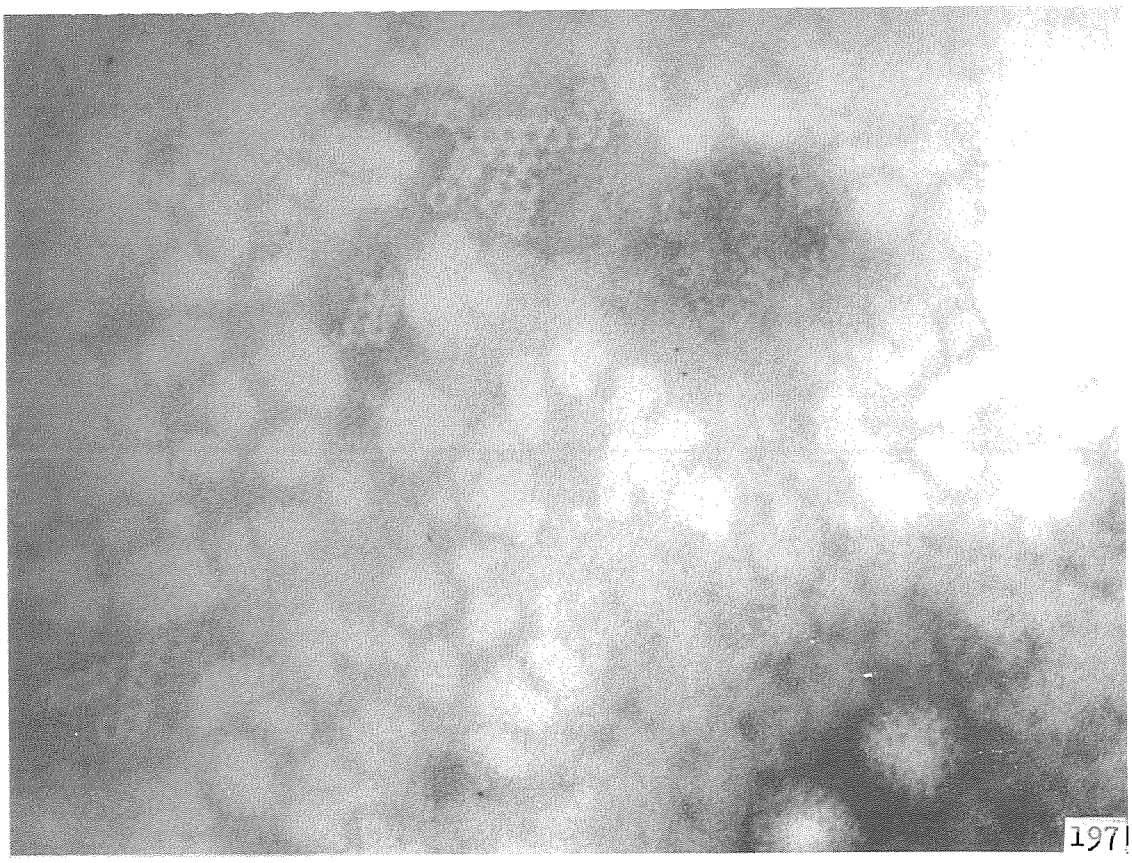
197

Fig. 198. ditto, × 550,000.

199. ditto, × 250,000.

200. dtito, A band of surface structure seems to be separeted from the disrupted particles. × 250,000.

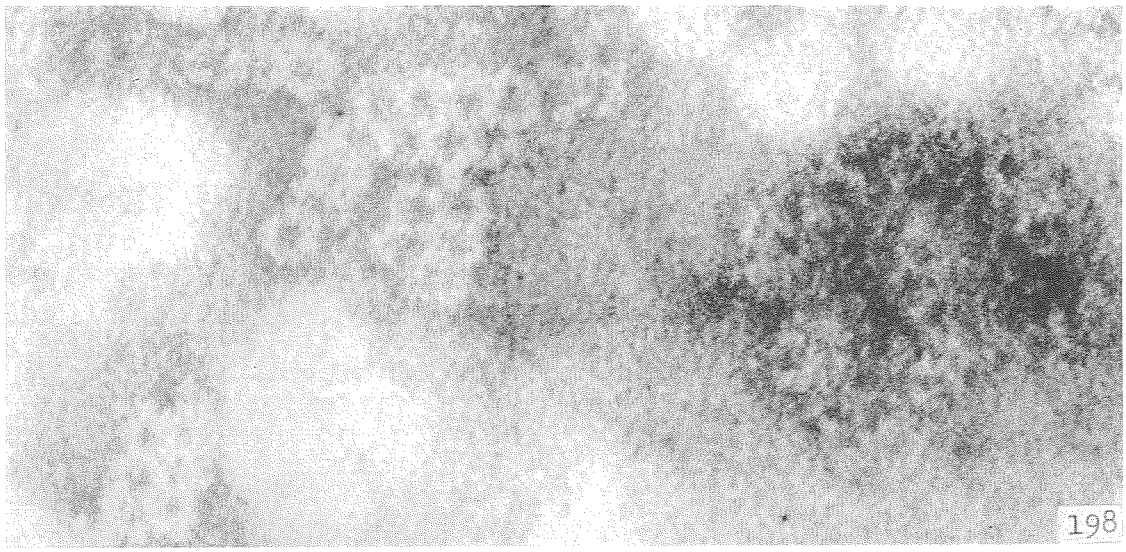
198

199

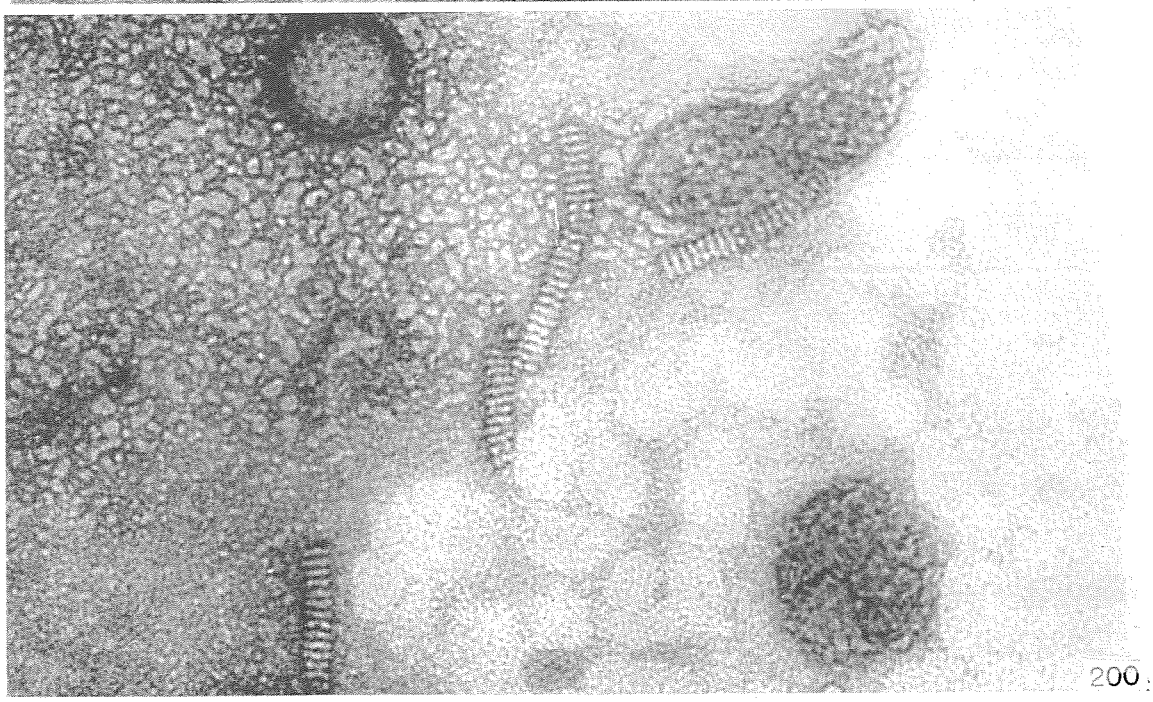
200

Fig. 201. ditto, × 550,000.

202. Ultrathin section of purified virus pellets, stained by 2% uranyl acetate, showing some inner structures. × 170,000.

201

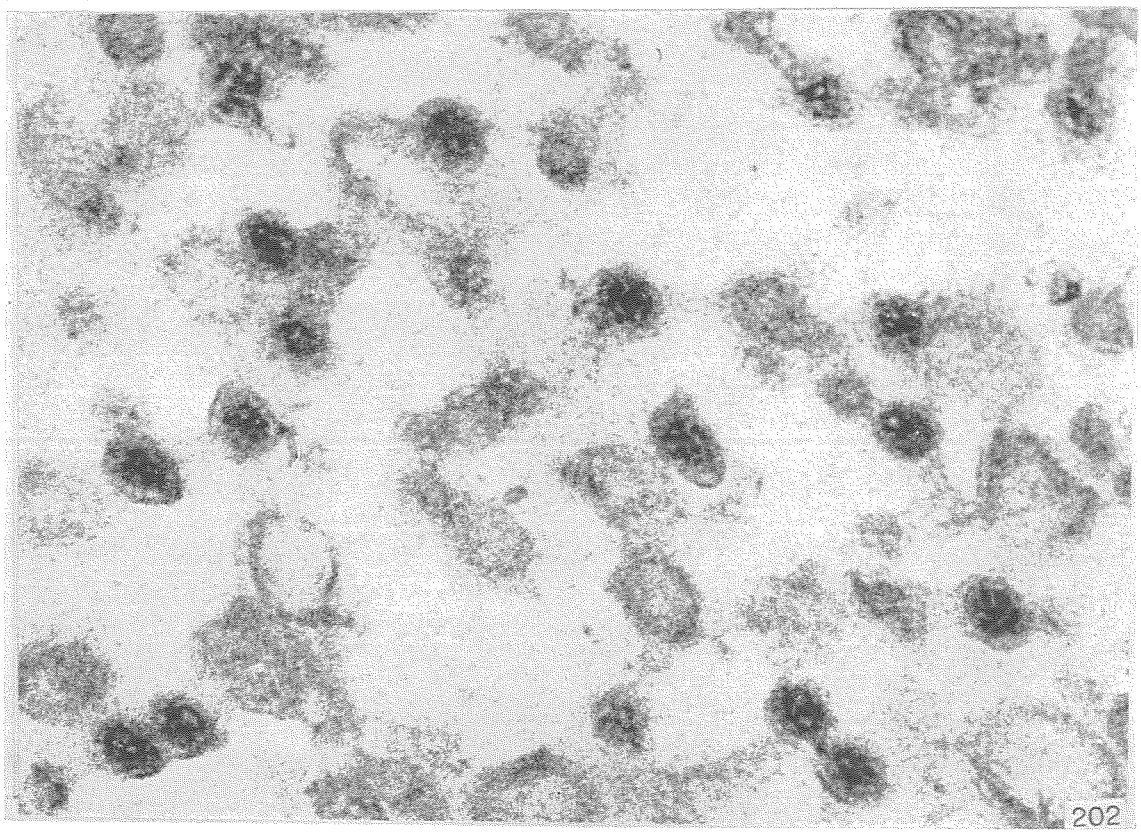

202

Fig. 203, 204. ditto, showing loose accumulation of virus particles in the pellets, some membraneous structures which seems to be envelopes, and a empty particles. Fig. 203. × 160,000; Fig. 204. × 240,000.

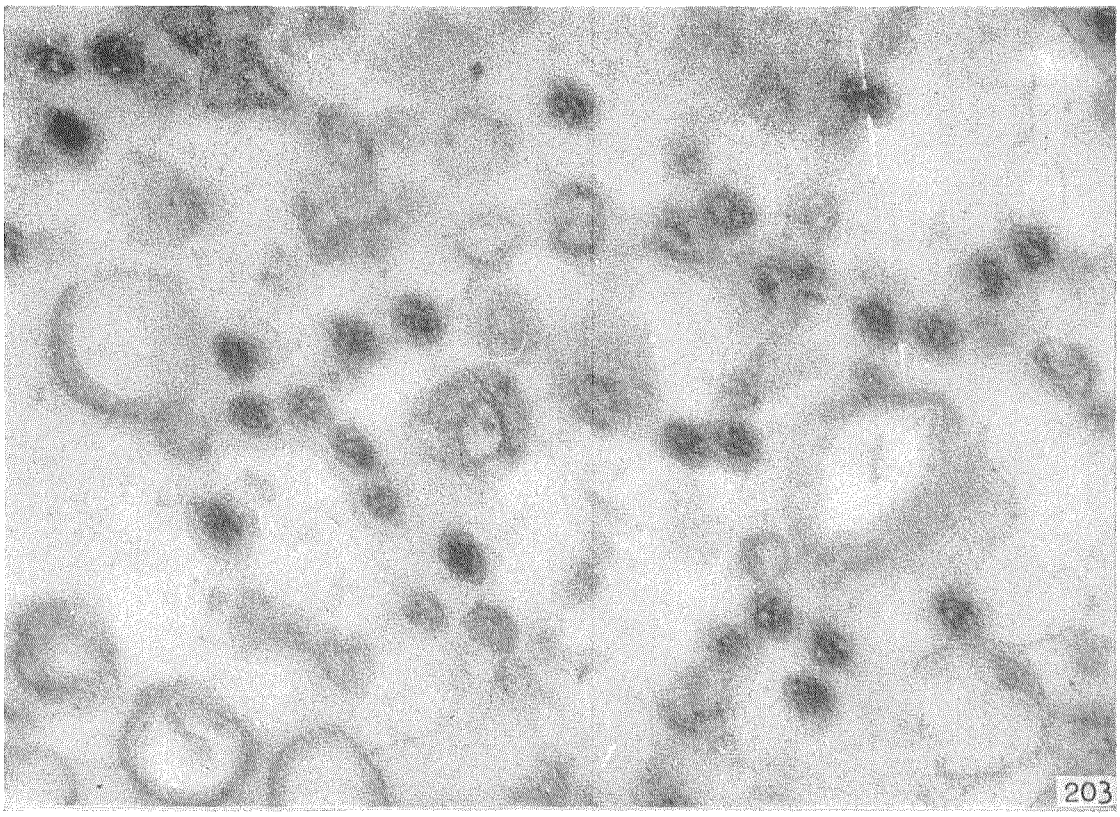
203

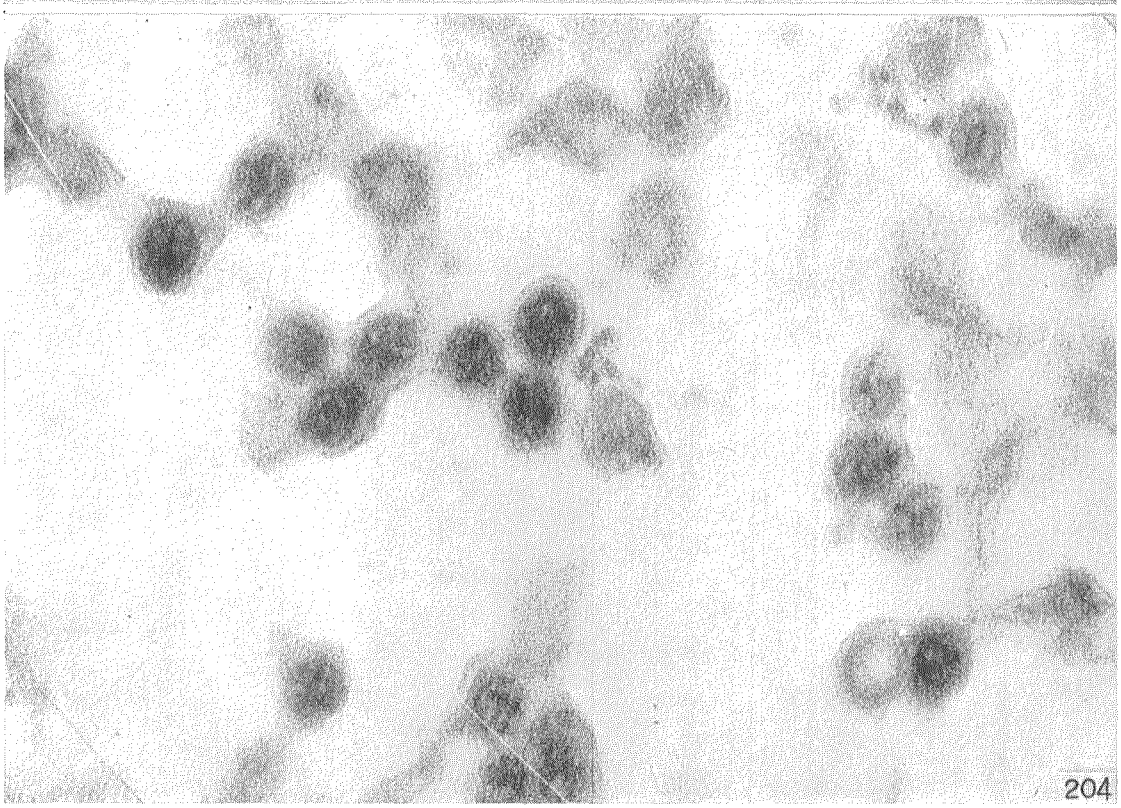
204

Fig. 205. Ultrathin section of chlorotic portion of diseased rice leaves. Ch; chloroplast, N; nucleus, V; rice dwarf virus particles. × 9,500.

206. ditto, A large virus cluster beside the nucleus. × 22,000.

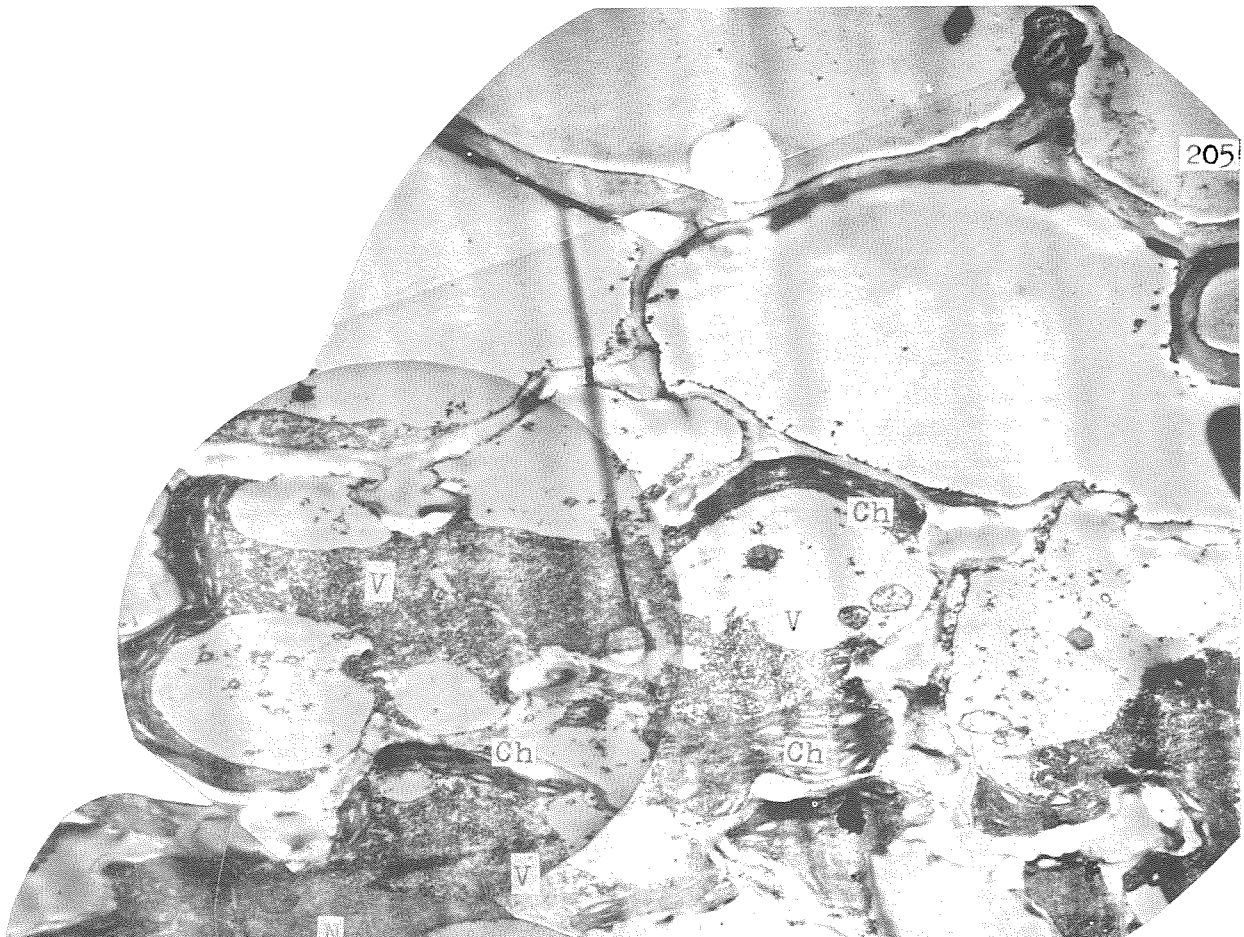
205
Ch
V
V
Ch
Ch
V
N
Ch

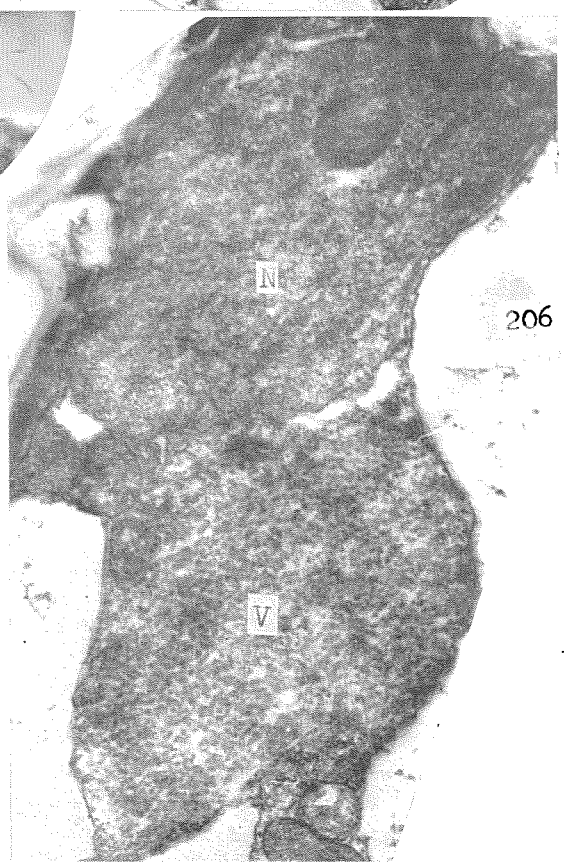
N
206
V

Fig. 207. A ultrathin section of chlorotic portion of rice leaves infected with rice dwarf virus 20 days after infection. Virus particles are filled loosly in cytoplasm of a infected cell. M; Mitochondria × 12,000.

208. ditto, 30 days after infection showing compactly arranged virus particles. Chloroplast (Ch) are disintegrated. × 42,500.

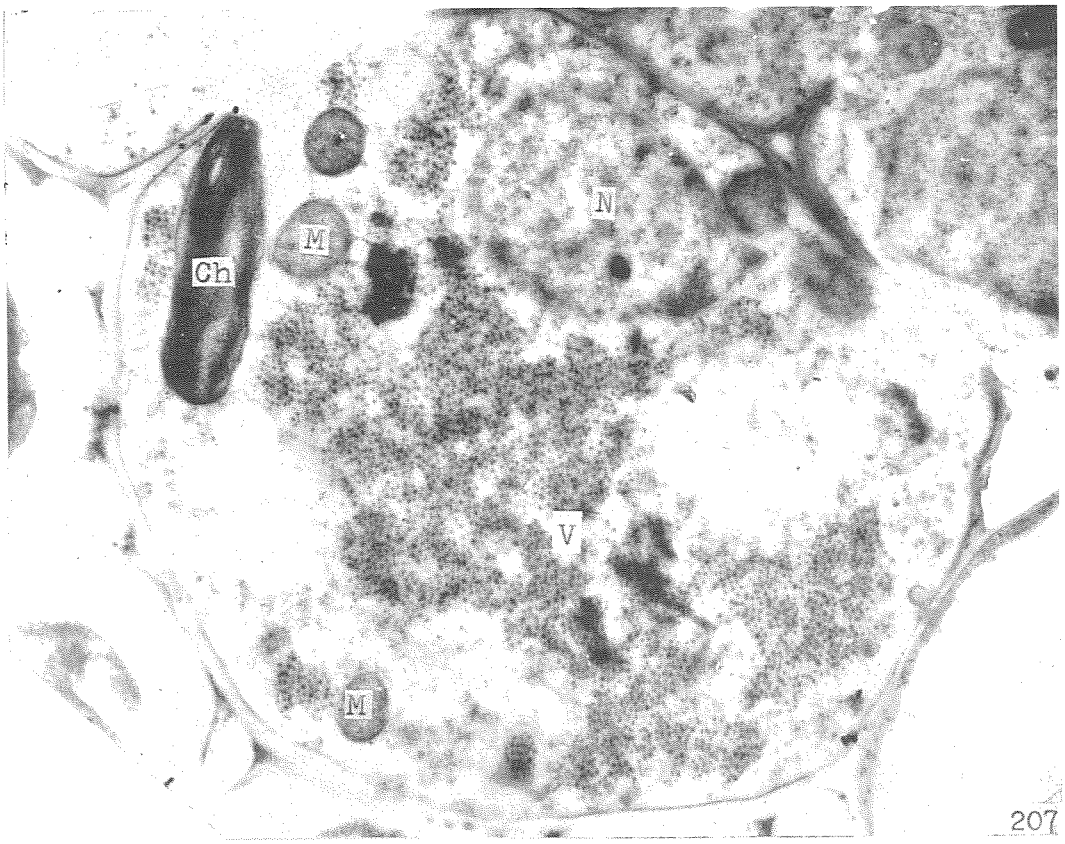

207

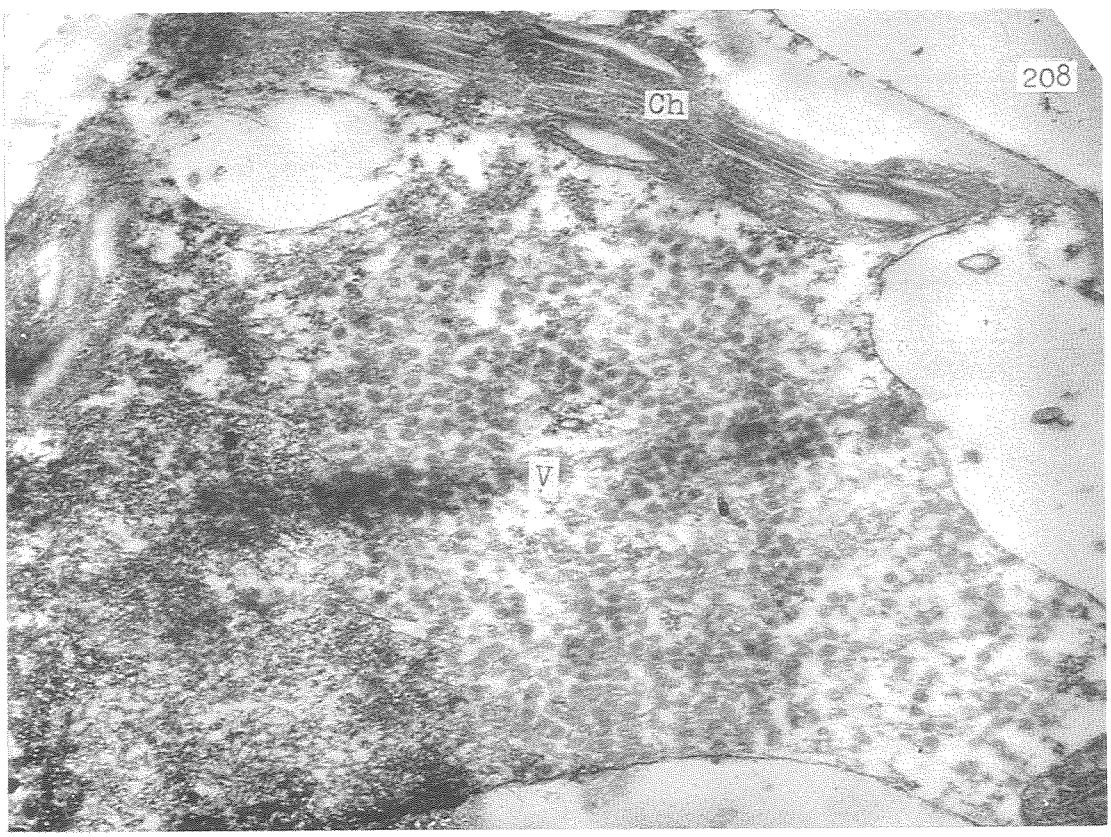

208

Fig. 209, 210. ditto, Cr shadowed after removing the methacrylate resin. Fig. 209; × 21,000, Fig. 210; × 60,000 Particles similar to the isolated rice dwarf virus particles are encountered.

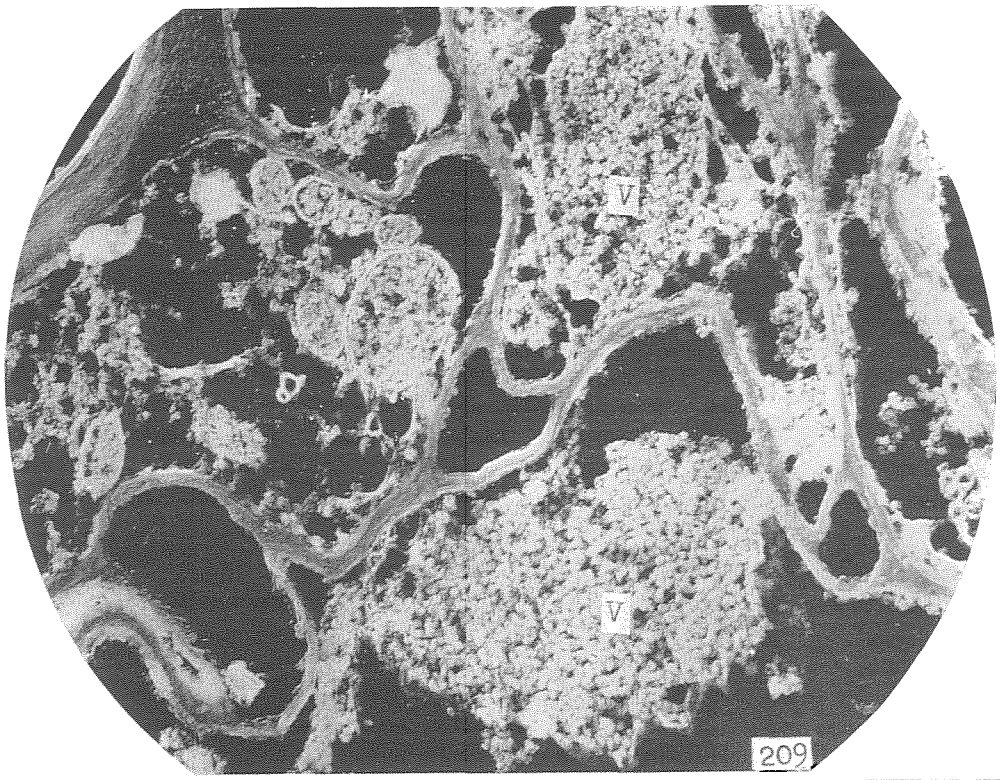
V
V
209

210

Fig. 211–213. ditto, particles similar to the isolated rice dwarf virus particles are encountered in Fig. 211. × 73,000. Fig. 212. shows regular arrangement of virus particles in a cell of diseased rice leaves. × 22,000. Fig. 213. represents the membraneous structure enclosing virus particles. 73,000.

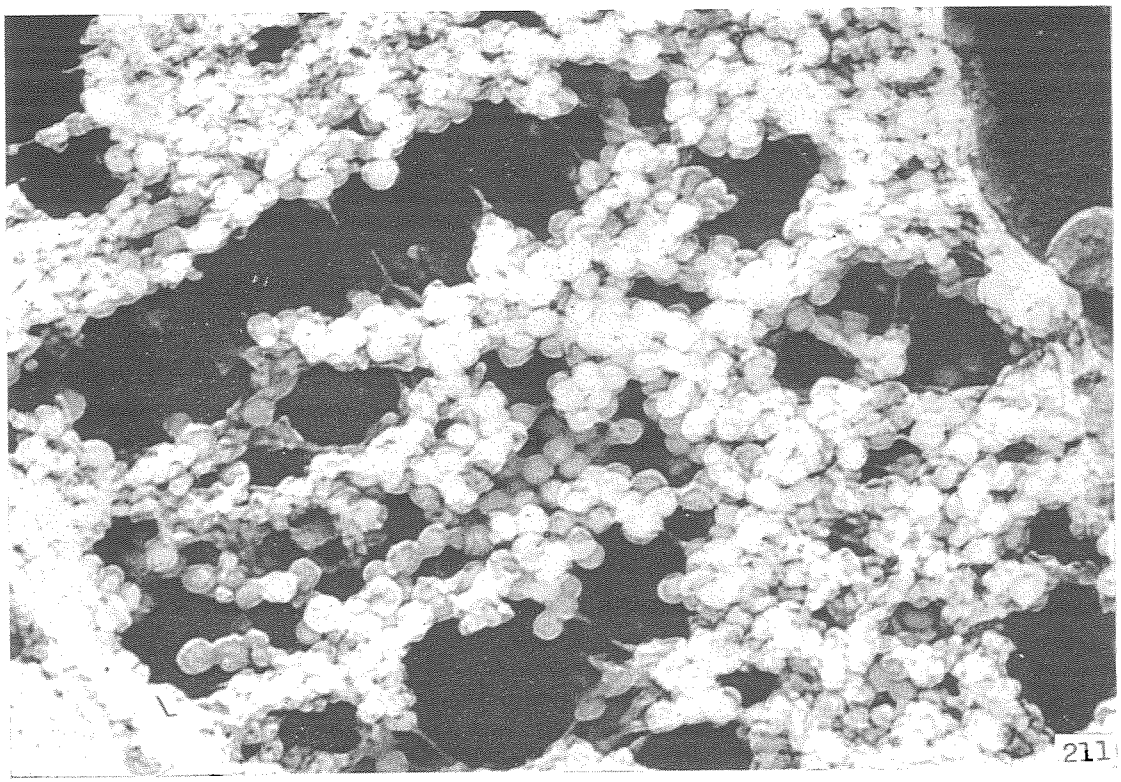

211

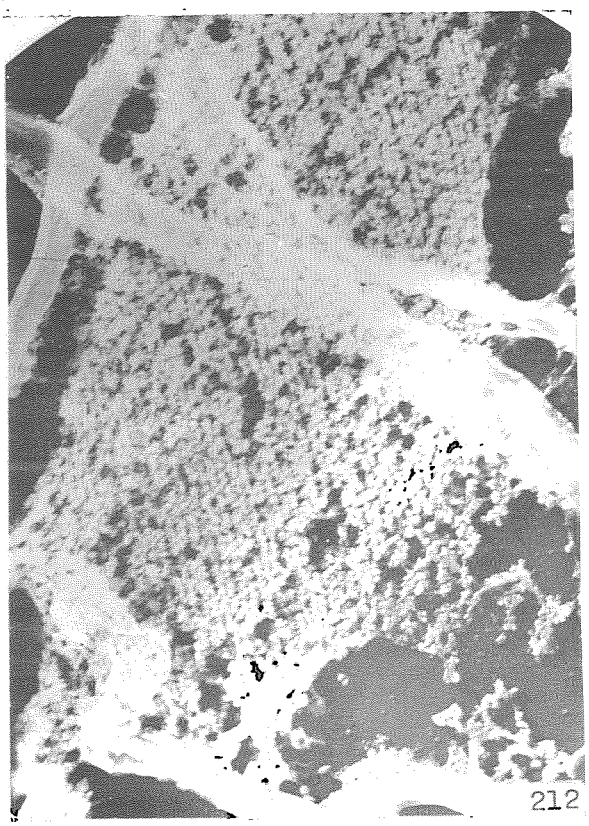

212

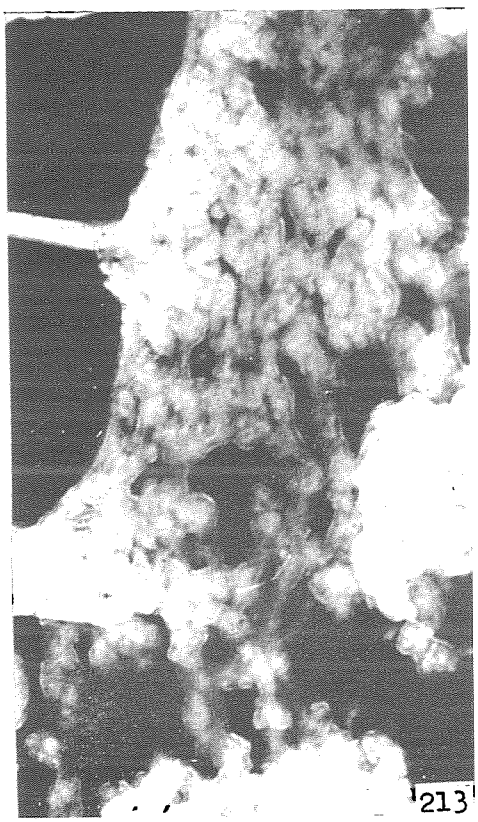

213

Fig. 214, 215. ditto, rice dwarf virus particles are loosely accumulated in the cytoplasm of a cell. Some tubular structures in cross section and in longtudinal section are visible. × 32,400.

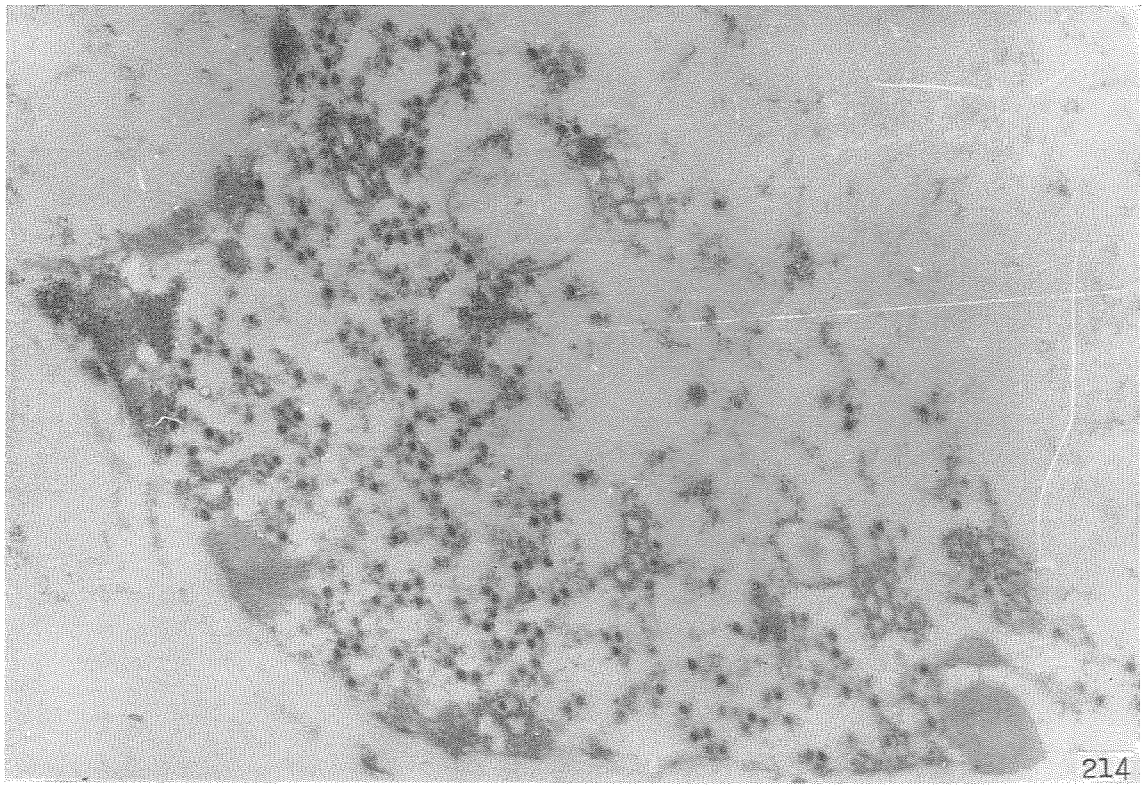

214

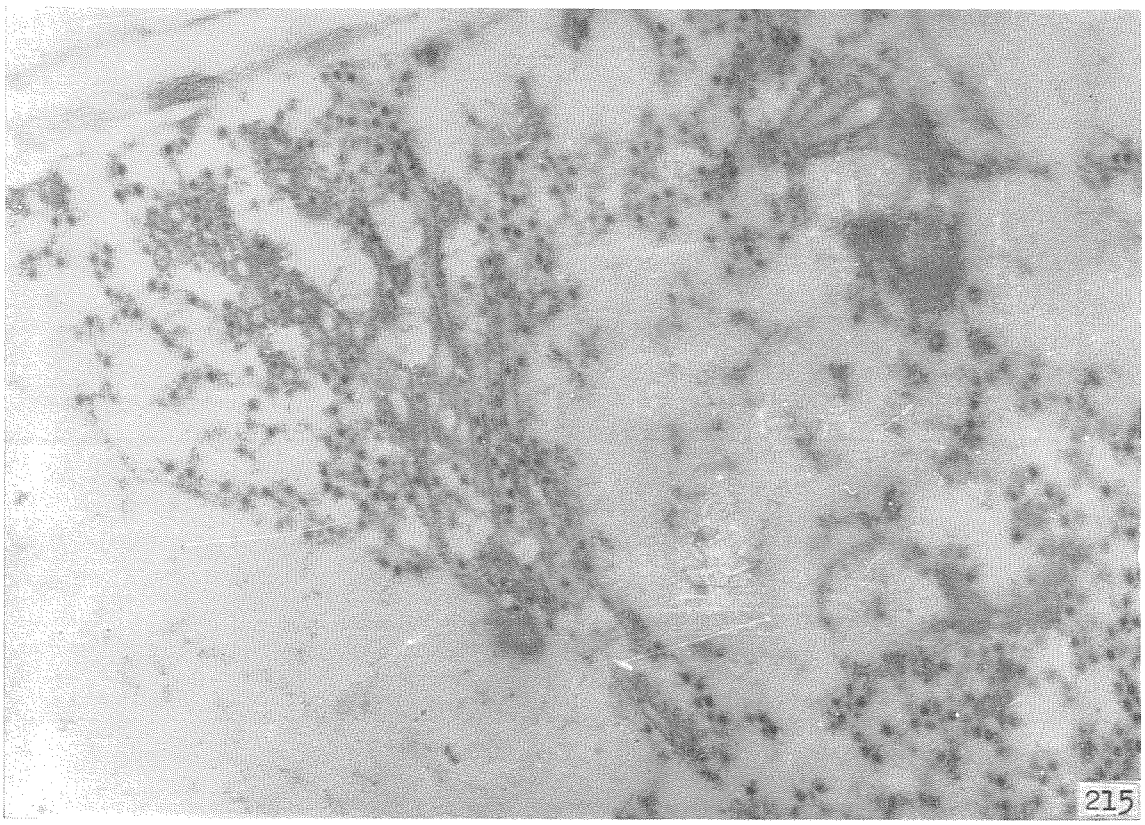

215

Fig. 216, 217. ditto, showing virus particles arranged on some membraneous structure, also in tubular structures, Fig. 216, × 96,000; Fig. 217, × 66,000.

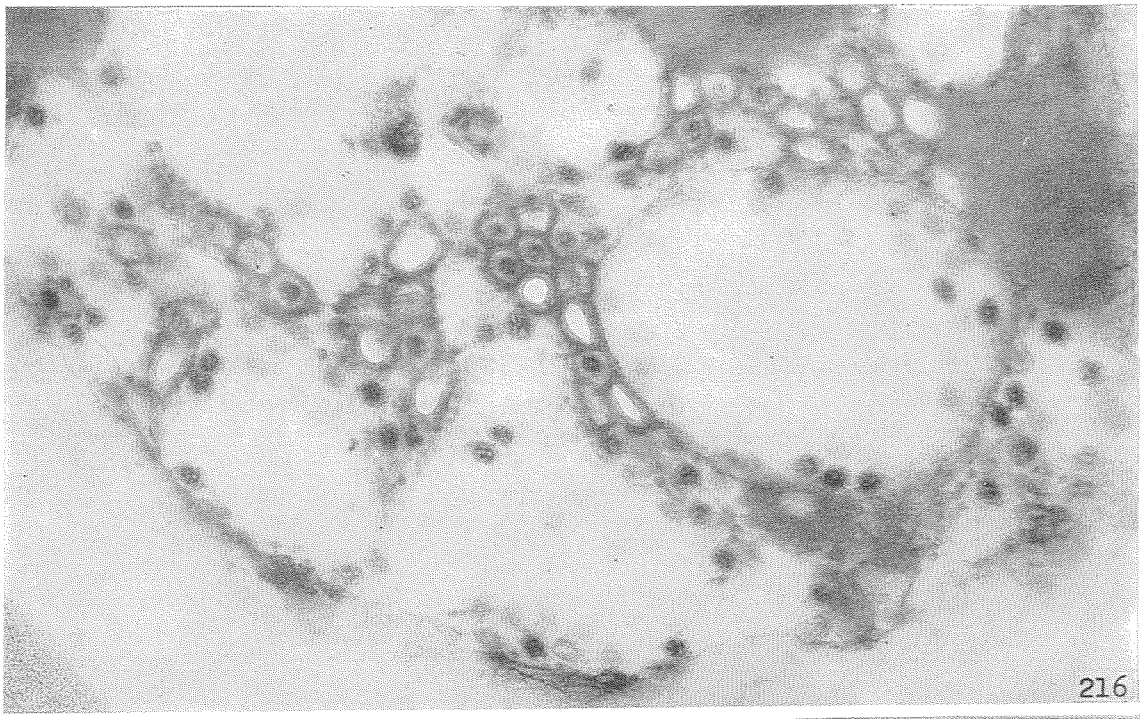

216

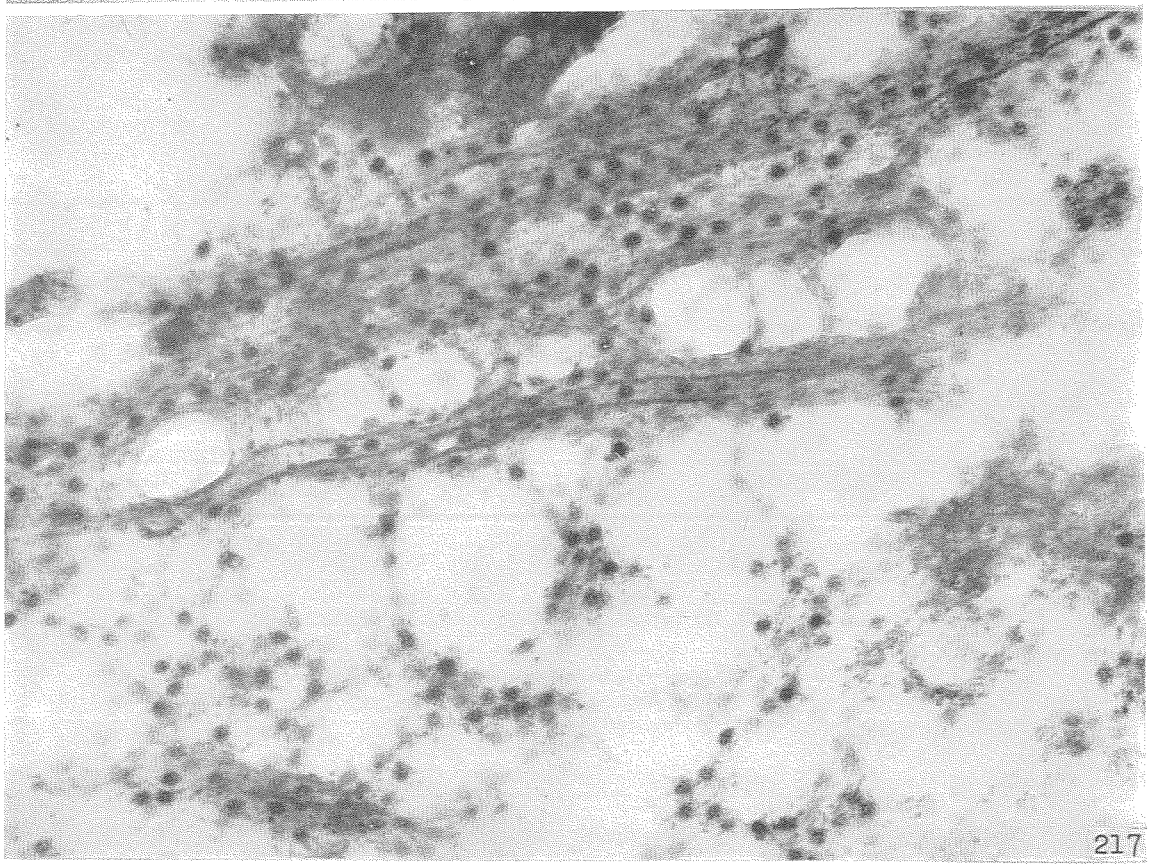

217

Fig. 218. Ultrathin sections of healthy rice leaves.

219. Ultrathin sections of diseased rice leaves, cutting through from green portion to chlorotic portion, very near to the infected cells, but no virus particles are detected in the cells.

Ch
218

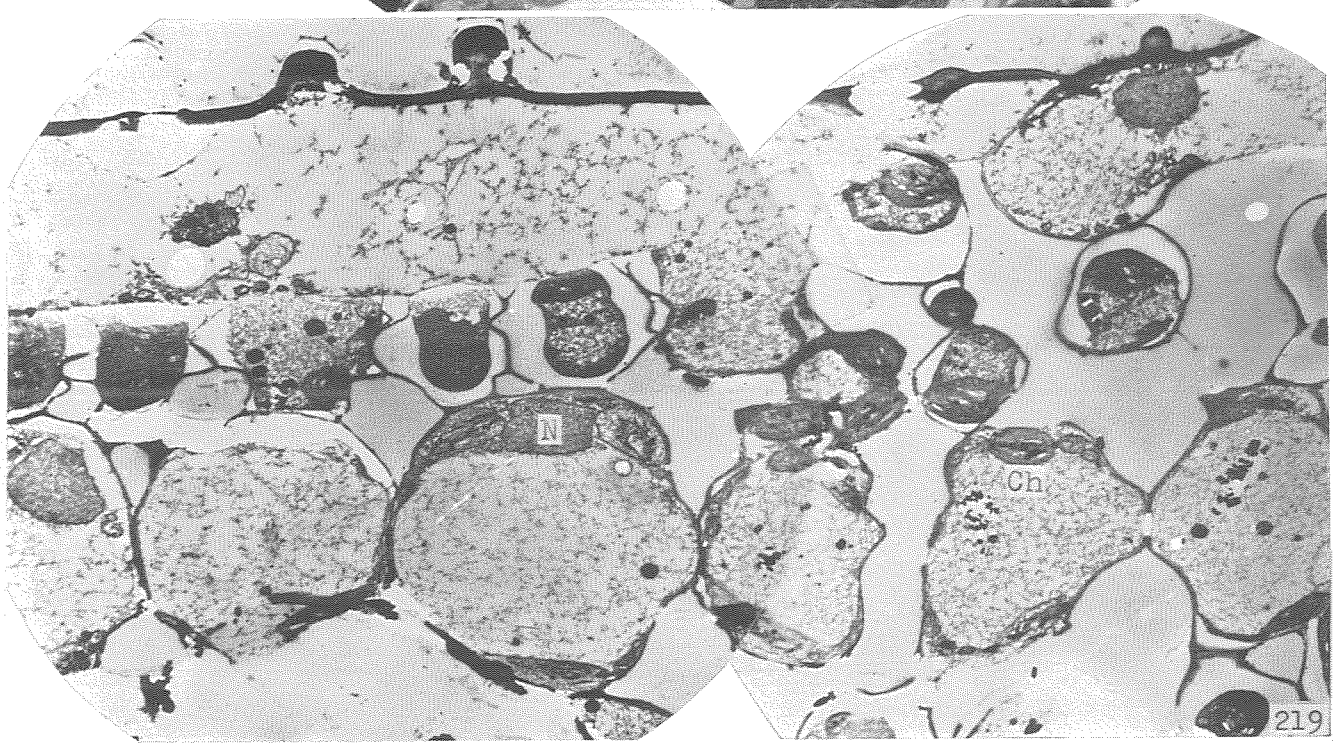
N
Ch
219

Fig. 220. advanced portion of the same specimen as shown in Fig. 219, Virus clusters are visible in a cell, surrounded by a limiting membrane in the cytoplasm of a cell.

221. ditto, high magnification of the above. × 20,000.

220

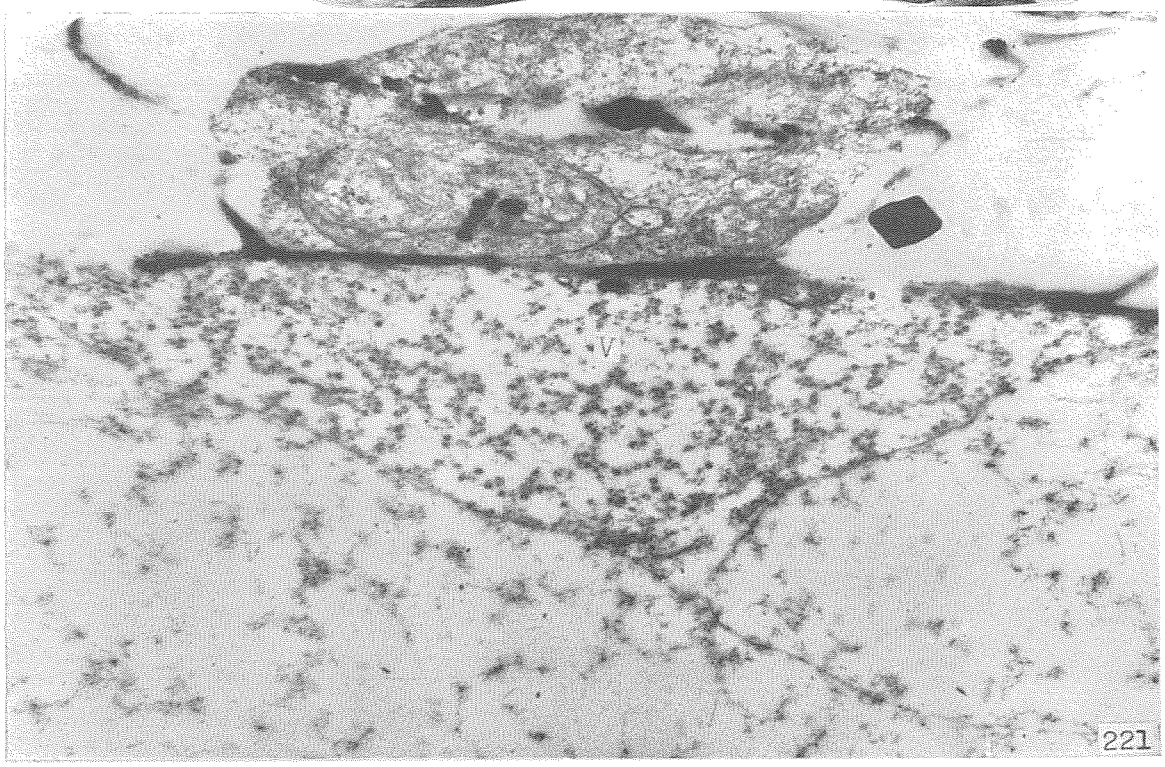

221

Fig. 222, 223, Cr shadowed thin sections reveal virus particles scattered in cytoplasm of the cell, arranging with some cytoplasmic structure. × 30,000.

224, 225. Ultrathin sections of diseased rice leaves, Fig. 224. shows the section of cytoplasmic structure of a cell in green portion. Fig. 225. shows cytoplasmic changes in a cell very near to chlorotic portion. × 90,000 & 76,500 respectively.

226. Ultrathin section of fatbody from a viruliferous leafhopper, showing scattered virus particles (V). × 23,000.

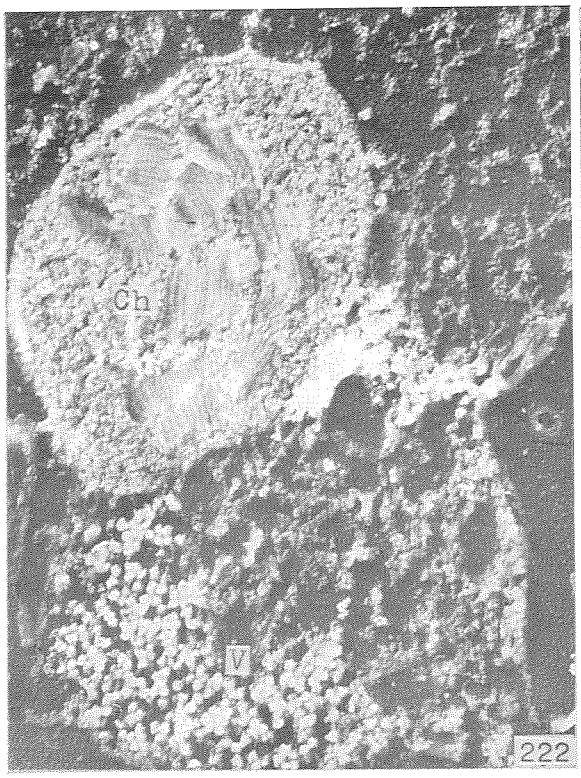
Ch
V
222

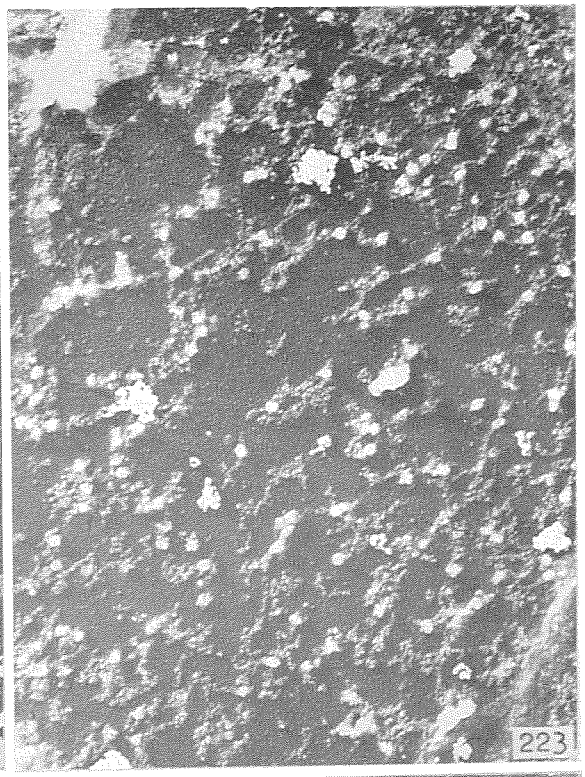
223

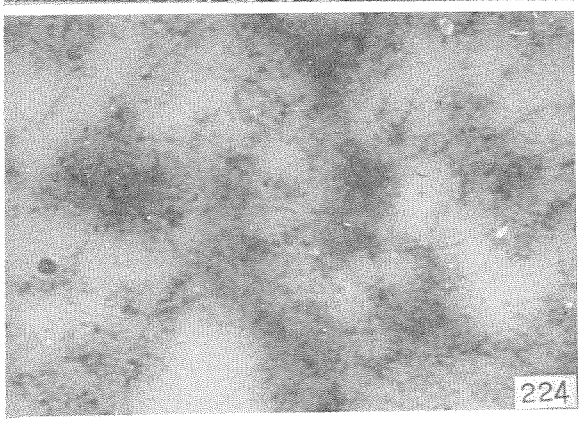
224

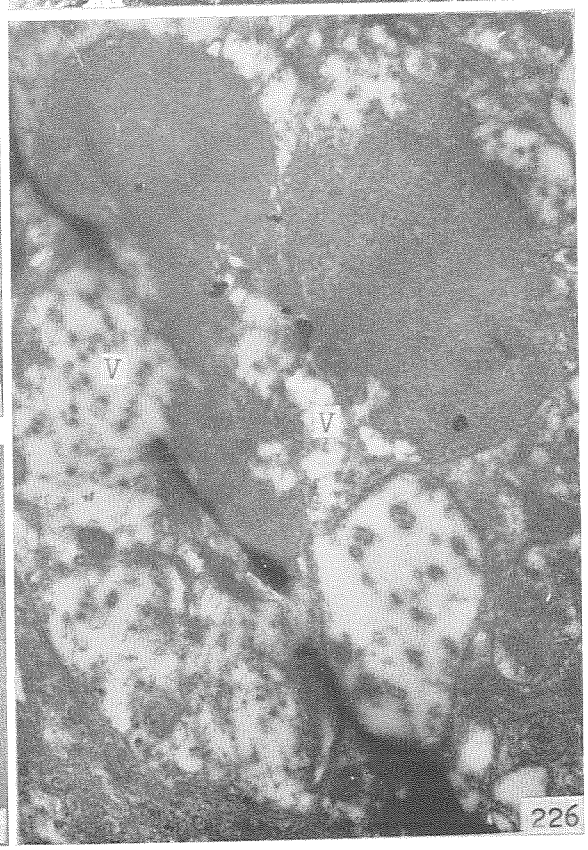
V
V
226

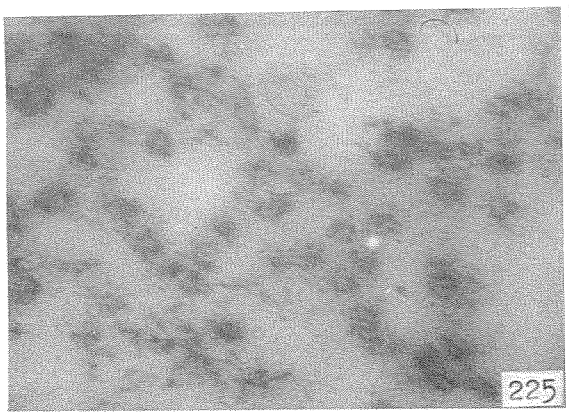
225

Fig. 227, 228. A rice dwarf virus cluster encountered in fatbody of infective leafhopper. Cr shadowed, Fig. 227. × 65,000. Fig. 228 represents the same cluster as shown in Fig. 227 whithin fat body.

229. Unknown structure frequently found in infective abdomen, seemed to be a blood cell, not in healthy leafhoppers. × 34,000.

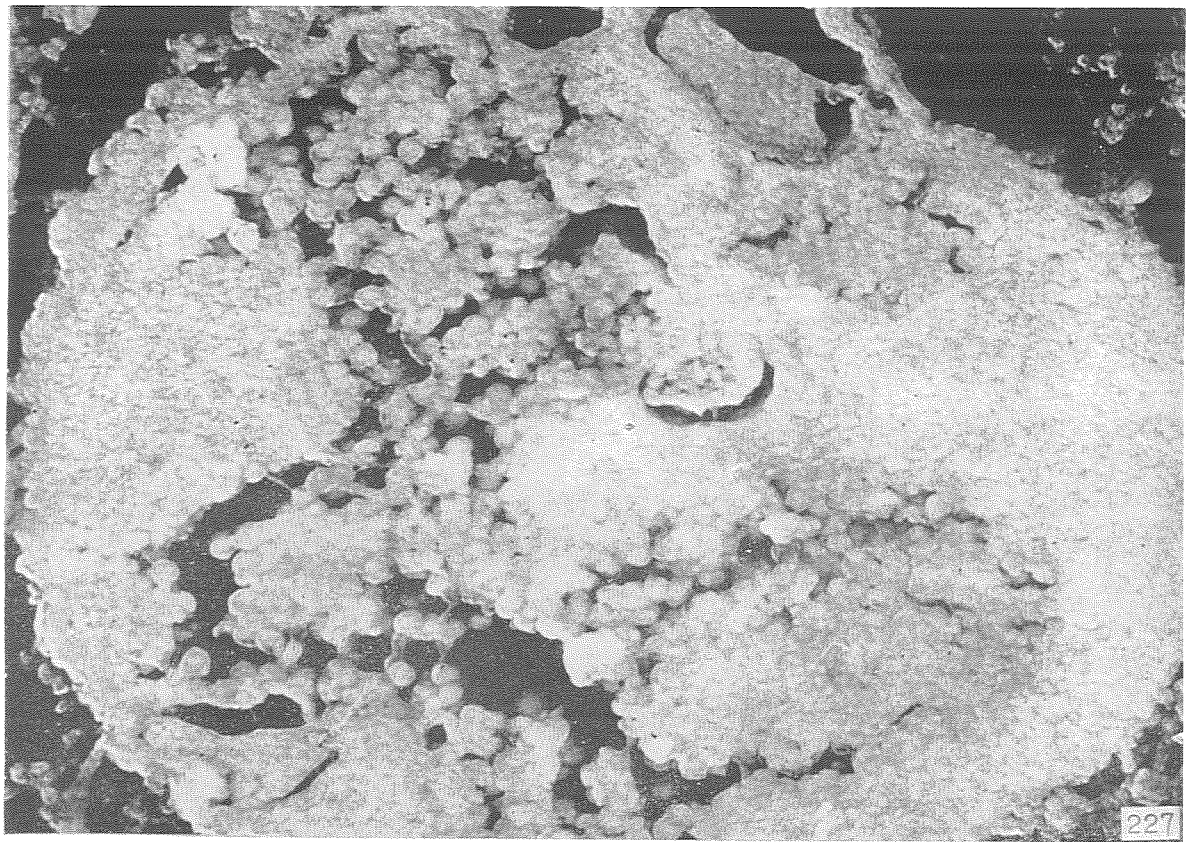
227

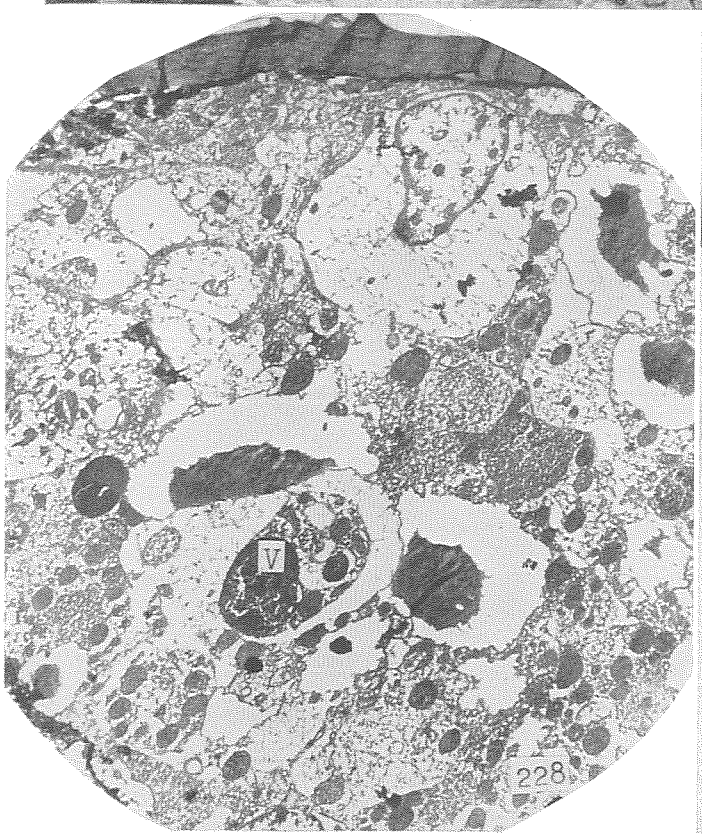
V
228

229

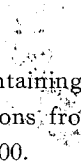

Fig. 230, 231. These structures containing virus clusters seem to be blood cells in a ultrathin sections from abdomen of infective leafhoppers. × 18,000 & × 25,000.

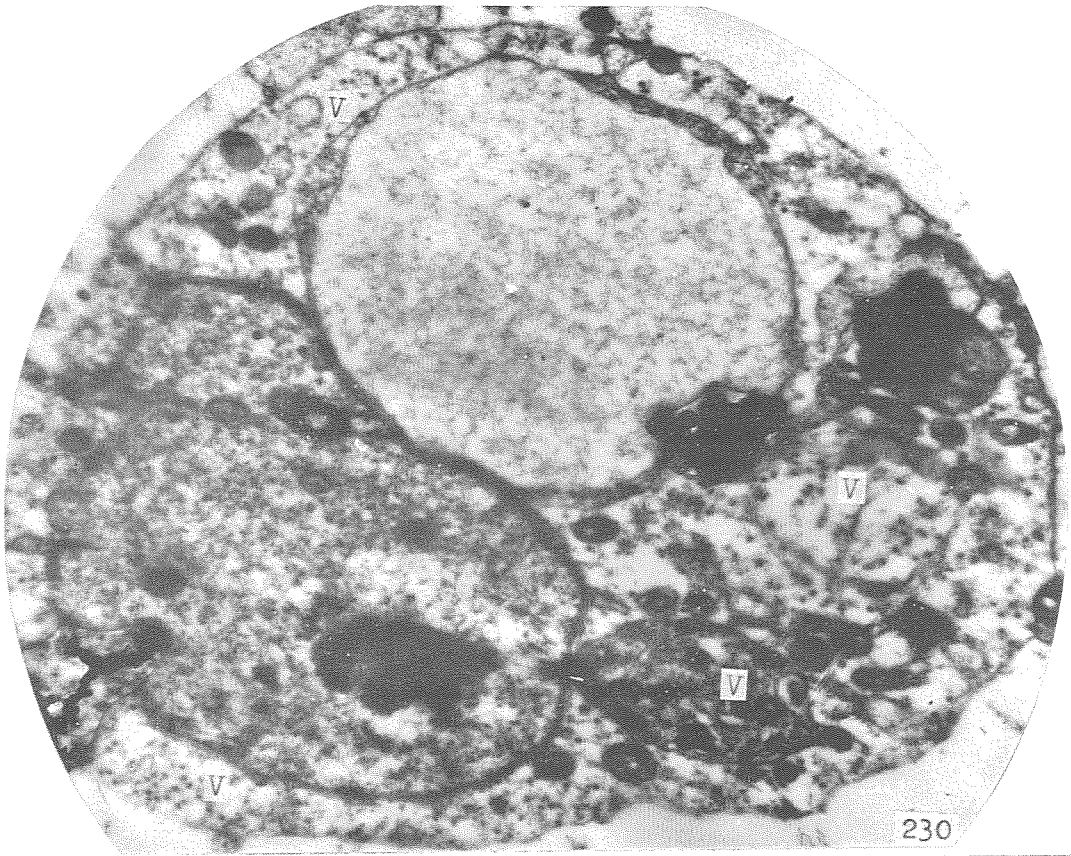

230

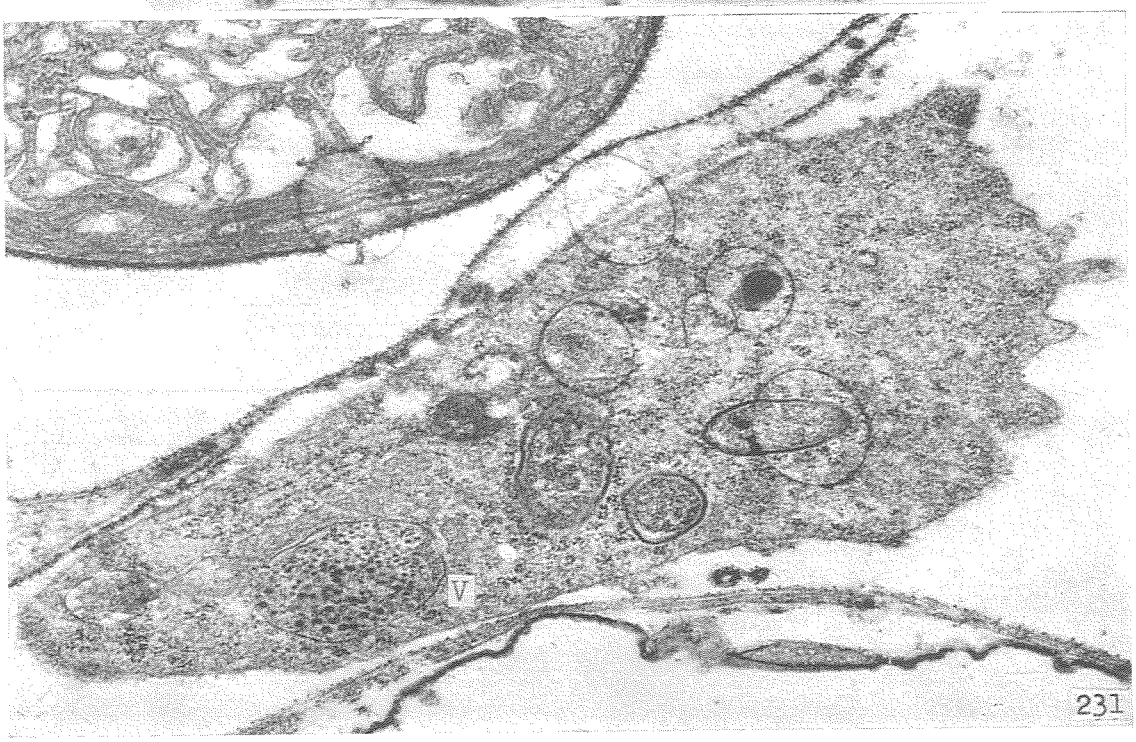

231

Fig. 232. A virus cluster encountered through ultrathin sections from abdomen of infective leafhoppers, showing regular arrangement of virus particles. × 37,000.

233. High magnification of virus cluster encountered in a cell of Malphighian tubules. Arrows show a hexagonal shape of virus particles with central darker area surrounding less dense portion. × 155,000.

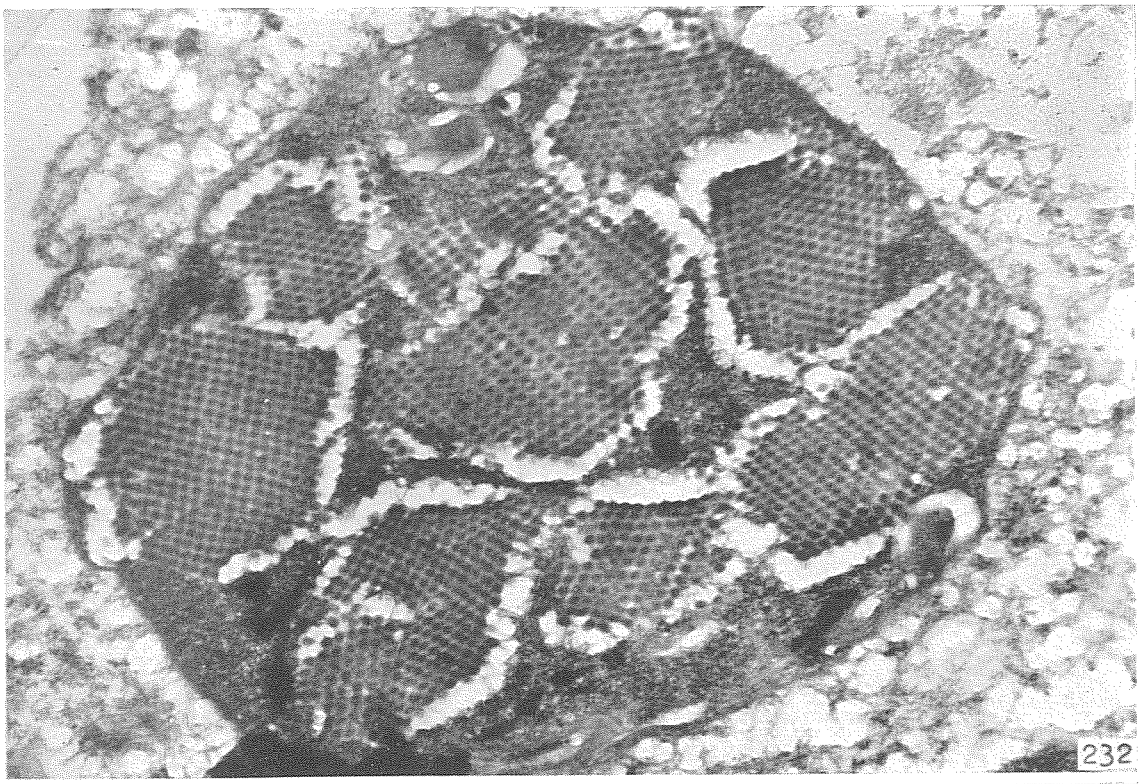
232

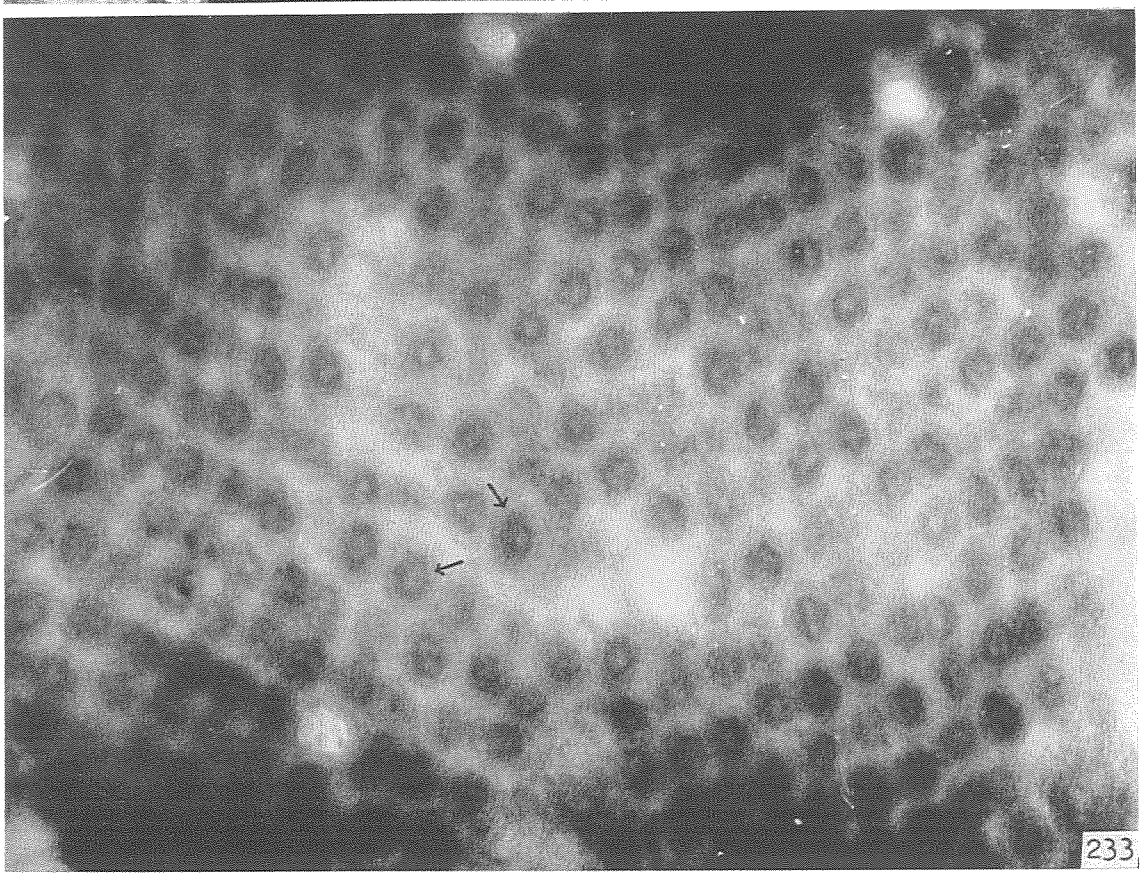
233

Fig. 234. A ultrathin section of Malphighian tubules from infected leafhoppers, showing a virus cluster in a defined structure, B represents Brochosome; V represents Virus particles. × 27,000.

235. Crystalline arrengement of virus particles in a cell of abdomen from infective leafhopper. × 27,000.

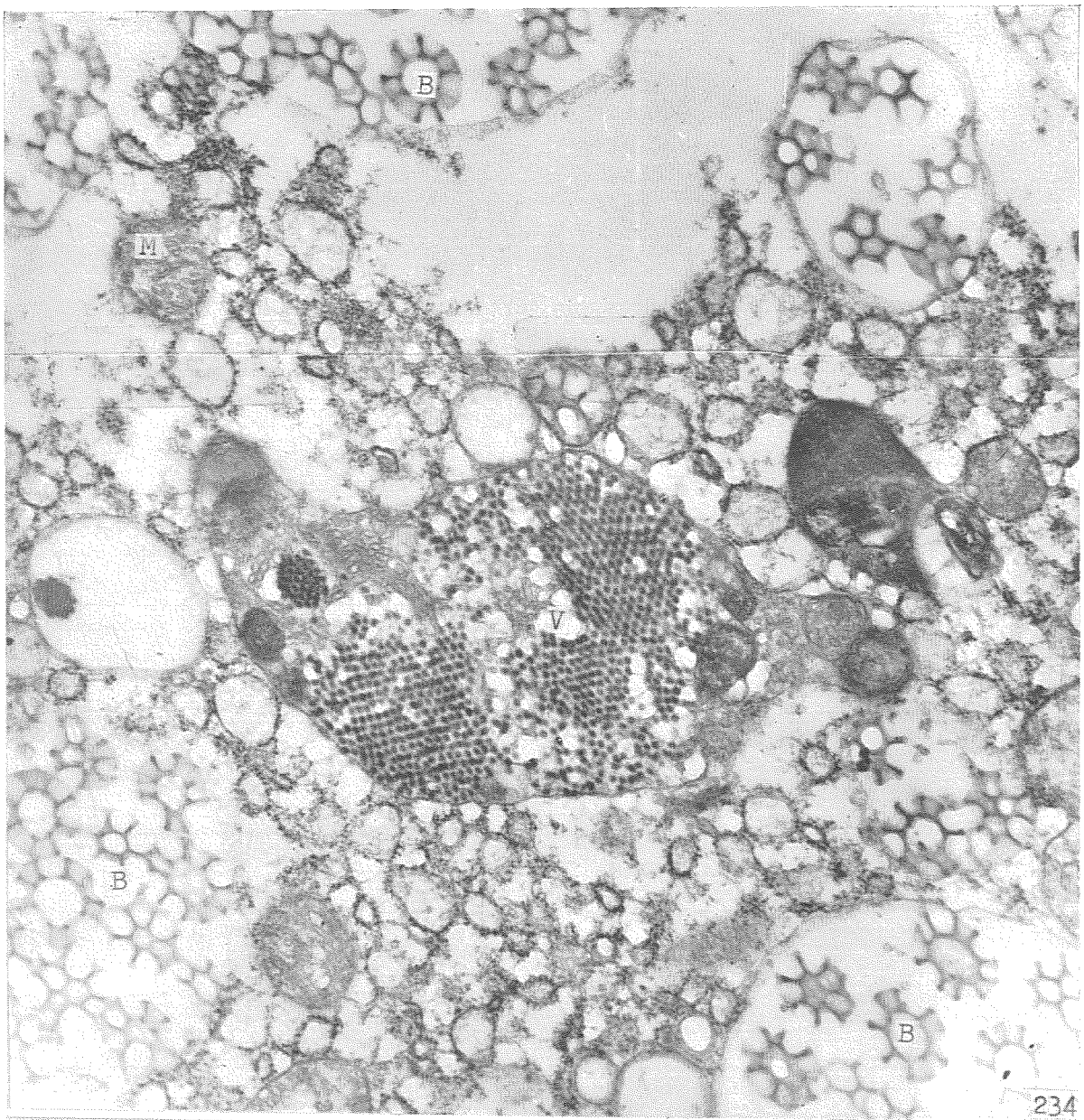
B
M
V
B
B
234

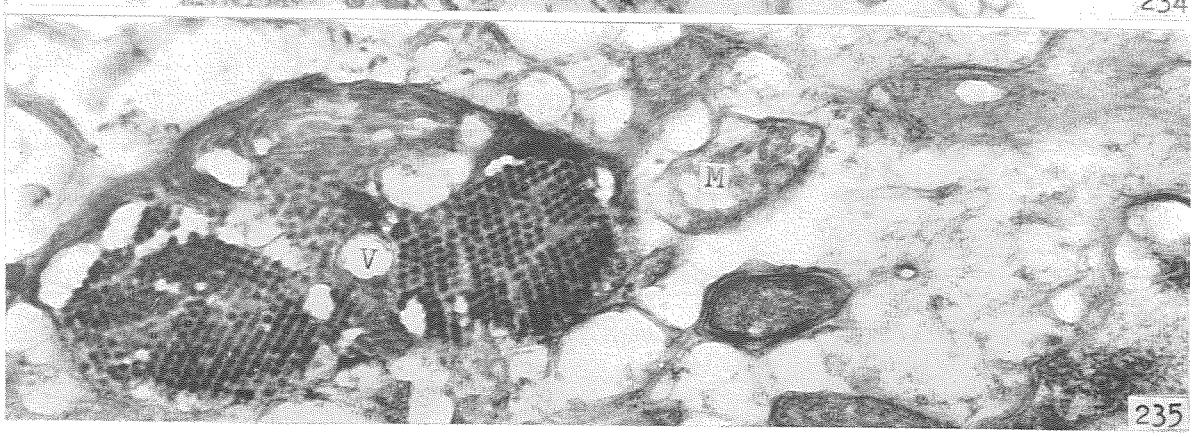
M
V
235

Fig. 236, 237. Ultrathin sections through fatbody of diseased leafhopper, showing defined structures enclosing virus particles. V; virus particles, M; mitochondria. × 16,000 & 30,000 respectively.

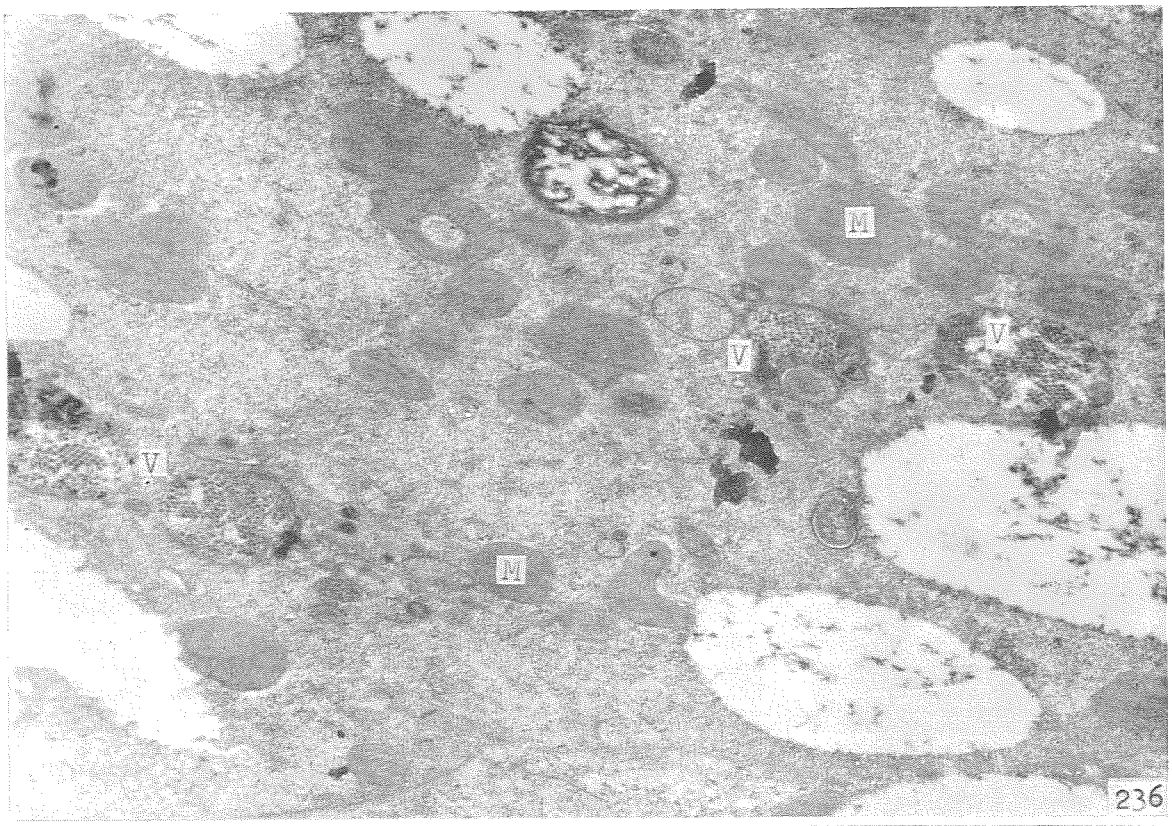

236

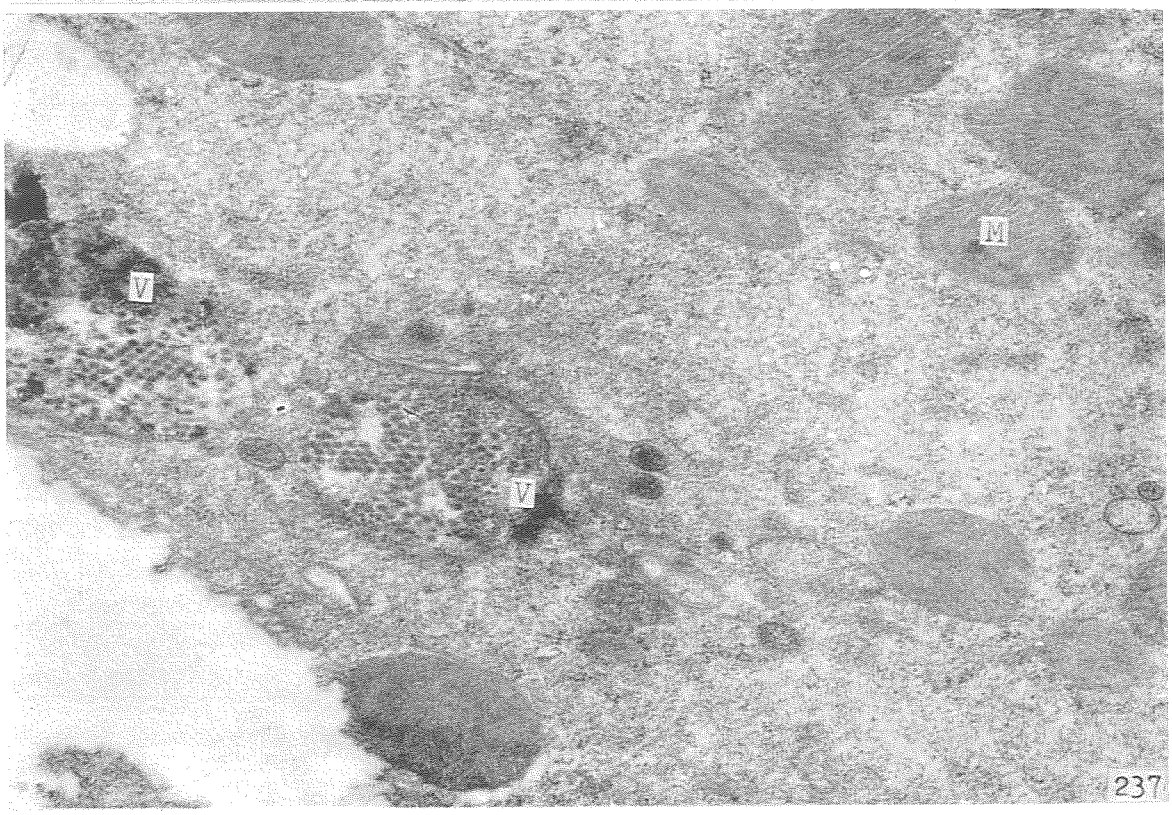

237

Fig. 238. ditto, showing small dense particle accumulation other than virus particles within defined structure including virus particles. × 30,000.

239. ditto, Virus clusters surrounding by several layers of cytoplasmic membrane, which seems to be smooth endoplasmic reticulum, are visible. × 33,000.

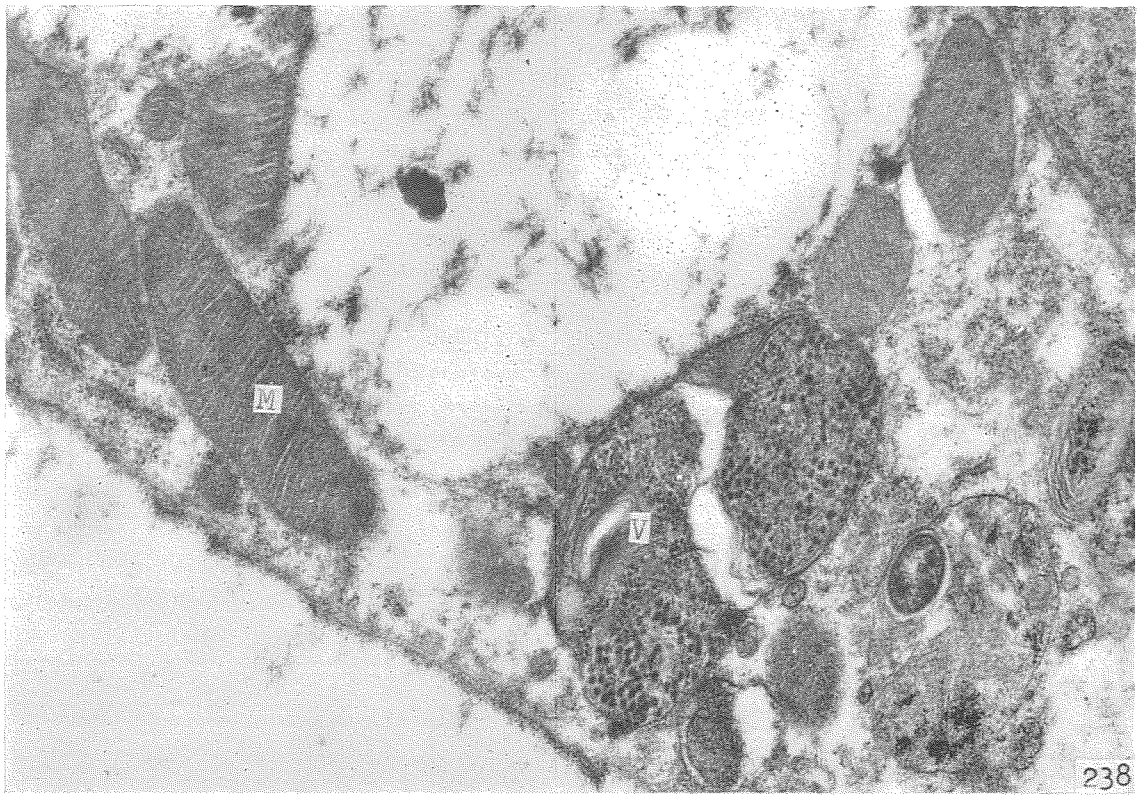
M
V
238

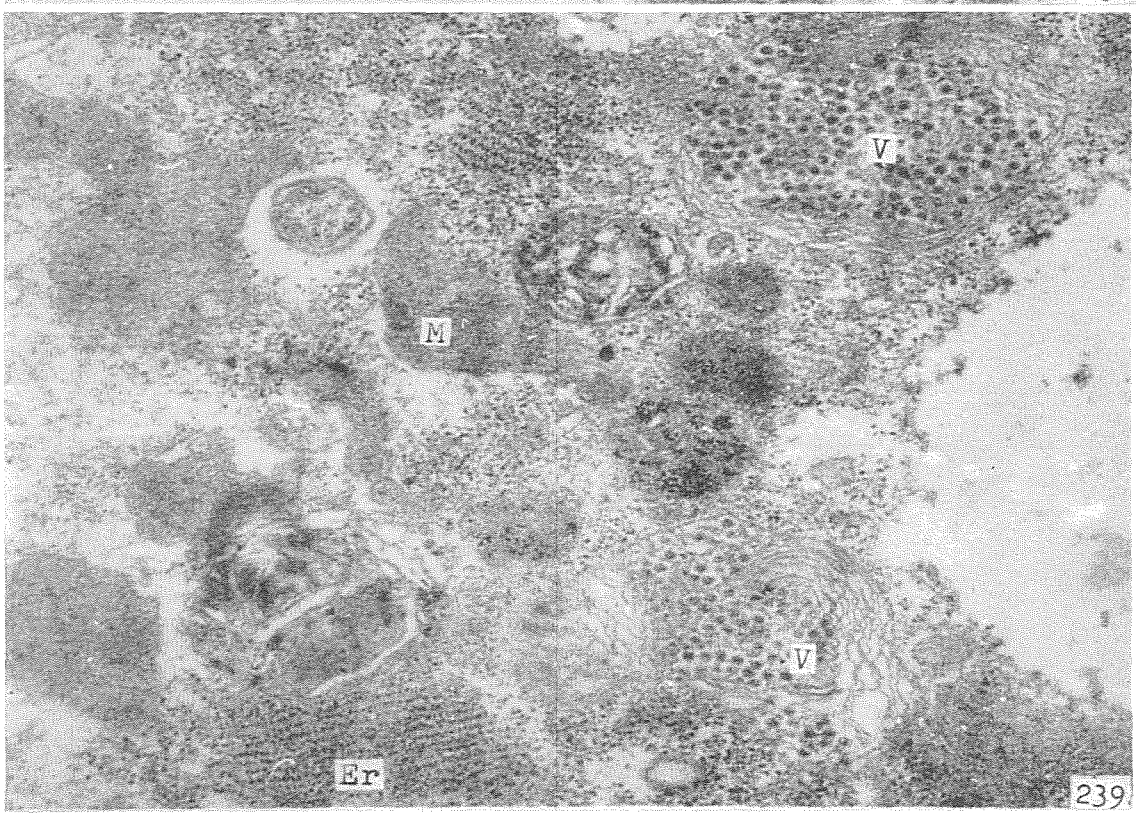
V
M
V
Er
239

Fig. 240–242. ditto, showing tubular structures including a string of virus particles (V) in Fig. 240, 241. Well developed smooth endoplasmic reticulum (ER) were frequently appeared near virus clusters in Fig. 241, 242. M; Mitochondria. × 70,000.

240

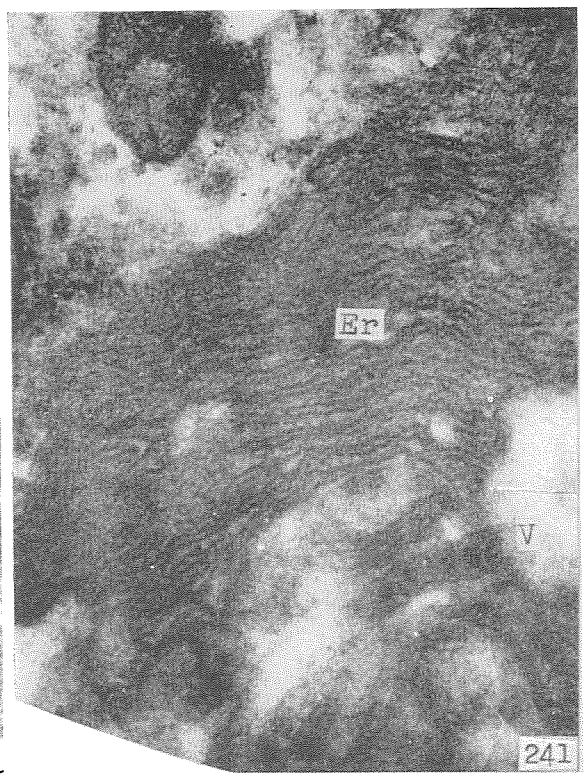

241

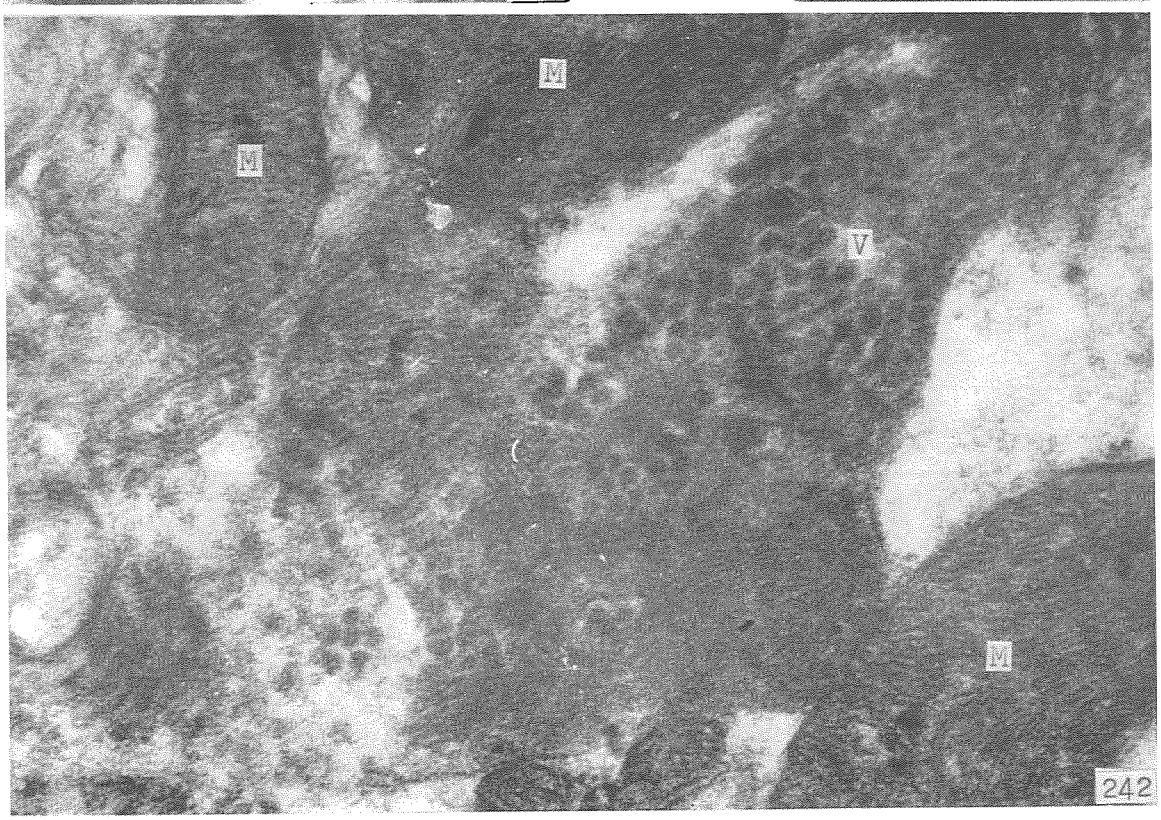

242

Fig. 243, 244. Ultrathin sections of epitherial cells of intestine from infective leafhoppers. Crystalline arrangement of virus particles are encountered. N; nucleus, V; virus clusters. × 30,000 & 33,000.

245. A ultrathin section of salivary gland of infective leafhopper. Showing virus accumulation (V) in a vesicle. × 5,600.

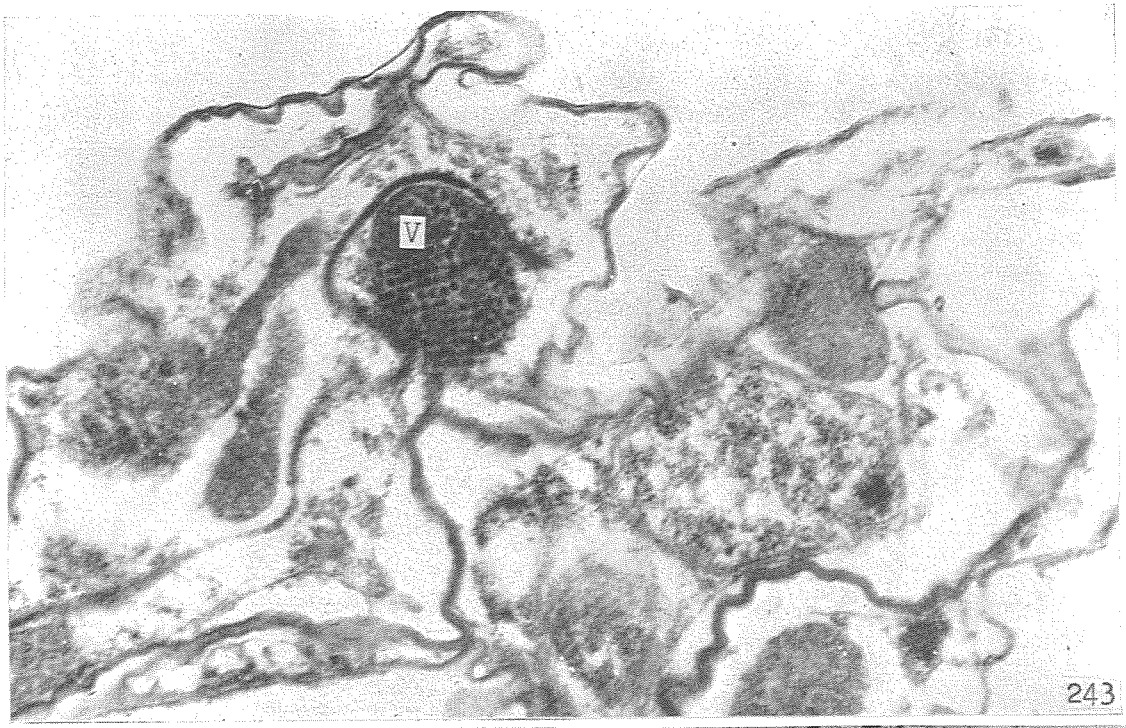
V
243

V
N
V
244

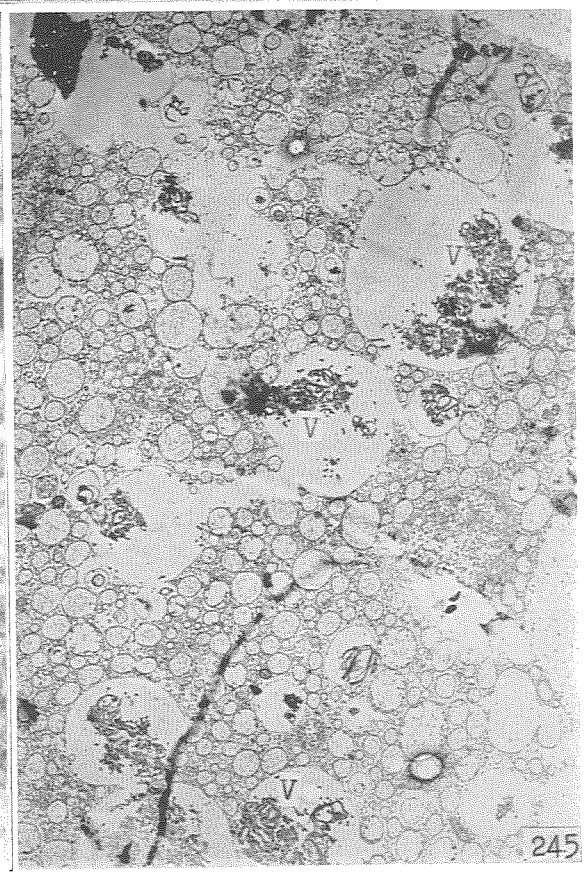
V
V
V
V
245

Fig. 246, 247. ditto, showing a vesicle including virus clusters. Virus particles are enclosed in dense membraneous substances, or scattered in the vesicle. × 24,750 & 60,000.

246

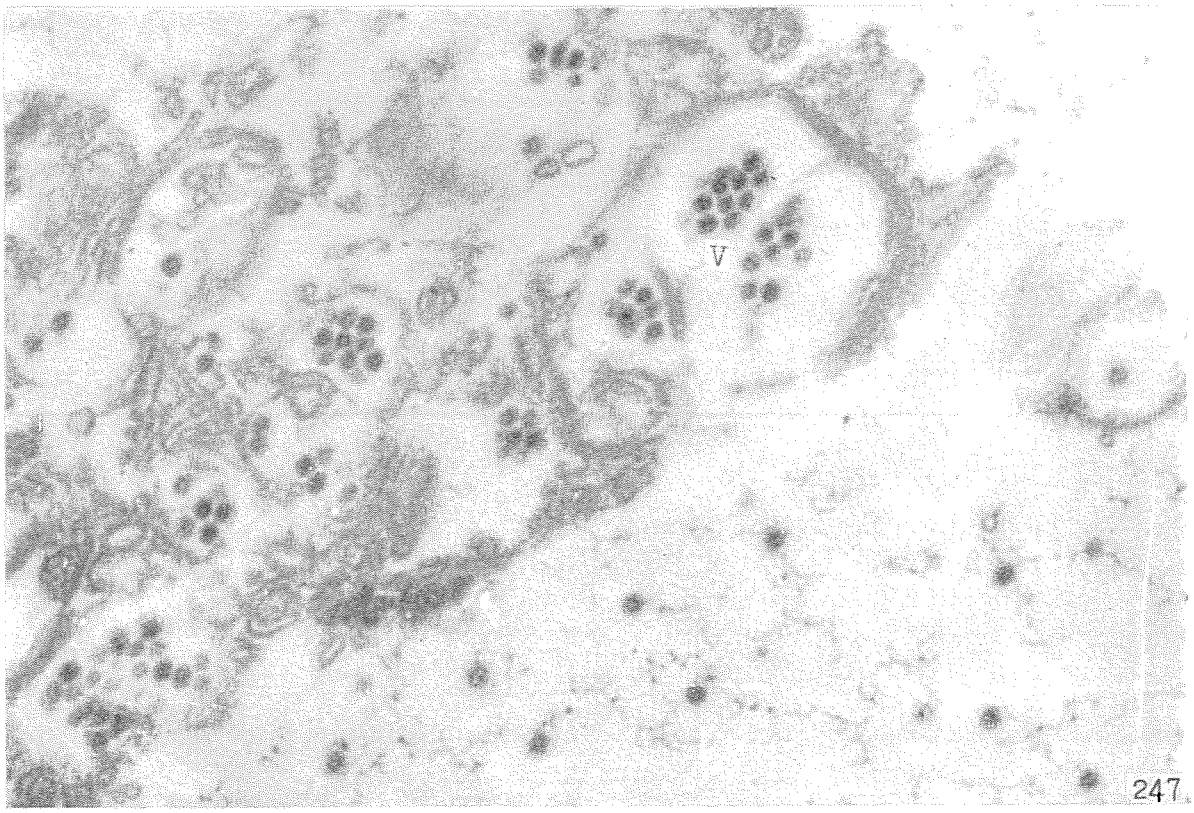

247

Fig. 248, 249. ditto, a lot of virus particles are compactly accumulated in the vesicles in the sarivaly gland cells. × 37,500.

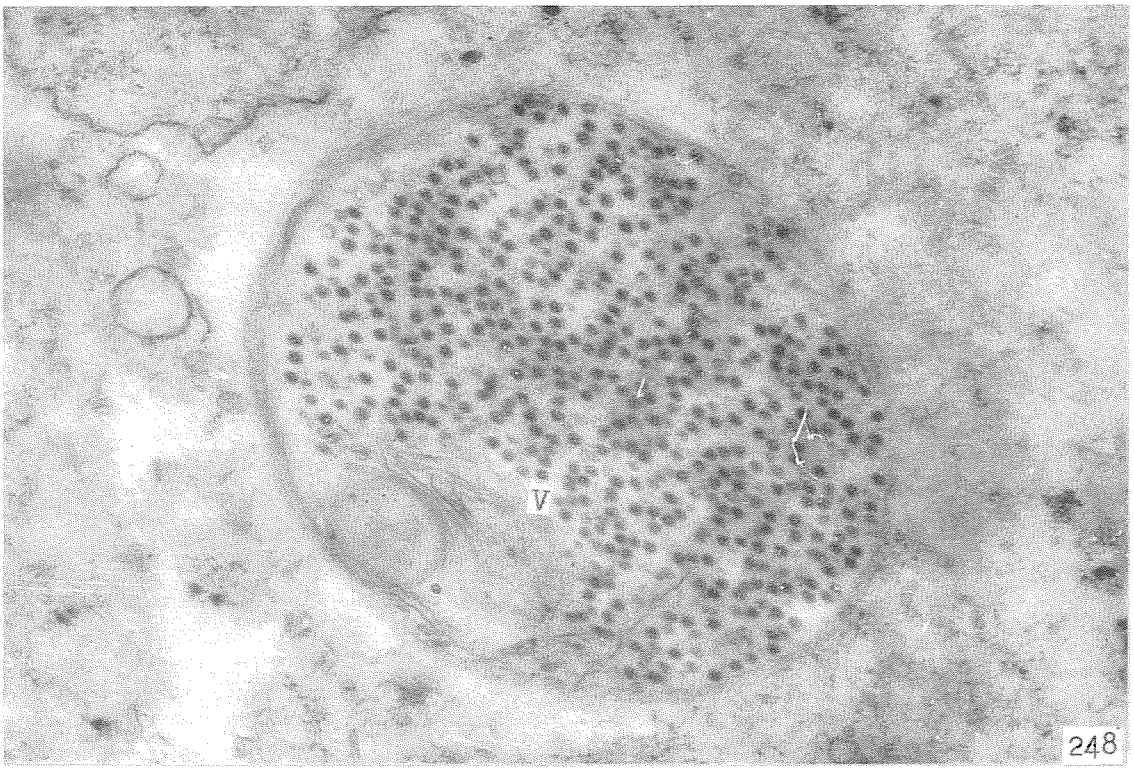

248

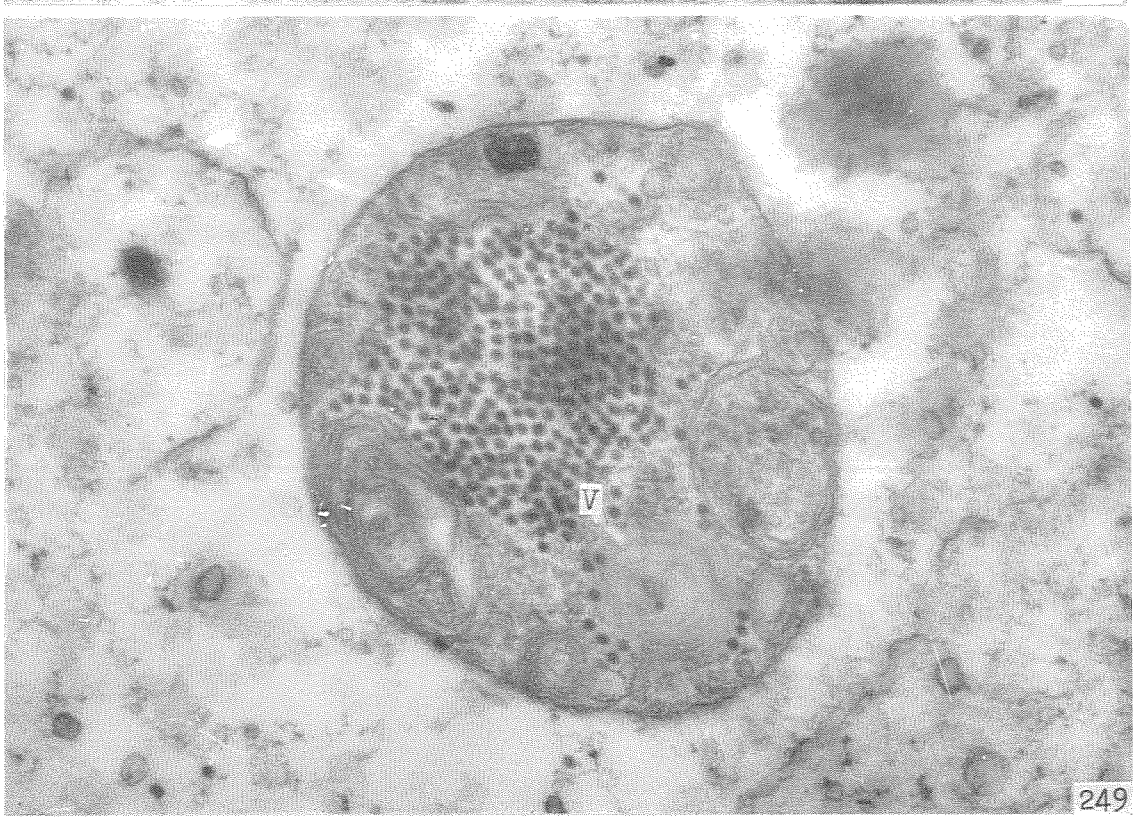

249

Fig. 250, 251. ditto, a string of virus particles arranged in the tubular structures in the vesicle of salivary gland cells. × 45,000 & 82,500.

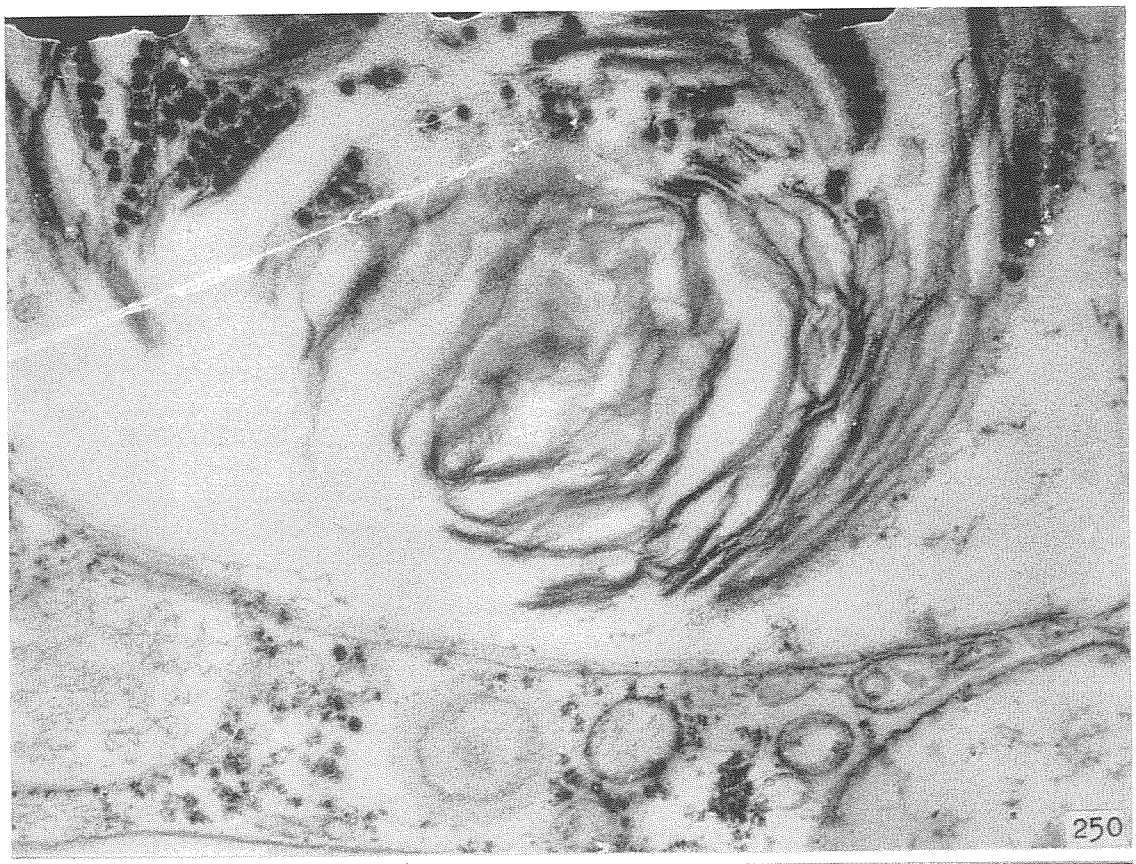

250

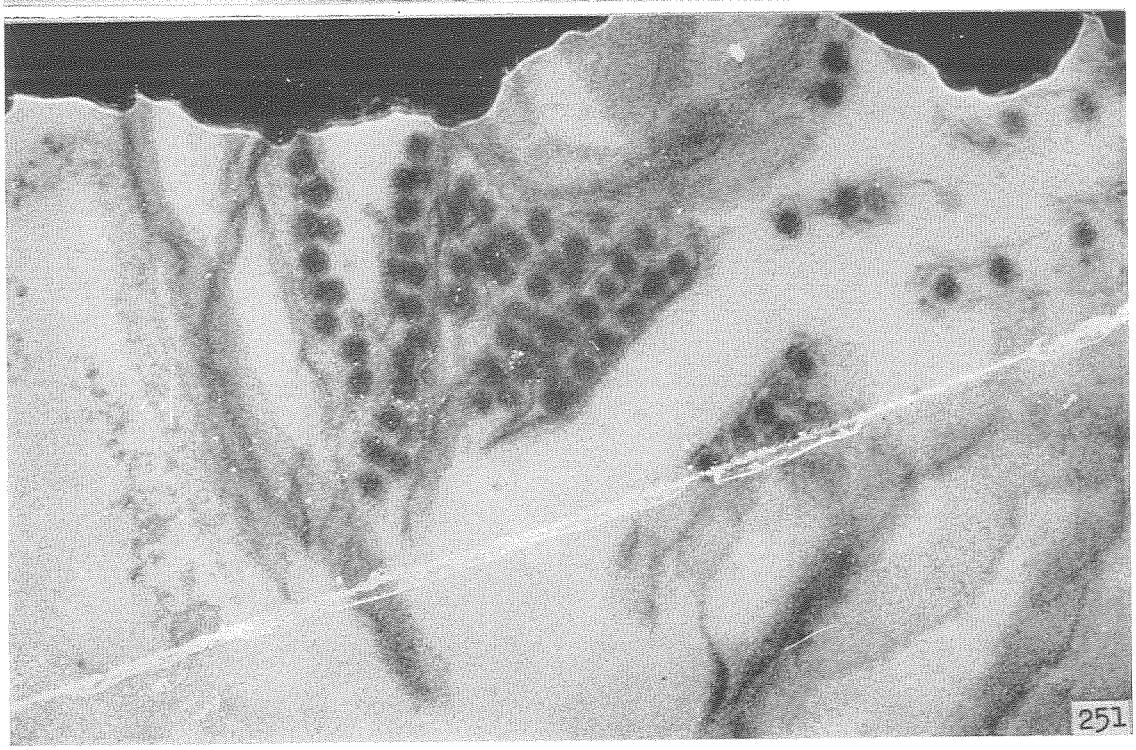

251

Fig. 252. ditto, A virus containg vesicle including a lot of virus particles and micro tubular structure in a salivery gland. × 20,000.

253. ditto, another tubular structures containing a string of virus particles in the vesilces of salivery gland cells. × 45,000.

252

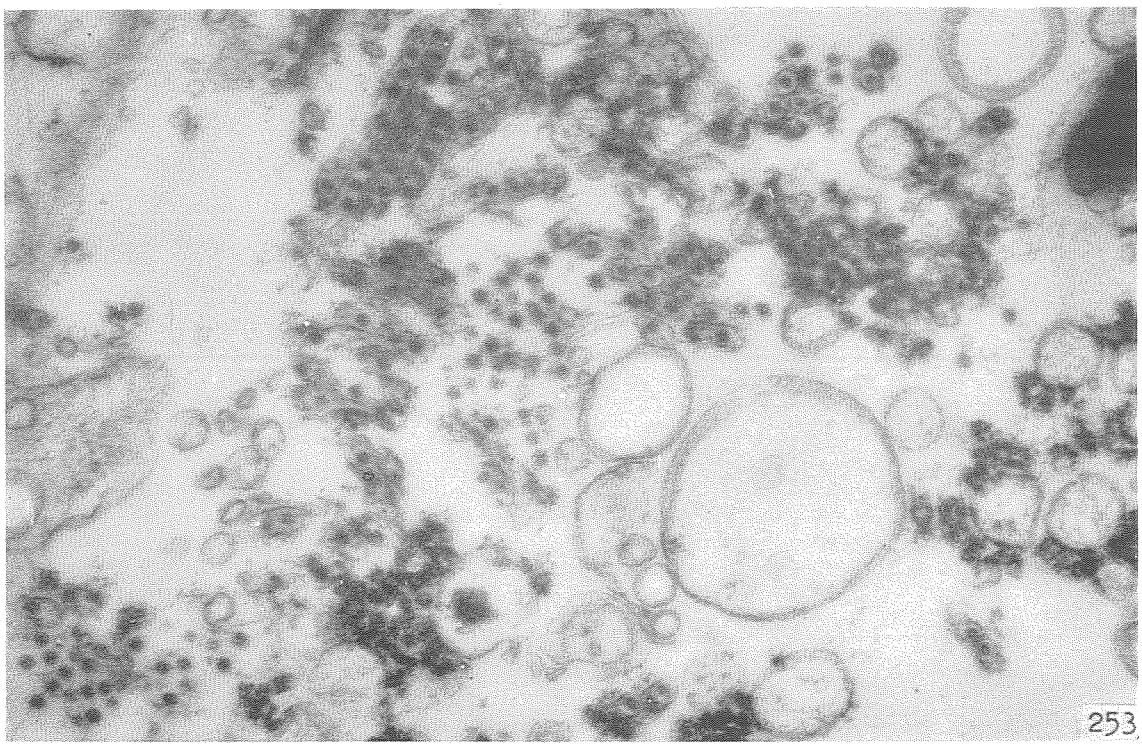

253

Fig. 254, 255. Ultrathin sections of ovarian tubules from infective leafhoppers reveales a lot of virus clusters of rice dwarf virus. × 29,700.

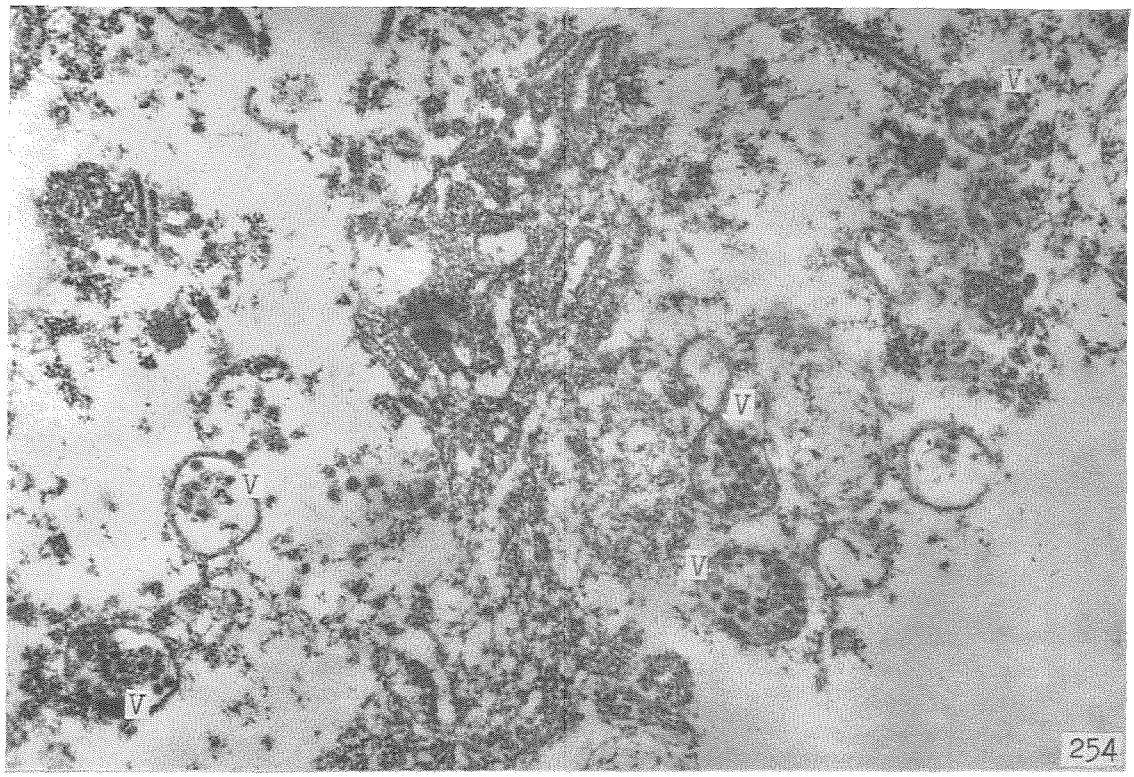
V
V
V
V
V
254

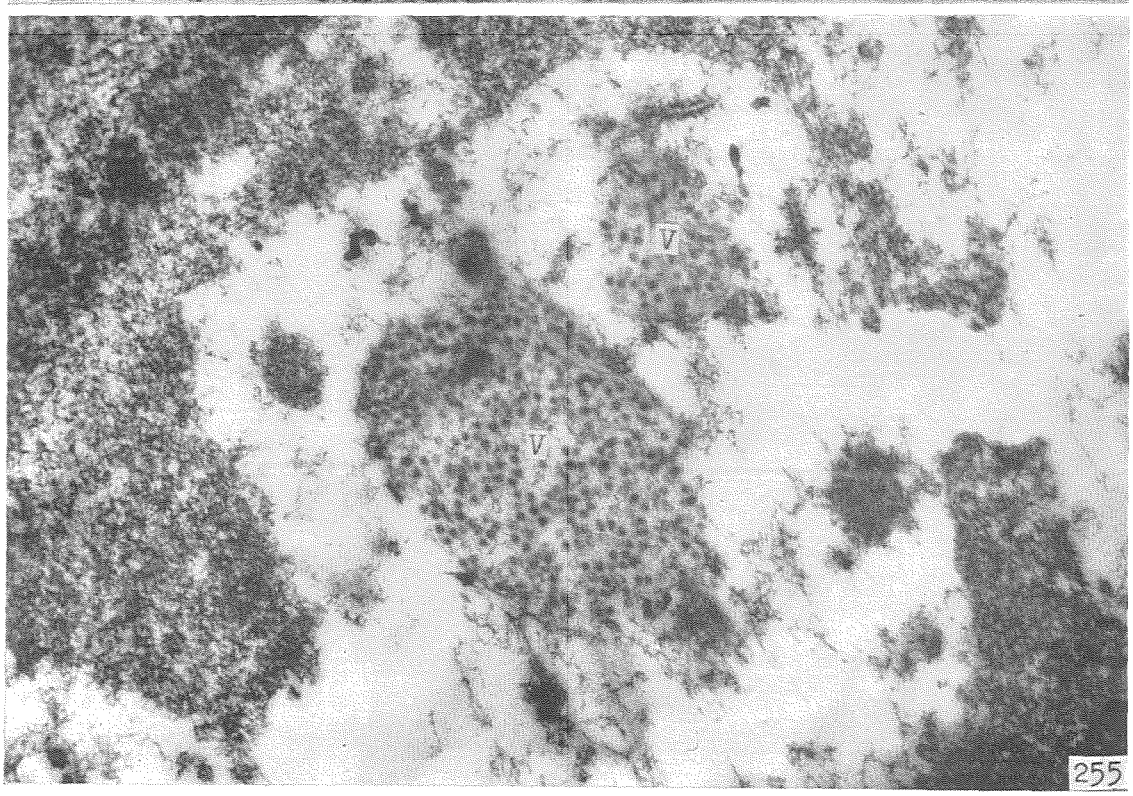
V
V
255